

This volume was originally prepared by myself, and the work described
herein is the property of the University of Edinburgh.

Harold G. Corwin, Jr.

Harold G. Corwin, Jr.

September 1981

THE INDUS SUPERCLUSTER

Harold G. Corwin, Jr.

Ph. D.

University of Edinburgh

1981



This thesis was entirely composed by myself, and the work described in it was entirely done by myself unless specifically noted otherwise.

Harold G. Corwin, Jr.

September 1981.

Abstract

A survey of rich galaxy clusters, redshifts for many of those clusters, and galaxy counts by eye to $B = 19.0$ show the Indus Supercluster to be an annular (in projection) configuration of nine rich clusters at $0.073 \lesssim z \lesssim 0.080$ apparently connected by bridges of galaxies.

Photoelectrically calibrated photographic photometry of galaxy images on six U.K. Schmidt plates using the COSMOS machine at the Royal Observatory, Edinburgh, gave photometric information for about 150,000 galaxies. From this, the luminosity function of the Indus Supercluster was extracted. To $B = 21.5$, the Supercluster includes about 25,000 galaxies, its estimated total luminosity is $7 \times 10^{13} L_{\odot}$, and — if its mass-to-light ratio is typical — its total mass is $\sim 1 \times 10^{16} M_{\odot}$. Its diameter is about 40 Mpc. These parameters make it similar to other known superclusters.

In addition, the integrated apparent field luminosity function for galaxies, derived from the 140 square degrees of sky scanned on Schmidt plates by COSMOS, agrees with most previous determinations.

The general picture of a sponge-like cellular distribution of galaxies as developed by Einasto and his colleagues is confirmed. Though there are some indications that this structure is primordial, neither data nor theories are yet sufficient to allow an adequate explanation of the development of such structure in the universe.

Table of Contents

Abstract	3
Table of Contents	4
Acknowledgements	6
Dedication	9
Chapter 1 -- The Distribution of Galaxies and Macrostructure in the Universe	
I. Introduction	10
II. Early Studies of the Distribution of Galaxies	11
III. Beginning of the Modern Era in Galaxy Distribution Studies	13
IV. Modern Surveys Pertaining to the Galaxy Distribution Problem	21
V. Statistical Investigations of the Modern Catalogues	23
VI. Observational Studies of the Distribution of Galaxies and Clusters: Individual Superclusters	27
VII. Macrostructure in the Universe	40
VIII. Purpose and Overview of the Present Work	42
Chapter 2 -- Southern Optical Sky Surveys and the Discovery of the Indus Supercluster	
I. Introduction: Historical Southern Sky Surveys	44
II. Southern Schmidt Surveys	47
III. A Suspected Supercluster	49
Chapter 3 -- A Preliminary Redshift Survey of the Indus Supercluster Area	
I. Introduction and Assumptions	73
II. Selection and Positions of Galaxies	74
III. Observations	75
IV. The Redshift Survey	78
V. Beyond the Indus Supercluster	91
Chapter 4 -- Photometry, COSMOS Scans, and the Luminosity Function of the Indus Supercluster	
I. Introduction	92
II. Plate Material	93
III. The COSMOS Machine	93
IV. Relative Calibration of UK Schmidt Plates	96
V. Absolute Calibration of Galaxy Magnitudes	101
VI. COSMOS Data Processing	119
VII. Possible Sources of Systematic Errors in the Star-Galaxy Separation	129
VIII. Luminosity Functions	141
Chapter 5 -- The Structure of the Indus Supercluster	
I. Introduction	163
II. Data: Review and Desiderata	163
III. Comparison with Other Supercluster Observations	167

IV. Formation of Superclusters	169
References	175
Appendix A -- Optical Spectra and Redshifts for Eighty Galaxies by Harold G. Corwin, Jr. and David Emerson	
Appendix B -- UBV Photoelectric Photometry and Photometric Parameters for 40 Galaxies by Harold G. Corwin, Jr.	

Acknowledgements

I have been most strongly influenced in this work by the ideas of and by my contact with three astronomers: Prof. George Abell, Dr. Jaan Einasto and Prof. Gérard de Vaucouleurs. Without their help and friendship, I could not have found or studied the Indus Supercluster.

My professors, V. C. Reddish and M. S. Longair, are patient and tolerant gentlemen. I thank them for having me at Edinburgh.

Dr. David Emerson, my supervisor in the Department of Astronomy, has been steadfast in his friendship, help, and cheerful criticism, all valuable to me. He and Richard Dodd struggled through the long South African winter nights with me, chasing galaxies. I appreciate their help.

Drs. Russell Cannon and Robert Stobie, my supervisors at the Royal Observatory, made the full facilities of the U.K. Schmidt Telescope Unit and of the Image and Data Processing Unit (which they, respectively, lead) available for my use. Their ideas and answers also helped me to get the work done.

Dr. Harvey MacGillivray was more than generous in sharing his COSMOS data reduction software and experience. A large part of this work would have been much more difficult without his continued aid.

Among others in the Astronomy Department or at the Royal Observatory who helped significantly were (in no particular order): Keith and Sue Tritton, John and Jo Barrow, Robert Smyth, Ralph Martin, Bernie McNally, Eve Thomson, Liz Sim, Mary Davidson, Joyce Shand, Susan Hooper, Mary Brück, Peter Brand, Arthur Dent, Brian

Hadley, Tim Hawarden, Andy Longmore, Angus MacDonald, Susan-Jane and Ann and Rita, Russell Eberst, Marjorie Fretwell, Steven Beard, Paul Hewett, Mike Hawkins, Gillian Pickup, Lindsay Ellery, John Cooke, Dennis Kelly, Neil Pratt, Neil Reid, Gerry Gilmore, Ford Prefect, Bruce Guthrie, Mauricio Tapia, Kashi Nandy, John Dawe, Bill Zealey, Michael and Mary Smyth, Len Lawrence, Rudy Lutz, Graham Smith, Dorothy Skedd, Victor Clube, Fred Watson, Calum Barclay, Bill Robertson, Harry Seddon, Andy Brooks, Arthur Trew, Bob Smith and Ray Sharples. To those whom I may have forgotten here, my apologies — anonymous thanks are not quite the same, are they?

The Astronomy Group at the University of Durham (Drs. Dick Fong, Richard Ellis, Tom Shanks, Steve Phillipps and Martin Green) had valuable comments on this work and contributed data as well. They also introduced us to a lovely British town.

Chip Arp, Guido Chincarini and Massimo Tarenghi (as well as Tom Shanks and Martin Green) contributed redshifts that helped to fill in gaps in tables and diagrams. Guido Chincarini also has been a firm friend and gentle critic for many years.

Friends and relatives — especially my parents, Mr. and Mrs. H. G. Corwin; my brothers, John and Dean; and our lifetime friend Carolyn Jennings — helped in all the ways that make it possible for life to flow on enjoyably.

My typist, John Clifford, persevered under the difficulties of odd-sized paper, English spelling, and (most especially) my wretched penmanship. In spite of this, he managed not only to get the job done, but to correct my hasty punctuation, grammar, and American spelling (but any remaining mistakes are mine!) along the way.

The tables and figures are my own fault.

Finally, my wife Kay has suffered through countless days and nights of galaxies, galaxies, and more galaxies. Her patience and love are unrivalled, I'm sure, anywhere in the universe.

Financial support for this work came from the U.S. Veterans' Administration, and from the U.S. National Science Foundation (through research grants to Prof. G. de Vaucouleurs and to Prof. G. O. Abell, and through a USNC/IAU travel grant). I also gratefully acknowledge travel and subsistence grants from the U.K. Science and Engineering Research Council, the International Astronomical Union, the Estonian Academy of Sciences, and the French Centre National de la Recherche Scientifique.

Dedication

This thesis must be for

my lovely

Caitlin

who helped me through it;

and for

Les

who helped me get it started.

CHAPTER 1

The Distribution of Galaxies and
Macrostructure in the UniverseI. Introduction

The large-scale structure of the universe can best be studied at present by determining distances to galaxies and clusters of galaxies. Though the areal distribution of these objects can give clues to their true spatial distribution (see e.g. Peebles 1980 and references therein), the lack of well-determined distances has been a serious obstacle to our understanding of even the nature of the spatial distribution, let alone its origin or evolution.

Fortunately, the past decade has seen the development of image intensifier technology to the point where spectra of very nearly the faintest detectable objects can be obtained in a reasonable amount of observing time. At the time of the publication of the First Reference Catalogue of Bright Galaxies (RC1; de Vaucouleurs and de Vaucouleurs 1964) about a thousand extragalactic redshifts were known. Twelve years later at the publication of the Second Reference Catalogue (RC2; de Vaucouleurs, de Vaucouleurs, and Corwin 1976), the number had grown by a factor of four. The intervening five years to the present have seen yet another factor of four increase. This vast data explosion is allowing us to glimpse for the first time the true distribution of luminous matter in our local region of the universe (e.g. Einasto et al 1980a, b, Davis et al 1981).

The purpose of the present study is to see if the overall properties of the distribution as revealed by the nearby samples hold at greater distances. This first chapter summarizes the conclusions drawn from the previous areal and spatial surveys of galaxies, with emphasis on the phenomenon (or perhaps phenomena) that we call superclustering; that is, clustering of galaxy clusters. The second chapter of this thesis describes the areal search for and discovery of a candidate supercluster suitable for study. The third and fourth chapters discuss respectively spectroscopic and photometric surveys of this supercluster. The fifth chapter finally brings together the conclusions of the work in this thesis, and compares them with the conclusions of other investigators. As we shall see, a coherent picture emerges of the distribution of galaxies in space.

II. Early Studies of the Distribution of Galaxies

The first one and a half centuries of the study of the distribution of the "nebulae" were necessarily devoted to (because the study was confined by) the brightest ($m_{pg} \lesssim 14$) galaxies. These are now known to be, for the most part, members of the Local Supercluster. De Vaucouleurs (1981) gives an excellent review of the discovery and properties of the Local Supercluster. The interested reader is directed to that article for an introduction to this nearest and most easily studied of the known superclusters, though a brief review of its structural properties is also given in Section VI below.

In general, the census of fainter galaxies discovered visually was too incomplete to allow more than glimpses of structure in their distribution. The early investigators, too, were hampered by lack of proof that the majority of the nebulae were indeed "island universes" separate from our own Milky Way system. This was the theory adopted by most astronomers working on the problem (e.g. W. Herschel 1784, J. Herschel 1847; von Humboldt 1866, Proctor 1869, Abbe 1867, Waters 1873, 1894), but modern notions of the distances involved did not fully develop until the second and third decades of the present century.

However, structure beyond William Herschel's great "stratum" of nebulae was occasionally noted in the 19th century. Several streams of nebulae and clusters stretching across the sky are easily visible on maps of John Herschel's so-called "General Catalogue" (GC; J. Herschel 1864), and were commented on immediately (von Humboldt 1866, Proctor 1869). John Herschel (1847) himself noted a stream of nebulae extending northward from the Large Magellanic Cloud to Pisces, and Waters (1873, 1894) also mentioned several clusters and streams of nebulae in the GC and in its revision, the New General Catalogue (NGC; Dreyer 1888). Stratonoff (1900) and Hinks (1911) used the NGC objects for further studies of the nebular distribution, reaching the same general conclusions as the earlier investigators.

Though photographic studies of the clustering of nebulae began at Harvard in the 1890's (e.g. Pickering 1899), it was not until the 1920's that Shapley and his collaborators began to consider the large-scale distribution as revealed by the Harvard plates. In the meantime, Hardcastle (1914) and Reynolds (1921a, b)

had used the Franklin-Adams plates for studies of the distribution of the nearer galaxies, and Fath (1914) used the Mt Wilson 60-inch reflector for a photographic study of the nebulae in Kapteyn's Selected Areas. With respect to the distribution problem, Fath only noted that a) "the clustering [around the northern galactic pole] is much more marked than around the southern" and b) that "the number of nebulae in a region does not depend wholly on the galactic latitude." Sanford (1917) and Seares (1925) discussed Fath's data in more depth concluding that large-scale aspects of the galaxy distribution are real, while the smaller scale details may be the result of galactic absorption. Lundmark (1927) working from plates taken with the Bruce 16-inch telescope at Heidelberg reached essentially identical conclusions. It is interesting to note that the Local Supercluster did not escape the attention of any of these astronomers, and some devoted much of their work to it (e.g. Reynolds 1921a, b, 1923, 1924, 1934).

III. Beginning of the Modern Era in Galaxy Distribution Studies

A. Harlow Shapley and the Harvard Surveys

Not surprisingly, the first great photographic studies of the distribution of nebulae came in the 1920's at the same time as the confirmation of the extragalactic nature of most of these nebulae was announced. Hubble (1925, 1926) was of course responsible for the latter work using the largest telescope in the world at that time (the Mt. Wilson 100-inch Hooker Reflector), but the work done by Shapley and his collaborators depended entirely on the much smaller wide-field telescopic cameras at Agassiz, Arequipa, and

Bloemfontein. The 30-year series of papers that resulted from that work is summarised in Shapley's 1957 book The Inner Matagalaxy.

Among the more important of Shapley's conclusions is the general smoothness of galactic absorption (see e.g. Shapley 1940, 1951, Shapley and Ames 1929, Shapley and Jones 1938a, 1940). Though patchy in places near the galactic plane (as shown by Shapley's discovery of several "windows" in the absorbing layer along our line of sight toward the galactic plane), the numbers of galaxies in any field can be taken as a general indication of the amount of absorption. This large-scale feature of our own Galaxy was used to good advantage by Shapley in many of his galactic studies.

At the same time, Shapley's explorations into further regions of space showed again and again the same features revealed by the earlier distribution studies: a strong tendency toward clustering of galaxies, and an equally apparent tendency for the clusters themselves to be found embedded in extensive clouds of galaxies. This particular aspect of the Harvard work was quantified by Bok (1931, 1934) who found that no sample of galaxy counts, to whatever magnitude limit, was distributed randomly as compared with predictions from the binomial, normal, and Poisson distributions. This applied to the Shapley-Ames (1932) catalogue of bright galaxies, to the other Harvard counts to fainter limits then available, and to Hubble's (1934) counts. However, when Bok counted faint stars in the same fields as the galaxies, he found that their distribution could be accurately characterized as random. Thus, he discarded the notion that the non-randomness of the galaxy counts was caused by galactic absorption — this would have affected

the faint (therefore distant) stars just as it would have the galaxies.

Therefore, at higher galactic latitudes ($|b| \gtrsim 30^\circ$), the apparent clustering of galaxies, indeed all features of the galaxy distribution, were attributed by Shapley and the rest of his Harvard group (e.g. Warwick 1950) to the actual distribution of galaxies in space.

This is especially noteworthy in Shapley's discovery of large-scale gradients in the galaxy counts across the sky (Shapley 1934a, 1938a, b, 1940). These gradients implied clustering on scales of hundreds of megaparsecs, and led Shapley to his notions of the existence of metagalactic clouds (Shapley 1933, 1934b, c, 1935a, b, c, 1937a, b, c). Our own galaxy (Shapley 1929), the Coma Cluster (Shapley 1934b), the Perseus Cluster (Shapley and Jones 1938b), the Virgo Cluster (Shapley and Ames 1930a, b, Shapley and Paraskevopoulos 1940), the Hercules Cluster (Shapley 1933, 1934c), and many other galaxies, groups and clusters were all noted as belonging to one or another of these metagalactic clouds. Well-studied examples of these extensive clouds are those in Horologium (Shapley 1933, 1935a, b, 1938b) and Dorado (Shapley 1934b, 1937a, b, c, 1938b).

Shapley's ideas were solidly based in the observations, so have not become dated — even in retrospect, his view of the structure of the universe is surprisingly modern. He also made other important pioneering contributions. These will be considered below as appropriate.

B. Other Studies of Galaxy Distribution, 1930-1950

Though Shapley and his Harvard collaborators dominated galaxy distribution studies in the 1930's and 1940's, other investigators were also active during this time. Zwicky (1938, 1942a, b) began his studies with the Palomar 18-inch Schmidt, finding — as did Shapley — that the galaxies were distributed non-randomly. He continued his work (e.g. Zwicky 1951, 1952, 1953) when the Palomar 48-inch Schmidt came into operation in 1949, and he summarized his ideas in his book Morphological Astronomy (Zwicky 1957a). He stressed the existence of clusters of galaxies as well as the existence of clouds of galaxies and clouds of clusters. These are identical to Shapley's metagalactic clouds, but Zwicky (see also Zwicky and Rudnicki 1963) considered them as individual "cluster cells" of about 40 Mpc diameter. Each of these cluster cells contains the equivalent of one large cluster, though some may be made up of several smaller clusters. The centers of the cells are distributed randomly throughout space, though the galaxies within each cell are primarily found in groups and clusters. Zwicky also stressed the probable influence of galactic and intergalactic absorption on the distribution of galaxies and clusters (Zwicky 1952, 1957a, Zwicky and Rudnicki 1966). Zwicky's influence on current thinking has been strong, and his ideas mentioned above will return later, though in slightly altered form.

Lundmark's (1927) study of galaxies on the Heidelberg plates has already been mentioned. This same plate material was also used by other northern European astronomers in studies of galaxy distribution. Their conclusions are similar to those

already presented: a) the bright galaxies are primarily found in a flattened metagalactic cloud with our own galaxy toward one edge of this system (Holmberg 1937, Reiz 1941); b) though galaxies are concentrated near the galactic poles, there is only a rough correlation of their numbers with galactic latitude (for $|b| \gtrsim 30^\circ$), c) there are many clusters of galaxies (Wirtz 1923); and d) streams of galaxies and clusters, e.g. the Perseus-Pegasus stream, are readily apparent (Bernheimer 1932a, b).

Other contemporary studies giving added weight to the conclusions reached above are those by Tombaugh (1937), Mowbray (1938), and Katz and Mulders (1942). Tombaugh's work at Lowell Observatory on the "great Perseus-Andromeda stratum of extra-galactic nebulae" was one of the first in which the differentiation of galaxy types in clusters was mentioned: early-type galaxies are generally found in the central regions of clusters, later-type galaxies in the outskirts. Tombaugh also supported Shapley's observation that clusters of galaxies usually occur "in extensive regions rich or moderately rich" in galaxies.

Mowbray (1938) repeated Bok's (1934) tests on Hubble's (1934, 1936b) counts, and extended them to the counts given by Mayall (1934) and by Shapley (1937b). Again, Mowbray found that all the samples were distributed non-randomly across the sky. Katz and Mulders (1942) worked only with the Shapley-Ames (1932) sample of bright galaxies, applying Zwicky's (1942a) dispersion-subdivision test to the data. The Local Supercluster, of course, dominates the Shapley-Ames catalogue — Katz and Mulders found that the probability of the great belt of galaxies arising at random is 4.2×10^{-8} . Thus, the Local Supercluster — and all other clusters,

clouds, strata, and streams so far observed — is not likely to be due to chance.

Two other important papers on galaxy distribution have so far been mentioned only in passing. These are by Hubble (1934) and by Mayall (1934), both of whom found, contrary to all other evidence, that the areal large-scale distribution of galaxies is essentially random. Both also found that the numbers of nebulae per unit area increased as the square root of the distance, indicating that galaxies are also distributed randomly in depth. In spite of noting that Seares and Reynolds had called attention to William Herschel's band of nebulae across the northern galactic hemisphere, Hubble went on to state, "There are as yet no indications of a super-system of nebulae analogous to the system of stars."

Recall that the quantitative tests performed by Bok (1934) and by Mowbray (1938) showed that Hubble's galaxy counts indicated a non-uniform distribution, and that Mowbray also showed the same for Mayall's counts. This seeming contradiction with Hubble's and Mayall's own results is simply due to their not having performed adequate tests on their own data.

Hubble (1936a) went on to incorporate his ideas in his book The Realm of the Nebulae, and the randomness, homogeneity, and isotropy of the universe became dogma in spite of the incontestable observational facts to the contrary.

One other paper by Hubble (1936b) appeared that discussed the spatial distribution of galaxies, this time also considering their redshifts. Hubble's suggestion from this study was that

the galaxian redshifts are not Doppler shifts, an idea already mentioned by him in a 1935 paper with Tolman.

C. The Lick Survey

The studies thus far mentioned were based on either "test" probes in depth of small sky areas (Fath 1914, Hubble 1934, Mayall 1934) or on areal surveys of large portions, but not all, of the sky (the Harvard surveys eventually covered about one-third of the sky). It would obviously be desirable to have an areally complete galaxy survey of as much of the sky as possible in as homogeneous a fashion as possible. This was the reasoning behind the inception in the 1940's of the galaxy counts on 20-inch astrograph plates taken at Lick Observatory.

Though the $6^\circ \times 6^\circ$ plates were originally taken for the Lick proper motion survey, Mayall and Shane realized that they were also ideal for the galaxy survey. The 20-year effort that followed is summarized by Shane and Wirtanen (1967) who also give the counts (by square degree, though the plates were originally counted in ten minute squares), and display them in the form of isopleths reduced to numbers of galaxies per square degree. The survey covers the sky from the north celestial pole to -20° , and has a limiting magnitude of $B = 18.9 \pm 0.5$ (Kron and Shane 1974).

This survey has been particularly useful in statistical studies of the distribution of galaxies. During the 1950's, Neyman and Scott (1959 and references therein) developed a theory of galaxy distribution that was directly inspired by the Lick counts. The predictions of this theory, which placed all galaxies in clusters, ignored interstellar or intergalactic absorption, and

distributed the positions of the clusters randomly in space, was compared by Scott et al (1954) with the actual distribution of galaxies on one of the Lick plates. The results were startling: the actual galaxy distribution was even more clustered than the theoretical distribution. Neyman et al (1956), after modifying the basic theory to take redshift and galactic absorption into account, attributed the discrepancy between the theory and the observation to superclustering.

Other similar work done at the time included that by Agekian (1957), Layzer (1956, 1975), Limber (1953, 1954, 1957), Rubin (1954), and van Albada (1960, 1962). (Chandrasekhar and Münch 1952 developed a method for detecting discrete absorbing clouds in our own galaxy by studying the fluctuations in galaxy counts. Apparently never applied, this approach would be unlikely to succeed in any case because of the manifestly non-random distribution of the galaxies.) Most of these studies reached the same conclusion: clustering, on scales of less than about 5-10 Mpc, is the major characteristic of the galaxy distribution. Neyman et al (1956) and van Albada (1960) also suggest statistical evidence for clustering on larger scales.

[Note should be made here that distances in this thesis are on the extragalactic distance scale defined by de Vaucouleurs (de Vaucouleurs and Bollinger 1979 and references therein).

$H_0 = 100 \text{ km sec}^{-1} \text{ Mpc}^{-1}$ on this scale and is assumed to hold true for all extragalactic distances beyond the Local Supercluster.]

Shane and Wirtanen (1954) and Shane (1956) had earlier noted from preliminary reductions of their galaxy counts that superclustering and clumping of galaxies and clusters into

"multiple clusters" was a common feature in the Lick work. Shane and Wirtanen (1967) and Shane (1975) reiterated their earlier conclusions, and also noted possible evidence for inhomogeneities on the order of 200 Mpc across. De Vaucouleurs (1971) in an excellent review also mentioned this, and noted that the Hubble counts, when smoothed, also showed very large scale fluctuations of the same order of size.

The Lick counts by Shane and Wirtanen thus provided a major impetus for attempting to understand the nature of the clumpy distribution of galaxies in space. During the past dozen years, they also provided material for the first serious attempts at understanding the origin of the non-random galaxy distribution. Several other observational efforts contributed to these attempts; they are reviewed in the following section.

IV. Modern Surveys Pertaining to the Galaxy Distribution Problem

Though Shane and Wirtanen (1967) published only the counts added together in one degree squares, the original ten minute counts were made available to the Princeton group led by Peebles. These were reduced anew by Seldner et al (1977) and presented in a form that more graphically than any other demonstrates the nature of the galaxy distribution. Using a gray scale to represent the number of galaxies in each ten minute square, the resulting matrix was displayed photographically in polar coordinates. It resembles nothing so much as it does a cross-section of a sponge, filamentary and cellular.

This sponge-like structure so easily seen in these nearest

10^6 galaxies (most are within 300 Mpc if $M_{pg} \approx -18$ is the peak of the gaussian luminosity function of "normal" galaxies counted in such surveys; Brown 1978) is repeated for the even nearer 3×10^4 galaxies in the catalogue by Zwicky and his associates (CGCG; Zwicky et al 1961, 1963, 1965, 1966, 1968a, b). Peterson (1974) and Fall (1979) have maps of these galaxies which are brighter than $m_{pg} \approx 15.5$ and generally within 100 Mpc.

The same sort of structure is visible in the distribution of rich clusters of galaxies, catalogued by Abell (1958) and by Zwicky in the CGCG. Similarly, the nearby groups, clouds, and poor clusters listed by de Vaucouleurs (1975a), Corwin (1967), Karachentsev (1970), and Turner and Gott (1976) are roughly arrayed in chains and filaments, the very nearest generally following and aligned with the plane of the Local Supercluster (de Vaucouleurs 1975a, b, c).

Finally, the most distant sample yet analysed for distribution, that in the so-called "Jagellonian Field" (named after the Polish university where the work was done by Rudnicki et al 1973) shows an identical structure. This sample of 15650 galaxies in a 36 square degree field photographed with the Palomar Schmidt Telescope reaches to $m_{pg} \approx 21.0$ and represents the universe at a distance of about 1000 Mpc. This probably also represents the extreme limit of the Abell and Zwicky cluster catalogues, but with nominal limits of 600 to 700 Mpc, they do not on average penetrate as deeply into space. However, their coverage of the entire northern sky (in the case of Abell's catalogue, the coverage is to $\delta = -27^\circ$, nearly 3/4 of the sky) gives them an advantage when very large scale structures are being studied.

Other galaxy counts to varying limits are those by Nilson (UGC; 1973), Vorontsov-Velyaminov et al (MCG; 1962, 1963, 1964, 1968, 1974), and Zonn (1968). (Catalogues and surveys specifically relating to the southern sky will be covered in the next chapter.) These too are limited to the northern sky (Nilson) or to the southern limit of the Palomar Schmidt (Zonn and MCG), and are all based on the Palomar Schmidt Survey (PSS). Since they are essentially duplications of other efforts, they have not received in themselves much attention in distribution studies, except where their additional data could help (see e.g. Davis and Geller 1976 and MacGillivray et al 1981a).

Finally, galaxy surveys with the COSMOS machine at ROE are currently being made for selected parts of the sky. While the long range goal of a complete coverage of the sky to $m_{pg} \approx 21-22$ is far from being met, several studies already published have indicated the feasibility of such a project (see e.g. MacGillivray and Dodd 1979a, b, 1980a, b, MacGillivray et al 1976, Hewett et al 1981, Shanks et al 1980, Phillipps et al 1978; and references therein).

V. Statistical Investigations of the Modern Catalogues

Since accurate distances are generally lacking for most of the galaxies and clusters in the above catalogues, various statistical tests have been used to search for non-randomness in the areal distribution of the objects. These tests fall into several different general groups, as follows:

1) The n-point correlation functions, especially the two-point correlation (or covariance) function and its Fourier

transform the power spectrum. Though first used for studying the clustering of galaxies by Totsuji and Kihara (1969), the n-point correlation functions have been developed and used most extensively by Peebles (1980 and references therein) and his Princeton group. Fall (1979) also has a thorough review of the methods involved, their shortcomings, and the general results.

2) Zwicky's (1942a, 1952) dispersion-subdivision test, applied by Zwicky (1957b), Zwicky and Rudnicki (1966), and by Karpowicz (1967a, b, 1970a, b, 1971c) to the CGCG cluster data; and by Hewett et al (1981) to one of the COSMOS galaxy samples.

3) The index of clumpiness test (Neyman and Scott 1952) applied by them to the Lick counts as noted above (see also Neyman and Scott 1959 and references therein). This test has also been used by Kiang (1967) to study superclustering of the Abell (1958) clusters, and by Kalinkov (1974) to search for higher order clustering among the Abell and CGCG clusters.

4) Nearest neighbour tests have been applied by Bogart and Wagoner (1973), by Rood (1976, 1979), and most recently by Thuan (1980) to the Abell cluster data; and by Kalinkov (1974) to the CGCG cluster data. These tests are the only ones to require distance estimates. Thus, while their present applicability is limited, they have perhaps the greatest potential of any of the statistical tests for giving easily interpreted results.

5) Abell (1958), Fullerton and Hoover (1972), and Kalinkov (1974) have applied χ -squared tests to the Abell cluster data.

Abell and Seligman (1965, 1967), Gusak (1969), and Kalinkov (1974) have also applied these tests to the CGCG data.

6) Smoothing and filtering of the CGCG cluster data has been done by Kalinkov and his colleagues (see Kalinkov 1977 for references).

7) Zieba's (1975) "method of statistical reduction" has been used by Zeiba and Zeiba (1975) and by Flin (1974 and references therein) to examine various catalogues of extragalactic objects.

8) Mead's analysis (Mead 1974; Shanks 1979 and references therein) was applied by Shanks (1979) to the Zwicky galaxies and to the Jagellonian catalogue; and by Hewett et al (1981) as well as by Shanks to COSMOS samples from UK Schmidt plates.

9) The area of the largest CGCG clusters was studied by Zwicky and his collaborators (Zwicky and Rudnicki 1963, Zwicky and Berger 1964, Zwicky and Karpowicz 1965, 1966, and Karpowicz 1971a, b). Though not a statistical test in the same sense as the others noted above, these studies have still provided the characteristic dimensions of typical (as well as the largest) CGCG clusters (8 and 25 Mpc, respectively).

Most of these tests (other than the last one, as just noted) are conceptually similar. Angular (or spatial) distances are measured from a given object to its nearest neighbour, to its next nearest neighbour, and so on; or the numbers of objects within cells of a given size are counted and compared with counts in different sized cells. Unfortunately, since these tests generally

take no account of possible systematic errors in the data, the results can be misleading. This has been stressed by Paal (1964), Reaves (1968, 1974), Reaves and Stern (1967), Kiang (1967), Fullerton and Hoover (1972), Ozernoy and Reinhardt (1976), Soneira and Peebles (1977), and Kalinkov (1977) all of whom have pointed to possible sources of error in the basic data. These are usually simple selection effects that might be functions of galactic absorption, distance, richness, etc. Often these can be corrected to some extent (see e.g. Corwin 1974, Seldner et al 1977), but usually are not. Taken to its logical extreme (by e.g. Fesenko 1979a,b) the presence of selection effects has even been used to argue against the very existence of rich clusters of galaxies.

More fundamental problems exist in the interpretation of the tests, however. Nearly all of them have been used to show non-randomness in the distribution of extra-galactic objects. (Indeed, the current general acceptance of superclustering is due in large part to the widespread application of these tests, especially the covariance function, over the past dozen years.) But few have suggested that the indicated non-randomness is due to anything but clumping of the galaxies or clusters. Holmberg (1974) attributes the apparent distribution to patchy galactic absorption, while Zwicky and his colleagues (references above) have cited intergalactic absorption as the cause (it will be seen in Chapter 2 that there is as yet little hard evidence for patchy absorption dense enough to cause the non-randomness).

Even more basic yet is the problem encountered in the present work of trying to a) isolate a supercluster for detailed

study or b) determine structural parameters for superclusters. Only the nearest neighbour tests as applied by Rood (1976) and Thuan (1980) are capable of providing the detailed answers to these questions. The other tests may indicate the existence of superclustering, but generally provide no more than a characteristic scale length for the clustering [see especially Abell (1958), Abell and Seligman (1965), Kiang (1967), de Vaucouleurs (1971), Kalinkov (1977 and references therein), and Hewett et al (1980)]. Or they may indicate no specific scale length at all [e.g. the n-point correlation functions, but see Wesson (1976), and Zieba's (1975) "method of statistical reduction"]. These results generally come from studies where the tests essentially integrate data in depth, wiping out any large scale features that might be present (Fall 1979). Other problems with the tests themselves have been discussed by e.g. Peebles (1980), Shanks (1979), and Hewett (1980, unpublished). These problems (e.g. "edge corrections" in covariance function analyses) can have very considerable effects on the results (Hewett 1980, unpublished).

VI. Observational Studies of the Spatial Distribution of Galaxies and Clusters: Individual Superclusters

A. Introduction and Definitions

The lack of firm answers from most of the statistical tests outlined in the previous section has been part of the motivation behind the recent observational studies of several superclusters. This lack was also instrumental in initiating the present study.

How, though, are superclusters defined? De Vaucouleurs (1971) calls the "classical" supercluster one which has a major diameter of 30 to 50 Mpc, an axis ratio of 1/4, a velocity dispersion on the order of 1000 km sec^{-1} , and (in the examples he cites) containing only a few rich clusters but many groups, clouds, and individual galaxies. Abell (1961, 1974, 1975) defines superclusters primarily in terms of the rich clusters in his catalogue (Abell 1958), but finds the same characteristic diameter as did de Vaucouleurs. An Abell supercluster contains an average of 10 rich clusters, it may be elongated, and has a velocity dispersion of 2000 to 3000 km sec^{-1} . Its mass is in the range 10^{15} to $10^{17} m_{\odot}$, and contains many more groups and poor clusters (perhaps 10 times as many) as rich clusters. Abell (1961) gives a list of 17 superclusters drawn from his 1958 cluster catalogue.

Rood (1976) and Thuan (1980) also define superclusters in terms of Abell clusters: from a sample of nearby Abell clusters with known velocities, spatial separations of neighbouring clusters are computed. Neighbouring clusters within 25 Mpc (Rood) or 35 Mpc (Thuan) of a given cluster are identified, all clusters within the same distances from the neighbouring clusters are identified and so on until no more clusters can be added. The resulting group of clusters constitutes a supercluster. The superclusters so formed tend to be linear or sheet-like in space with typical diameters of about 30 Mpc. About 60% of the superclusters are simply binary clusters, with another 25% to 30% being triplets or quadruplets. These superclusters, then, are "classical" superclusters as defined by de Vaucouleurs, except that groups, clouds and "field" galaxies

must necessarily be ignored.

A different definition is adopted by Einasto et al (1980a,b and references therein). From redshift surveys, they find that space is separated into supercluster "cells" roughly 40-50 Mpc across. In projection, the cell "walls" form filamentary bridges connecting rich clusters which are at the intersections. A single supercluster, then, is a nearly empty "hole" with its surrounding filaments and sheets of galaxies, and with the embedded rich clusters and poorer clouds and groups. Adjoining superclusters in this model share elements in common. The "classical" supercluster, then, is just one filament or sheet of clusters, groups, and galaxies in the cellular (annular in projection) supercluster.

Most of the studies cited below concern themselves with "classical" superclusters, that is, parts of Einasto's and his colleague's cellular superclusters. A more restrictive definition used by Jones (1976) and by Hoffmann et al (1980) for the Local Supercluster will be considered below.

Finally, Zwicky (1957a) has suggested that a "supercluster" might be defined as a vast, spherically symmetric gravitationally bound collection of hundreds or thousands of clusters of galaxies. The simple fact that such "superclusters" obviously do not exist led Zwicky and his collaborators to deny repeatedly the existence of clusters of clusters (see e.g. Zwicky and Rudnicki 1966 and Karpowicz 1971b and references therein). Zwicky's concept of the large scale distribution of galaxies involved their being grouped into cluster cells perhaps 40 Mpc across with each cell containing the equivalent mass and luminosity of one rich cluster. Within

each cell, there might be several smaller clusters, groups, and clouds of galaxies, and even clouds of clusters (Zwicky 1957a). This is very close to how the "classical" supercluster has been visualized by most astronomers (e.g. de Vaucouleurs, Rood, and Thuan as noted above). Zwicky's insistence on the non-existence of superclusters is thus seen to be mostly a matter of definition.

B. The Local Supercluster

Though known as a belt of galaxies about 10 degrees wide across the northern sky since its discovery in 1783-4 by William Herschel (1784), it was only gradually that the Local Supercluster was recognized to be a supercluster in the "classical" sense as noted above. It was not until 1953 that de Vaucouleurs gave a modern description of it, calling it the "Local Supergalaxy" and noting its proximity in space to a "southern supergalaxy," seen stretching from behind the Large Magellanic Cloud north to Eridanus.

De Vaucouleurs has remained the most active astronomer in the study of the Local Supercluster. His latest reviews (de Vaucouleurs 1978, 1981) cover our current state of knowledge of it well. Its structural characteristics as set out by de Vaucouleurs (1978, 1981) are briefly summarized here.

The Local Supercluster is a flattened system with an apparent axial ratio of about 3 or 4 to 1. It includes one rich cluster, the Virgo Cluster, at a distance of about 12 to 15 Mpc from our own Local Group. The many other groups and clouds of galaxies in the Supercluster are arrayed in filaments or chains within its plane, and extend perhaps 20 Mpc in various directions from the

Virgo Cluster. A small number of "field" galaxies, probably no more than 10% of its total number of galaxies, are found between the various groupings of the Local Supercluster.

There may be gas and dust associated with the Supercluster, but the evidence is marginal and contradictory. Many of its galaxies are radio sources, and a few are X-ray sources. Aside from the Virgo Cluster, however, there are no X-ray sources associated with clusterings in the Local Supercluster. Even the Virgo Cluster X-ray emission is dominated by one peculiar object, M87. In general, it can probably be said that the Local Supercluster is a rather small one, and perhaps atypical in some ways because of its size. However, exploration of its further reaches in the northern sky is far from complete, so conclusions as to its total size (~ 40 Mpc) and mass ($\sim 10^{15}$ to $10^{16} m_{\odot}$) may be premature.

Since the Local Group and the Galaxy are a part of the Local Supercluster, redshifts of other galaxies as we view them will be somewhat affected by any motion of our own Galaxy within the Supercluster (an analogous situation to the solar motion within the Galaxy apparently perturbing the motions of the nearby stars). De Vaucouleurs first found evidence of this motion in 1958 using the Humason, Mayall and Sandage (HMS; 1956) list of redshifts from Lick and Mt. Wilson. These data were fit reasonably well with a flat rotating-expanding model of the Supercluster. This sort of model (with minor adjustments, e.g. allowing for galaxy motions perpendicular to the supergalactic plane) continues to model well the ever-accumulating totality of the redshift and distance data for the nearby galaxies (de Vaucouleurs 1981 and references therein).

Nevertheless, it is felt by many that the motion of the Local Group is primordial rather than rotational (e.g. Mould et al 1980). In other words, the local motion is a reflection not of present supercluster dynamics or even of recent evolution, but of conditions at the time of its creation. Some weight is given to this point of view by studies of alignments of galaxies with respect to the plane of the Local Supercluster. The most recent, based on the largest amount of data, is that by MacGillivray et al (1981a,b) who find that the spin axes of a significant number of galaxies are perpendicularly aligned with the Supergalactic equator. Because of the problems involved in changing the directions of the spin axes, such correlations are usually taken as primeval. De Vaucouleurs (1975c) has also found alignments of the major axes of galaxy clouds with the Supergalactic equator. This puts even firmer constraints on any structural evolution as the crossing times for galaxy clouds are generally about one Hubble time or longer. (see e.g. Turner and Sargent 1974, Rood et al 1970).

Thus, the Local Supercluster (and, by extension, other superclusters) is probably an only slowly evolving relic of inhomogeneities in the early universe.

Jones (1976) and Hoffmann et al (1980) have taken a somewhat different view of the Local Supercluster. Assuming it to be a spherically symmetric body of galaxies centred on the Virgo Cluster (they refer to it as the "Virgo Supercluster"), they then find that the properties of this body resemble those of a rich cluster. The space density of galaxies falls off roughly as r^{-3} (Jones) and their velocity dispersion drops with increasing radius

(Hoffmann et al). The techniques used in these two studies are in fact very well suited to rich clusters, but the assumption of spherical symmetry makes the application to a supercluster considerably less likely to yield meaningful results.

C. Other Superclusters

Though several external superclusters were noted in the Harvard survey of the 1930's (Shapley 1957 and references therein), structural parameters could not be estimated with any certainty because of a lack of firm distances. Though Shapley (1933) did estimate distances for several clusters now known to be in superclusters (i.e. Hercules and Horologium), he gave no specific data for the superclusters themselves.

The same was true for the many other studies of superclusters from that time until the mid-1970's when redshifts for a significant number of clusters started to become available (e.g. Noonan 1973, Corwin 1974). Working without redshifts, however, it was at least possible to isolate many superclusters purely on the basis of examining the galaxy distribution on the sky (e.g. Bernheimer 1932a,b; Tombaugh 1937, Zwicky 1942b, Shane 1975 and references therein; de Vaucouleurs 1956a, Kalinkov 1967, Herzog 1967, Reaves 1968, 1974) or by using the rough distance estimates given in the Abell and Zwicky cluster catalogues (Abell 1961, 1962, van den Bergh 1961, Karachentsev 1966, Gusak 1969, Rood and Sastry 1971, Fullerton and Hoover 1972, Kalinkov 1974, Murray et al 1978).

Working with distances found from luminosity and diameter functions, Corwin (1967) isolated several superclusters and

determined diameters for them. Rood (1974, 1976) and Nottale (1976) using distances from known redshifts did the same, extending the studies into the realm of dynamics. Karachentsev and Shcherbanovskii (1978) drew up a list of pairs and triplets of Abell clusters, derived mean separations for them, and hinted at possible dynamical interactions from the few redshifts available.

All of these studies give a generally consistent view of superclustering: clusters form elongated associations (with "field" galaxies scattered between them in some cases) with sizes ranging from ~ 30 Mpc to ~ 70 Mpc. Axial ratios vary from about 2 to 1 to about 8 to 1 in the extreme case of the Perseus-Pegasus Stream. The superclusters are expanding with the general Hubble flow, though clusters with spatial separations of less than about 5-10 Mpc give some signs of gravitational interaction. There are also indications that all groups, clouds, and clusters - perhaps even all galaxies (Corwin 1967) - are members of one supercluster or another, though the evidence for this is mostly statistical. Finally, there is also evidence from many sources (e.g. Shapley 1938a, de Vaucouleurs 1971, Kalinkov 1977 and references therein, van den Bergh 1961, Dodd et al 1975, Kiang and Saslaw 1969, Hauser and Peebles 1973, Shane and Wirtanen 1967, Chincarini and Rood 1979) that very large scale inhomogeneities of the size expected of third-order clusters (i.e. several hundred megaparsecs) exist. Beyond this, the data run out, but the clues are tantalizing: perhaps our universe is a vast if irregular hierarchy of matter (e.g. de Vaucouleurs 1970). Only more data can give us a definite answer.

[At this point, it is worth mentioning that the largest scale inhomogeneities detected in the optical data are not confirmed in many studies in other wavelengths. See e.g. Golden (1974) and Webster (1976a,b) for statistical studies showing the randomness of the extragalactic radio source distribution, and Weiss (1980) for evidence that the microwave background radiation is smooth to better than one part in a thousand. However, a few puzzles remain even here. For example, Bell (1969), Karoji (1975), Burbidge (1977) and Bolton and Savage (1978) report inhomogeneities in the number of QSO's over the sky and in redshift space, and Sofue et al (1968) suggest that measures of Faraday rotation in distant radio sources are correlated by a "metagalactic" magnetic field of $\sim 10^{-9}$ gauss intensity. All of these studies imply inhomogeneities of hundreds of megaparsecs extent - but the data are scanty, so not too much should be made from them.]

D. Studies of Individual Superclusters

In this section, we shall concentrate on the structural features of known superclusters. Though it is possible to go beyond structural studies with the data at hand [to determine e.g. the deceleration parameter (Jones 1976) or the ratio of "present" density to critical density (Ford et al 1981)], the structure of superclusters and the distribution of matter and luminosity within them are our main concerns here.

1) The Coma Supercluster

The first radial velocity observations suggesting that the

Coma Cluster might be a part of a larger supercluster came in the 1950's from Lick, Mt. Palomar and Mt. Wilson (HMS, Zwicky 1957a). However, it was not until Chincarini and Rood (1976a) had collected 50 redshifts from a magnitude limited sample to the west of the Coma Cluster itself that it became clear just how great the extent of the Coma Supercluster might be. Chincarini and Rood traced it to about 15 Mpc from the centre of the Coma Cluster, while Gregory and Thompson (1978) showed that a "bridge" of galaxies extended all the way to another rich cluster, A1367, at a projected distance of about 20 Mpc. The redshifts of both clusters and of galaxies along the "bridge" are nearly identical, so that an association was assumed. Surprisingly, the velocity dispersion of the galaxies in the "bridge" is small compared to that within the clusters. It thus seems that redshifts may be used to fairly accurately map the structure of superclusters when other distance indicators are lacking (see Chapter 3, Section I for more evidence of this).

Others to suggest that Coma was a part of a supercluster were Shapley (1934b) and Tifft and Gregory (1976). Other galaxies and groups in the same redshift range have been found a considerable distance from the cluster by Zwicky (1957a), Eastmond (1976), Chincarini and Rood (1979) and by Corwin and Emerson (1981; Appendix A of this thesis). The most complete study to date is that by Tago (Einasto 1980, private communication); this will be discussed further in Section VII below.

2) The Pegasus and Hydra-Centaurus Superclusters

Chincarini and Rood (1976b, 1979) have called attention to other superclusters in Pegasus and in the Hydra-Centaurus region. Little is yet known of these superclusters aside from their association with well-known rich clusters. The Pegasus Supercluster contains the Pegasus II Cluster while Hydra-Centaurus contains the two clusters bearing those names (the clusters are connected by a bridge of galaxies as are Coma and A1367. Smyth 1980 has a thorough discussion of the Hydra Cluster - also called A1060 - and Dawe et al 1977 discuss the Centaurus Cluster).

3) The Hercules Supercluster

Shapley first noted this supercluster in 1933 and it has been an area of intense study ever since (e.g. Shane and Wirtanen 1954, 1967; the Burbidges 1959; Abell 1961; Corwin 1967, 1971 and Chincarini and Martins 1975). Abell suggested that the Hercules Supercluster might extend some 20° northward to include the two rich clusters A2197 and A2199 at the same redshift, and the present writer notes two other Abell clusters (A2052, A2063) nearly the same distance to the southwest, again with similar redshifts. Thuan (1980) extends the grouping even further in the same direction, including six more Abell clusters. If this entire complex is associated, its length would be on the order of 100 Mpc. Another interpretation, set out in the next section, seems more likely, however.

The most thorough study of the Hercules Supercluster to date is that by Tarenghi et al (1979a,b). Their work is restricted

to an area within a few degrees of the three rich clusters A2147, 51, and 52, but they show that this complex region contains several groups and clusters as well as a "dispersed component" rather similar to the "bridge" in the Coma Supercluster. They note two foreground "layers" of galaxies, one first mentioned as a possible group by Corwin (1967), both specifically noted by Chincarini and Martins (1975). Lately, Giovanelli et al (1981) have extended the study to the 21-cm HI line properties of the galaxies, showing that spirals in the area of the diffuse X-ray source coincident with A2147 are HI deficient compared with those outside this area. They also quote Corwin and MacGillivray (unpublished) who have two-colour COSMOS photometry of most of these galaxies: the HI deficient sample is significantly redder, though the mean morphological types of the two samples are the same. The conclusion is that these HI-deficient galaxies have been swept of much of their gas and dust that otherwise would have formed more young blue stars that give these galaxies their characteristic colour.

4) The Perseus Supercluster

The famous Perseus-Pegasus Stream, first specifically noted by Waters (1896), has recently received considerable attention (Tifft et al 1975, Aaronson et al 1980, Gregory et al 1981). Gregory et al (1981) find that the Stream is as deep in redshift space as it is wide on the sky (about 4 Mpc), and that the position angles of member galaxies are preferentially aligned with the Stream. The supercluster that the Perseus-Pegasus Stream is a part of will be discussed further in Section VII.

5) The Horologium Supercluster

Dawe et al (1979) have published a preliminary discussion based on about 130 redshifts of galaxies in the area of the well-known Horologium Cloud (Pickering 1899, Shapley 1935a, de Vaucouleurs 1956b). As with Hercules, this is a rich and complicated region with many groups and clusters, but Dawe et al find that several of them appear to form a supercluster at about 170 Mpc distance. One of the clusters is a well-known X-ray source and has been studied by several other groups [e.g. Havlen and Quintana 1978, Quintana and Havlen 1979, Dodd et al (1979), Chincarini et al (1981)].

6) The Ursa Major Supercluster

An important radio and optical study by Schuch (1979, 1981) of the Ursa Major Supercluster shows it to be an association of Abell clusters and many smaller groups at a velocity of about 18,000 km sec⁻¹. It appears to have a projected diameter of about 50 Mpc, and seems to be expanding with the Hubble flow. The radio properties of the included galaxies and clusters are apparently normal, differing little if at all from other radio surveys not specifically including superclusters.

7) Other superclusters

Ford et al (1981) and Harms et al (1981) have studied two of the more distant superclusters listed by Abell (1961) and by Murray et al (1978) with the view of deriving the mean mass density of the universe (their results strongly favour an open universe).

At the same time, they suggest that "gravity has noticeably slowed the Hubble expansion of both superclusters."

Finally, Perrenod and Lesser (1980) have redshifts in one of the apparent superclusters identified by Murray et al (1978) from Abell's (1958) catalogue. In a small area only two by two degrees square are eight Abell clusters all at the same nominal distance in an elongated configuration suggestive of the several other superclusters known. In redshift space, however, the eight clusters break up into three distinct streams, each well-separated from the others in redshift, but completely intermixed in position on the sky. Furthermore, apparent cluster members can belong in actuality to different physical clusterings.

VII. Macrostructure in the Universe

One aspect of the study of superclusters stressed again and again is the existence of empty "holes" in the three dimensional distribution of galaxies. In redshift histograms or in "cone" diagrams (redshift plotted versus right ascension, declination, or some combination thereof), these holes appear as gaps. Good examples are given by Chincarini and Rood (1976a), Gregory and Thompson (1978), and Perrenod and Lesser (1980).

Though first explicitly noted by Chincarini and Martins (1975) and Chincarini and Rood (1976a), the phenomenon had been mentioned earlier (e.g. de Vaucouleurs 1971 and references therein; Peterson 1974). It was first fully exploited however as a method for determining the macrostructure of the nearer parts of the universe by Jöeveer et al (1978a,b). The Estonian group has continued

its work to the present (see Einasto et al 1980a for references), and the picture that is emerging from their studies is in some ways revolutionary.

Other work continuing and confirming the general results presented below is that by Tully and Fisher (1978), Kirshner et al (1978), Tarenghi et al (1979a,b), Chincarini (1978), Einasto et al (1980a,b), Chincarini and Rood (1979), Perrenod and Lesser (1980), Thuan (1980), Tago (Einasto 1980, private communication), Ellis et al (1980, private communication), and Davis et al (1981). Since the conclusions of all the studies cited above are qualitatively similar, a general description following Einasto et al (1980a) and Davis et al (1981) is set out here.

Space is dominated not by galaxies or clusters, but by holes nearly devoid of galaxies. Surrounding these holes are filamentary chains and thin sheets of galaxies, groups and clusters. The richest clusters occur where these sheets and chains intersect in space (the Perseus cluster, A426, and the Hercules Clusters, A2147, 51, and 52 are good examples). The chains of clusters and groups can be traced through space around an almost empty "hole" to form in projection an irregular annular or ringlike association of objects. At rich clusters, the sheets and filaments may branch into two or more chains which in turn can be traced around other "holes." The Estonian group thus defines a supercluster as a hole with its surrounding filaments, sheets of galaxies and clusters. Thus, neighbouring superclusters share the separating "walls" and filaments. The Perseus-Pegasus stream, for example, belongs to not only the Perseus Supercluster, but also to the neighbouring

Andromeda Supercluster. Thus, the macrostructure of the universe might adequately be visualised as sponge-like. Not only do the sheets and filaments intersect, but so do the voids and holes. This visualisation might also be extended in two ways to include the very large scale density variations seen by some as "third-order clusters" (references in Section VI-C above) - the galaxy/cluster density within the filaments might be higher in some regions of the universe or alternatively the voids might be smaller (or both). This, however, is speculation - very little data yet exist which would allow a choice between these alternatives, or among others not amenable to the sponge analogy.

VIII. Purpose and Overview of the Present Work

As mentioned above in the first section, the purpose of this thesis is primarily to examine a more distant region of space in some detail to see if the general structure outlined in the previous section holds true, or if there might be discernible changes in it.

However, this particular goal grew out of another: to provide structural parameters for a moderately distant supercluster that might be easily studied via UK Schmidt plates and the COSMOS machine. This original goal guided the initial phases of the project through 1976 and 1977 when the sponge-like macrostructure set out in the previous section was only being hinted at. With the appearance or more and more work on the macrostructure over the past four years, however, the writer's ideas and the goal of this thesis inevitably changed.

A part of the change came about directly through this study, however. The work can be best put in perspective by noting that Sections II through VI of this chapter, and much of Chapter 2 and 4, are roughly contemporaneous in that they deal with superclusters as discrete entities. The remainder of the thesis reflects the shift to a different viewpoint regarding "superclustering" as just one aspect of the large-scale sponge-like distribution of luminous matter in the universe.

CHAPTER 2

Southern Optical Sky Surveys and the
Discovery of the Indus SuperclusterI. Introduction: Historical Southern Sky Surveys

The first telescopic survey of the southern sky was carried out by Lacaille at the Cape of Good Hope from 1751 to 1753. His prime goals were navigational and astrometric, however, so that the list of 42 non-stellar objects that he published (Lacaille 1755, Glyn Jones 1975) is hardly complete for even naked eye nebulae and star clusters. Dunlop's (1828) list of 629 southern deep sky objects is marred by very poor positions so that even today less than a third of his nebulae and clusters have been identified with certainty.

Thus, the first survey of any continuing use is that which John Herschel carried out at Feldhausen near Cape Town during the years 1834 to 1838. The Results of this survey were published by him in 1847 in a single volume devoted principally to nebulae, star clusters, and double stars. For the nebulae that we today call galaxies, Herschel's work is essentially complete to about the 13th (photographic) magnitude. However, there are tens of brighter galaxies not seen by Herschel (primarily of low surface brightness), and hundreds of fainter objects — to about the 15th magnitude — that he did find. Herschel's work thus remains valuable as a basic finding list for studies of the distribution of nearby galaxies in the south, and for work on groups and clusters there, also.

Unfortunately, the Revised New General Catalogue (RNGC; Sulentic and Tifft 1973) was published before the major southern Schmidt surveys (Section II, below) were generally available. Thus, 112 of Herschel's objects in the RNGC have no modern data. Such was the quality of Herschel's work, though, that only one of these 112 objects has been since found to be spurious (Corwin, unpublished). Therefore, the RNGC remains a useful finding list for Herschel's southern objects.

Using the Franklin-Adams plates taken soon after the turn of the century, Reynolds (1921 a, b) published a list of positions, diameters, position angles, and short descriptions of the brighter southern "spirals." For the most part, these galaxies are included in Herschel's catalogue, though the additional data proved useful in Reynolds' distribution studies mentioned in Chapter 1. So, until the late 1970's, John Herschel's remained the only areally complete survey of southern galaxies that penetrated much beyond our local neighbourhood.

In the years between Herschel's time and the present, photographic surveys to fainter magnitudes than reached by the Franklin-Adams plates were begun at Arequipa, Peru by Harvard College Observatory astronomers under the general direction of E. C. Pickering. A summary of the first few years of this work with extensive lists of southern objects is given by Pickering (1908). Some 800 southern nebulae and star clusters, found mostly by Stewart and Frost, are thus included in Dreyer's Second Index Catalogue (1910).

Under Harlow Shapley's inspired leadership beginning in the early 1920's the southern Harvard surveys continued from Peru and

South Africa until about 1940. In all, about half the southern sky was explored to the 17th magnitude. Detailed results with lists of galaxies for a few areas were published (e.g. Shapley 1935a, Baker 1933, 1937), but it was not until 1957 that the entire effort was admirably summarized by Shapley in his book The Inner Milky Way.

An important part of this work was the justly famous survey of galaxies brighter than the 13th magnitude (Shapley and Ames 1932; recently updated by Sandage and Tammann 1981). Though essentially "complete" only to the 12th magnitude (again, some tens of brighter galaxies are missing), the "Shapley-Ames catalogue" is still used as a census of the nearest and/or brightest 1250 galaxies.

The portion of the Shapley-Ames catalogue south of -35° was almost completely resurveyed by de Vaucouleurs (1956a) from 1952 to 1955 with the 30-inch Reynolds Reflector at Mt. Stromlo near Canberra. The publication of this "Reynolds' Survey" marked another important step in southern extragalactic work: for the first time southern groups, clouds, and clusters of galaxies received more than just passing attention. By this time, de Vaucouleurs and a few other astronomers recognized clustering to be a dominant property of the distribution of galaxies — modern studies of the spatial arrangement of luminous matter in the universe had begun.

II. Southern Schmidt Surveys

A. Basic Photographic Material

In the 1950's, it was recognized that large Schmidt telescopes would have to be erected in the southern hemisphere to complete the sky survey work of the 48-inch Schmidt at Palomar Mountain. It was twenty years, however, before the southern Schmidts came into existence.

In the meantime, surveys with smaller wide-field telescopes in South America and Australia were providing plate material for limited extragalactic surveys. Among these surveys are those by Klemola (1969, groups and clusters), Snow (1970, groups and clusters), Aguero (1971, peculiar galaxies), Sersic (1974, peculiar galaxies, groups, and clusters), and Rose (1976, groups and clusters). Though patchy in their coverage, these surveys still serve as finding lists for extragalactic studies south of the equator.

The early 1970's saw the European Southern Observatory (ESO) erect a 1.0-m Schmidt at La Silla in Chile; and the Royal Observatory, Edinburgh (ROE) built a duplicate of the Palomar Schmidt (with a few important improvements) at Siding Spring in Australia. Together, these telescopes are engaged in several surveys of the southern sky. One of these, the ESO/Uppsala Survey (Lauberts et al, 1981a,b; and references therein) lists about 18,500 non-stellar objects, most of them galaxies. Its major advantages are the inclusion of precise positions for all objects, and position angles for non-round galaxies. It is serving very well as a finding list for galaxies larger than ~ 1 arcmin south of $\delta = -17^\circ$.

The deepest of the surveys, and the one upon which this thesis is based, is that on hypersensitized Kodak IIIa-J fine-grain blue-green sensitive plates being taken with the United Kingdom's Schmidt (UKS) at Siding Spring. More details will be given when appropriate.

B. Surveys of the UKS "J" Plates

Working with Prof. Abell, the writer is engaged in a survey of southern galaxy clusters as seen on the J plates. This will extend Abell's (1958) northern cluster survey to the south celestial pole. The writer is also working with the de Vaucouleurs on a survey of large southern galaxies on the same plates. (See Corwin et al 1980, 1981 and references therein for details and preliminary results for late-type galaxies south of $\delta = -22^\circ$.)

It was realized that a realistic exploration— even a preliminary one — of a single supercluster for a thesis project would have to depend on more distant objects than those noted during the large galaxy survey. Inasmuch as a study of the supercluster with the COSMOS machine was also planned, the practical problems of data collection and handling dictated that no more than 10 to 15 UKS J plates be involved. The rich cluster survey was seen to be the perfect means for locating a supercluster satisfying these practical limitations. A candidate object was indeed quickly found.

(In addition to those mentioned just above, another noteworthy survey on the UKS J plates is that by Arp and Madore for peculiar galaxies. Complete from the south celestial pole to $\delta = -22^\circ$, it contains positions, diameters, types, and notes for

several thousand peculiar galaxies. Preliminary results are given by Arp and Madore (1977).)

III. A Suspected Supercluster

A. Desiderata

In addition to being distant enough to cover only a few UKS plates, the supercluster still had to be near enough to be accessible with the 1.0-m Elizabeth Reflector at the South African Astronomical Observatory (SAAO), and with the 1.9-m Knox-Shaw Reflector at SAAO. It was planned to calibrate the UKS plates by photoelectric aperture photometry of some of the brighter supercluster galaxies, and to obtain spectra for some of these same galaxies, with the SAAO telescopes.

The candidate object first seen in Southern Sky Survey field 145 (field center at $21^{\text{h}}32^{\text{m}}$, -60° , in an area of the sky not covered by any of the Harvard surveys) seemed to be ideal. It consists of two quite rich elongated clusters at an estimated redshift of $z \approx 0.07$ to 0.08 , along with several other clusters, groups, and clouds at the same apparent distance. If the candidate object was indeed a supercluster at approximately 200 to 250 Mpc, it would be expected to span about 10° if it had the typical supercluster diameter of ~ 50 Mpc as reported by e.g. de Vaucouleurs (1970, 1971) and Abell (1974, converting from his distance scale based on $H_0 = 50 \text{ km sec}^{-1} \text{ Mpc}^{-1}$). Therefore, to allow complete coverage of the suspected supercluster with a considerable amount of "field" around it, sixteen $6.4^{\circ} \times 6.4^{\circ}$ UKS fields, centred approximately on the position of the rich double cluster ($21^{\text{h}}48^{\text{m}}$, -58°), were chosen as

the initial survey area. Data for each of the plates of these fields are listed in Table 2-1. Their sky coverage is shown in Figure 2-1.

Figure 2-1 also shows the distribution of all galaxies in the initial survey area that are larger than $D_{25} = 2.0$ arcmin. These are the galaxies included in the large galaxy survey (Section II-B above). (Inasmuch as the reduction from measured diameters to D_{25} — the diameter at the 25.0 mag sec^{-2} isophote — is preliminary, the final selection of large galaxies in these fields may differ slightly from those shown in Figure 2-1.) Since additional data subsequently showed that none of these galaxies is associated with the suspected supercluster, they will not be discussed in detail in this thesis. At the moment, we only note that most of them are members of the nearby Pavo-Indus Cloud (de Vaucouleurs 1956a, 1975a) or the slightly more distant NGC 7014 Cloud (Sandage 1978; Chapter 3 of this thesis.)

B. Cluster Survey

Having delineated the initial survey field, UKS plates were obtained for the sixteen fields included. In several cases, the plates were copies on Kodak Process emulsion kindly made for the project by the UKS Telescope Unit at Siding Spring. The remainder were non-survey grade original UKS J plates judged adequate for the work.

The plates were scanned as usual for rich clusters, and parameters were estimated for the clusters found (see Abell 1958 for details; magnitude estimates for cluster galaxies are also discussed in Chapter 4 of this thesis.) The clusters estimated to

TABLE 2-1 -- Plates in the Initial Survey Area

Field	α (1950)	δ	Plates (C = copy)
106	20 32	-65	J1764, J2539C
107	21 16	-65	J908
108	22 00	-65	J1728
109	22 44	-65	J954
144	20 54	-60	J892
145	21 32	-60	J1578*, J1759C*
146	22 10	-60	J1873C*
147	22 48	-60	J1579, J1808C
187	20 54	-55	J1577, J3370C
188	21 27	-55	J1592C*
189	22 00	-55	J3474*, J4584C*
190	22 33	-55	J1765C*
235	21 00	-50	J3389
236	21 30	-50	J1823, J2391C*
237	22 00	-50	J2376, J3658C*
238	22 30	-50	J961



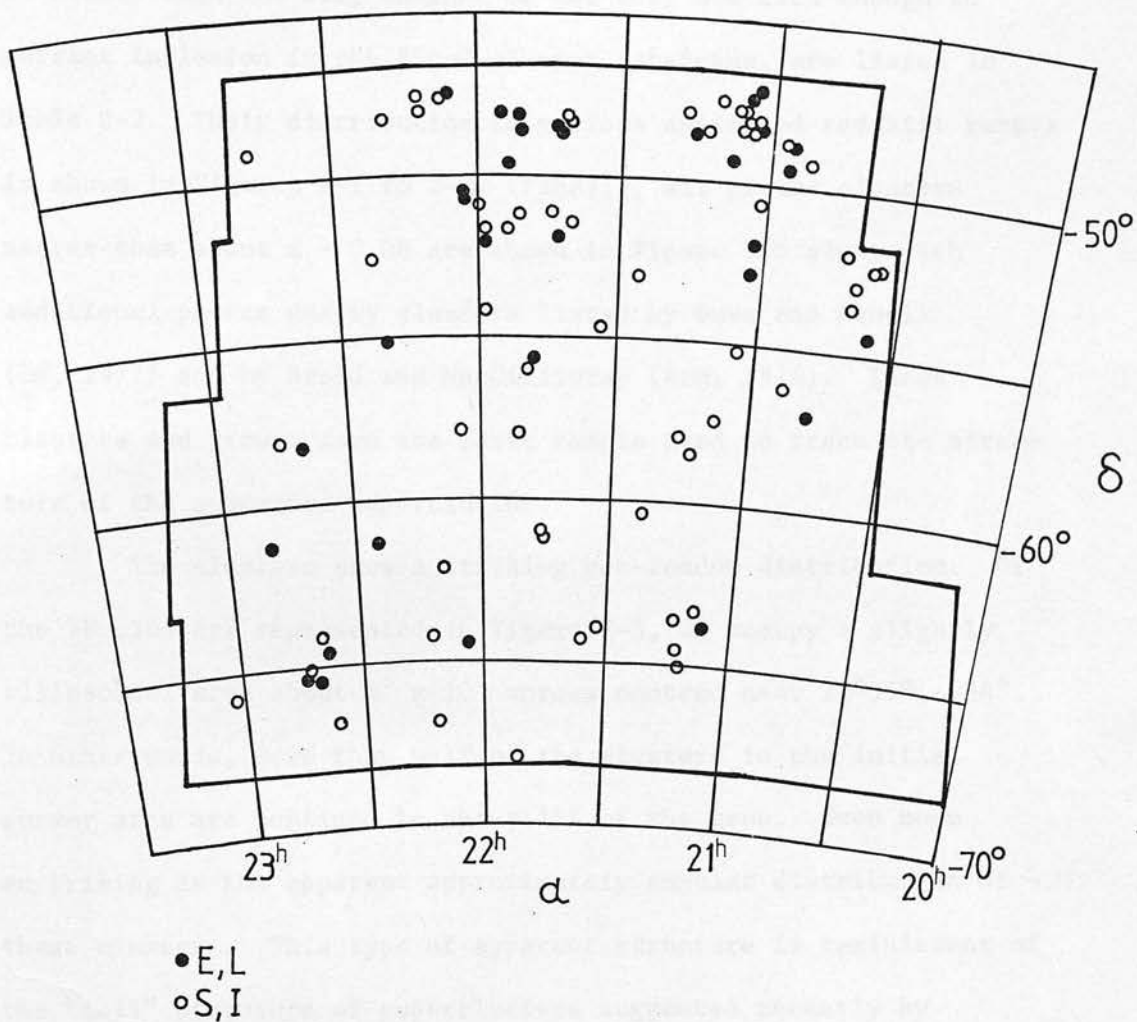


Figure 2-1. The initial survey area, comprising fields 106 - 109, 144 - 147, 187 - 190, and 235 - 238. Galaxies with $\log D_{25} > 1.3$ from the southern galaxy survey are also shown, ellipticals and lenticulars as closed circles, spirals and irregulars as open circles.

be closer than $z \approx 0.1$, whether or not they are rich enough to warrant inclusion in the final cluster catalogue, are listed in Table 2-2. Their distribution in various estimated redshift ranges is shown in Figures 2-2 to 2-4. Finally, all of the clusters nearer than about $z \approx 0.08$ are shown in Figure 2-5 along with additional poorer nearby clusters listed by Duus and Newell (DN, 1977) and by Braid and MacGillivray (BrM, 1978). These clusters and groups form the basic sample used to trace the structure of the suspected supercluster.

The clusters show a striking non-random distribution. Of the 48 clusters represented in Figure 2-5, 25 occupy a slightly ellipsoidal area about $8^\circ \times 10^\circ$ across centred near $21^{\text{h}}55^{\text{m}}$, -54° . In other words, more than half of the clusters in the initial survey area are confined to about 15% of the area. Even more surprising is the apparent approximately annular distribution of these clusters. This type of apparent structure is reminiscent of the "cell" structure of superclusters suggested recently by Jöeveer, Einasto, and their colleagues in a remarkable series of papers still in progress [Jöeveer and Einasto 1978, Jöeveer et al 1978, Einasto et al 1980a,b, Tago (Einasto 1980, private communication); and references therein]. Is this apparent annulus of clusters another example of a "cell" in space? Are galaxies and clusters arrayed in sheets and chains around an almost empty "hole"? The remainder of this chapter, as well as the next two, are devoted to observational tests of these questions.

An obvious first step is to extend the cluster survey to more fields around those already scanned. Unfortunately, J plates were not available for many of the fields. However, use of those

TABLE 2-2 -- Rich Clusters with $z_{est} \leq 0.12$ in the Initial Survey Area

Cluster	l	b	z_{est}	R	A	B-M	Other Names of Comments
2029.1	-6312	333.1	0.072:	0	R	III	BRM96, STR2029-632
2035.9	-6132	335.0	.072	1	I	II	STR2036-615
2036.3	-5314	345.3	.059	-1	I:	II-III	BRM161, STR2036-532
2047.8	-5255	345.5	.034	3	I	III	BRM162, 189
2048.7	-5208	346.5	.046	1	I	III	BRM163, 190, STR2049-521
2113.1	-5937	336.0	.059	0	I	II	STR2113-596
2115.1	-5325	344.1	.090	-1	I	III	STR2116-533
2126.1	-5102	346.8	.065	0	I	III	BRM193, STR2126-510
2130.7	-6215	331.7	.069	0	R	II:	BRM99, 129, STR2131-623
2131.0	-5351	342.7	.069	0	I	II	STR2131-537
2132.2	-5246	344.1	.069:	-1	I	III	Two clusters superposed
2132.7	-5625	339.1	.082	-1	I	I-II:	
2136.0	-5218	344.5	.115	-1	I	II-III	BRM195
2136.1	-5137	345.5	.094	-1	I	I-II	
2142.1	-5150	344.8	.040	0	RI:	I-II:	
2143.1	-5732	336.9	.061	3	R	II	BRM130, STR2143-575, SER149-05
2147.0	-5533	339.3	.039	0	I	I-II	STR2147-555
2150.6	-5805	335.6	.069	3	R	II-III	BRM132, STR2150-581, SER149-10
2152.3	-5549	338.5	.029	0	I	III	STR2152-556, 2153-558, SER149-02
2154.9	-6040	331.9	.056	2	R	III	BRM133, STR2155-606
2156.5	-5624	337.4	.035	1	I	II	
2158.2	-6011	332.2	.082	2	R	I	STR2159-602
2201.1	-5822	334.3	.061	-1	I	I-II	This is <u>not</u> SER149-11 = STR2201-585
2201.2	-5019	345.6	.043	0	R	I-II	
2206.2	-5204	342.5	.106	1	R	I	BRM200

TABLE 2-2 -- Continued

Cluster	l	b	zest	R	A	B-M	Other Names or Comments
2212.7	-5148	342.3	-52.0	0	R:	II-III	
2213.5	-5250	340.7	-51.7	0	I	I-II	
2217.0	-5245	340.4	-52.2	0	R	II	BRM203, 204, STR2217-526
2218.0	-5755	333.2	-49.7	-1	I	III	STR2218-579, ROSE73
2218.2	-5523	336.6	-51.1	1	I	II-III	STR2217-554, SER149-01, ROSE72
2221.0	-5644	334.4	-50.7	-1	I	II-III	STR2221-567, SER149-04, ROSE75
2221.6	-6431	324.9	-46.1	-1	I	III	BRM103, STR2221-645, SER150-03
2222.4	-5605	335.1	-51.2	-1	I	III	STR2223-561
2223.2	-4910	345.1	-54.6	2	R	I-II	BRM206, STR2225-491
2226.5	-5411	337.2	-52.7	-1	I	III	STR2226-542
2228.5	-5500	335.8	-52.5	-1	I	III	STR2228-551, ROSE78
2231.8	-5243	338.6	-54.1	-1	I	I-II:	STR2232-526, ROSE82
2234.5	-6014	328.3	-50.0	-1	I	III	BRM136, STR2235-602
2236.6	-6245	325.2	-48.6	-1	I:	II-III	BRM137, STR2234-628
2242.0	-6304	324.2	-48.8	-1	R	III	BRM107, 138, STR2242-631
2243.1	-5259	336.6	-55.4	-1	R	II-III	STR2243-530, ROSE85
2244.7	-5220	337.3	-56.0	-1	RI:	II-III	
2246.5	-6439	322.0	-48.0	2	R:	II	BRM108, STR2246-647

1950 positions. z estimated from m_{10} and R = Abell richness (Abell 1958).
 Abell types: R = regular, I = irregular, RI = intermediate. Bautz-Morgan types
 as usual. BRM = Braid and MacGillivray (1977); STR = Stromlo from Duus and Newell
 (1977); SER = Sersic (1974); ROSE = Rose (1977).

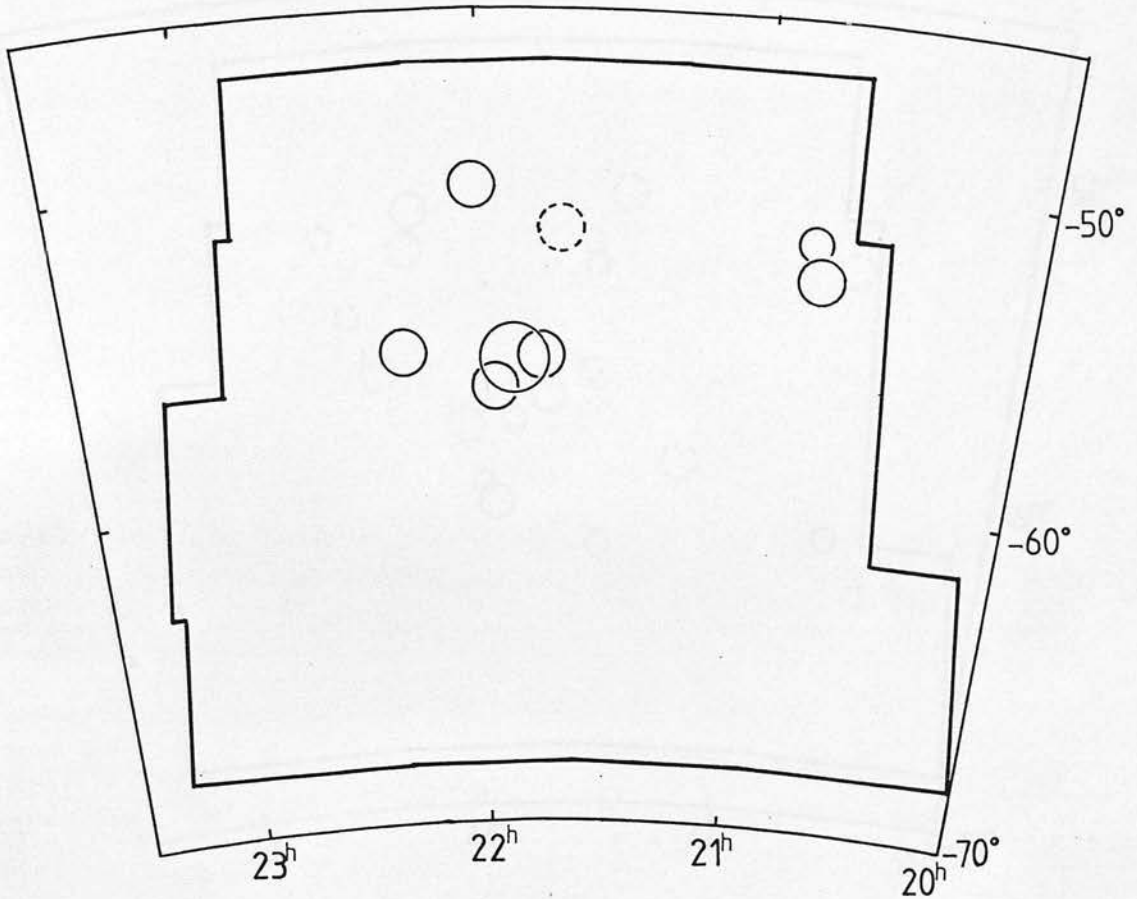


Figure 2-2. Clusters from the southern rich galaxy cluster survey with $z < 0.046$ (z estimated from m_{10}). Clusters shown as dashed circles have fewer than 50 members in the magnitude interval m_3 to $m_3 + 2$. Circle radii approximate the Abell radii.

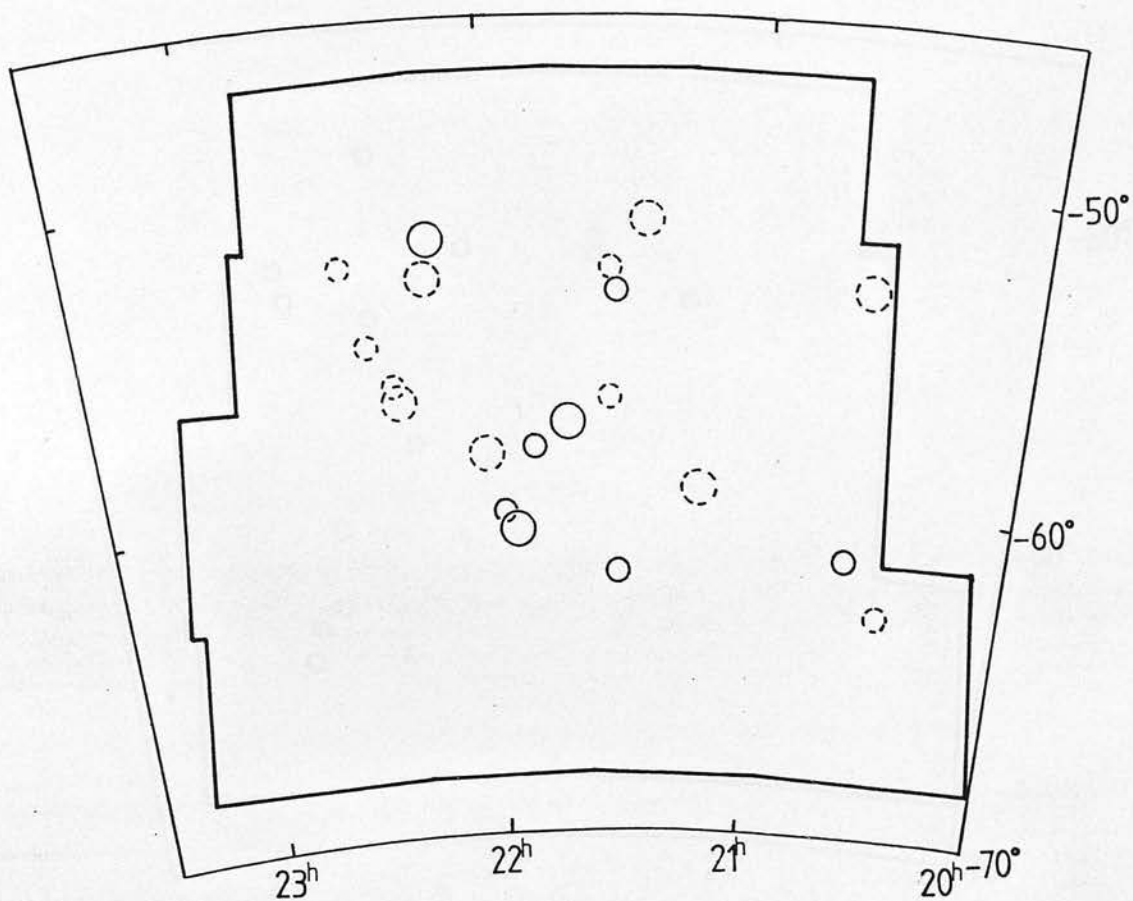


Figure 2-3. Same as Figure 2-2, but for clusters with $0.046 < z < 0.070$.

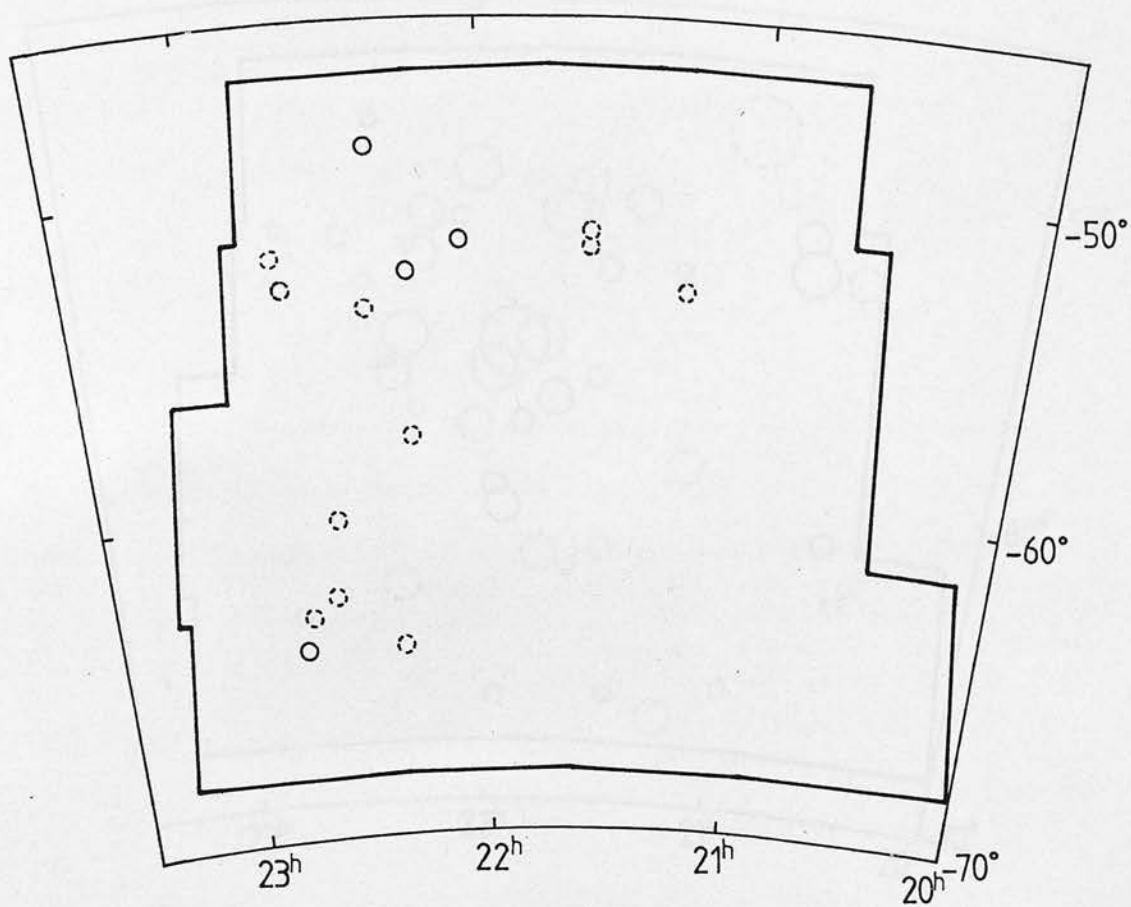


Figure 2-4. Same as Figure 2-2, but for clusters with $0.070 < z < 0.095$.

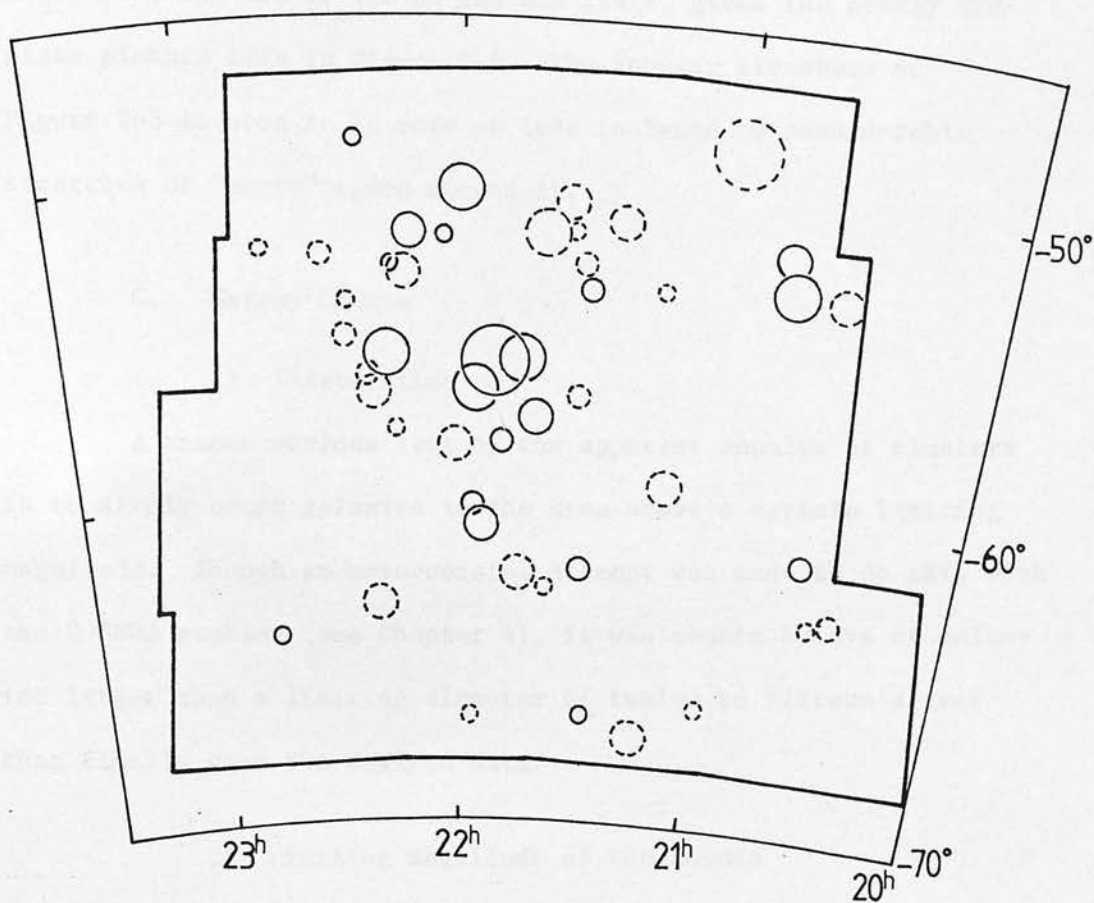


Figure 2-5. All clusters in the initial survey area with $z < 0.08$. Clusters are from Duus and Newell (1977) and Braid and MacGillivray (1977) as well as the southern cluster survey.

that were, and use of the DN and BrM lists, gives the nearly complete picture seen in Figure 2-6. The annular structure of Figure 2-5 is seen to be more or less isolated by considerable stretches of "empty" space around it.

C. Galaxy Counts

1) Introduction

A second obvious test of the apparent annulus of clusters is to simply count galaxies in the area above a certain limiting magnitude. Though an unsuccessful attempt was made to do this with the COSMOS machine (see Chapter 4), it was counts by eye of galaxies larger than a limiting diameter of twelve to fifteen arcsec that finally gave the desired data.

2) Limiting magnitude of the counts

The counts had to be made to a limiting diameter rather than to a limiting magnitude because no adequate magnitude calibration for the J plates existed when the counts were begun. However, it is still of some interest to know the approximate limiting magnitude to which the limiting diameter corresponds. Several different estimates of this limiting magnitude are possible.

1. The mean number of galaxies per square degree counted in the fields is 85 ± 15 . Luminosity functions for "field" galaxies (e.g. Brown 1978, Rainey 1977, MacGillivray and Dodd 1980b) entered at this number suggest a limiting magnitude of $B = 18.7 \pm 0.4$.

2. The number of galaxies per square degree is also the same (to within the errors) as given by the Lick counts. This

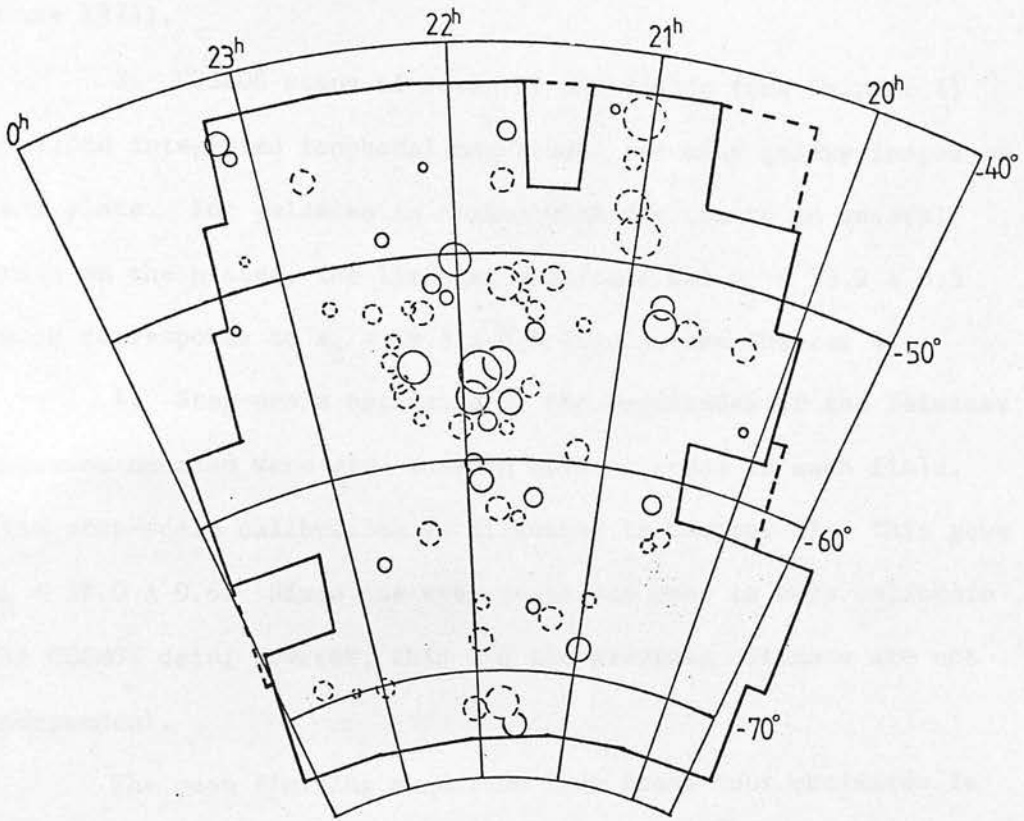


Figure 2-6. The extended survey area with clusters as in Figure 2-5.

implies the same limiting magnitude of $B = 18.9 \pm 0.5$ (Kron and Shane 1974).

3. COSMOS scans of seven of the fields (see Chapter 4) provided integrated isophotal magnitudes for many galaxy images on each plate. For galaxies in common with the counts in several areas on the plates, the limiting magnitude was $m_j = 18.9 \pm 0.5$ which corresponds to $m_B \approx 19.3 \pm 0.5$ (again, see Chapter 4).

4. Step-scale estimates of the magnitudes of the faintest galaxies counted were also made in several areas in each field. (The step-scale calibration is discussed in Chapter 4). This gave $m_B = 19.0 \pm 0.6$. Since the step scale was used to help calibrate the COSMOS data, however, this and the previous estimate are not independent.

The mean limiting magnitude from these four estimates is $B = 19.0 \pm 0.5$. The error is estimated and may be optimistic for two reasons: 1) isophotal magnitudes quoted above from the various sources refer to different (general unknown) isophotes; and 2) because galaxies of a given diameter have a wide range of surface brightnesses, the isophotal magnitudes for such a diameter limited sample will also cover a wide range.

3) Counting procedure

The plates were examined with a 10-power binocular microscope through transparent plastic overlay sheets. Each galaxy larger than the limiting diameter was marked on the plastic overlay directly above the galaxy's image on the plate. A coordinate grid was also marked on the overlay; it was transferred from standard equatorial coordinate grids aligned with reference to SAO stars in

the fields.

The overlay sheet with the positions of the galaxies marked on it was then placed on a sheet of paper ruled with 1-cm squares, and the number of galaxies in each square centimeter was counted. These 1-cm counts were then added by fours to give 2-cm counts, the number of galaxies in each 2-cm square across the plate. At the same time, a reduction factor was applied to reduce the raw counts to the counts in field 145. The reduction factors are simply the ratios of the total count in the overlap areas common between plates. Since the plates overlap by more than a degree, this procedure is reasonably accurate (Table 2-3, below). The process had to be performed stepwise for fields not directly overlapping field 145, but more than one "route" back to field 145 was often taken. For example, the plate factor for field 237 was found not only by comparing it with field 189 (which overlaps it and field 145), but also through comparison with field 236 which overlaps field 188, which in turn overlaps field 145. The largest difference in the plate factors derived by this stepwise procedure was 11%, with values of 4% to 6% being typical, showing that the procedure is accurate. This is also an indication of the accuracy of the counts on a single plate. In other words, the diameter limit was consistently maintained while counting across a single plate. The plate factors, which are listed in Table 2-3, show that the counts can vary up to 30% between plates. However, this still amounts to only ± 0.4 mag, which is more than adequate for the present purposes.

The reduced 2-cm counts, as well as the raw 1-cm counts, are available on request from the writer.

TABLE 2-3 -- Plate Factors

Fields		Count		$f_p = A/B$
A	B	A	B	
F145-F107		510	442	1.15
F145-F108		474	373	1.27
F145-F188		969	1004	0.97
F145-F189		769	647	1.19
F189-F190		1013	1289	0.78
F145-F190	Through F189			0.93
F146-F190		481	556	0.87
F145-F190	Through F146			0.87
F145-F190	Adopted			0.90
F145-F146		1404	1394	1.01
F146-F147		781	721	1.08
F145-F147	Through F146			1.09
F188-F236		853	1056	0.81
F145-F236	Through F188			0.78
F189-F236		207	310	0.67
F145-F236	Through F189			0.79
F145-F236	Adopted			0.78
F189-F237		766	825	0.93
F145-F237	Through F189			1.10
F236-F237		1226	818	1.50
F145-F237	Through F188, F236			1.17
F145-F237	Adopted			1.14
F237-F238		767	1170	0.66
F145-F238	Through F188, F236, F237			0.77
F145-F238	Through F189, F237			0.72
F190-F238		891	1192	0.75
F145-F238	Through F146, F190			0.65
F145-F238	Through F189, F190			0.69
F145-F238	Adopted			0.71

The raw counts were processed in no way other than reducing them to field 145. Specifically, most of the various correction factors used by Shane and Wirtanen (1967) to reduce the Lick galaxy counts to a uniform system across the sky are taken into account by the procedure outlined above. Only vignetting (and possibly other field effects; see Chapter 4) and differential atmospheric extinction might contribute to small residual errors in the counts. However, these errors will be much smaller than the uncertainty arising from counting galaxies to a limit which is several magnitudes above the plate limit.

Finally, isopleths were drawn through the reduced 2-cm counts field by field. To demonstrate the adequate repeatability of the counts in the overlap areas, the isopleths for four adjacent fields are shown in Figure 2-7. Isopleths for the entire prime survey area, the eleven fields containing the annular concentration of clusters noted above, are shown in Figure 2-8. The annulus can be seen in the isopleths, but the picture is of course irregular as well as contaminated by background galaxies and clusters.

In order to trace the large-scale structure in the region more easily, the reduced 2-cm counts in each field were smoothed by averaging the counts over nine 2-cm squares, giving the central square weight 3, and the other eight squares weight 1 (these smoothed 2-cm counts are also available from the writer on request.) The isopleths drawn through the resulting smoothed 2-cm counts are shown in Figure 2-9. This figure clearly confirms the picture given by the clusters in Figure 2-5: a large ring-like assembly of clusters, clouds, and groups is apparently seen in projection. Figure 2-9 adds the important information of apparent "bridges" of

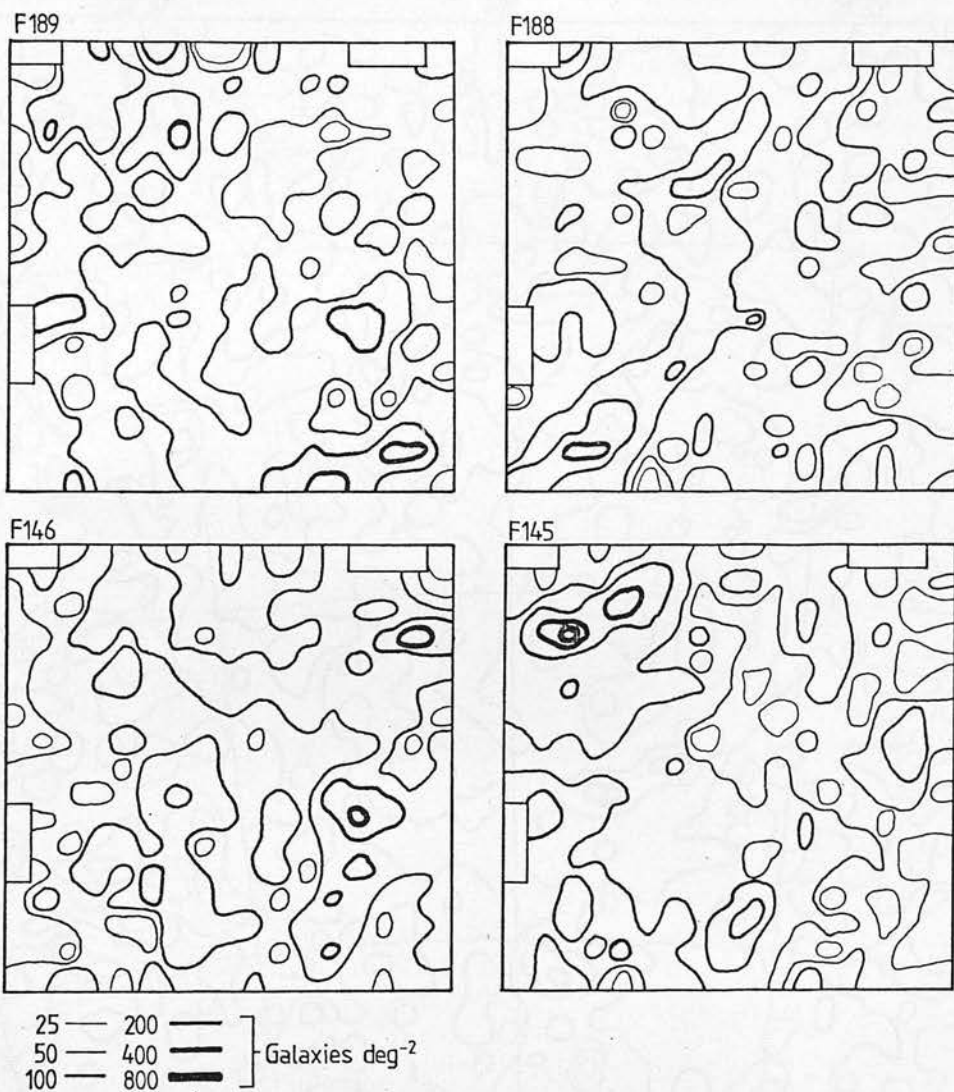


Figure 2-7. Isopleths for galaxies counted in 2 cm square cells for four plates in the prime survey area.

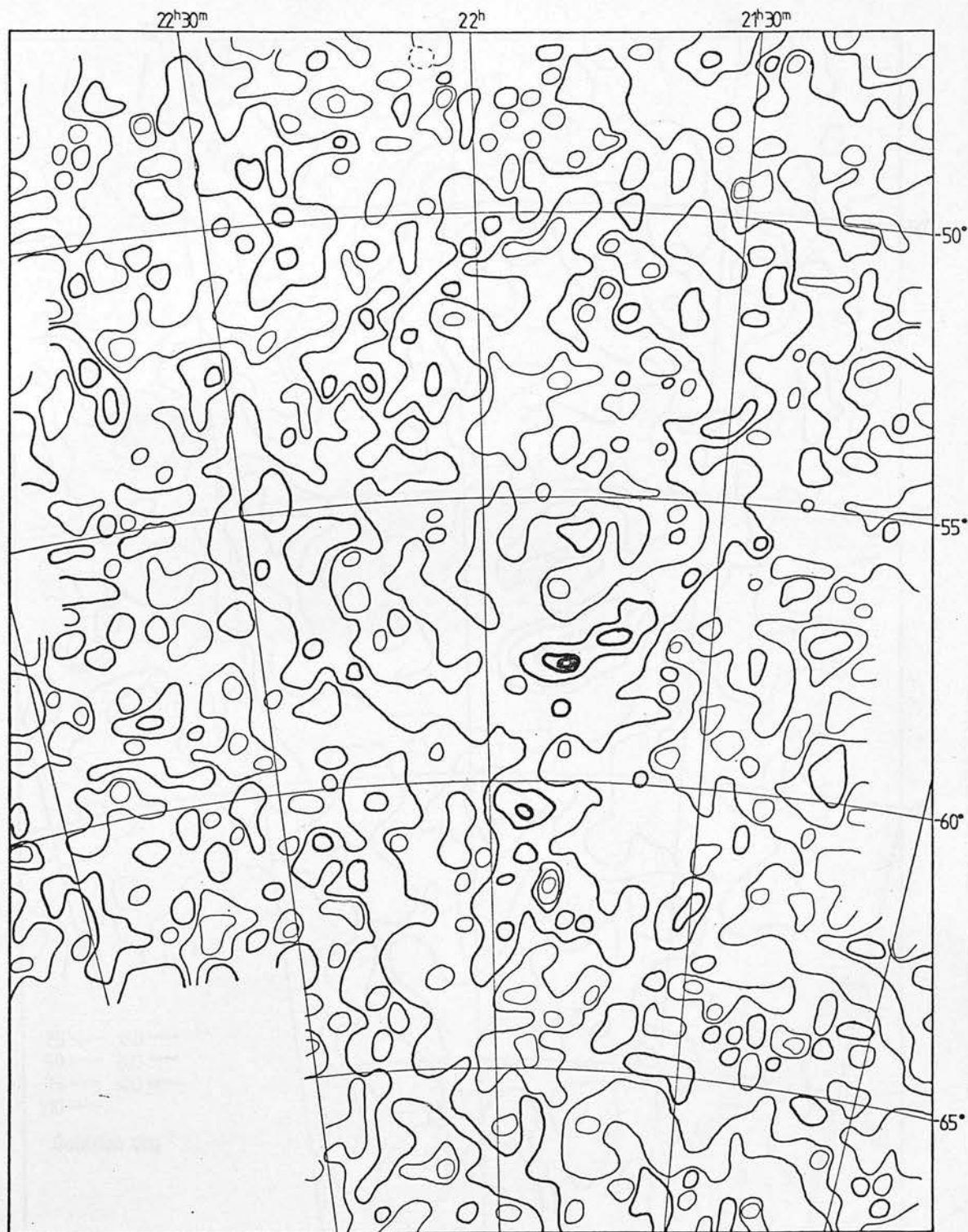


Figure 2-8. Isopleths as in Figure 2-7, but for all eleven plates in the prime survey area. The dashed circle at $22^{\text{h}} 05^{\text{m}} -47^{\circ} 12'$ locates the 2nd magnitude star α Gruis whose image obscures galaxies near it.

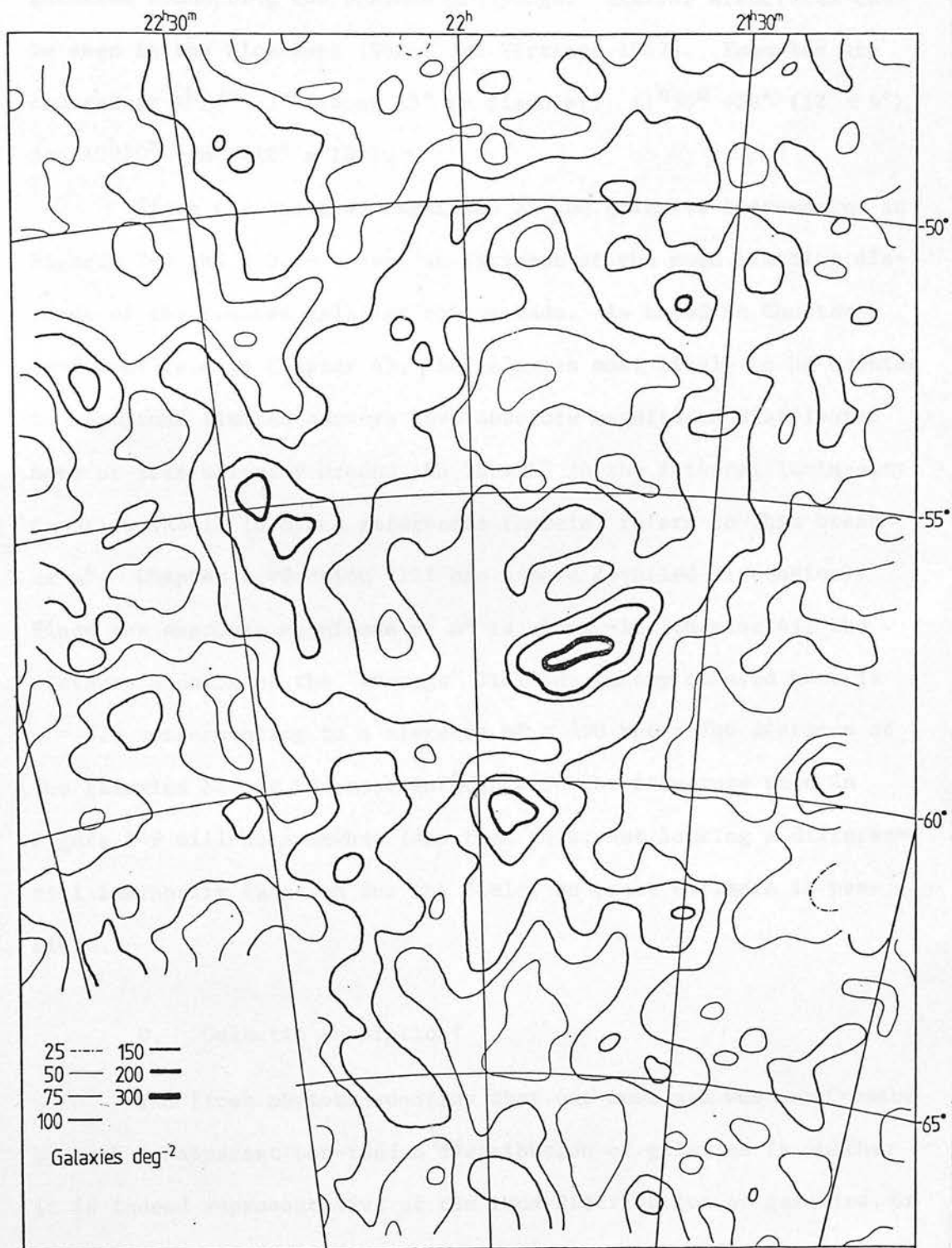


Figure 2-9. 2 cm smoothed isopleths for galaxies in the prime survey area.

galaxies connecting the various groupings. Similar structures can be seen in the Lick maps (Shane and Wirtanen 1967). Examples are centred at $1^{\text{h}}15^{\text{m}} -5^{\circ}$ (about 15° in diameter), $11^{\text{h}}30^{\text{m}} +28^{\circ}$ ($12^{\circ} \times 5^{\circ}$), and $10^{\text{h}}50^{\text{m}} +48^{\circ}$ ($18^{\circ} \times 10^{\circ}$).

Since the limiting magnitude of the galaxies represented in Figures 2-8 and 2-9 is known, an estimate of the mean limiting distance of the counted galaxies can be made. As noted in Chapter 1 (and confirmed in Chapter 4), the galaxies most likely to be counted in magnitude limited surveys have absolute magnitudes distributed more or less normally around the "break" in the integral luminosity function (Abell 1975 and references therein, refers to this break as m^* . Chapter 4, Section VIII has a more detailed discussion). Since the absolute magnitude of m^* is about -18 (Chapter 4), the distance modulus of the "average" limiting galaxy counted here is $\mu \approx 37$, corresponding to a distance of ≈ 250 Mpc. The distance of the galaxies having the most influence on the structure seen in Figure 2-9 will be somewhat less than this, but lacking a differential luminosity function for the field, no exact estimate is possible.

D. Galactic Absorption?

The first obvious question that one must ask when confronted by such an apparent non-random distribution of galaxies is whether it is indeed representative of the true distribution of galaxies, or whether it is an accident caused by galactic absorption.

Galactic latitudes in the prime survey area range from about -35° to -60° , and the star density is rather high. There is undoubtedly patchy absorption in the area. However, the smoothed

galactic absorption A_B , as given by the RC2 formulation, ranges only from 0.44 to 0.29 mag: relative smoothed absorption is small.

Some idea of the amount of patchy galactic absorption can be had by reference to the survey of galactic neutral hydrogen column densities by Heiles and Cleary (1979). Their data are plotted as isopleths in Figure 2-10 where it can be seen that there is no correlation of column density with galaxy count. This data, combined with the work of Burstein and Heiles (1978a,b), can also give an estimate of the range of absorption in the survey area. This predicts a maximum change in $E(B-V)$ across the field of 0.048 mag. With $R = A_B/E(B-V) = 3.1$ (Turner 1976), the maximum change in A_B through the prime survey area is $\Delta A_B = 0.15$ mag, in agreement with the value predicted by the RC2 formula. This figure reflects the patchy galactic absorption as revealed by HI column density measurements (with the variable gas-to-dust ratio taken into account), not just the change in the smoothed average absorption across the field. It thus puts a severe constraint of only $\sim 15\%$ on the allowable distortion to the galaxy counts by galactic absorption. Even the smoothed 2-cm counts of Figure 2-9 (note that the smoothing of both Figures 2-9 and 2-10 is about one degree; they are therefore directly comparable) show variations of factors of at least six. The range of galactic absorption would have to be nearly two magnitudes to account for this — and the factors of variation in the unsmoothed counts are much larger still. No reasonable model of galactic absorption can produce such drastic variations (see e.g. Spitzer 1978).

The conclusion is therefore nearly inescapable that the annulus of galaxies and clusters is indeed a projection of the true

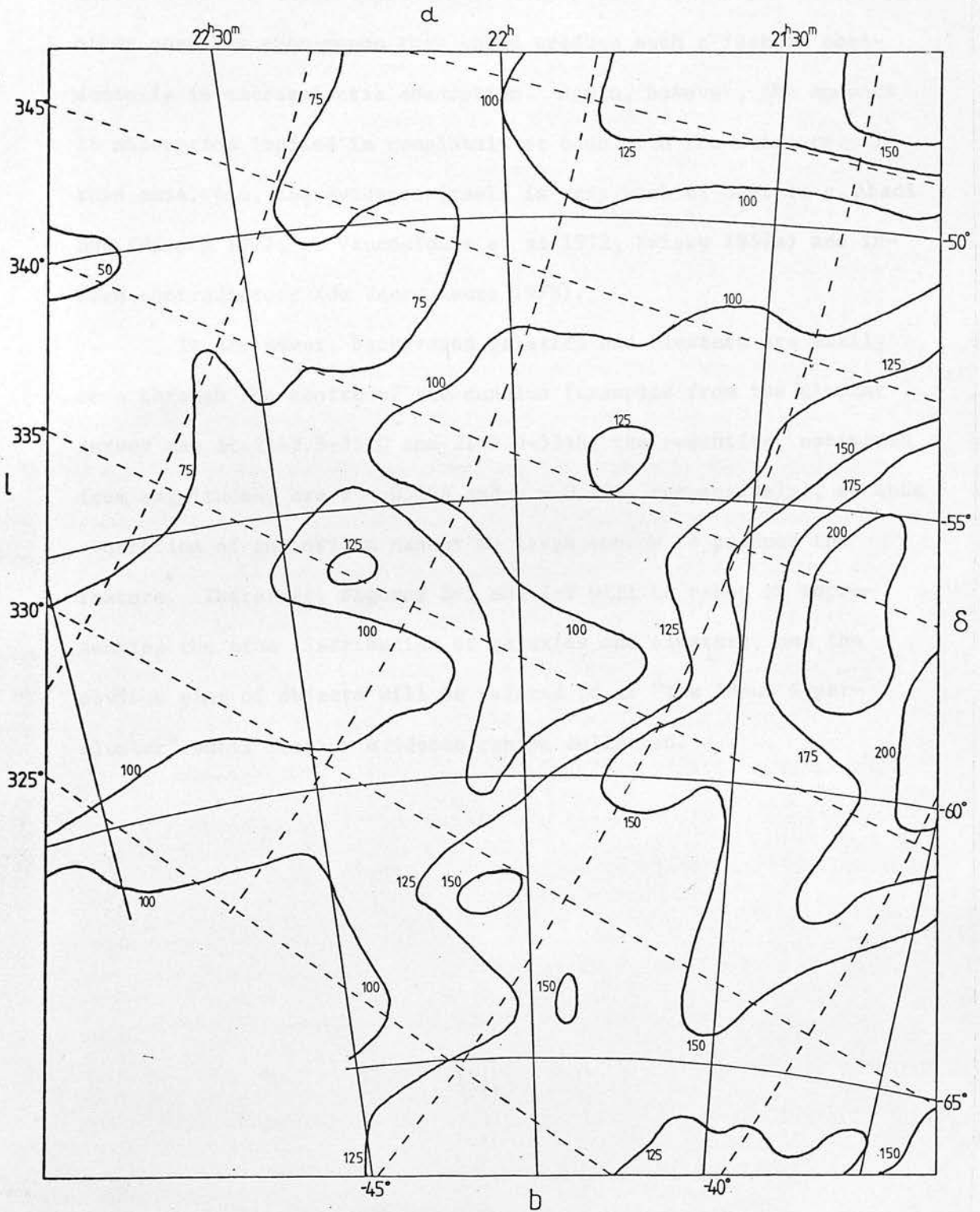


Figure 2-10. H I column densities in units of $2.23 \times 10^{18} \text{ cm}^{-2}$ integrated over the velocity range $-100 \text{ km sec}^{-1} < V_{\text{LSR}} < +100 \text{ km sec}^{-1}$ from Heiles and Cleary (1979). Galactic coordinates for the prime survey area are also shown as dashed lines.

distribution of these objects onto this part of the sky. The only other possible phenomenon that could produce such a feature accidentally is extragalactic absorption. Again, however, the amounts of absorption implied is completely at odds with the evidence. In this case, too, the evidence itself is very weak at best (e.g. Abadi and Edmunds 1977, de Vaucouleurs et al 1972, Zwicky 1957a) and indeed contradictory (de Vaucouleurs 1978).

In any event, background galaxies and clusters are easily seen through the centre of the annulus (examples from the cluster survey are at 2142.5-5320 and 2149.0-5348; the redshifts, estimated from magnitudes, are $z = 0.158$ and $z = 0.148$, respectively), so that absorption of any origin cannot be large enough to produce the feature. Therefore, Figures 2-5 and 2-9 will be taken as representing the true distribution of galaxies and clusters, and the obvious ring of objects will be referred to as "The Indus Super-cluster" until further evidence can be collected.

CHAPTER 3

A Preliminary Redshift Survey
of the Indus Supercluster AreaI. Introduction and Assumptions

Magnitude estimates of galaxies in the rich clusters in the area of the Indus Supercluster provided crude distances in the previous chapter. (Other photometric methods of determining distances of the Indus Supercluster members will be discussed in Chapter 4.) However, it is obviously desirable to have much more accurate distance estimates in order to examine the large-scale distribution of matter in the Supercluster. This can be most easily done by 1) assuming a constant Hubble parameter in the direction of the Supercluster and 2) measuring redshifts for galaxies suspected to be Supercluster members, both in and out of rich clusters.

The assumption of a constant Hubble parameter carries with it the assumption of a very small velocity dispersion outside of rich clusters if one wishes to use redshifts as distance estimators. Velocity dispersions of a few tens or a few hundreds of kilometers per second are commonly reported for galaxy groups (see e.g. de Vaucouleurs 1975a, Tammann and Kraan 1977, Tully and Fisher 1978, Materna 1979; and references therein) and for galaxies in clouds and bridges between rich clusters (Chincarini and Rood 1976a; Gregory and Thompson 1978, Einasto et al 1980 a,b; Davis et al 1981; and references therein). Therefore, redshifts have been used extensively by the investigators quoted above to study the spatial distribution of galaxies.

Adopting a constant Hubble parameter also assumes no change in its value with direction due to e.g. the disturbing influence of the Local Supercluster (de Vaucouleurs 1958, 1978; de Vaucouleurs and Bollinger 1979; Mould et al 1980; Yahil et al 1980; Tonry and Davis 1981; and references therein). However, the area under study here (the initial survey area) is relatively small so that any differential perturbation due to local motion of whatever origin or velocity will also be small.

This chapter, then, describes a first redshift survey of the Indus Supercluster, and the observational results of that survey, based on the assumptions above.

II. Selection and Positions of Galaxies

Most of the 216 galaxies chosen as candidates for spectroscopic observation are apparent members of rich clusters or of groups or clouds. All had precise positions measured with respect to SAO stars using the ROE X-Y machine. This has digital readout of 10 μ m in both x and y directions; exact repeatability of the readings in both axes was verified by experiment. Therefore, error intrinsic in the readings amounted to about 0.7 arcsec in α and δ .

Measurements were reduced using the standard method of dependencies (see e.g. König 1962). For 48 galaxies measured on two or more plates, the average deviations are $\pm 0^{\text{S}}.10 \pm 0^{\text{S}}.01$ (m.e.) in α , and $\pm 0''43 \pm 0''04$ in δ . The standard deviations are $\pm 0^{\text{S}}.12$ and $\pm 0''39$, respectively. Assuming a mean declination of -57° for the initial survey area, the figures in α become $\pm 0''83$ and $\pm 1''00$. The larger right ascension errors may reflect x-axis machine hysteresis, eyepiece parallax errors, or some unknown observer

bias. The declination errors, smaller than those intrinsic in the machine, must be fortuitous. Whatever the source of the mean errors, however, they are taken to be on the order of one arcsec for all objects.

The galaxies were once again examined, morphological types estimated, and observing priorities assigned. Brightest galaxies in rich clusters generally received highest priority, followed by brightest galaxies in poor clusters or in groups, other apparent cluster members, and finally apparent field galaxies.

III. Observations

A. Introduction

Three main series of redshifts were used:

1. Twenty-five spectra of twenty-four galaxies obtained with the Image Tube Spectrograph (ITS) on the 1.9-m SAAO telescope by the writer and Dr. David Emerson;

2. Schectman scanner observations of twenty-two galaxies with the Las Campanas 2.5-m telescope kindly obtained by Dr. H. C. Arp at the writer's request; and

3. ITS observations of eight galaxies with the Cerro Telolo 4-m telescope also kindly obtained at the writer's request by Drs. G. Chincarini and M. Tarenghi.

Additional redshifts were kindly communicated in advance of publication by Drs. M. Green and T. Shanks. The three main series of redshifts are further described below, and all data are collected in Table 3-1.

B. Series 1: SAAO 1.9-m ITS Spectroscopy

Though this series is described in detail by Corwin and Emerson (1981; Appendix A of this thesis), a summary is given here for the convenience of the reader. The spectra were obtained during a two-week observing run in June 1978. The ITS was used with its No. 1 grating which gave a reciprocal dispersion of about 215 \AA mm^{-1} at 5400 \AA : this varied only slowly with wavelength.

The spectra, on baked IIA-0 plates with argon comparison spectra, were measured with a single-screw travelling microscope. The relationship between screw position (read to $1 \text{ }\mu\text{m}$) and wavelength was modelled with a second-order polynomial. This gave wavelengths for absorption features and emission lines in the galaxy spectra, and for night sky emission lines which were subsequently used to zero the galaxy redshifts.

After several cycles of refining the rest wavelengths of the galaxy absorption features, the redshifts were computed using the usual non-relativistic formula $V = c(\Delta\lambda/\lambda)$. The external errors in the redshifts, derived through comparison with published and other unpublished data, are on the order of $\pm 60 \text{ km sec}^{-1}$. Possible small systematic errors in the redshifts are negligible for the purposes of this thesis, as is the error introduced by using the non-relativistic approximation for the computing the redshifts.

C. Series 2: Las Campanas 2.5-m Sheckograph Spectroscopy by Arp

Details of observing and reduction procedures will be found in Arp (1981). The present observations were made in

September 1980, were reduced by Arp to wavelength calibrated tracings, then were measured by the writer.

The centres of all recognizable features were estimated by eye, and the wavelengths read to 0.1 \AA by interpolation along the wavelength scale provided. Redshifts were then calculated using the rest wavelengths given by the de Vaucouleurs (1967), Sandage (1978), Dawe et al (1977), or listed in Tables 2, 4, 5, and 6 of Appendix A. Five to twenty-four (average 15) features were used in each spectrum for redshift determination. The internal mean errors averaged $\pm 32 \text{ km sec}^{-1}$, compared with Arp's (1981) estimate of $\pm 50 \text{ km sec}^{-1}$ external error. The implied error factor $f_{\sigma} = \sigma_e / \sigma_I = 1.6$ is typical (see Appendix A, the RC2, and Sandage 1978).

Only two objects in Series 2 have been observed by others. One, a peculiar irregular galaxy (A2201-585) from a short list by Pedreros (1978) cannot be used for comparison as different parts of the galaxy were measured by the two observers. However, there is no gross disagreement. The same is true for the galaxy measured by Shanks. Thus, while the true external error cannot be found from the present observations, there is no reason to doubt Arp's (1981) estimate of $\pm 50 \text{ km sec}^{-1}$.

D. Series 3: CTIO 4-m ITS Spectroscopy by Chincarini and Tarenghi

These redshifts have been measured and reduced by the usual procedure adopted by Chincarini and his colleagues (see e.g. Chincarini et al 1981). They are from a single run in November 1977.

Only the H and K features were regularly measured, though

the G, H, Mg I, and Na D features were also measured when strong. The resulting redshifts have internal mean errors averaging $\pm 60 \text{ km sec}^{-1}$. This is in agreement with the external error estimated as $\pm 70 \text{ km sec}^{-1}$ by Rood (1981). The three redshifts in common with Series 1 agree to within the errors, but suggest a systematic error in one series or the other. Evidence from other redshifts suggest that the error is in the Series 1 redshifts, as mentioned above and in Appendix A.

E. Other Redshifts

The literature was searched for other redshifts of galaxies in the initial survey area; 41 additional redshifts for objects beyond the Pavo-Indus Cloud were found. (Data for the Pavo-Indus galaxies were not collected. These galaxies, with a mean redshift near 3000 km sec^{-1} , are in the foreground and have no direct connection with the Indus Supercluster.) Unfortunately, only two of these 41 redshifts were in common with redshifts in the three major series, so that evaluation of errors must stand as set out above. While all data are accurate enough for the present purpose — mapping the space distribution of galaxies in the initial survey area — confirmation of their accuracy will be necessary before they can be used in dynamical studies of groups and clusters.

IV. The Redshift Survey

All 99 known redshifts for the 91 observed galaxies in the initial survey area beyond the Pavo-Indus Cloud are listed in Table 3-1. (Identification charts for the galaxies are available on request from the writer.) The distribution of the 91 galaxies

TABLE 3-1
Galaxy Redshifts in the Initial Survey Area

	α	Galaxy (1950)	δ	V	σ_v	V_0	S	Cluster	N
20	28	41.9	-63 11 57	+22984	± 78	+22873	CE	2029.1-6312	
	35	53.1	-61 30 37	21306	36	21258	CE	2035.9-6132	
	36	33.8	-53 12 38	13227	39	13167	CE	2036.3-5314	
	48	18.0	-52 56 29	13866	20	13808	CE	2047.8-5255	
	48	21.7	-52 56 36	12992	50	12934	CE	"	
	48	39	-48 57.9	5288	30	5250	E2	N7014 Cloud	1
	48	39	-48 56.0	5488	65	5450	E2	"	
	49	07.6	-52 13 00	13777	27	13723	CE	2048.7-5208	
	49	08.3	-52 21 13	14330	37	14275	CE	"	
	54	19	-52 03.8	4492	45	4439	S		2
21	55	02	-54 22.9	12950	200	12890	F2		
	57	37	-65 26.2	36100	63	35980	E3	2058-654	
	00	00	-48 24.1	5270	63	5235	S	N7014 Cloud	
	01	15	-48 23.3	4818	49	4787	S	"	
	02	07	-47 14.7	4955	37	4924	S	"	
	03	24	-47 23.3	5174	41	5143	S	"	
	03	49	-47 45.4	4491	55	4460	E2,4	"	
	03	49	-47 45.4	4618	42	4587	E2,4	"	
	04	29	-47 22.8	4760	25	4731	S	"	3
	07	29	-64 13.8	28030	100	28090	A		4
	11	46	-47 25.7	4814	67	4783	S	N7014 Cloud	5
	11	55.1	-59 47 33	17619	54	17527	CE	2113.1-5937	
	13	04.6	-59 43 05	17456	64	17364	CE	"	
	"	"	"	17336	75	17244	CT	"	
	13	10.9	-59 32 35	18130:	--	18040:	E2	"	6
	17	45	-66 03.0	5166	20	5044	R		7
	23	43	-61 02.5	4200	50	4100	E1		
	25	54.2	-51 06 12	23955	66	23907	CE	2126.1-5102	
	29	05.3	-60 55 06	8589	74	8491	CE		
30	38.5	-53 47 40	23551	36	23489	CE	2131.0-5351		
"	"	"	23414	90	23352	W	"		
30	49.3	-53 51 34	22874	180	22812	W	"		
31	21.9	-62 18 08	16856	48	16751	CE	2130.7-6215		
"	"	"	16756	82	16651	CT	"		
31	27.7	-62 10 56	16695	32	16591	CE	"		
31	46.0	-56 27 31	12302	29	12226	AC			
"	"	"	12050	100	11975	Sh			
32	24.1	-60 54 24	18246	77	18148	CT			
32	27.0	-56 28 01	20786	50	20710	AC	2132.7-5625		
32	33.9	-52 41 50	19245	45	19188	AC	2132.2-5246		

Table 3-1 -- Continued

	Galaxy	α	(1950)	δ	V	σ_V	V_0	S	Cluster	N
21	33	53.1	-52	50 44	+34455	± 55	+34397	AC		
	36	07.3	-51	37 19	22716	33	22664	AC	2136.1-5137	
	36	12.9	-50	55 03	16464	76	16416	CE	2136-509	
	39	40	-52	55.0	5296	58	5238	E2, ⁴		
	42	08.5	-51	50 17	16101	68	16048	CE	2142.1-5150	
	42	50.4	-57	31 04	22413	136	22331	CE	2143.1-5732	
	"			"	22342	150	22260	G	"	
	"			"	22292	89	22210	CT	"	
	44	46	-50	47.8	4997	61	4949	S		8
	46	32.3	-55	29 54	20320	45	20248	AC	2147.0-5533	
	46	34.9	-62	25 08	19456	20	19350	CT	2147-624	
	48	03.7	-55	34 16	11536	33	11463	AC	2152.3-5549	
	48	27.7	-57	43 14	12008	57	11925	CE		
	"			"	12066	43	11983	CE		
	50	40.3	-58	05 09	22477	3	22392	CT	2150.6-5805	
	50	41.0	-58	04 51	22619	113	22534	CT	"	
	50	44	-58	02.9	23090	150	23005	G	"	
	51	50.3	-57	53 40	23265	56	23181	CE	"	
	53	05.1	-55	48 15	11371	32	11297	AC	2152.3-5549	
	53	12.0	-55	47 33	11160	25	11086	AC	"	
	54	51.7	-60	39 53	22413	6	22315	CT	2154.9-6040	
	56	12.1	-56	26 51	10294	25	10216	AC		
	56	58	-60	13.3	9000	110	8900	E1		9
	56	59.8	-56	25 07	22675	30	22597	AC	2156.5-5624	
	58	21.6	-60	11 12	29903	53	29807	CE	2158.2-6011	10
21	58	21	-60	11.2	30250	100	30150	E1, ³	"	11
22	01	07.4	-50	17 25	10937	24	10890	AC	2201.2-5019	
	01	10.8	-58	18 44	12260	21	12173	AC	2201.1-5822	
	01	23.3	-58	32 10	6595	17	6513	AC		
	"			"	6449	16	6367	P		
	01	24.4	-58	21 19	12188	45	12100	AC	2201.1-5822	
	01	27.3	-50	29 39	11034	28	10986	AC	2201.2-5019	
	04	33	-59	47.7	48400	90	48300	E1	2205.8-5955?	
	08	43	-62	58.3	8430	10	8320	E2		
	12	21.9	-51	45 12	20436	40	20380	CE	2212.7-5148	
	13	47.8	-52	46 37	15967	52	15906	CE	2213.5-5250	
	14	32.7	-52	46 05	16050	200	15990	F2	"	
	17	15.9	-55	22 36	11959	61	11884	CE	2218.2-5523	12
	17	45	-49	01.6	9150	200	9110	F2		
	21	13.7	-56	46 02	10724	34	10642	AC		

Table 3-1 -- Continued

	α	Galaxy (1950)	δ	V	σ_V	V_0	S	Cluster	N
22	21 14	-64	32.0	+28200	± 48	+28080	E3	2221.6-6431	
	21 29.8	-56	43 21	26634	23	26552	AC	2221.0-5644	
	21 35	-62	28.0	12890	200	12780	F1		
	22 44.7	-56	08 14	24215	38	24136	AC	2222.4-5605	
	22 51.5	-56	09 57	23269	35	23189	AC	"	
	30 18.0	-55	03 08	22617	59	22542	CE	2228.5-5500	
	31 35	-62	08.6	7945	200	7840	F1		
	32 03.7	-52	38 32	16844	21	16780	AC	2231.8-5243	
	32 05.0	-52	38 58	16514	26	16450	AC	"	
	33 22	-61	39.6	12560	170	12440	E1		
	38 25	-62	16.5	27730?	--	27620?	F1		13
	46 42	-49	06.9	12450	200	12400	F2		
	48 54	-67	41.1	11840	200	11700	F1		14
	56 34	-65	23.7	12000?	--	11870?	F1		15
	57 00	-65	20.3	12890?	--	12760?	F1		13
	58 29	-59	54.4	10007	72	9903	E2,4		
22	58 29	-59	54.4	10212	103	10108	E2,4		
23	05 28	-62	28.6	8245	200	8130	F1		
	12 51	-59	19.6	13371	24	13267	E2,5		

Positions are accurate to ± 1 in the last place given. Redshifts are heliocentric with internal mean errors. Source (S) codes: A = Arp (1981), AC = Arp and Corwin, this thesis, CE = Corwin and Emerson (1981), CT = Chincarini and Tarenghi (private communication), E1 = West (1977), E2 = Bergwall et al (1978), E3 = West and Frandsen (1981), E4 = Borchkhadze et al (1977), E5 = West et al (1978), F1 = Fairall (1979), F2 = Fairall (1981), G = Green (1978), P = Pedreros (1978), R = Rubin et al (1976), S = Sandage (1978), Sh = Shanks (private communication), W = Whiteoak (1972). Clusters from Table 2-2 or Duus and Newell (1977).

Notes: 1) N6970. 2) N6984. 3) N7014. 4) N7020 1.8' p.
 5) N7038. 6) Weak H only. 7) I5101. 8) N7124.
 9) I5110. 10) Component D; B is a star. 11) Components A, D, and E. 12) N7249. 13) Possible K and H only.
 14) I5257. 15) Possible K, H, and G only; I5272 5' sp.

is shown in Figure 3-1. In spite of the preliminary nature of the redshift survey, the distribution of the observed galaxies adequately mimics that of the Indus Supercluster galaxies and clusters as shown in Figures 2-5 and 2-9. Therefore, these galaxies will be taken as tracers of the overall distribution of matter in this area. Much more data will be needed, however, to fully delineate the structure of the Supercluster.

The data for clusters with known redshifts are summarised in Table 3-2. As mentioned in the previous chapter, however, there are other poorer clusters and groups which need redshifts to confirm their distances. For convenience, these unobserved clusters are listed in Table 3-3.

Figure 3-2 is a histogram of the redshift sample. The hatched bars represent galaxies in the prime survey area (solidly outlined in Figure 3-1) while the open bars represent galaxies in the five additional fields also included in the initial survey area (enclosed by dashed lines in Figure 3-1). Peaks in this histogram occur at around 5000 km sec^{-1} (the NGC 7014 Cloud), 12000, 16000, and $23000 \text{ km sec}^{-1}$ (and possibly at 8000 and $20000 \text{ km sec}^{-1}$). Troughs are also apparent at 6500 , 15000 , and $21000 \text{ km sec}^{-1}$. There may also be a trough at $25000 \text{ km sec}^{-1}$. This is perhaps due to selection (but see Section 5, below).

These same peaks and troughs are also apparent in the "cone" diagrams shown in Figures 3-3 and 3-4. Several filaments and chains of galaxies and clusters can be traced in these diagrams. Again, selection effects may play an important role in shaping these diagrams. More redshifts, especially in the critical range

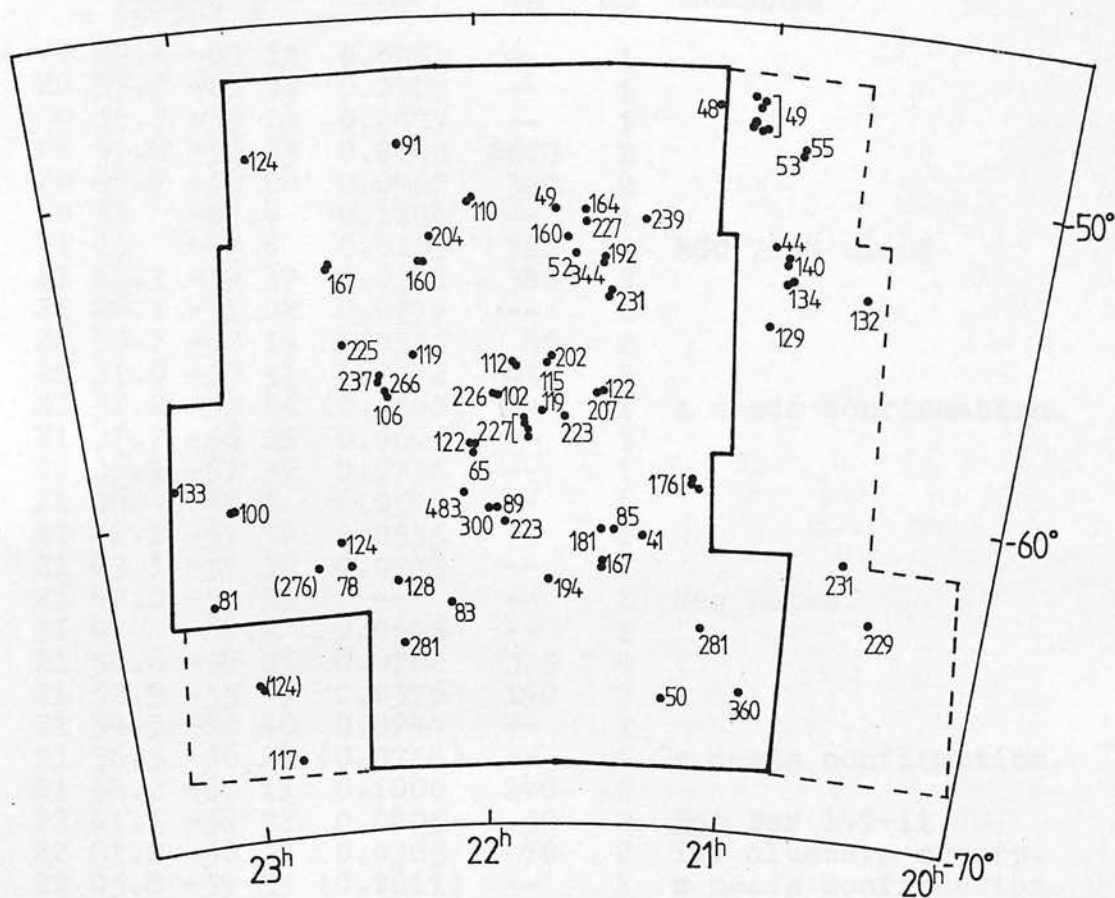


Figure 3-1. Distribution of galaxies with known redshifts in the initial (dashed outline) and prime (solid outline) survey areas. Numbers are $V \times 10^{-2} \text{ km sec}^{-1}$, in parentheses if uncertain.

TABLE 3-2 -- Cluster Redshifts

	Cluster		\bar{z}_0	σ_V	n_g	Comments
	α	(1950) δ				
20	29.1	-63 12	0.0763	--	1	
20	35.9	-61 32	0.0709	--	1	
20	36.3	-53 14	0.0439	--	1	
20	47.8	-52 55	0.0446	± 620	2	
20	48.7	-52 08	0.0467	390	2	
20	58	-65.4	0.1204	--	1	
21	05	-47.8	0.0165	322	10	NGC 7014 Cloud
21	13.1	-59 37	0.0588	380	3	
21	26.1	-51 02	0.0797	--	1	
21	30.7	-62 15	0.0555	80	2	
21	31.0	-53 51	0.0772	450	2	
21	32.2	-52 46	(0.0640)	--	1	z needs confirmation.
21	32.7	-56 25	0.0691	--	1	
21	36.1	-51 37	0.0756	--	1	
21	36	-50.9	0.0548	--	1	
21	42.1	-51 50	0.0535	--	1	
21	43.1	-57 32	0.0743	--	1	
21	47.0	-55 33	--	--	2	See Notes.
21	47	-62.4	0.0645	--	1	
21	50.6	-58 05	0.0760	375	4	
21	52.3	-55 49	0.0376	190	3	
21	54.9	-60 40	0.0744	--	1	
21	56.5	-56 24	(0.0754)	--	1	z needs confirmation.
21	58.2	-60 11	0.1000	240	2	
22	01.1	-58 22	0.0405	50	2	<u>Not</u> Ser 149-11.
22	01.2	-50 19	0.0365	70	2	Two clusters superp.
22	05.8	-59 55	(0.1611)	--	1	z needs confirmation.
22	12.7	-51 48	0.0680	--	1	
22	13.5	-52 50	0.0532	60	2	
22	18.2	-55 23	0.0396	--	1	
22	21.0	-56 44	--	--	2	See Notes.
22	21.6	-64 31	0.0941	--	1	
22	22.4	-56 05	0.0789	670	2	
22	28.5	-55 00	0.0752	--	1	
22	31.8	-52 43	0.0554	230	2	

Clusters from Abell-Corwin survey (in preparation) or from Duus and Newell (1977). n_g = number of galaxies with redshifts.

Notes: 21 47.0 -55 33, one galaxy has $z_0 = 0.0382$, the other has $z_0 = 0.0675$. 22 21.0 -56 44, one galaxy has $z_0 = 0.0355$, the other has $z_0 = 0.0886$.

TABLE 3-3 -- Nearby Indus Area Clusters
Without Known Redshifts

Cluster α (1950) δ	l	b	R	z_{est}	Source
20 34 -63.3	332.9	-36.0	(0)	0.08	STR
20 58 -48.9	350.6	-41.2	(0)	0.01	STR
20 58 -66.2	328.6	-37.8	(0)	0.08	STR
21 15.1 -53 25	344.1	-43.2	-1	0.09	AC, STR
21 18 -67.5	326.1	-39.1	(0)	0.06	STR
21 28 -67.0	326.2	-40.2	(0)	0.08	STR, BrM
21 38 -62.8	330.6	-43.0	(1)	0.08	STR
21 45 -58.5	335.5	-45.6	(1)	0.08	STR
21 57 -67.0	324.2	-42.6	(0)	0.08	STR
22 06.2 -52 04	342.5	-51.0	1	0.10	AC, BrM
22 17.0 -52 45	340.4	-52.2	0	0.10	AC, STR, BrM
22 18.0 -57 55	333.2	-49.2	-1	0.10	AC, Rose 73
22 20 -63.4	326.3	-46.7	(0)	0.06	BrM, Ser 150-02
22 26.5 -54 11	337.2	-52.7	-1	0.09	AC, STR
22 46.5 -64 39	322.0	-48.0	2	0.10	AC, STR, BrM

Sources: AC = Abell and Corwin (in preparation), STR = Duus and Newell (1977), BrM = Braid and MacGillivray (1977), Ser = Sersic (1974), and Rose (1977).
Richness (R) and redshift estimated on AC scale from data given in other sources.

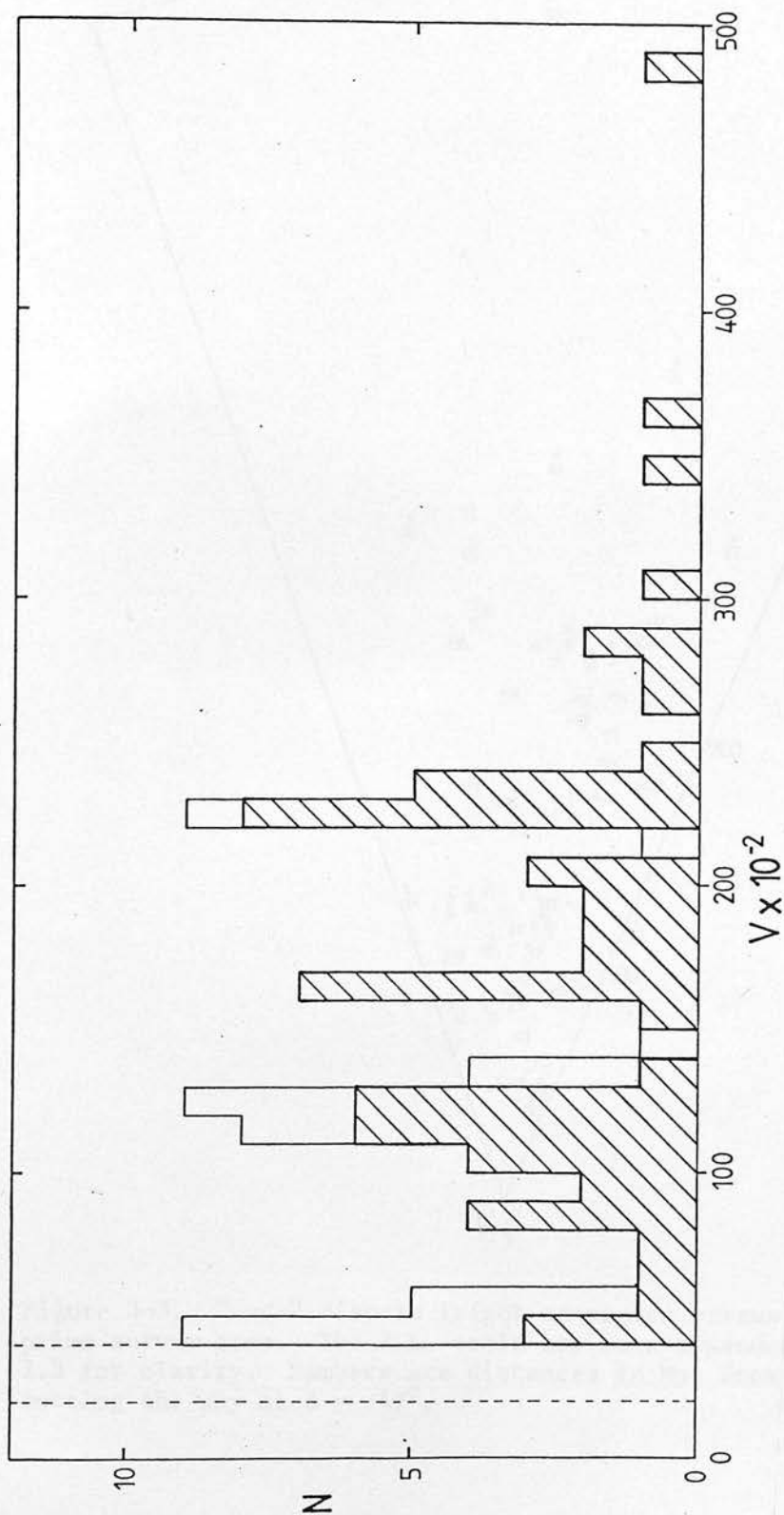


Figure 3-2. Histogram of known redshifts in the initial (open boxes) and prime (cross-hatched boxes) survey areas. The Pavo-Indus Cloud in the 2000 to 3000 km sec⁻¹ redshift range, is shown by dashed lines.

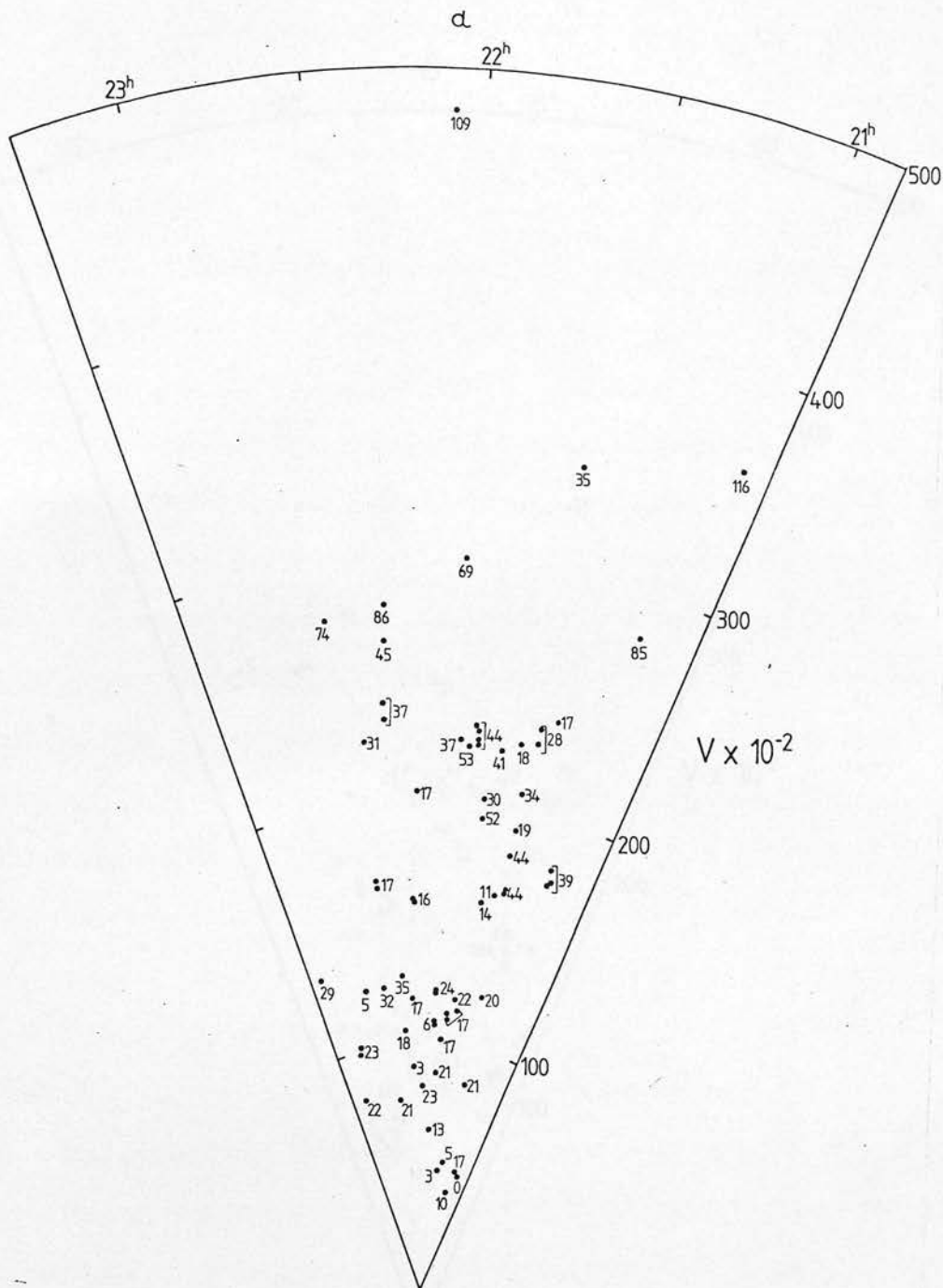


Figure 3-3. "Cone" diagram (right ascension versus redshift) for the prime survey area. The R.A. scale has been expanded by a factor of 2.3 for clarity. Numbers are distances in Mpc from a plane intersecting the sky at $\delta = -47^\circ$.

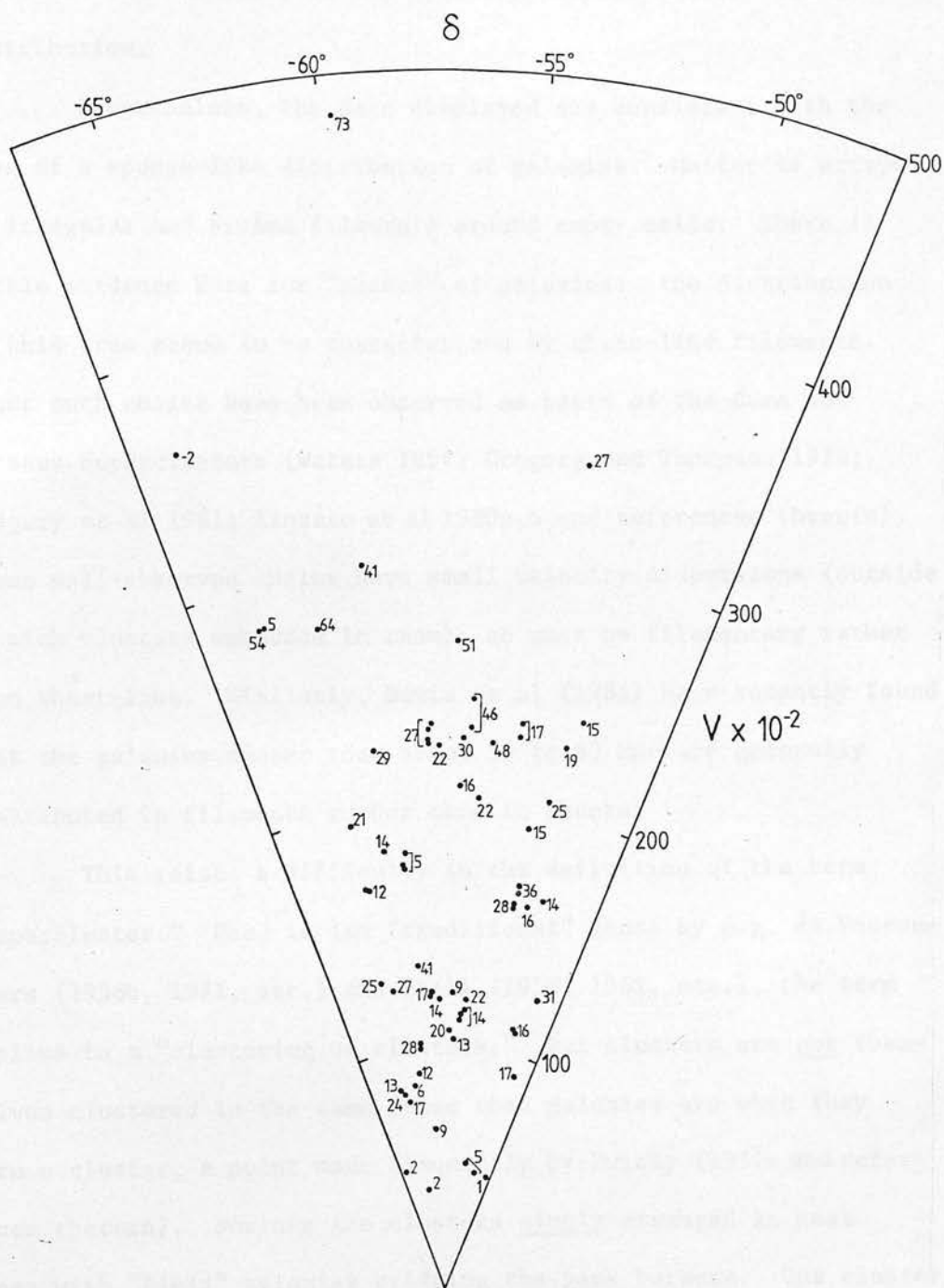


Figure 3-4. "Cone" diagram as Figure 3-3, but declination versus redshift. Numbers are distances in Mpc from a plane intersecting the sky at $\alpha = 21^{\text{h}}$.

15000 km sec⁻¹ to 25000 km sec⁻¹, would help to clarify the distribution.

Nevertheless, the data displayed are consistent with the idea of a sponge-like distribution of galaxies. Matter is arrayed in irregular and broken filaments around empty cells. There is little evidence here for "sheets" of galaxies: the distribution in this area seems to be characterized by chain-like filaments. Other such chains have been observed as parts of the Coma and Perseus Superclusters (Waters 1894; Gregory and Thompson 1978; Gregory et al 1981; Einasto et al 1980a,b and references therein). These well-observed chains have small velocity dispersions (outside of rich clusters embedded in them), so must be filamentary rather than sheet-like. Similarly, Davis et al (1981) have recently found that the galaxies nearer than about 50 to 60 Mpc are generally distributed in filaments rather than in sheets.

This raises a difficulty in the definition of the term "supercluster." Used in its "traditional" sense by e.g. de Vaucouleurs (1956b, 1971, etc.) and Abell (1958, 1961, etc.), the term applies to a "clustering of clusters." But clusters are not themselves clustered in the same sense that galaxies are when they form a cluster, a point made frequently by Zwicky (1957a and references therein). Nor are the clusters simply arranged in neat lines with "field" galaxies bridging the gaps between. One cluster may be at the intersection of two or more filaments. So, if "supercluster" is taken to mean a chain of clusters and their connecting galaxies, can their size be finite? Are "kinks" allowed in the filamentary superclusters? Are "branching" filaments parts of the same supercluster or two new ones?

There are as yet no clear answers to these (mostly semantic) difficulties. They arise almost purely from the rudimentary state of our knowledge of galaxy distribution. However, the model suggested by Einasto et al (1980a,b and references therein) in which the empty cells and their surrounding "walls" are taken as superclusters seems to match what we do know with the least strain. In this model, neighbouring superclusters share elements in common. Thus, the Perseus Supercluster and the Andromeda Supercluster share the famous Perseus-Pegasus chain (Einasto et al 1980a,b). By this model, the "Indus Supercluster" seen in Figures 2-5, 2-6, and 2-9 is actually several adjacent superclusters on the evidence of Figures 3-1, 3-3, and 3-4.

Somewhat arbitrarily, then, the "Indus Supercluster" is taken to be the complex of clusters at 22000 to 25000 km sec⁻¹. Even this breaks up into two or three sub-units on inspection. However, the entire assemblage seems to be fairly isolated in space (see also the next section) so that we can (cautiously) consider it as a "separate" unit of matter in the universe.

The mean redshift of the fourteen observed galaxies in the clusters in this redshift range is $+22930 \pm 157$ (m.e.) km sec⁻¹, standard deviation ± 587 km sec⁻¹. In the prime survey area, there are no objects closer than 3.8 standard deviations to this mean redshift other than the fourteen galaxies used to derive it. The Indus Supercluster is thus at least a statistically significant feature if not a "real" one.

V. Beyond the Indus Supercluster

Though the redshift survey carried out here reliably penetrates only to about $25000 \text{ km sec}^{-1}$, there are suggestions in the data that another 2000 to 3000 km sec^{-1} gap exists just beyond this limit. Beard (1980, private communication) has measured crude redshifts from an object prism plate for several hundred galaxies in an area of four square degrees including the rich cluster 2150.6-5805. This cluster appears on Beard's histogram of redshifts, and the gap just behind it is verified. Though only 0.005 wide in z , one would have expected the mean error in the prism redshifts ($\sigma_z = \pm 0.01$) to completely obscure this gap. Since it is still present, it must in reality be on the order of 0.01 wide in z , agreeing with the scanty information in Figures 3-2 to 3-5.

Since Beard's study covers only a small area, it too must be given rather low weight in this attempt to delineate the Indus Supercluster. However, it does offer supporting evidence from an independent source, so the present conclusion as to the extent of the Supercluster remains unchanged.

CHAPTER 4

Photometry, COSMOS Scans, and the Luminosity

Function of the Indus Supercluster

I. Introduction

Though the redshifts collected in the previous chapter constitute strong evidence for the existence of the Indus Supercluster as a reasonably isolated collection of galaxies and clusters, they can only delineate the skeleton of any structure that the Supercluster might have. In particular, there are no redshifts currently available for "field" galaxies in the Supercluster. This leaves unanswered the questions: 1) Do filamentary "bridges" of galaxies connect the rich clusters of the Indus Supercluster in space as is indicated by the distribution shown in Figure 2-9? or 2) Is the overall annular structure seen there merely an accident of projection?

A relatively straightforward answer to these questions can be obtained from the luminosity functions of selected areas in and out of the apparent density enhancements. Another more fundamental question might also be asked: Are the density enhancements seen in the eye counts real? In other words, do objective (as well as subjective) galaxy selection procedures reveal the annular structure of the Indus Supercluster?

This chapter addresses these questions.

II. Plate Material

Because of problems encountered during the on-going development of COSMOS, useable machine data was not obtained until December 1979. It was therefore decided to limit the COSMOS work to the seven U.K.Schmidt fields which contained the bulk of the Indus Supercluster. Though this would limit the amount of "field" available for comparison, it was felt that the advantages of having the "field" areas on the same plates as the "supercluster" areas would outweigh any disadvantages incurred. The plates scanned by COSMOS are indicated by asterisks in Table 2-1. Figure 4-1 shows the areas scanned superposed on Figure 2-9. Field 236 is shown in dashed outlines as the COSMOS data for it ultimately had to be discarded. Note that all of the plates finally used are copy plates; this later became important (Section VII, below).

III. The COSMOS Machine

Pratt (1977) gives a general overview of the COSMOS measuring machine. It has also been discussed and used extensively for galaxy photometry by e.g. Pickup (1979), Smyth (1980), and MacGillivray and Dodd (1980a and references therein). Its operation and performance current at the time of the present study (December 1979 to June 1980) are discussed by Stobie et al (1979) and by Dodd et al (1979). Interested readers are advised to turn to those articles and others cited therein for a full description of COSMOS, though a brief description is included here for the reader's convenience.

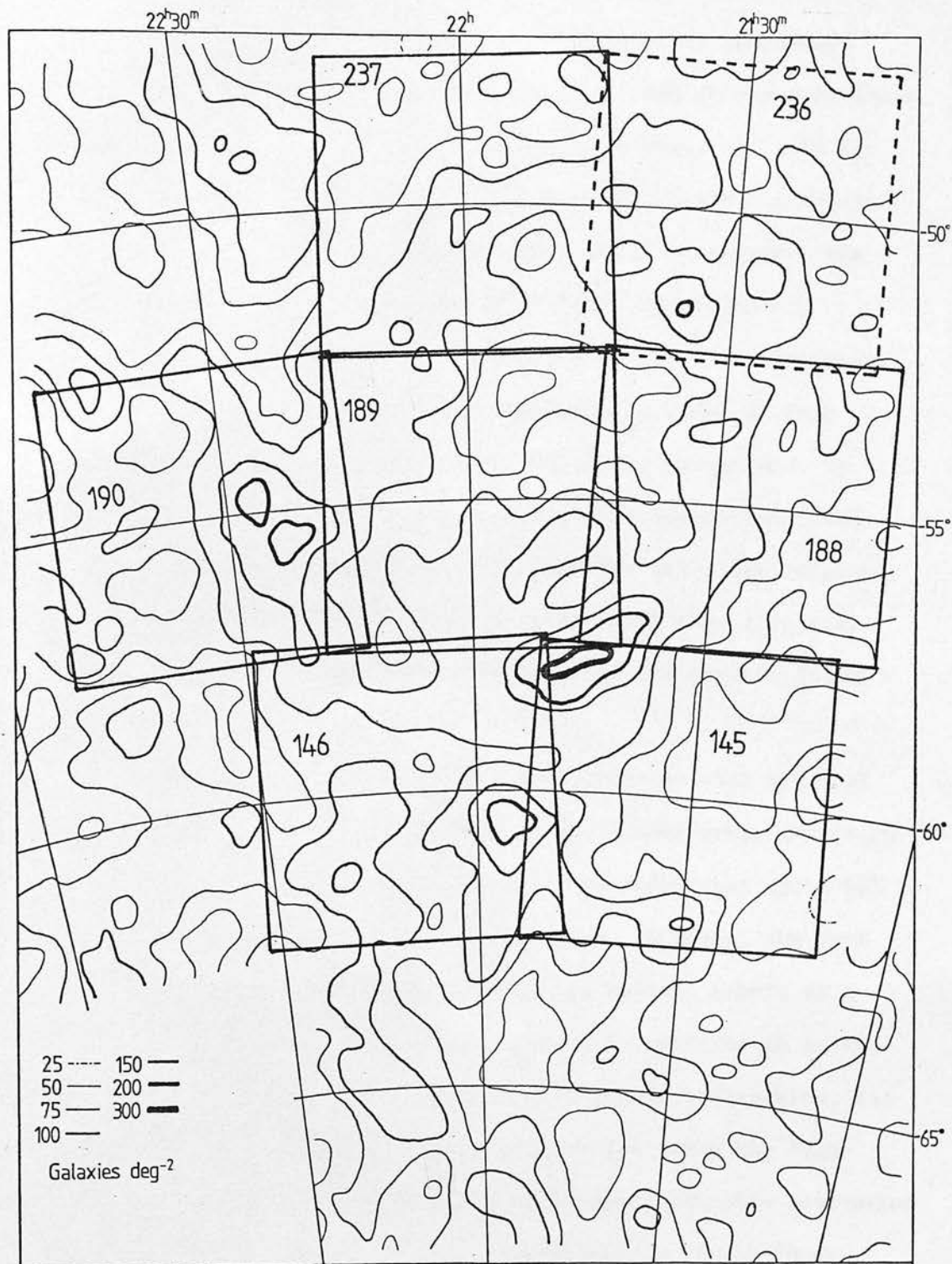


Figure 4-1. Approximate outlines of fields scanned by COSMOS (the COSMOS survey area) superposed on Figure 2-9.

As the plate is moved in the y-direction by the COSMOS plate carriage, a flying spot generated by a cathode ray tube scans a one millimetre "lane" of the plate in the x-direction. In its thresholded mapping (TM) mode, COSMOS is controlled by an online microprocessor using a thresholding algorithm. In essence, the algorithm samples an area of the plate (here 1 mm square or 5 mm x 1 mm) and, by examining a histogram of pixel transmissions, determines the mean sky background transmission level of that area. A preselected threshold, here 10% of the background, is applied to the data and only those pixels of transmissions less than the threshold are selected. The data for the selected pixels are then output to magnetic tape for further off-line analysis. The scanning process takes about 18 hours for the central 250 mm x 250 mm area of a UK Schmidt plate.

The plates were scanned in 8 μm increments with the spot defocused to a nominal 32 μm . Tests by the COSMOS group (Williams and Stobie 1980, private communication) have shown that about 60% of the light is within the nominal spot size. However, the spot is still detectable 16 millimetres from its centre, albeit at a very low level. This broad aureole (generally referred to as the spot "halo") is masked by a 3 mm wide slit in the y-direction, but cannot be masked effectively in the x-direction since the high-speed operation of COSMOS depends on rapid electronically controlled motion of the flying spot. This is undoubtedly a factor in determining the limited density range that COSMOS can measure ($\Delta D \approx 2$), though the 128 step digitization of the analogue signal from the photomultiplier also imposes limits.

Off-line processing of the thresholded data is handled by an algorithm designed and implemented by Lutz (1979) that detects images in the thresholded data. After joining those images that straddle lane boundaries, several image parameters are calculated from the zero, first, and second moments of the pixel distribution within the image. Those parameters that are used in this study are listed in Table 4-1. Image parameters are stored on magnetic tape which may then be used as an input medium for further processing and study.

IV. Relative Calibration of UK Schmidt Plates

Each Schmidt plate used carried on it two seven-step calibration "wedges," one near the north edge of the plate, the second near the east edge. Relative calibration of the plates was made using only the east wedge.

In order that the transmission levels measured by COSMOS be converted first to density, then to intensity, the step wedges were scanned and the transmission readings converted to the so-called "Baker density" through the equation

$$\omega = [(t_o - t_b)/(t - t_b)] - 1 \quad (4-1)$$

where t_o is the transmission of a clear plate area, t_b is the "transmission" of an opaque plate area (i.e. it is a measure of machine noise), and t is the measured transmission to be converted to density.

A plot of $\log \omega$ versus $\log I$, the relative step wedge intensity (provided by the UK Schmidt Unit) will generally be linear for densities up to 2 or 3, at least for photographic plates

TABLE 4-1 -- COSMOS IAM Parameters Used

X_I	} Intensity-weighted rectangular coordinates
Y_I	
a_u	} Unweighted major and minor axes
b_u	
Area	Total image area within a_u , b_u
m_{raw}	$-250 \log (\sum I - I_{sky})$
I_{sky}	Sky intensity interpolated to image centroid

in general use before about 1970 (see e.g. Baker 1925, de Vaucouleurs 1968). Unfortunately, experience showed that this characteristic curve is not linear for the fine-grained IIIa-J emulsion used here (Dawe 1980, unpublished). The several characteristic curves for the plates used in this study are superposed in Figure 4-2 which confirms Dawe's finding of non-linearity.

However, the COSMOS scanning procedure required a linear characteristic for conversion of the measured transmission t to the "Baker density" ω . The actual linear approximations used are superposed on the measured points in Figure 4-2. Except at relatively high or low densities, these linear approximations are adequate. The slopes of the linear characteristics, Γ ($= 1/\gamma$, where γ is the slope of the "linear" part of the so-called "H and D" characteristic curve, $\log D$ vs $\log I$) are listed below in Table 4-3. They are not unusual for IIIa-J plates (M. E. Sim 1980, private communication).

The slopes may have been slightly influenced by one incorrect $\log I$ value for the least dense step wedge. This point, shown by crosses in Figure 4-2, was in use during 1978 to mid-1980. Recent measurements of the sensitometer steps (K. P. Tritton 1980 private communication) confirmed all the values of $\log I$ except the faintest. The history of the $\log I$ measurements, from various UKSTU newsletters and circulars, is given in Table 4-2. Except for the one measurement for step 7 in 1977, there is no evidence of significant changes in the step wedges from 1972 to 1980. In general, the COSMOS operator ignored the faintest point when estimating the linear approximation to the characteristic curve. However, slight inaccuracies introduced by this incorrect point may

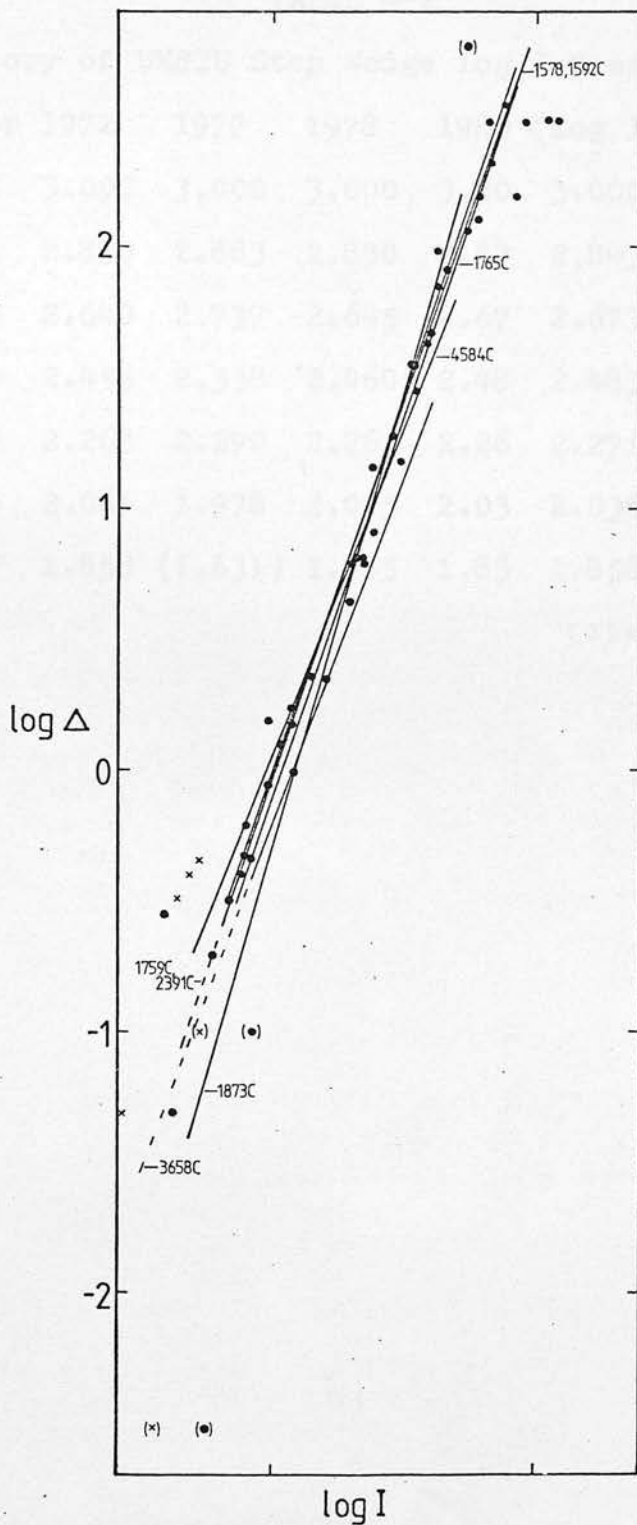


Figure 4-2. Relative calibration curves for plates scanned by COSMOS. Curves were superposed by shifting in $\log I$ axis only. Uncertain points are in parentheses, the points affected by the one incorrect $\log I$ value are shown as crosses, and the adopted linear calibration curves are labeled with their plate numbers.

TABLE 4-2

History of UKSTU Step Wedge log I Measurements

Step	1972	1977	1978	1980	$\langle \log I \rangle$	σ
1	3.000	3.000	3.000	3.00	3.000	--
2	2.830	2.883	2.830	2.83	2.843	± 0.027
3	2.640	2.737	2.645	2.67	2.673	0.045
4	2.455	2.538	2.460	2.48	2.483	0.038
5	2.268	2.290	2.265	2.26	2.271	0.013
6	2.061	1.978	2.075	2.03	2.036	0.043
7	1.858	(1.631)	1.885	1.83	1.858	0.028

$\langle \sigma \rangle = \pm 0.032$

have had some influence on the magnitudes of the objects measured on the plates.

Once the characteristic curves were known, the plates were scanned by COSMOS as outlined above. The various image parameters were found, and the tape with the parameters was given to the writer for analysis.

V. Absolute Calibration of Galaxy Magnitudes

A. Introduction and Photoelectric Photometry

Three different sets of magnitudes in the COSMOS measures need to be calibrated against photometric standards. These are:

- 1) The limiting isophote μ_ℓ to which the COSMOS measures of diameters and magnitudes refer (this is a surface brightness),
- 2) The background sky level m_J^S (this is also a surface brightness), and
- 3) The COSMOS magnitudes themselves m_J (measuring the brightness of an image within its limiting isophote).

The photometric standards used here were nineteen galaxies within the initial survey area which were measured by Corwin (1980; Appendix B of this thesis). The measurements and reductions are fully explained in Appendix B. A few brighter galaxies with published photometry were also used.

B. Magnitude Systems

Because the IIIa-J plates cover a broader wavelength range than do the standard filters of the UBV system in which the

photoelectric photometry was done, a transformation between the two systems was needed. Though several studies have derived the transformations for stellar data (e.g. Konzitas 1977, Kron 1980), none have yet done so for the composite spectra of galaxies. It is well-known that these composite systems require different transformations than do stars (see e.g. de Vaucouleurs 1961, Sandage and Visvanathan 1978).

Havlen and Quintana (1979) and Kron (1980) have published data from which the transformation coefficient in

$$m_J = B + a(B - V) \quad (4-2a)$$

may be estimated. Figure 4-3 is a plot of the residual $B - m_J$ versus $B - V$ colour index. The solid line is an impartial least squares solution

$$B - m_J = -0.21 + 0.34(B - V), \quad \sigma = \pm 0.04$$

$$\pm 0.04 \quad \pm 0.04$$

The transformation coefficient is well-determined and is significantly larger than that found for stars ($a_{\text{stars}} = -0.23$). Therefore, in what follows,

$$m_J = B - 0.35(B - V) \quad (4-2b)$$

shall be adopted for galaxies of all types. (Note that transformations to/from other m_J systems such as that used by Oemler (1974) do not apply to the IIIa-J plates used here.)

C. Limiting isophote, μ_ℓ

The following information is needed to find the limiting isophote corresponding to the threshold cut used:

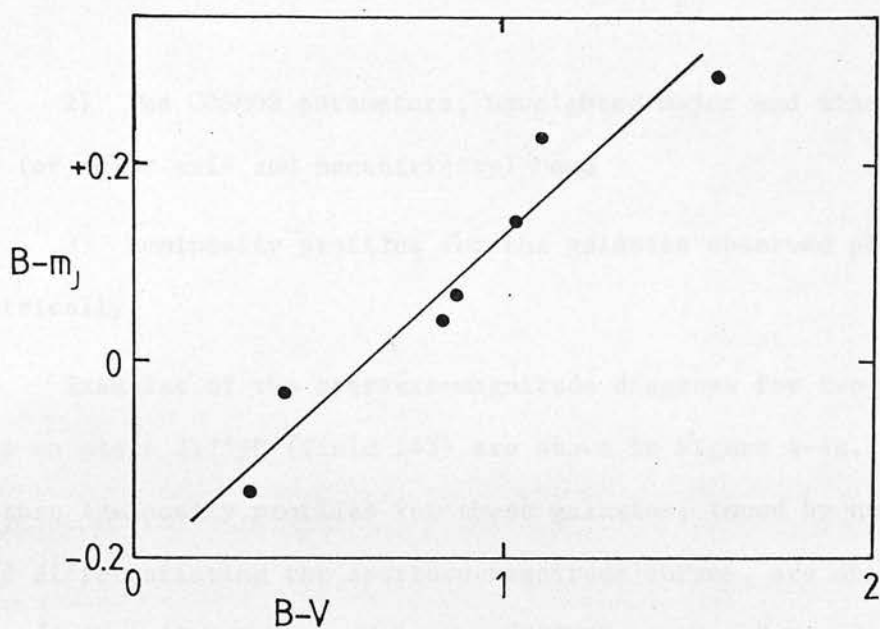


Figure 4-3. Relationship between standard B magnitudes and magnitudes from IIIa-J plates (plus GG385 or 395 filter) as a function of B-V for galaxies. The solid line represents the impartial solution $B - m_J = -0.21 + 0.34(B-V)$.

1) Aperture-magnitude diagrams for as many galaxies as possible which were also measured by COSMOS on the plate in question

2) The COSMOS parameters, unweighted major and minor axes (or major axis and eccentricity) and

3) Luminosity profiles for the galaxies observed photoelectrically.

Examples of the aperture-magnitude diagrams for two galaxies on plate J1759C (Field 145) are shown in Figure 4-4a. The aperture luminosity profiles for these galaxies, found by numerically differentiating the aperture-magnitude curves, are shown in Figure 4-4b. Also indicated is the "COSMOS aperture" A_u , defined as follows:

$$\log A_u = \log D_u - 0.5 \log R_u \quad (4-3)$$

where D_u is the unweighted major axis measured by COSMOS, and

$$R_u = D_u / d_u = 1 / (1 - e_u)$$

where d_u is the unweighted minor axis and e_u the unweighted eccentricity. Equation (4-3) gives an "aperture" of the same area as is contained in the COSMOS image, assuming the COSMOS image to be elliptical. Though equation 4-3 is strictly applicable only to thin disk models of galaxies, a solution for the empirical coefficient of $\log R$ gave 0.48 ± 0.03 . The sample included over 100 galaxies with $0 \leq \log R_{25} \leq 0.8$, with well-determined diameters D_{25} at the 25.0 mag sec⁻² isophote, and with A_{25} derived from aperture luminosity profiles such as those shown in Figure 4-4b. Though

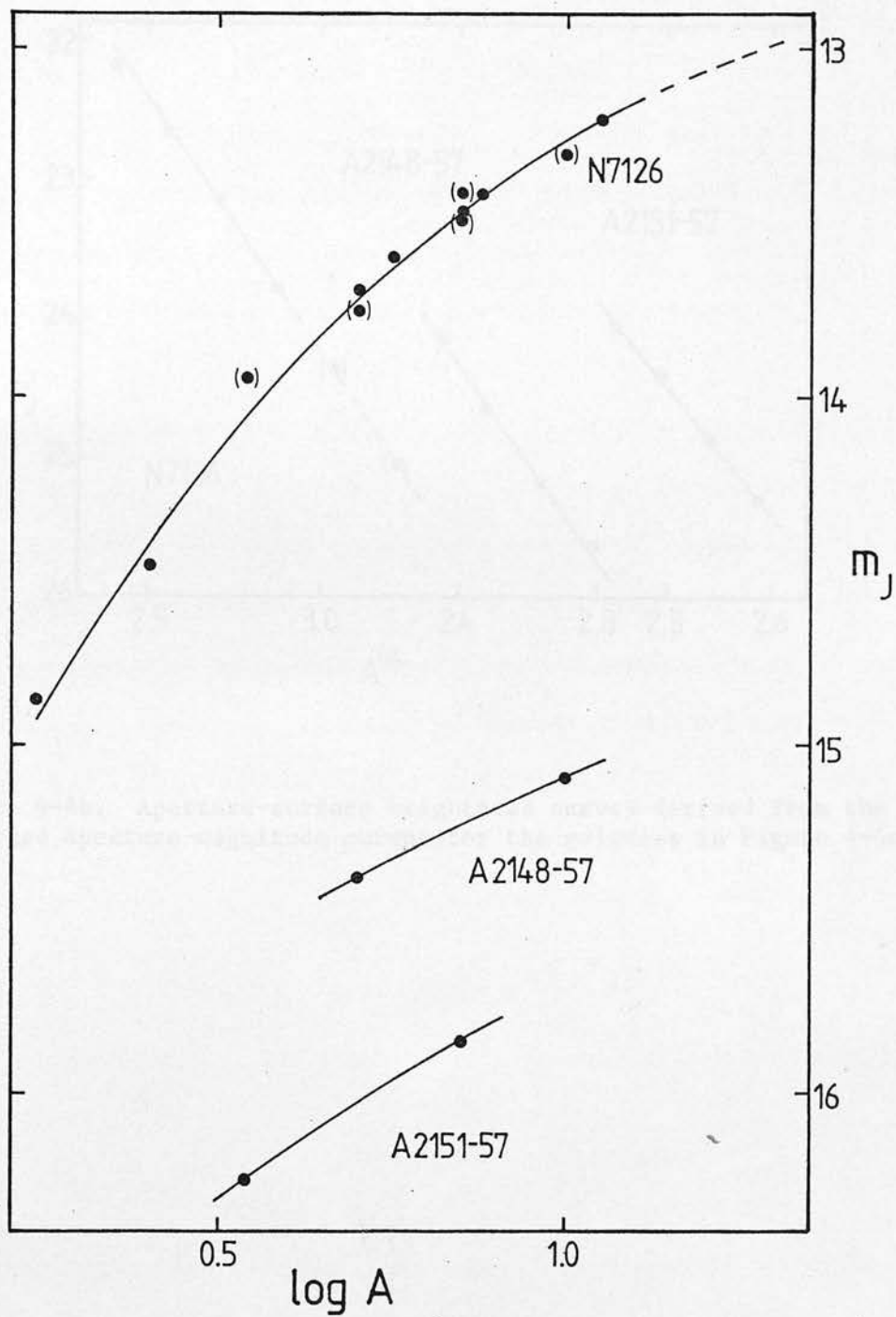


Figure 4-4a. Aperture-magnitude curves for three photoelectrically observed "standard" galaxies.

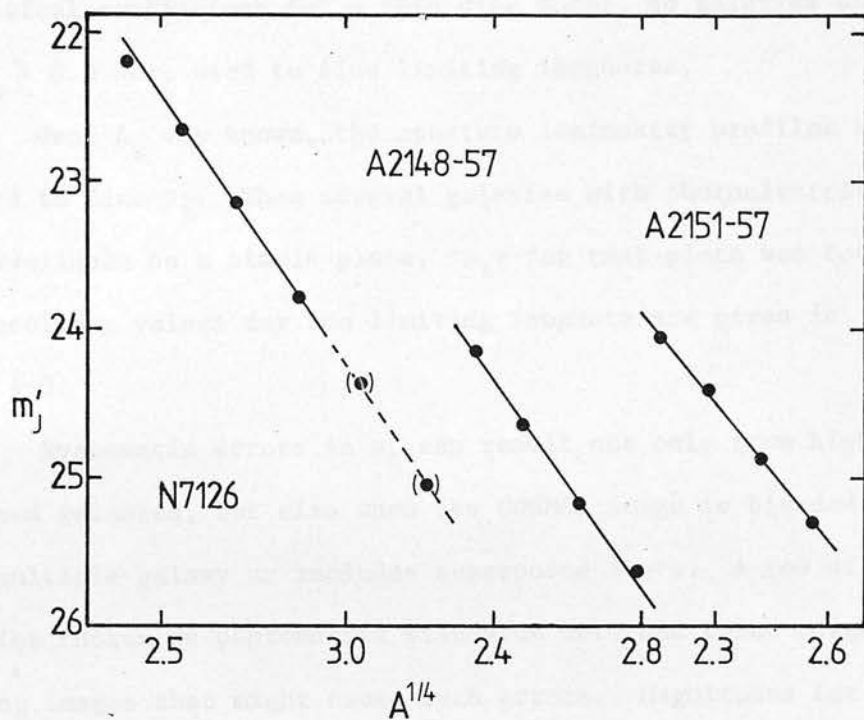


Figure 4-4b. Aperture-surface brightness curves derived from the smoothed aperture-magnitude curves for the galaxies in Figure 4-4a.

the empirical coefficient is not significantly different from the theoretical coefficient for a thin disk model, no galaxies with $\log R_u > 0.3$ were used to find limiting isophotes.

Once A_u was known, the aperture luminosity profiles were entered to find μ_ℓ . When several galaxies with photoelectric data were available on a single plate, $\langle \mu_\ell \rangle$ for that plate was found. The resulting values for the limiting isophote are given in Table 4-3.

Systematic errors in μ_ℓ can result not only from highly inclined galaxies, but also when the COSMOS image is blended, i.e. is a multiple galaxy or includes superposed stars. A few of the galaxies chosen as photometric standards here had faint neighbouring images that might cause such errors. Magnitudes for these neighbouring images were estimated with a calibrated step scale (Section V-F below) and were subtracted from the COSMOS magnitude. The largest change in magnitude from this procedure was $\Delta m = 0.07$, well within the systematic mean errors in the COSMOS data.

D. Sky Background Level, m_J^S

The sky background level is simply related to the threshold cut T by

$$m_{JP}^S = -2.5 \log (T^{-1} 10^{-0.4 \langle \mu_\ell \rangle}) \quad (4.4)$$

These values compare reasonably well with the sky values from the UK Schmidt night sky photometer. The mean difference is -0.02 ± 0.17 (m.e.) with a standard deviation of ± 0.47 , or $+0.10 \pm 0.14$ and ± 0.38 with the largest difference (-0.81 for plate J3658C, field 237) rejected. Note that the night sky photometer was pointed at the

TABLE 4-3

Parameters for Plates Scanned by COSMOS

Plate	Field	Γ	$\langle \mu_g \rangle$	m_{JP}^S	m_{JNS}^S	m_{JSB}^S	m_{JSS}^S
1578	145	0.32	24.30 ± 0.04	22.17	22.67	22.15	---
1592C	188	0.36	25.0	22.5	22.48	22.5	22.15
1759C	145	0.34	24.95 ± 0.07	22.45	22.87	22.50	22.20
1765C	190	0.32	24.81 ± 0.12	22.31	---	22.30	21.90
1873C	146	0.29	25.3	22.8	22.31	22.3	21.90
2391C	236	0.35	25.3	22.8	22.68	22.4	---
3474	189	0.41	25.0	22.5	22.41	22.4	---
3658C	237	0.24	25.6 ± 0.4	23.1	22.29	22.8	22.50
4584C	189	0.41	24.9	22.4	22.87	22.9	22.60
			$\langle m_J^S \rangle =$	22.56	22.57	22.47	22.21
			$\sigma_n =$	± 0.10	± 0.08	± 0.08	± 0.12
			$\sigma_1 =$	± 0.29	± 0.23	± 0.24	± 0.29

m_J^S = night sky brightness, mag sec⁻¹, from:

P -- photoelectric galaxy photometry

NS -- night sky photometer

SB -- magnitude residual - surface brightness relationship (equation 4-8)

SS -- step scale calibration.

south celestial pole during the period when the plates were taken, and that the recorded sky brightness readings must be corrected for a slow drift in the "standard" source in the photometer (see the UKSTU Newsletter No. 3, June 1981, for details). Thus, perfect agreement cannot be expected between these two estimates of the sky background.

Two other estimates of the sky background are available. These are discussed below in the next two sections.

E. Systematic Errors in m_J

Once the sky background is known, the raw COSMOS magnitude,

$$m_{\text{raw}} = -250 \log \left[\sum_i (I_i - I_{\text{sky}}) \right] \quad (4-5a)$$

can be converted to a "true" magnitude through

$$m_I = (m_{\text{raw}}/100.0) + 2.5 \log I_{\text{sky}} + 2.5 \log \left\{ [(1000)/PS]^2 \right\} \quad (4-5b)$$

where I_{sky} is the background intensity interpolated to the centre of the image, P is the plate scale ($= 67.14 \text{ arcsec mm}^{-1}$) and S is the COSMOS step size (increment) in microns ($= 8 \text{ } \mu\text{m}$ here). The observed m_J magnitude is then just

$$m_J = m_I + m_J^S \quad (4-6)$$

It is necessary to examine m_J for systematic errors. This was done by comparing it with the m_{JP} photoelectric magnitudes for the standard galaxies. The aperture-magnitude curves for these objects (Fig. 4-4a) were entered at the COSMOS aperture A_u to find the corresponding m_{JP} . The residuals $\Delta m_J = m_J - m_{JP}$ were then examined for systematic errors due to e.g. galaxy type, surface brightness, axis ratio, etc.

Only surface brightness proved to be systematically correlated with Δm_J . This is shown in Figures 4-5a and b where

$$m'_J = m_J + 5 \log D_u - 2.5 \log R_u - 5.26 \quad (4-7)$$

$$m'_{JP} = m_{JP} + 5 \log A_u - 5.26$$

are the surface brightnesses from COSMOS and photoelectric photometry, respectively. Note that D_u and A_u are expressed in tenths of arc minutes, as in RC1 and RC2. The solid line in Figure 4-5a represents

$$\Delta m_J = m_J - m_{JP} = 0.12 - 0.58(m'_J - 14.2), \sigma = \pm 0.062$$

$$\pm 0.02 \quad \pm 0.07 \quad . \quad (4-8)$$

The slope of this relationship has been confirmed by data from photometry of galaxies in the Hercules Cluster (MacGillivray and Corwin, unpublished) where much more photoelectric photometry exists (Buta and Corwin, in preparation) than for the plates used here. The zero point is entirely dependent on the value of the sky background. A change of sky brightness of -0.1 mag would cause the relationship to change as shown by the dashed lines in Figure 4-5. Therefore, this relationship is capable of providing yet another estimate of the sky background brightness. The values so derived are given in Table 4-3, and were used to minimize the scatter in equation 4-8 above.

Note that the relationship is much steeper for the COSMOS data than for the photoelectric data. This comes about through the

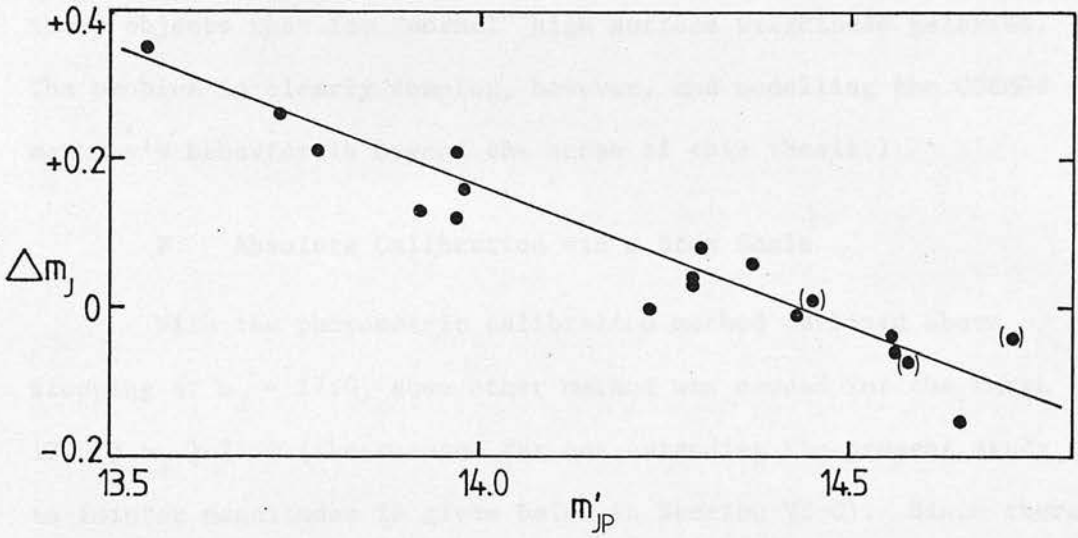
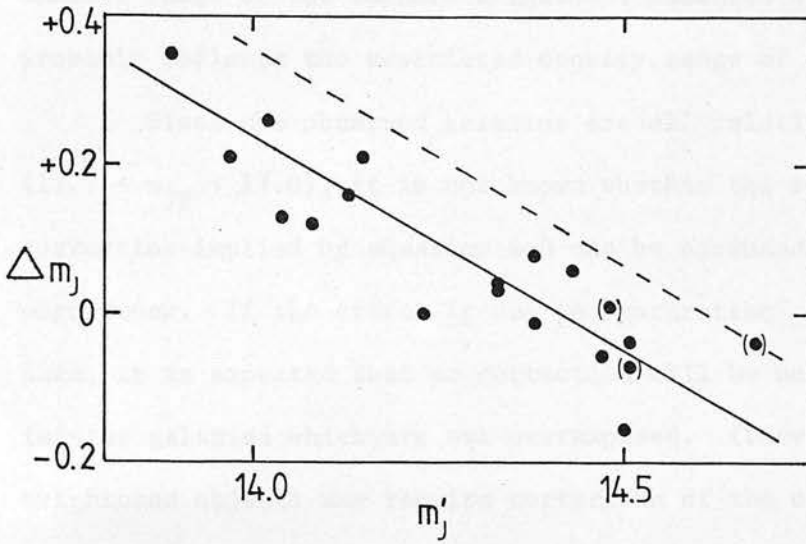


Figure 4-5. $\Delta m_J = m_J - m_{JP}$ as a function of surface brightness as measured by COSMOS (top) and photoelectrically (bottom). The solid lines are the adopted impartial solutions and the dashed line shows the effect of changing the sky background level by $+0.1$ magnitude.

smaller range of the surface brightness measured by COSMOS and probably reflects the restricted density range of the machine.

Since the observed galaxies are all relatively bright ($12.7 < m_{JP} < 17.0$), it is not known whether the surface brightness correction implied by equation 4-8 can be extended to fainter magnitudes. If the effect is due to "saturation" in the COSMOS data, it is expected that no correction will be necessary for fainter galaxies which are not overexposed. (Very low surface brightness objects may require correction of the opposite sign as light in the COSMOS aureole will contribute to the signal more for these objects than for "normal" high surface brightness galaxies. The problem is clearly complex, however, and modelling the COSMOS machine's behavior is beyond the scope of this thesis.)

F. Absolute Calibration via a Step Scale

With the photometric calibration method outlined above stopping at $m_J \approx 17.0$, some other method was needed for the range $17.0 \lesssim m_J \lesssim 21.0$ (the reasons for not extending the present study to fainter magnitudes is given below in Section VI-C). Since there is no photometry in this range in any of these fields, an indirect method had to be used.

As mentioned in Chapter 2, Prof. Abell and the writer are currently engaged in extending the rich galaxy cluster survey (Abell 1958) to the south celestial pole using the IIIa-J plates. As in the 1958 work, magnitudes are being estimated with step scales of galaxy images. The step scale being used by the writer is composed entirely of elliptical galaxy images. A calibration curve for this step scale was built up by estimating step readings

(to one-tenth of a step) for galaxies in the central thirty-six square degrees of the Virgo Cluster as seen on UK Schmidt plate J2137. Many galaxies to $m_J \sim 14.0$ in this field have well-determined total magnitudes listed by de Vaucouleurs and Head (1978). These are in the system of RC2, but with the addition of data from other sources and with a small systematic error depending on inclination removed (see de Vaucouleurs and Corwin 1977 and de Vaucouleurs et al 1977).

In the poorly observed range $14.0 \lesssim m_J \lesssim 17.0$, a large portion of the photoelectric calibrating data come from Appendix B. The data for the 19 Indus area galaxies plus one galaxy in A2670 act as secondary standards in this range.

The calibration at fainter levels rests on photoelectric observations of three galaxies in the galaxy cluster A1553 by Sandage (1972), and on photoelectrically calibrated photographic photometry of galaxies, stars, and globular clusters around M87 by Hanes (1975, 1977). Hanes' work verifies earlier photographic photometry of objects around M87 by Racine (1968) and Ables et al (1974).

The mean errors in the calibrating data at all magnitude levels are better than $\sigma_{B,V} \approx \pm 0.15$. However, systematic errors in estimating step-scale readings depend on surface brightness. Low surface brightness objects are generally estimated too faint because "integration" by eye of the light in the object's image is difficult (this is the primary reason for surface brightness dependent errors in the survey photometry of Shapley and Ames 1932 and in the CGCG. See Holmberg 1958, de Vaucouleurs 1957, de Vaucouleurs and Pence 1979, and Corwin 1979 for details). Similarly,

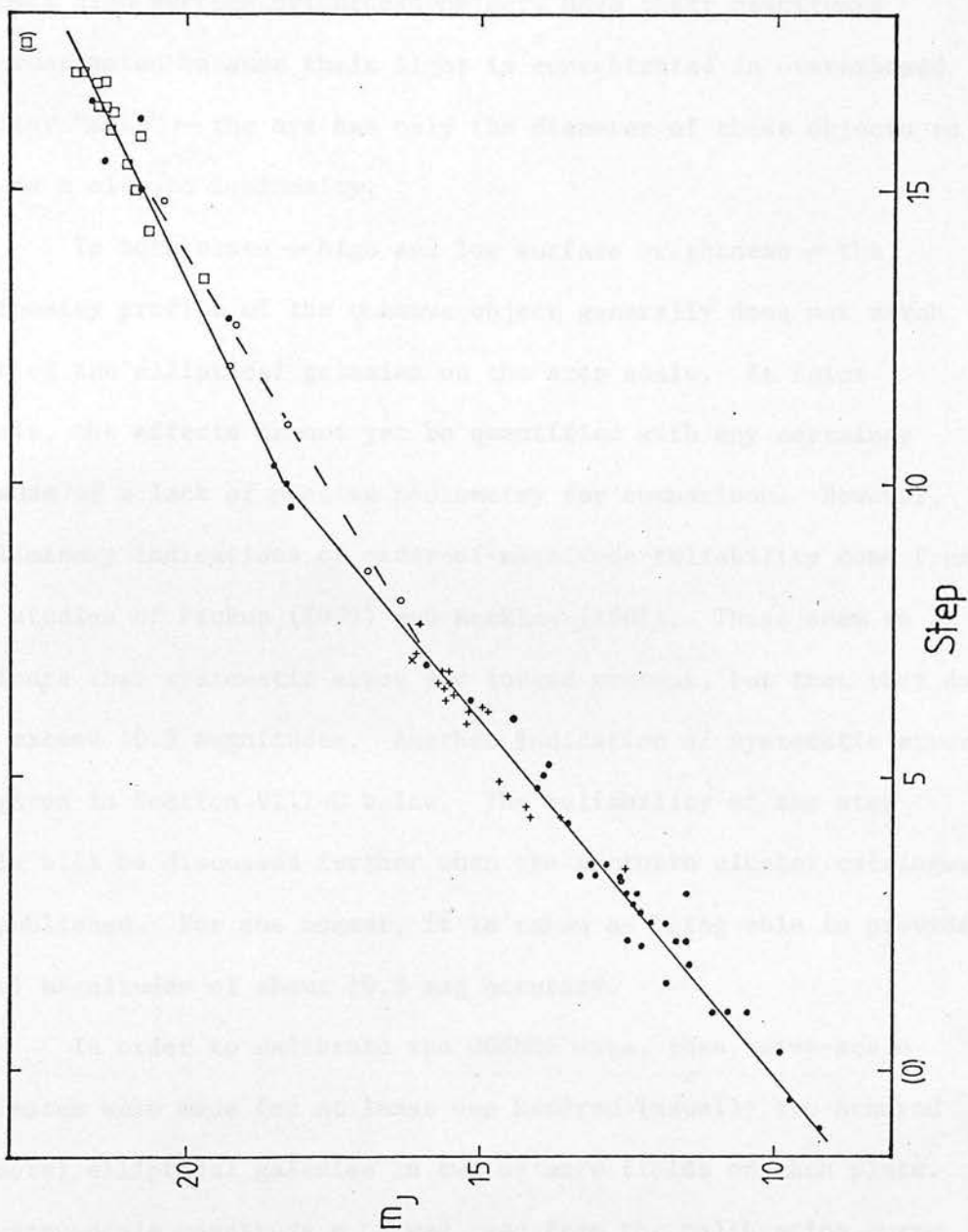


Figure 4-6. Step scale calibration curve. Dots are photoelectrically (step < 12) or photographically (step > 12) observed galaxies in the Virgo Cluster area (prime calibrators), plus signs are photoelectrically observed galaxies in the Indus area (secondary calibrators), the cross is a photoelectrically observed galaxy in A2670 (see Appendix B), the open squares are photographically observed globular clusters around M87, and the open circles are photographically observed stars near M87. The adopted calibration curve is shown by the solid lines; the dashed line is a possible alternative calibration for stars.

compact high surface brightness objects have their magnitudes underestimated because their light is concentrated in overexposed stellar "dots" — the eye has only the diameter of these objects to use as a clue to luminosity.

In both cases — high and low surface brightness — the luminosity profile of the unknown object generally does not match that of the elliptical galaxies on the step scale. At faint levels, the effects cannot yet be quantified with any certainty because of a lack of precise photometry for comparison. However, preliminary indications of order-of-magnitude reliability come from the studies of Pickup (1979) and Hawkins (1981). These seem to indicate that systematic errors are indeed present, but that they do not exceed ± 0.5 magnitudes. Another indication of systematic error is given in Section VIII-C below. The reliability of the step scale will be discussed further when the southern cluster catalogue is published. For the moment, it is taken as being able to provide total magnitudes of about ± 0.5 mag accuracy.

In order to calibrate the COSMOS data, then, step-scale estimates were made for at least one hundred (usually two hundred or more) elliptical galaxies in two or more fields on each plate. The step-scale magnitude m_{JSS} was read from the calibration curve (Figure 4-6) and simply plotted against m_{T} (eq. 4-5b). The calibration plot for plate J3658C is shown as Figure 4-7. This plate is atypical in that it has fewer calibrating galaxies in the range $14.0 < m_{\text{JSS}} < 18.0$ and more galaxies at $m_{\text{JSS}} > 18.0$ than average, but it demonstrates the characteristics of the other calibration plots. The entirety of the data from all six plates finally used are superposed in Figure 4-8. The calibration adopted is shown by

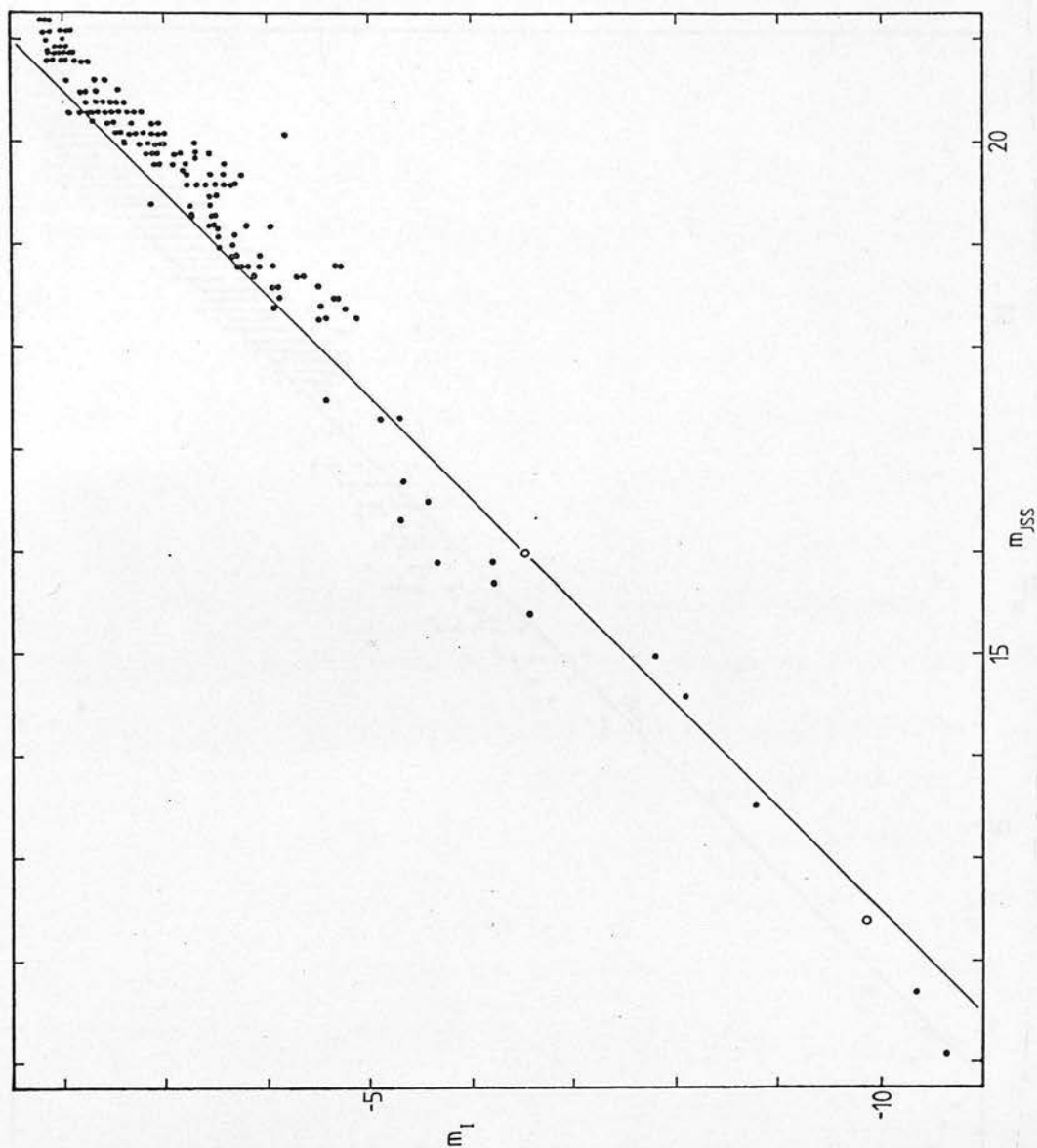


Figure 4-7. Step scale magnitude versus COSMOS magnitude for plate J3658C. Photoelectrically observed "standard" galaxies are shown by open circles. The 45° solid line is the adopted calibration.

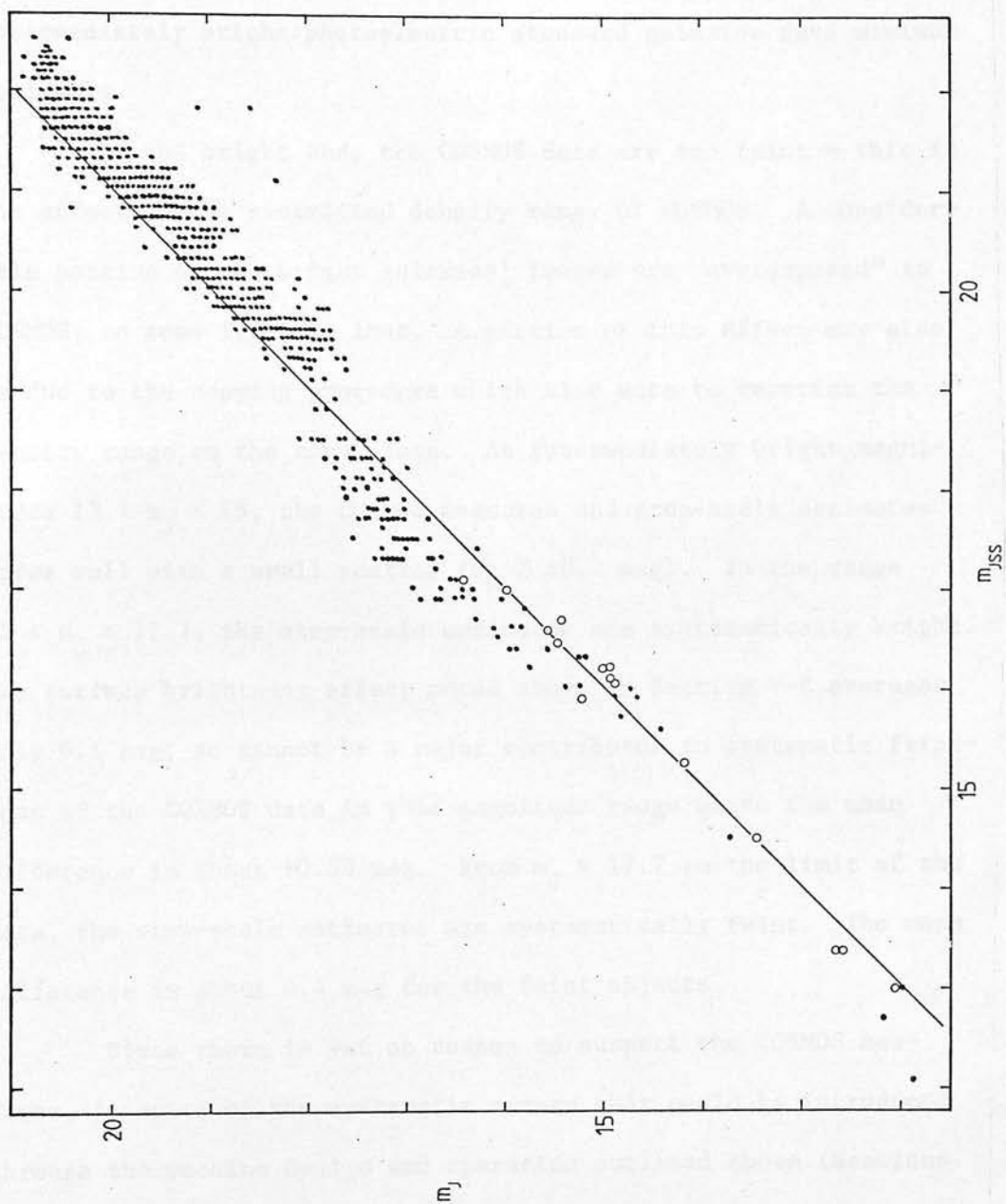


Figure 4-8. Same as Figure 4-7, but plates J1592C, J1759C, J1765C, J1873C, and J4584C added.

the solid line of slope 1.0. It was fitted to the data so that the intermediately bright photoelectric standard galaxies gave minimum residuals.

At the bright end, the COSMOS data are too faint — this is the effect of the restricted density range of COSMOS. A considerable portion of the bright galaxies' images are "overexposed" to COSMOS, so some light is lost. A portion of this effect may also be due to the copying procedure which also acts to restrict the density range on the copy plate. At intermediately bright magnitudes $13 < m_J < 15$, the COSMOS measures and step-scale estimates agree well with a small scatter ($\sigma_m \approx \pm 0.2$ mag). In the range $15 < m_J < 17.7$, the step-scale estimates are systematically bright. The surface brightness effect noted above in Section V-E averages only 0.1 mag, so cannot be a major contributor to systematic faintness of the COSMOS data in this magnitude range where the mean difference is about +0.35 mag. From $m_J = 17.7$ to the limit of the data, the step-scale estimates are systematically faint. The mean difference is about 0.4 mag for the faint objects.

Since there is yet no reason to suspect the COSMOS measures, in spite of the systematic errors that could be introduced through the machine design and operation outlined above (Sections III and IV), the systematic errors here will be attributed to the step scale. Some indirect support for this conclusion comes from noting that very few magnitude estimates are made with the galaxy image at step 10 on the step scale. This image is more compact and more obviously elongated than the other step-scale images. The only direct evidence however of a systematic error in the step-scale estimates comes from Hawkins (1981). (Pickup 1979 used

another step scale in her study, so her results, though also indicating a systematic error, cannot be applied to the present problem.) Hawkins' work suggests the step-scale estimates to be too bright by 0.21 mag at the faint end ($18 < m_J < 22$). In the face of this contradiction, it can only be concluded that a) estimating magnitudes for faint ($m_J > 18$) galaxies by means other than photoelectric photometry or photoelectrically calibrated photometry is still subject to systematic errors of up to ± 0.5 mag; and b) that while the faint COSMOS magnitudes may contain such systematic errors, there is as yet no way of detecting them with the data available here.

Therefore, it will be assumed in the remainder of this thesis that the COSMOS magnitudes are correct (exclusive of zero-point) with errors on the order of $\sigma_m \approx \pm 0.15$ to ± 0.2 mag (Dodd et al 1979, MacGillivray 1981 private communication). Furthermore, the calibration as indicated by Figure 4-8 shall be adopted until evidence indicates otherwise. The implied values of the sky background are listed in Table 4-3. They are generally brighter than the other estimates probably because the step-scale magnitudes are calibrated against total magnitudes, while the COSMOS data are isophotal.

VI. COSMOS Data Processing

A. Introduction: Special Acknowledgement

The computer software used in the data processing described in this section was primarily written by Dr. H. T. MacGillivray. I am very grateful to him for permission to use his programs, and

I am also grateful for his help with the programs which he freely gave. A few generally available COSMOS user's routines were also used here, and I am indebted to the various members of the COSMOS group for their help with these programs.

B. Preprocessing: Removal of Bright Stars, Satellite and Meteor Trails

In areas around bright stars where the density of the sky background changes rapidly, the background following algorithm cannot cope adequately with the steep density gradients. The result is the detection of a halo of images around the star. Ghost images of bright stars are also often detected. These effects are shown in Figures 4-9 a, b and c which also show satellite trails detected as lines of highly elliptical images.

Most of these false images are of moderate to low surface brightness. This means that they will be detected as galaxies in the star-galaxy separation procedure used (see Section VI-C below). It thus becomes necessary to remove them. To do this, a duplicate tape is made with the spurious image parameters not copied to the new tape. Figure 4-10 shows a dot-plot (all images regardless of magnitude or size plotted simply as dots) with most spurious images removed. The process was repeated until all detectable defects were removed from the data.

C. Star-Galaxy Separation

Several different schemes were tried for the necessary procedure of separating stars from galaxies. (Since it was estimated that the seven plates scanned by COSMOS contained about

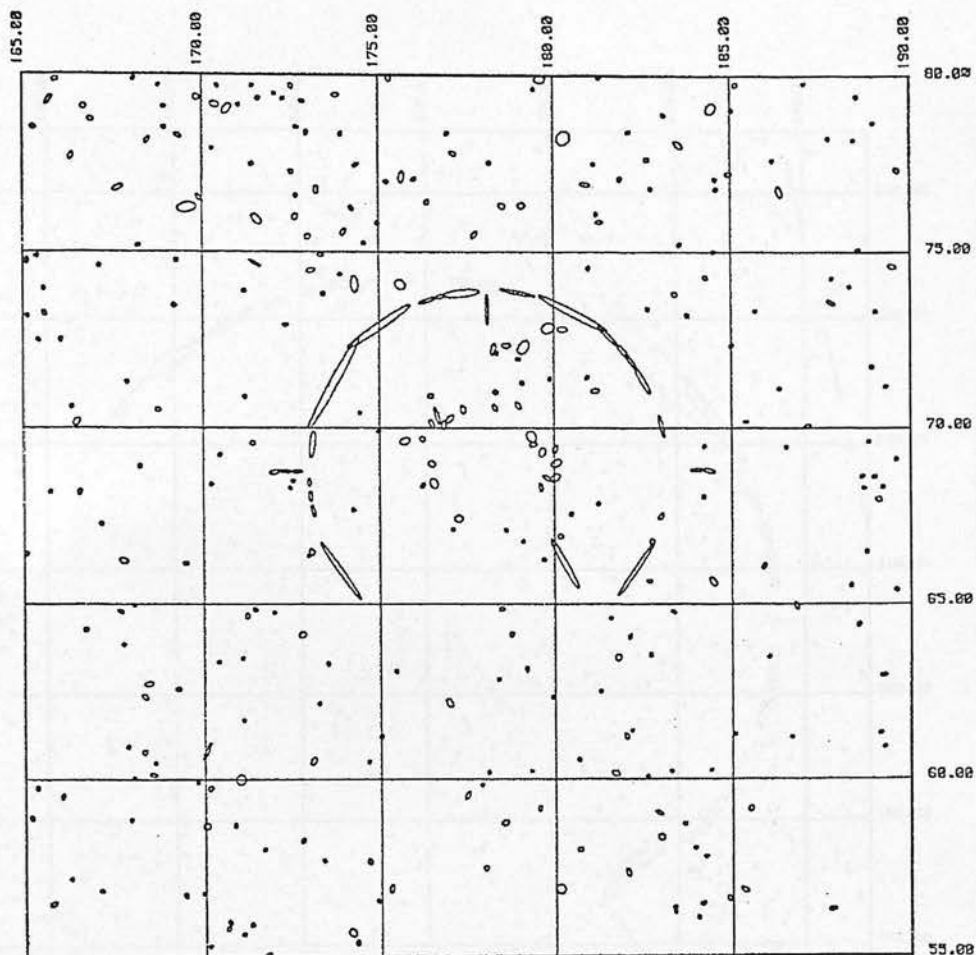


Figure 4-9a. False images detected by COSMOS around a bright star on plate J4584C.

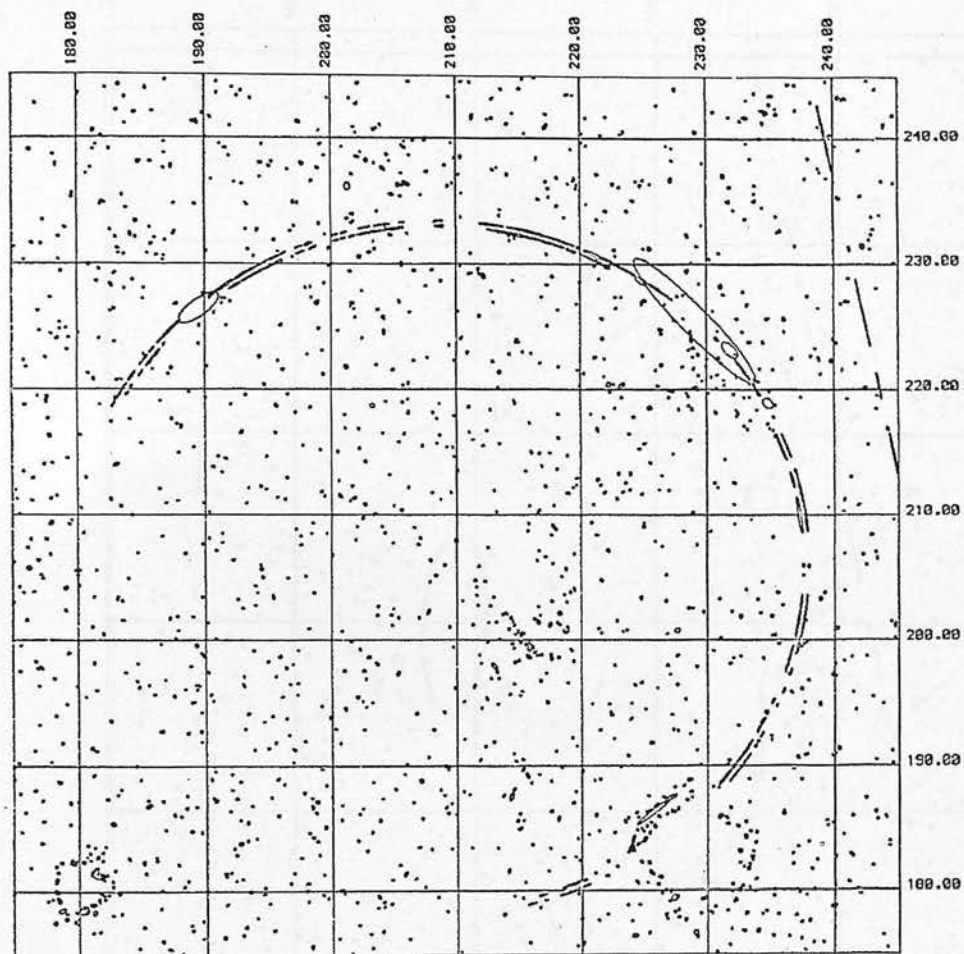


Figure 4-9b. Ghost image of a bright star detected by COSMOS on plate J1873C. A satellite trail and three rings of false images around bright stars are also apparent.

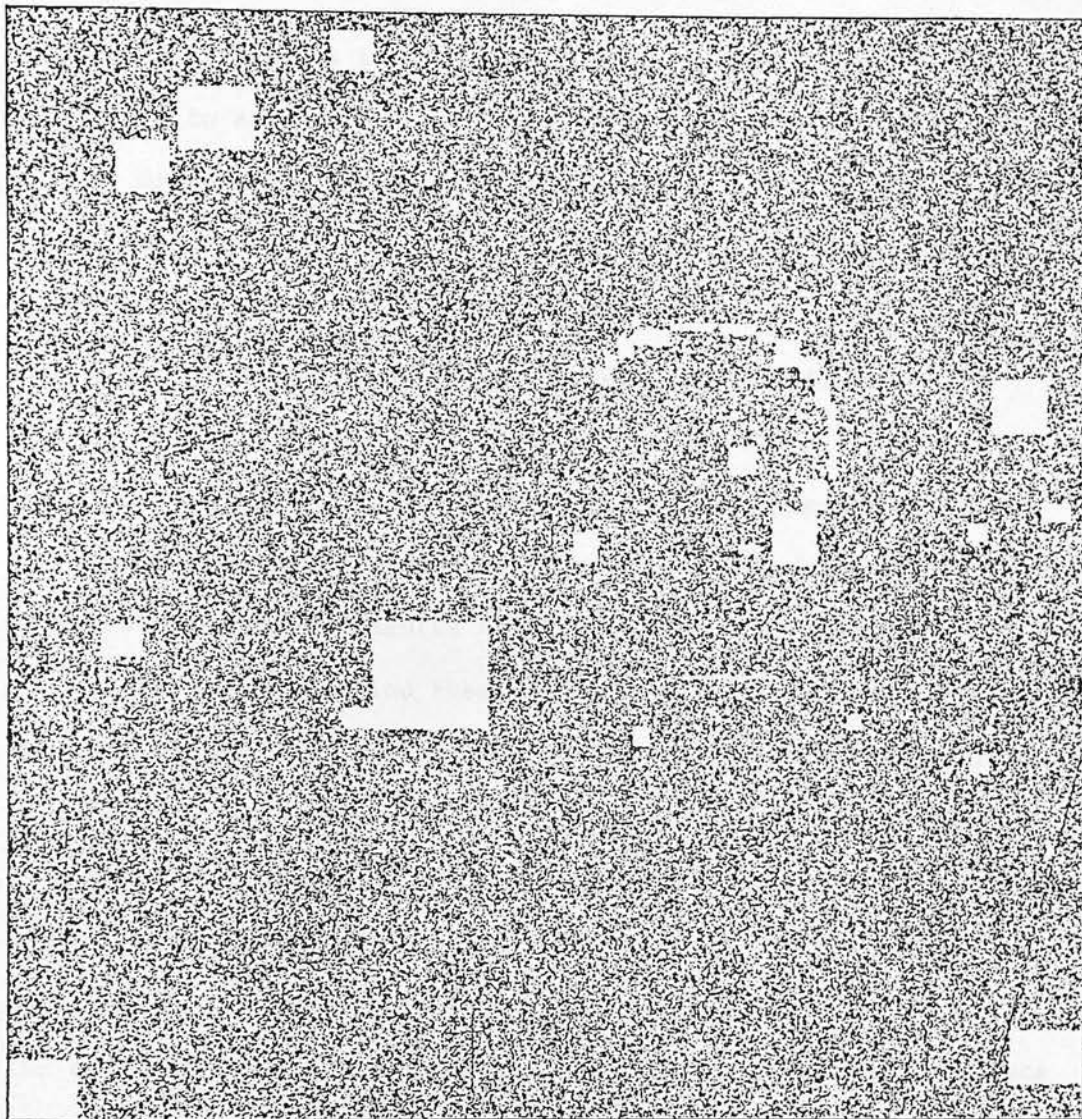


Figure 4-10. All images detected by COSMOS on plate J1873C after removal of most false images. A few faint satellite trails and other linear defects can still be seen.

150,000 galaxy images to $m_J \sim 21$, it would have obviously been impossible to attempt a manual separation of the data.)

Of the several semi-automatic methods tried, a simple plot of the COSMOS magnitude (equation 4-5b) against the logarithm of the area enclosed by the limiting isophote gave the best separation over the widest range of magnitude. Figure 4-11 is one of the test plots done on a copy plate (J1759C). Since a fairly good separation is apparent here from $m_J \sim 15$ to 21, computer plots of the same variables were made and separation lines drawn on them. Examples are shown as Figures 4-12a and b.

The concept behind these plots is simple. Since stars all have similar surface brightnesses, they will occupy a very narrow strip of the log A-magnitude plot. Galaxies of the same magnitude as a given star will usually have much larger areas, so will be scattered to the low surface brightness side of the stellar sequence. At the bright end, this technique breaks down because the star images develop haloes and spikes which lower their surface brightnesses into the part of the diagram occupied by normal galaxy images. This occurs about eight or nine magnitudes above the plate limit. At the faint end, stars and galaxies become indistinguishable by any criteria on the Schmidt plates. The smallest images on the plates used here are about 30 to 50 μm in diameter, only a few pixels across. As star images become unsaturated, they appear progressively similar to faint galaxy images. At the same time, the galaxy images shrink toward the size of the seeing disks on the plate, becoming more and more stellar in appearance. Both visually and in the machine separation, stars and galaxies become indistinguishable about two magnitudes above the plate limit (on deep,

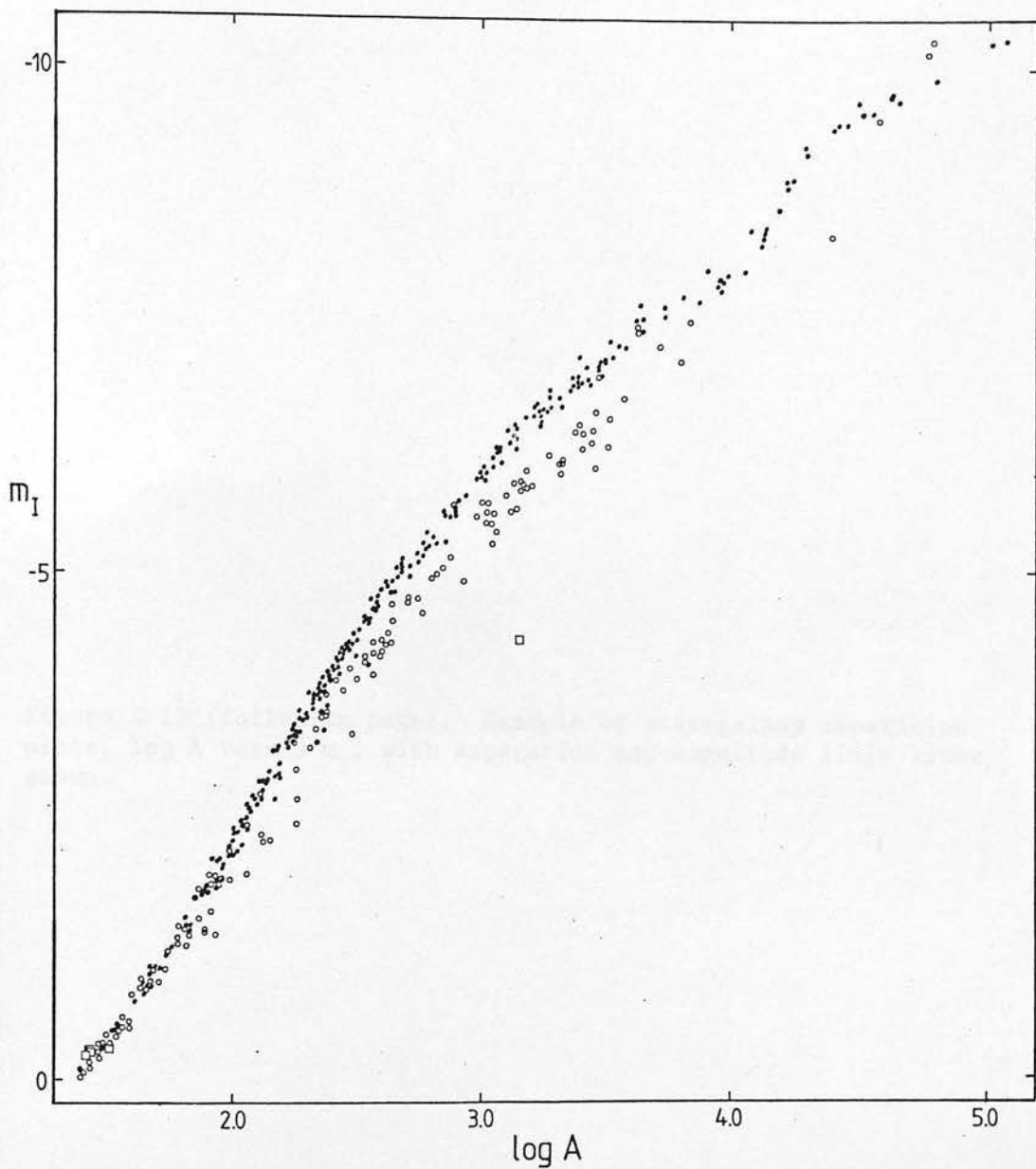
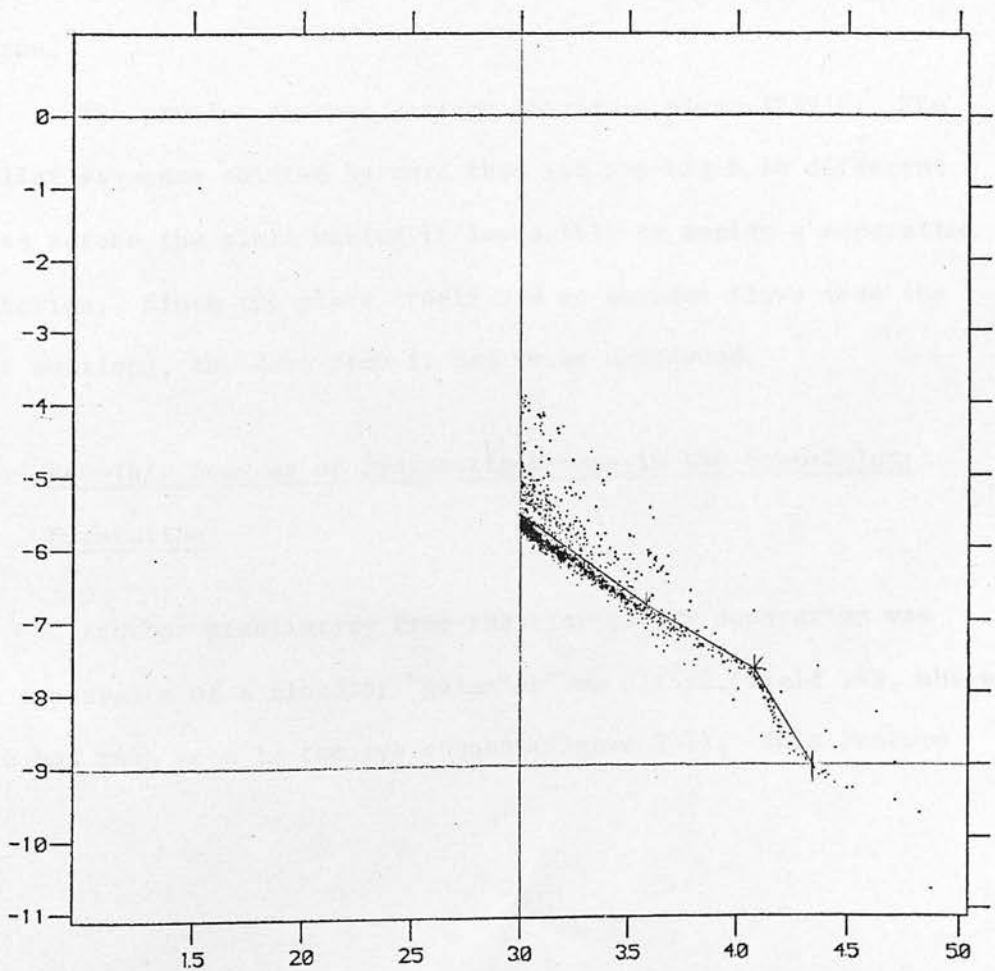
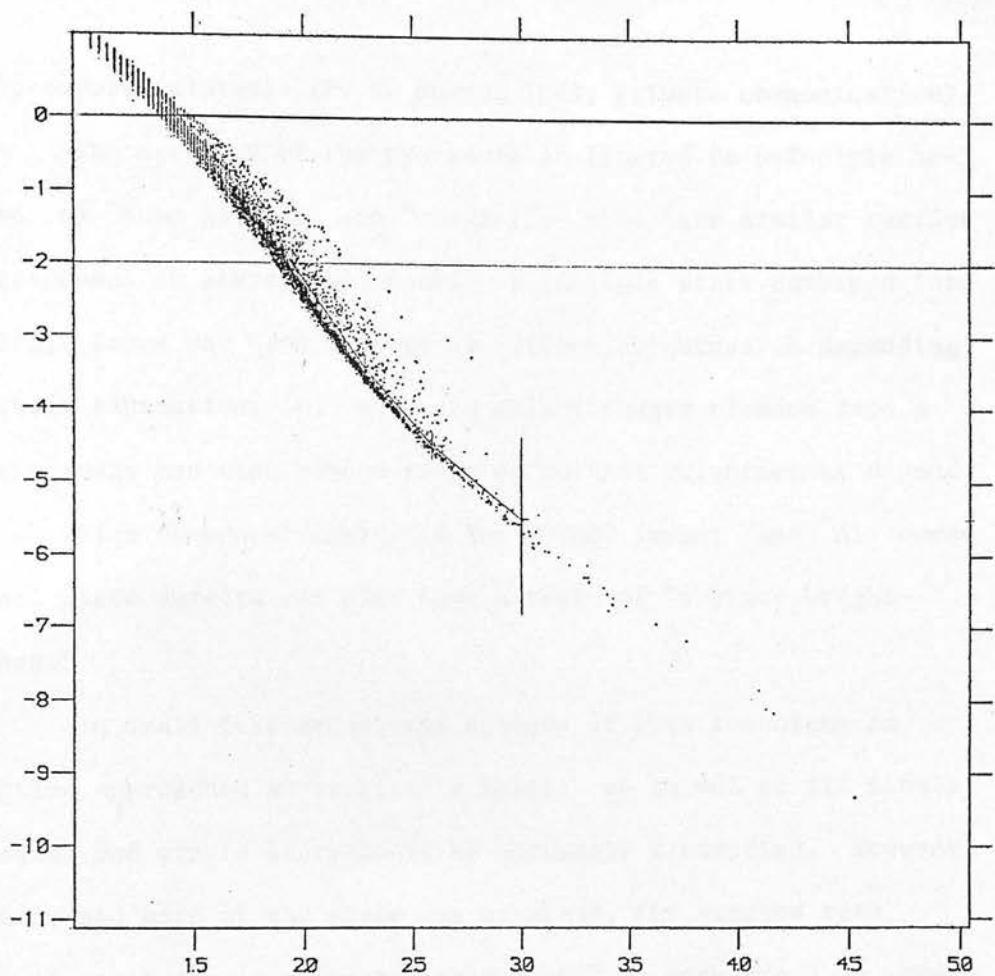


Figure 4-11. Star-galaxy separation plot, $\log A$ versus m_I . Stars, multiple stars, and star-dominated images are shown as dots. Galaxies, multiple galaxies, and galaxy-dominated images are shown as open circles. Defects are shown as open squares.

Figure 4-12 (following page). Example of star-galaxy separation plots, $\log A$ versus m_I , with separation and magnitude limit lines shown.



fully-exposed plates) (P. C. Hewett 1981, private communication).

The accuracy of the procedure is limited in principle because a) some galaxies are "compact" - they have similar surface brightnesses to stars; b) double or multiple stars combined into a single image may have a range of surface brightnesses depending on their separation; c) star and galaxy images blended into a single image can also have a range of surface brightnesses depending on which component dominates the COSMOS image; and d) occasional plate defects can also have a range of "surface brightnesses."

In small test areas, the success of this technique in practice approached an acceptable level: up to 90% of all single galaxies and single stars could be correctly classified. However, as more and more of the plate was examined, the success rate dropped until it was no better than 50-60% in some areas on some plates.

The problem reached extreme levels on plate J2391C. The stellar sequence shifted by more than its own width in different areas across the plate making it impossible to assign a separation criterion. Since the plate itself had no obvious flaws (see the next section), the data from it had to be abandoned.

VII. Possible Sources of Systematic Errors in the Star-Galaxy Separation

Another peculiarity from the star-galaxy separation was the appearance of a cloud of "galaxies" on J1759C, field 145, where none had been seen in the eye counts (Figure 2-7). This feature

shows well in the dot-plot (Figure 4-13) as the strong enhancement roughly two degrees across centred at $21^{\text{h}}32^{\text{m}}$, $-60^{\circ}50'$. A dot plot of the "stars" to the same magnitude limit (Figure 4-14), while much more uniform, shows a deficiency in the same area. This excess of "galaxies" and deficiency of "stars" was confirmed by contour plots (Figures 4-15, 4-16) to several different magnitude levels. A contour plot made from an early scan of the same field on plate J1578 showed no trace of the "galaxy cloud" (Figure 4-17).

A contour plot of the background intensity values (I_{sky}) is shown in Figure 4-18. There is no obvious correlation between this and Figures 4-15 and 16. Finally, the writer asked Ms. S. B. Tritton of the UK Schmidt Unit (she is in charge of quality control of the later issues of the SERC half of the Southern Sky Survey) to examine the copy of J1759 scanned by COSMOS. Her examination showed that the size of the smallest images varied across the plate as shown in Figure 4-19. The area of the "galaxy cloud" is seen to be in poor focus relative to the remainder of the plate. This has led to the hypothesis that the 3 mm thick copy plate was not in perfect contact with the positive copy of the original when it (the negative copy) was made.

Other plates show similar though not (with one exception) such drastic imperfections. The single exception is plate J3658C where the imperfection is coincident with variations in I_{sky} (Figures 4-20a, b, c).

The cause of the star-galaxy separation problem with J2391C may be due to background variations. There are no extreme focus variations across this plate, but the range of I_{sky} is somewhat

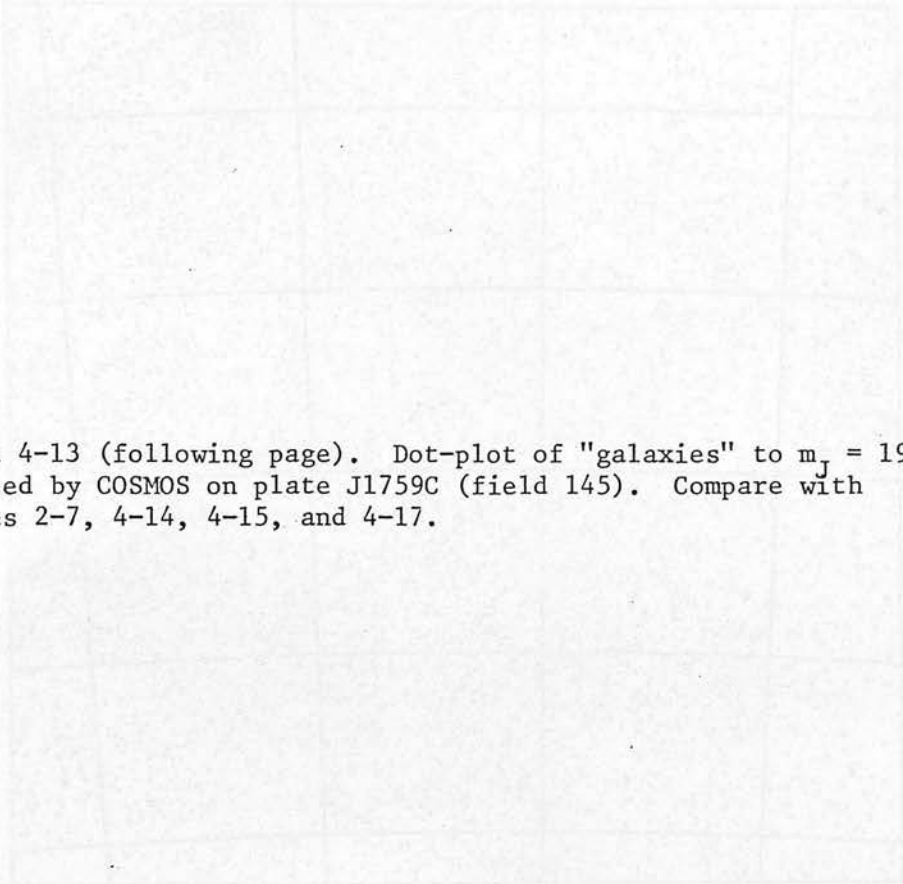


Figure 4-13 (following page). Dot-plot of "galaxies" to $m_J = 19$ detected by COSMOS on plate J1759C (field 145). Compare with Figures 2-7, 4-14, 4-15, and 4-17.

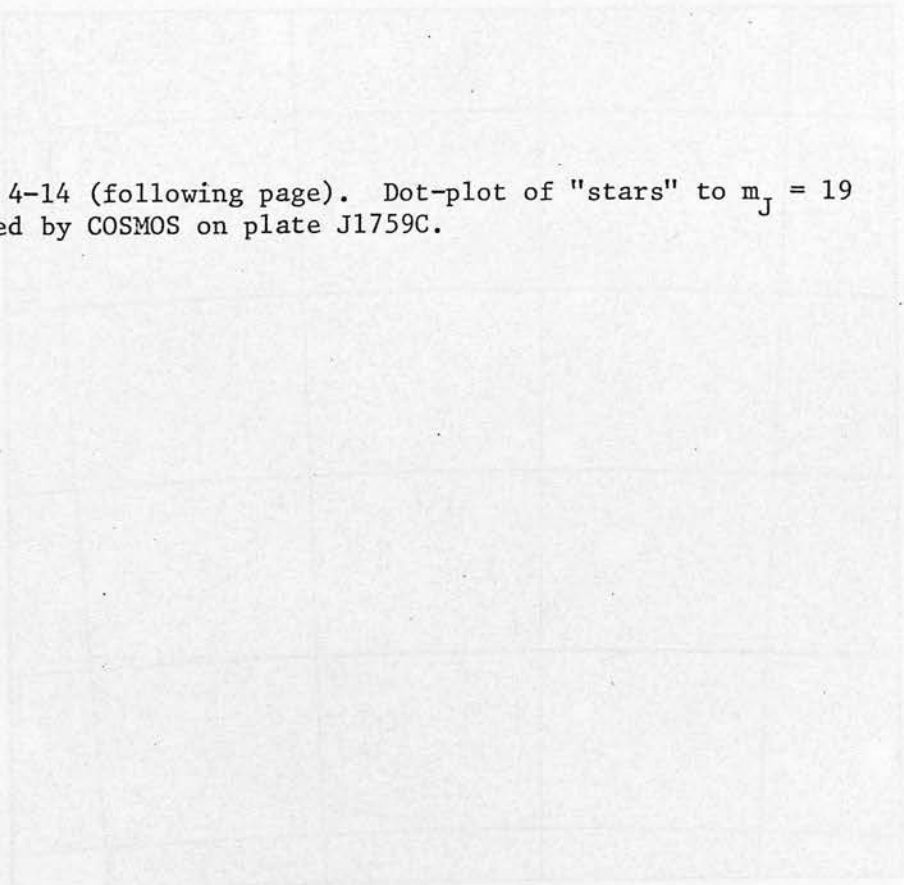
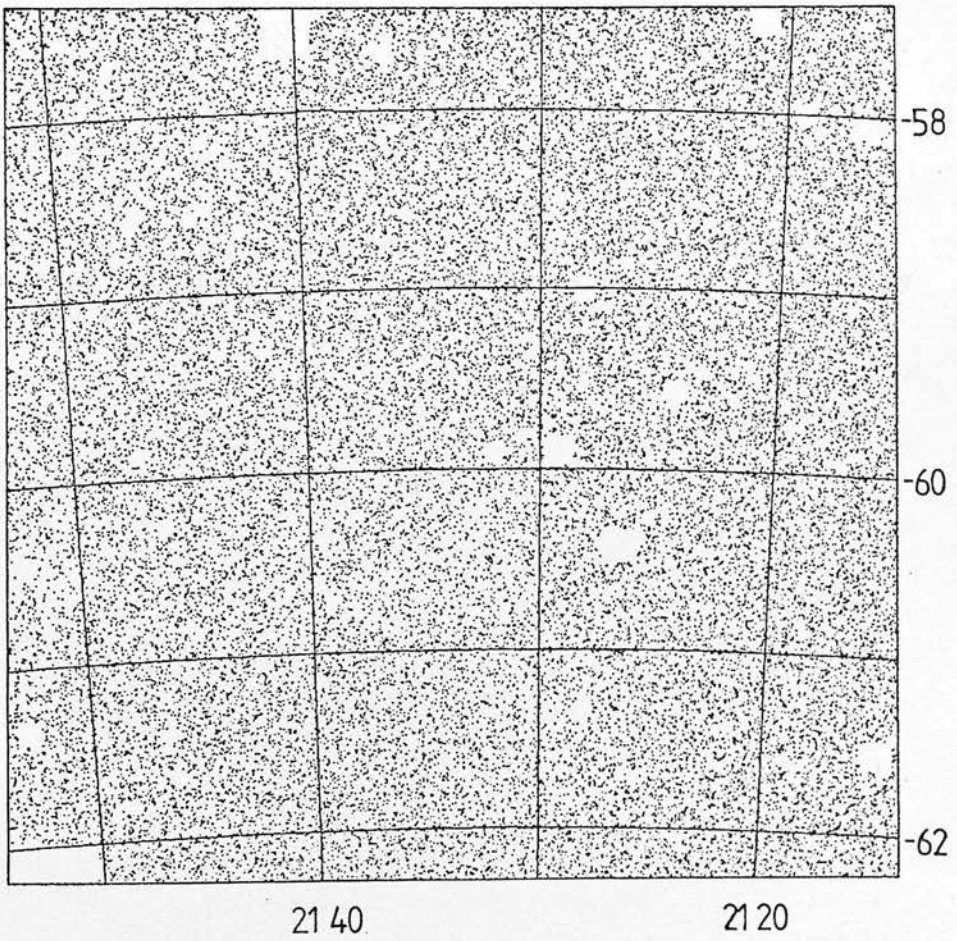
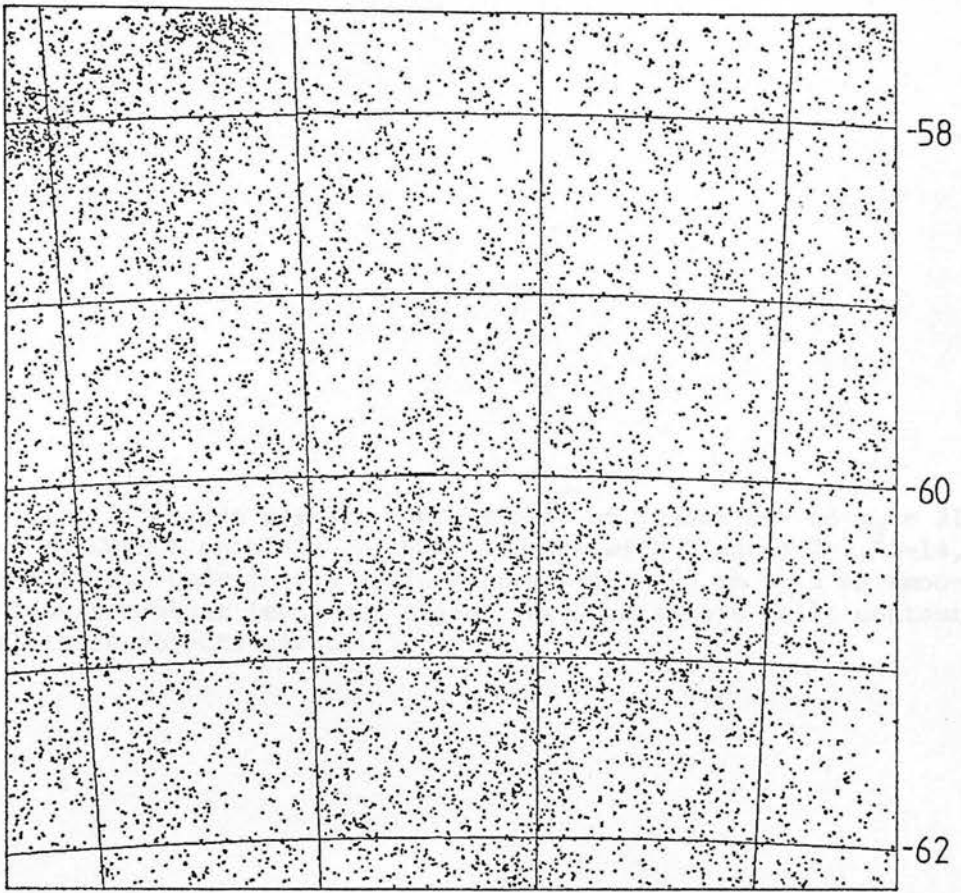


Figure 4-14 (following page). Dot-plot of "stars" to $m_J = 19$ detected by COSMOS on plate J1759C.



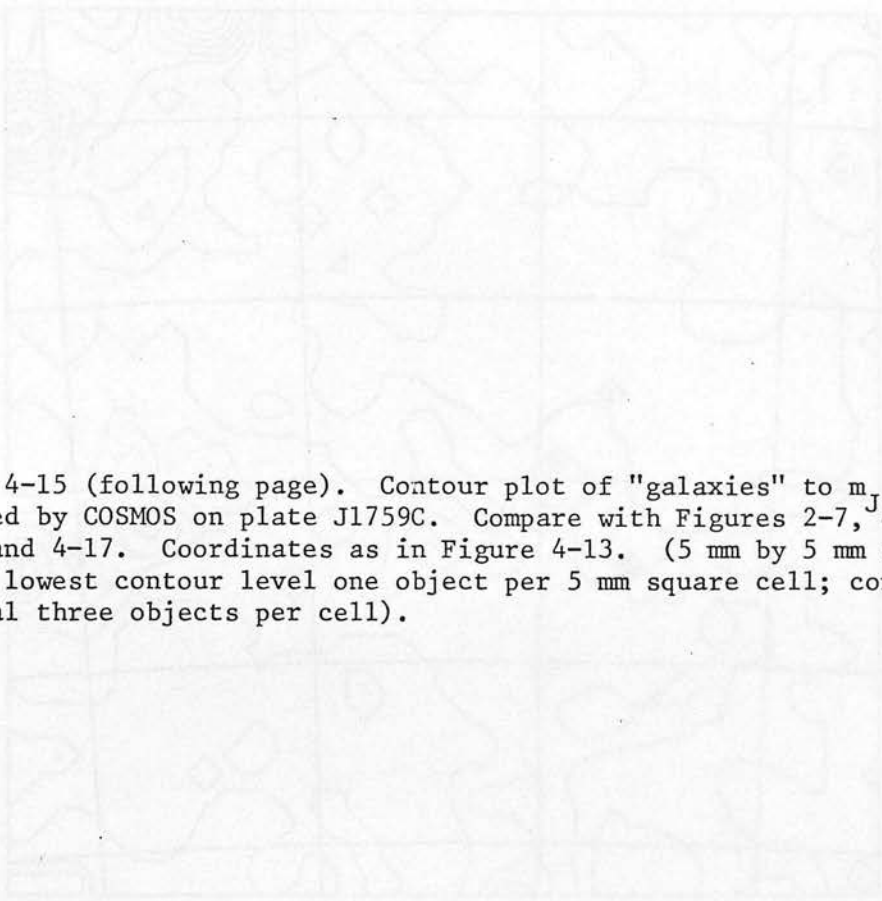


Figure 4-15 (following page). Contour plot of "galaxies" to $m_J = 21$ detected by COSMOS on plate J1759C. Compare with Figures 2-7, 4-14, 4-16, and 4-17. Coordinates as in Figure 4-13. (5 mm by 5 mm smoothing, lowest contour level one object per 5 mm square cell; contour interval three objects per cell).

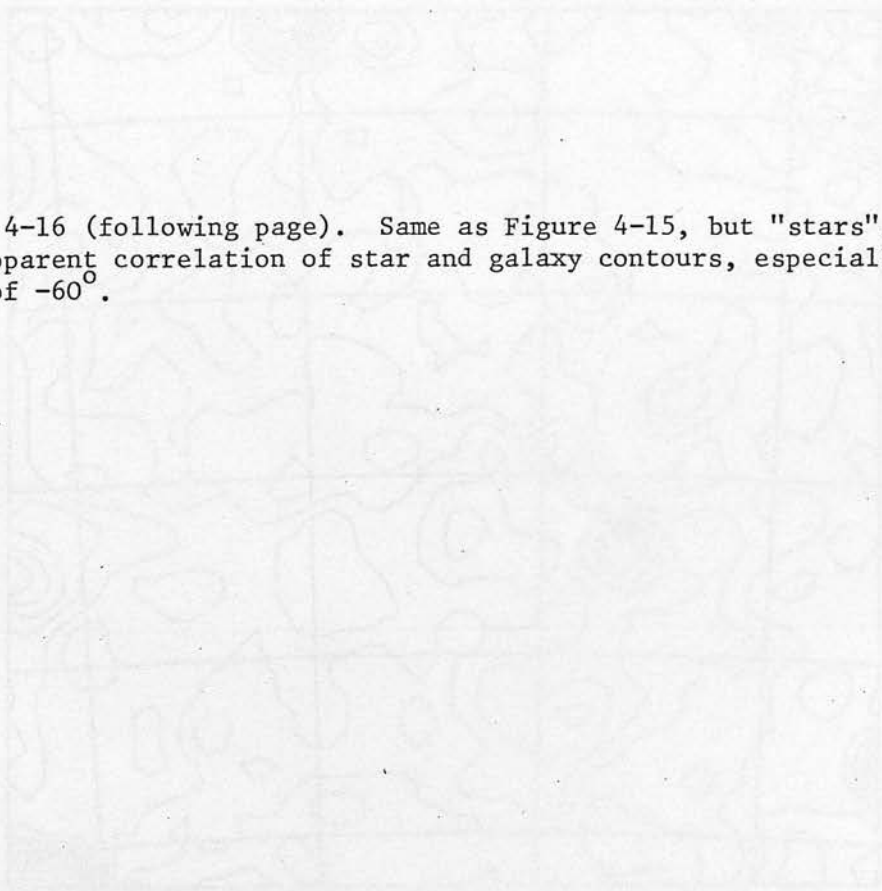
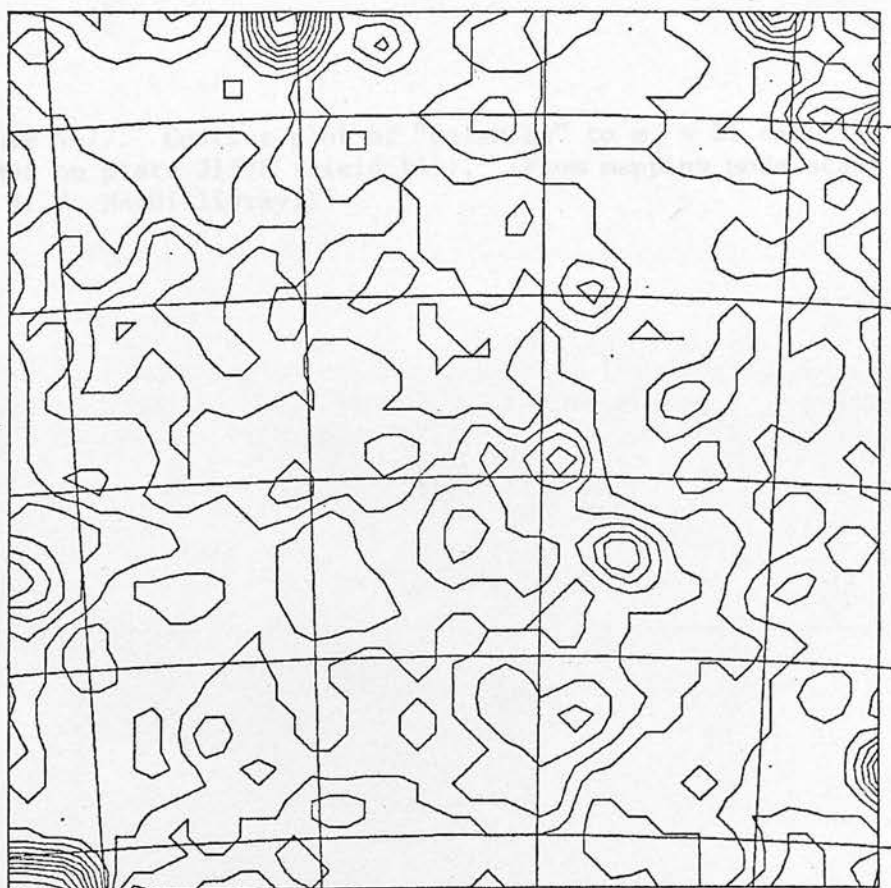
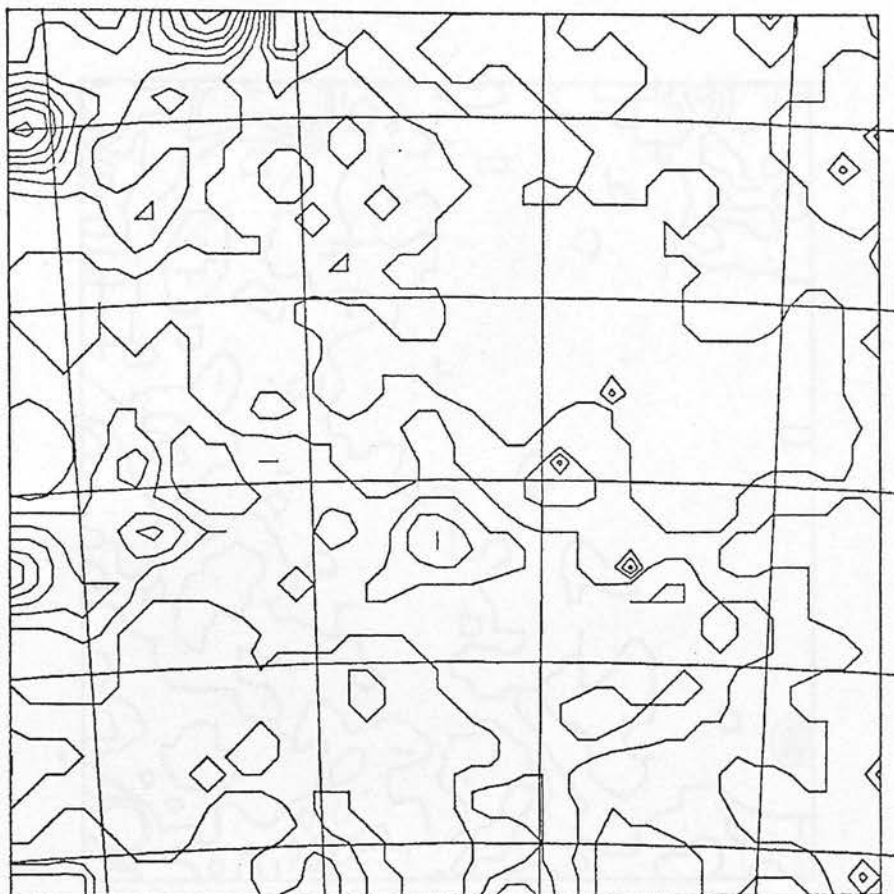


Figure 4-16 (following page). Same as Figure 4-15, but "stars". Note apparent correlation of star and galaxy contours, especially south of -60° .



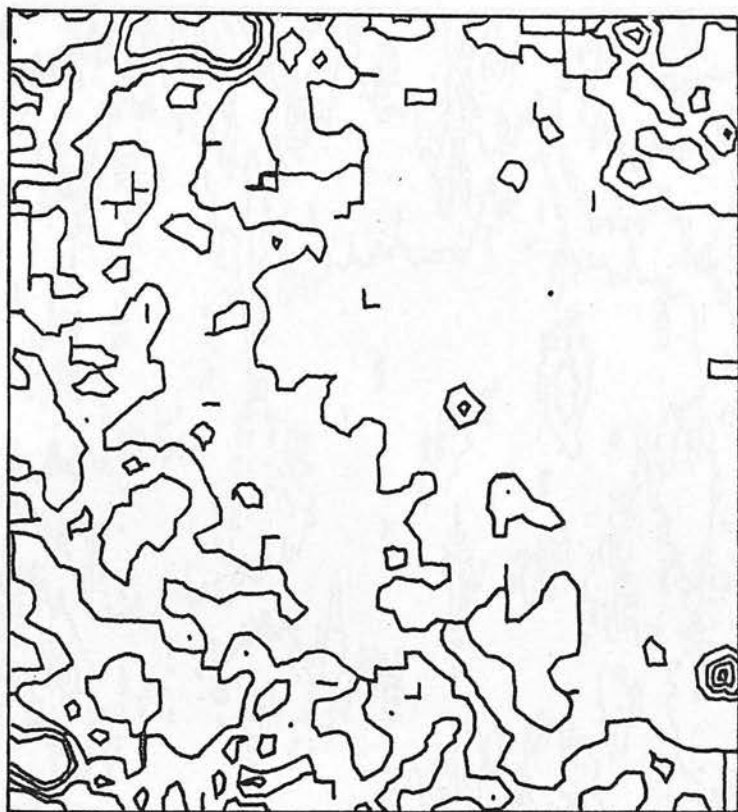


Figure 4-17. Contour plot of "galaxies" to $m_J \sim 21$ detected by COSMOS on plate J1578 (field 145). (From mapping mode scans by Dr. H. T. MacGillivray.)

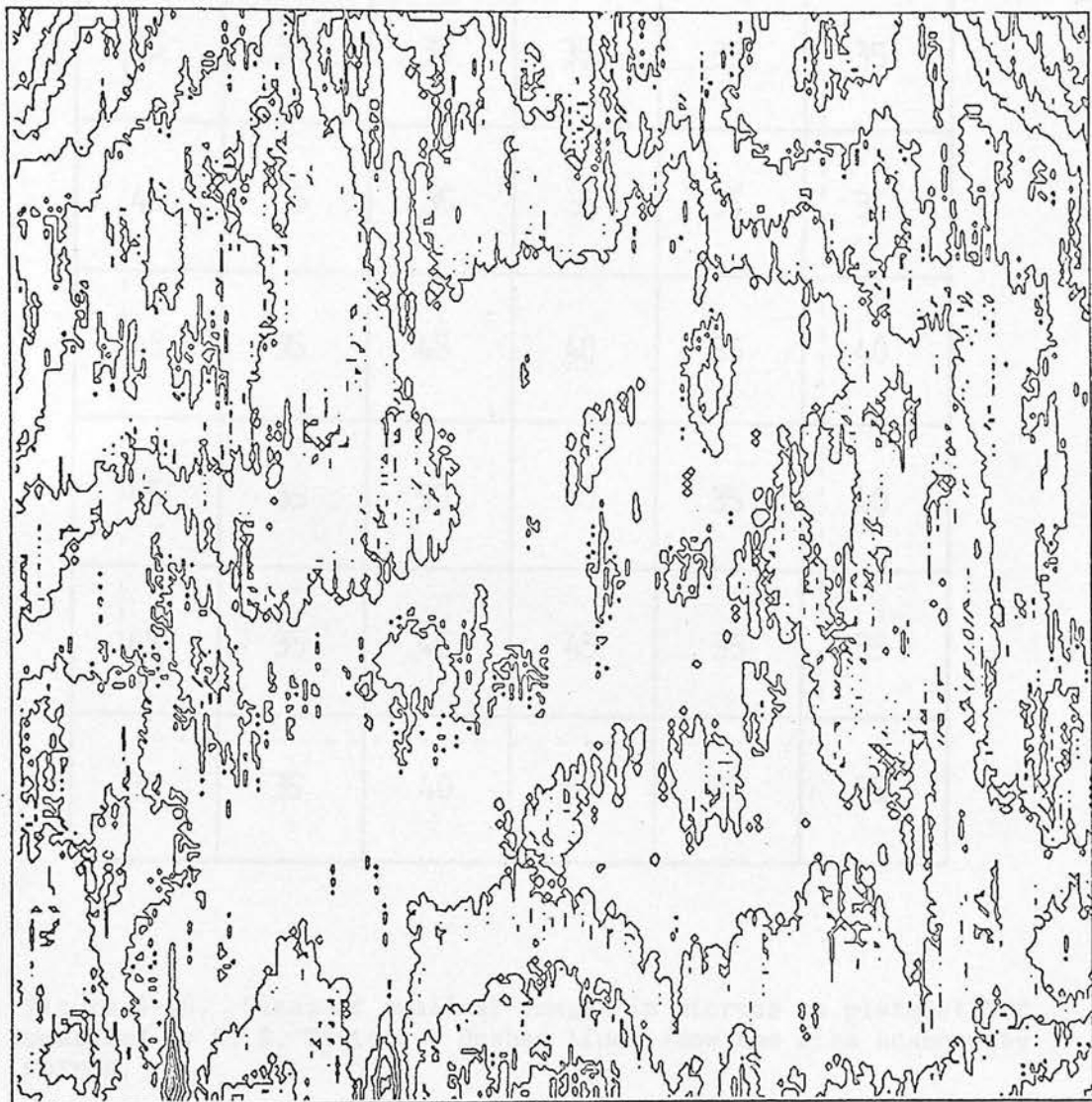


Figure 4-18. Contour plot of sky background intensities as measured by COSMOS on plate J1759C. Contours are through $\log I_{\text{sky}}$ values in 1 mm by 5 mm cells. $I_{\text{sky}}(\text{min}) = 152$, $I_{\text{sky}}(\text{max}) = 208$.

35	35	35	35	35	35
45	35	35	35	35	35
45	35	45	40	35	40
45	35	50	50	35	40
45	35	45	45	35	35
35	35	40	35	35	35

Figure 4-19. Sizes of smallest images in microns on plate J1759C measured by S. B. Tritton. Dashed lines show the area scanned by COSMOS.

Figure 4-19c. All "galaxies" detected by COSMOS on plate J1759C.



Figure 4-20a. All "galaxies" detected by COSMOS on plate J3658C.

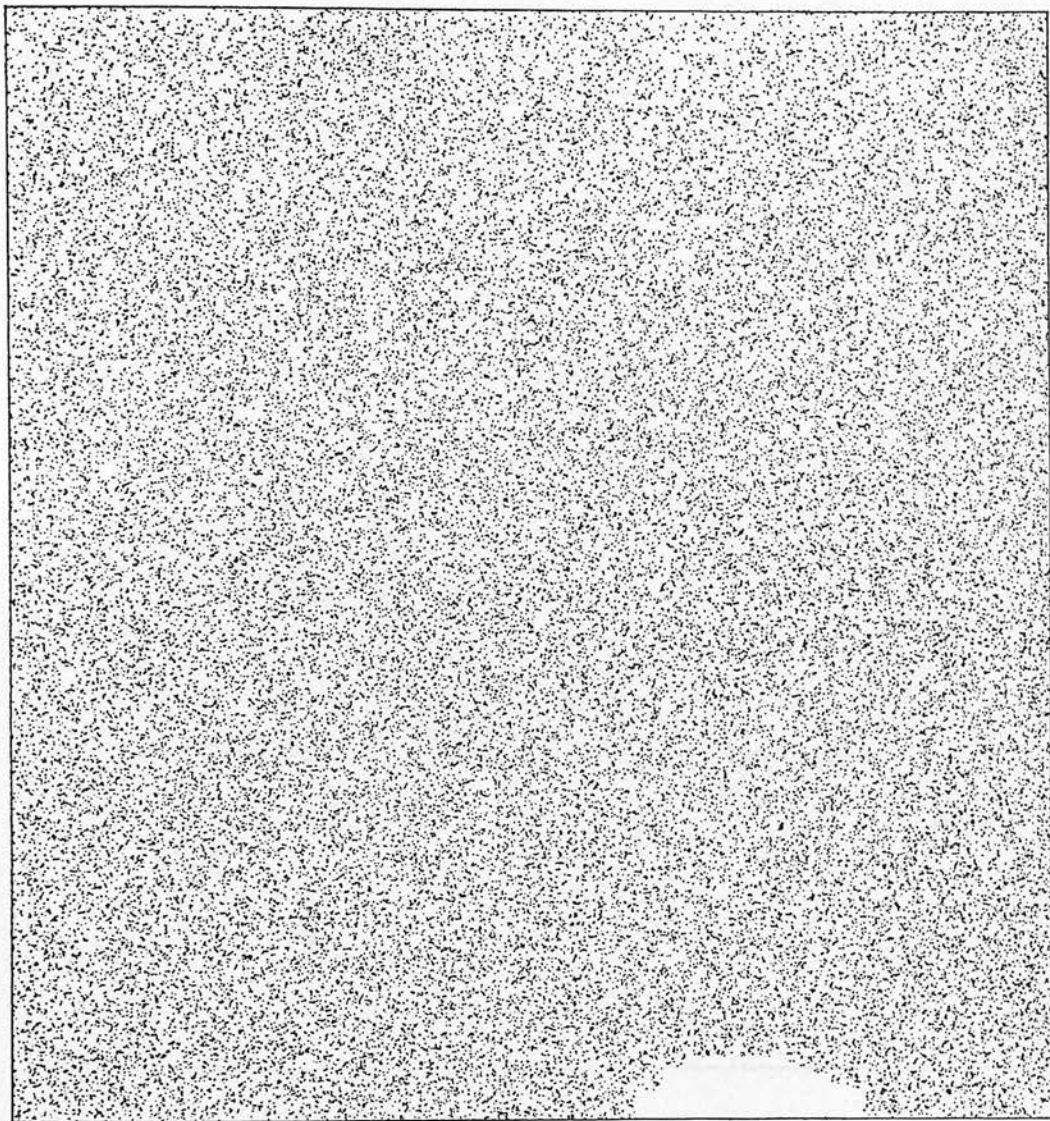


Figure 4-20b. All "stars" detected by COSMOS on plate J3658C.

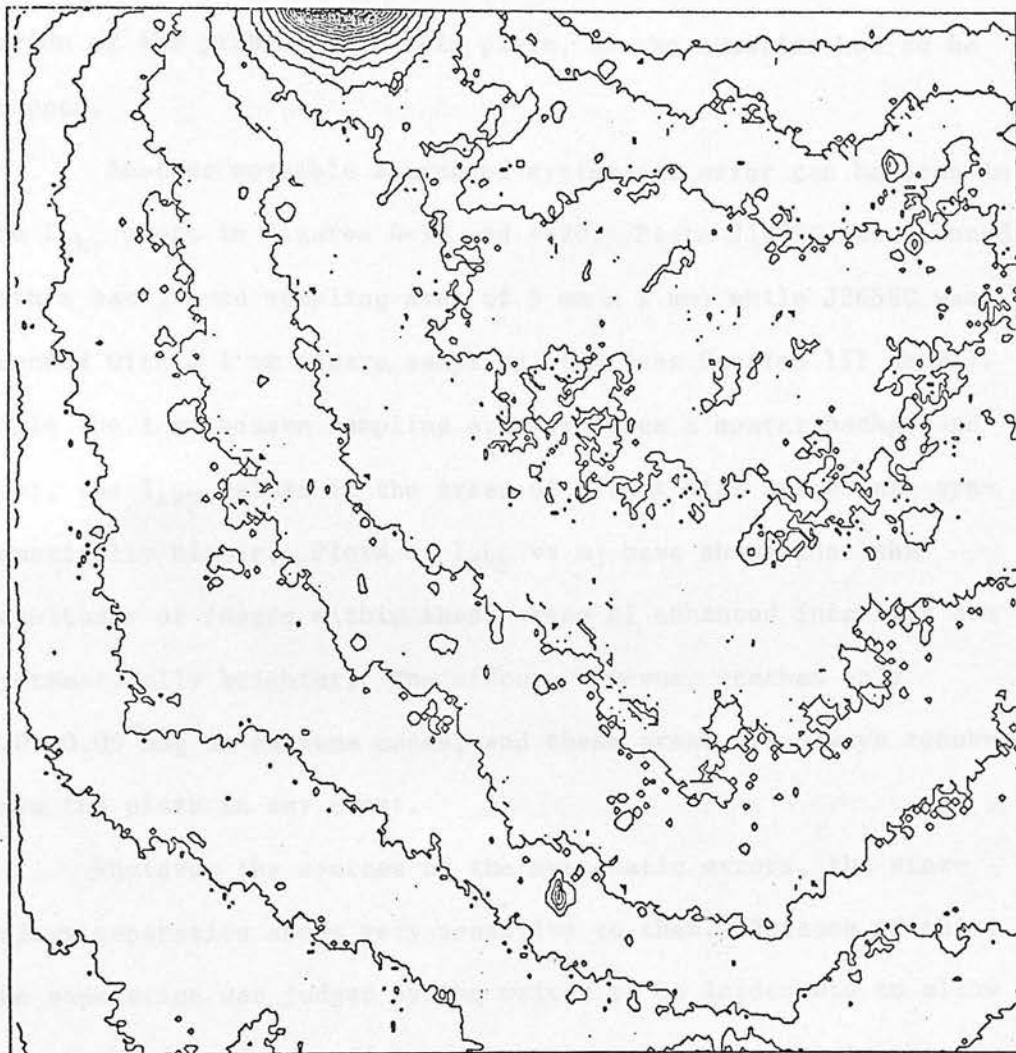


Figure 4-20c. Contour plot of sky background intensities as measured by COSMOS on plate J3658C. Contours are through $\log I_{\text{sky}}$ values in 1 mm by 1 mm cells. $I_{\text{sky}}(\text{min}) = 288$; $I_{\text{sky}}(\text{max}) = 934$ near image of α Gruis at top of field.

larger than typical. However, time did not allow a detailed examination of the problem with this plate, so the question had to be dropped.

Another possible source of systematic error can be seen in the I_{sky} plots in Figures 4-18 and 4-20. Plate J1759C was scanned with a background sampling area of 5 mm x 1 mm, while J3658C was scanned with a 1 mm square sampling area (see Section III above). While the 1 mm square sampling area produces a neater background plot, the I_{sky} values in the areas of bright star images are systematically higher. Plots of I_{sky} vs m_J have shown that the magnitudes of images within these areas of enhanced intensity are systematically brighter. The effect, however, reaches only 0.04-0.05 mag in extreme cases, and these areas are always removed from the plate in any event.

Whatever the sources of the systematic errors, the star-galaxy separation seems very sensitive to them. Because of this, the separation was judged by the writer to be inadequate to allow use of the data for studies of the galaxy distribution in the Indus Supercluster Area.

VIII. Luminosity Functions

A. Introduction

Abell (1975, 1977 and references therein) has argued that the integrated luminosity function $\log \Sigma N (< m)$ versus m of rich clusters of galaxies is similar for all clusters. Specifically, he points out (e.g. Abell 1975, Bautz and Abell 1973) that such

luminosity functions have a "break" at an invariant absolute magnitude which he calls M^* . This M^* may thus be used as a distance indicator (e.g. Mottmann and Abell 1977).

Similarly, Abell (1978) has argued from data by Rainey (1977) that the "field" integrated luminosity function is invariant in shape and value no matter where in the sky it is measured.

In general, the available data for clusters (e.g. Krupp 1974, Oemler 1974, Dressler 1978, Godwin and Peach 1977 and references therein) and for the "field" (e.g. Brown 1978, Karachentsev 1980 and references therein) support these contentions though with some exceptions for the clusters (Dressler 1978).

Since the integrated isophotal photometry from COSMOS does not seem to have been much affected by the star-galaxy separation problems (Section V above), an attempt was made to derive luminosity functions for various small fields in and out of the Indus Supercluster and for rich clusters in it. The fields so selected had to be outside of the areas known to be strongly affected by the star-galaxy separation problems, however.

This was done a) to provide a further check on Abell's ideas as outlined above and b) to provide redshift-independent distance estimates for the clusters in the Indus area.

B. Cluster Luminosity Functions

The luminosity functions for nineteen rich clusters present on the plates scanned by COSMOS are shown in Figure 4-21. These have had background corrections made by subtracting the "field" luminosity functions for each plate (see Section VIII-C below) from

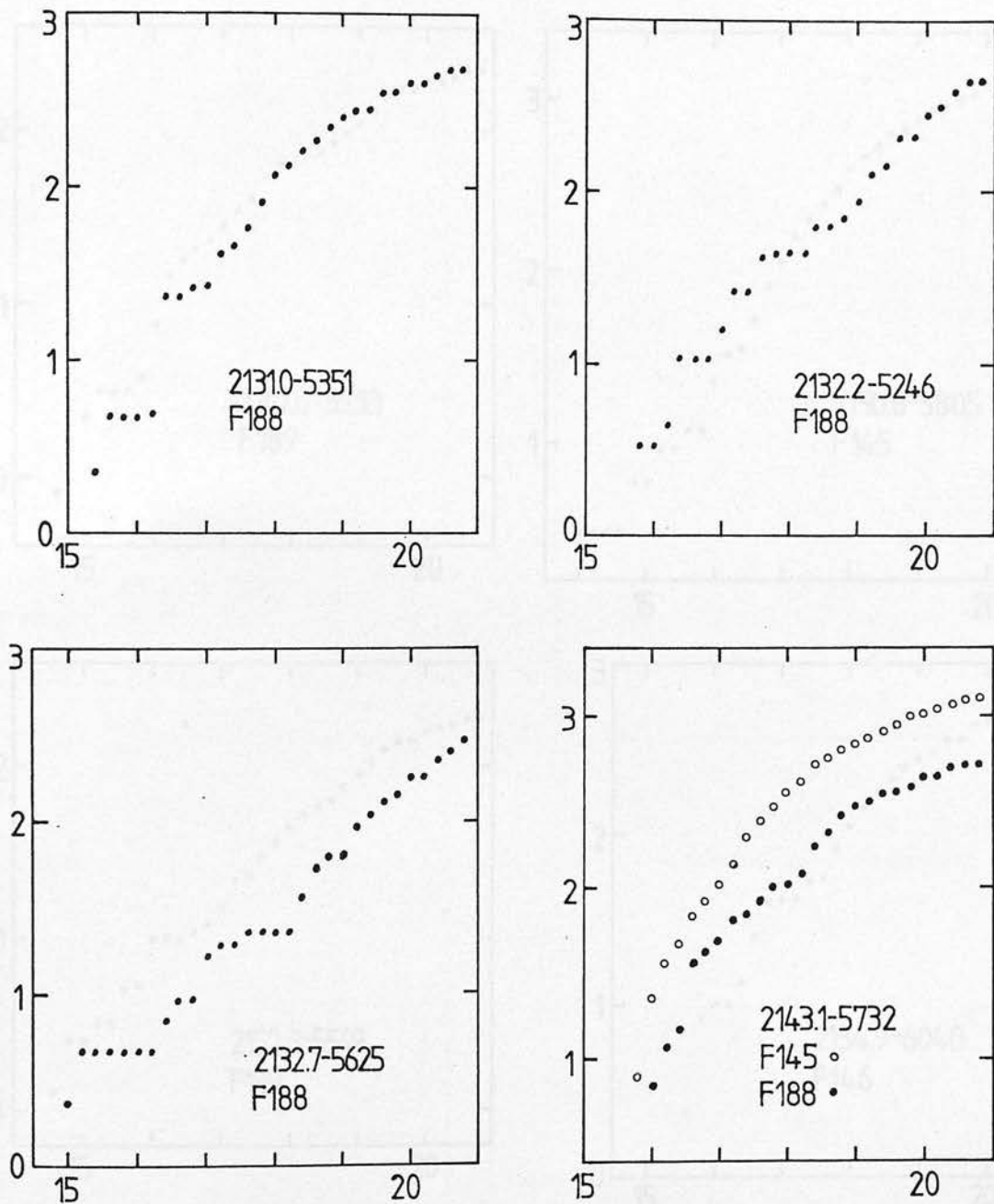


Figure 4-21. Integrated luminosity functions for 19 rich clusters scanned by COSMOS, and (for comparison) for the Coma Cluster as measured by Abell (1977) and by Godwin and Peach (1977). Abscissae are COSMOS magnitudes m_J (m for the Coma Cluster), ordinates are $\log \Sigma N(\leq m)$. N has been reduced to galaxies per square degree.

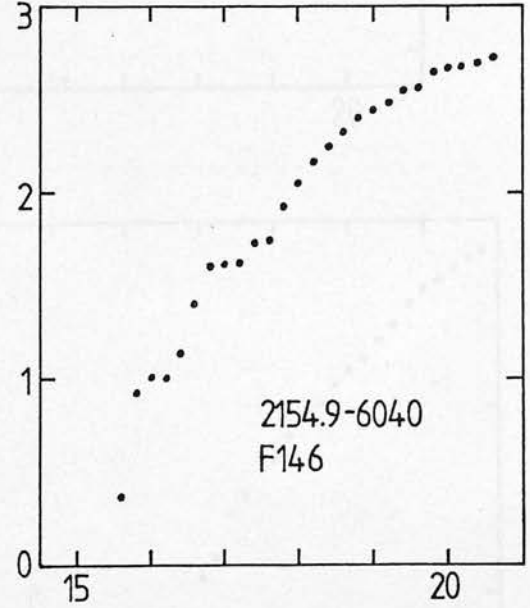
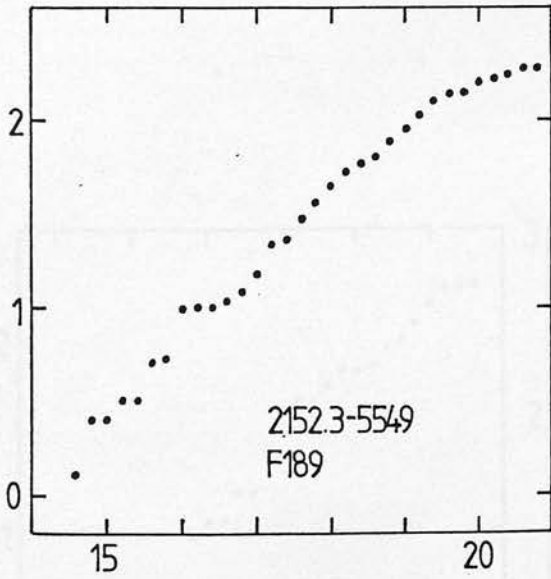
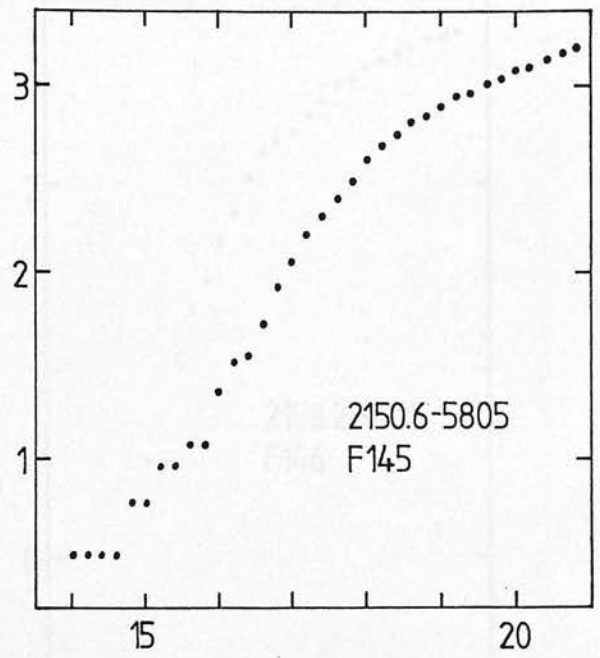
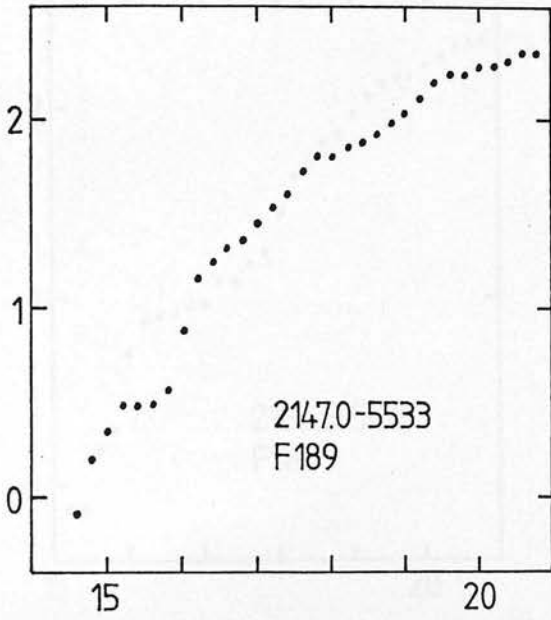


Figure 4-21 (continued).

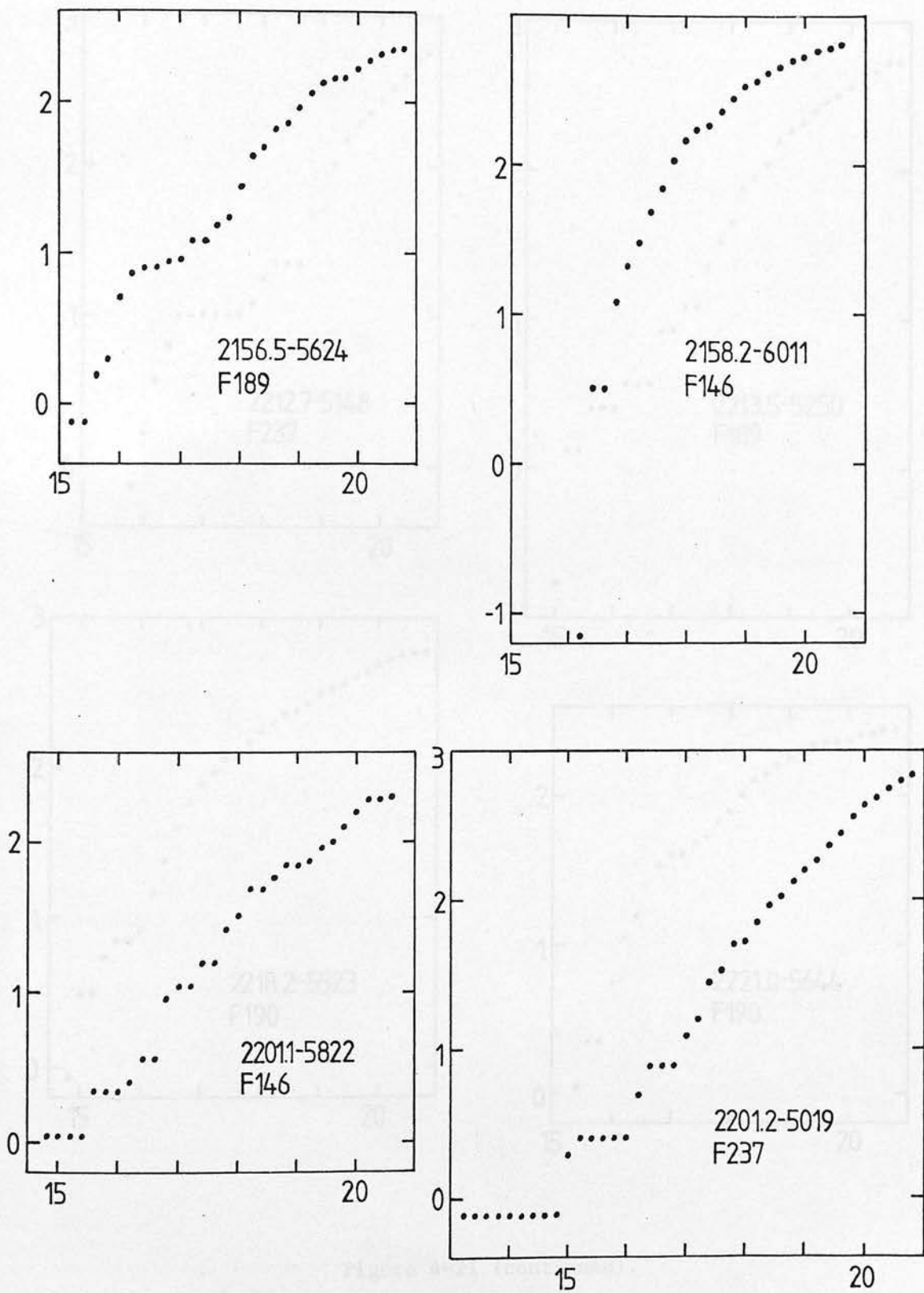


Figure 4-21 (continued).

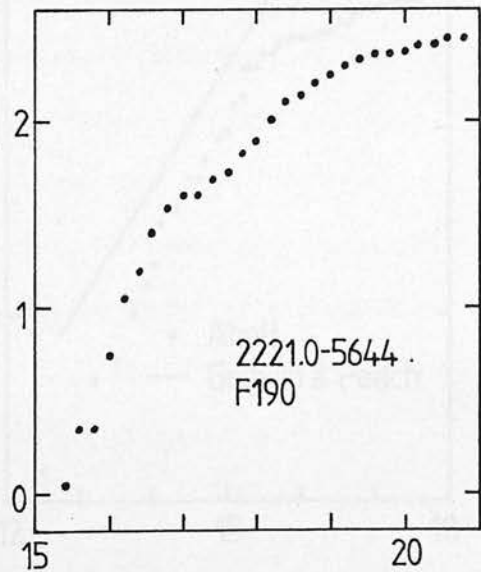
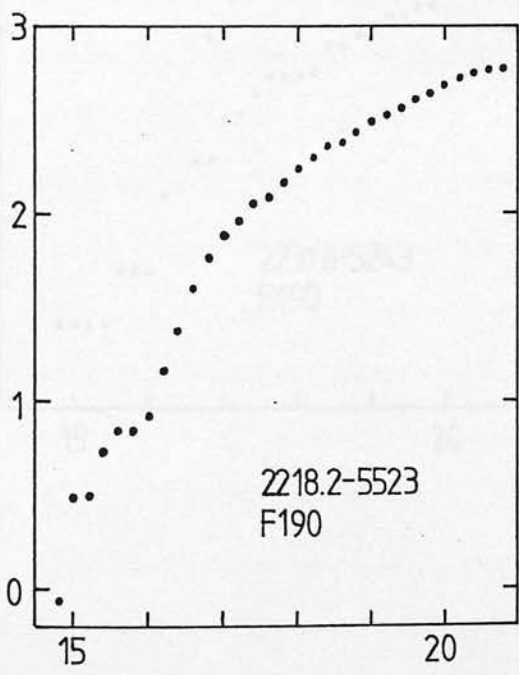
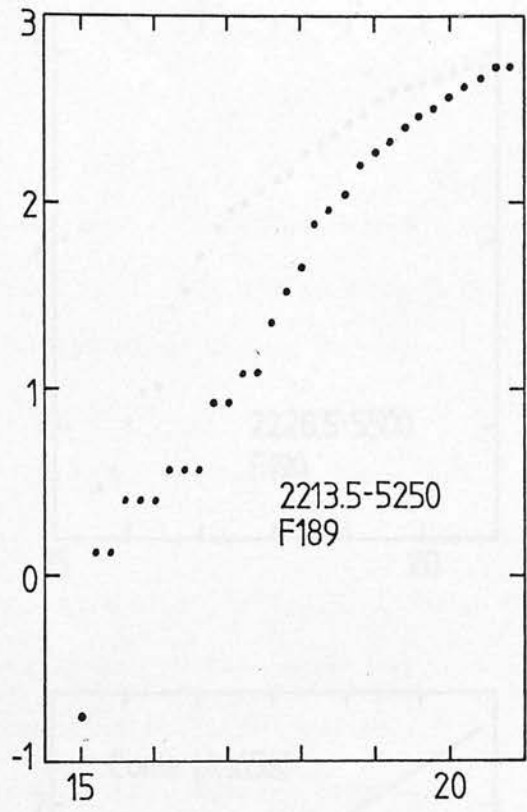
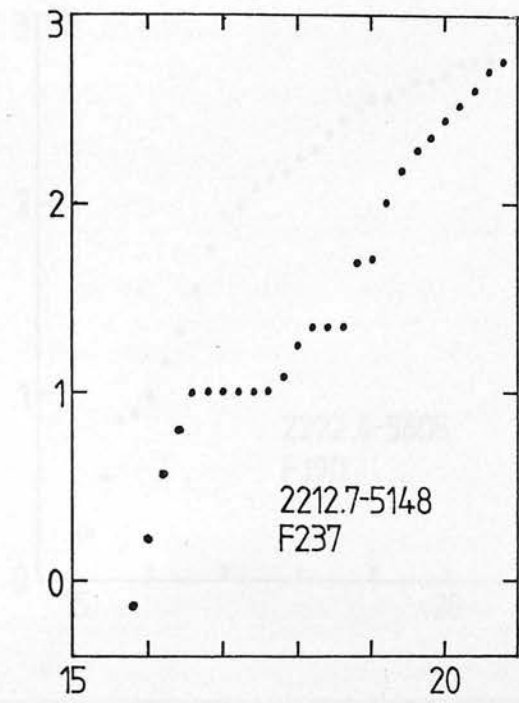


Figure 4-21 (continued).

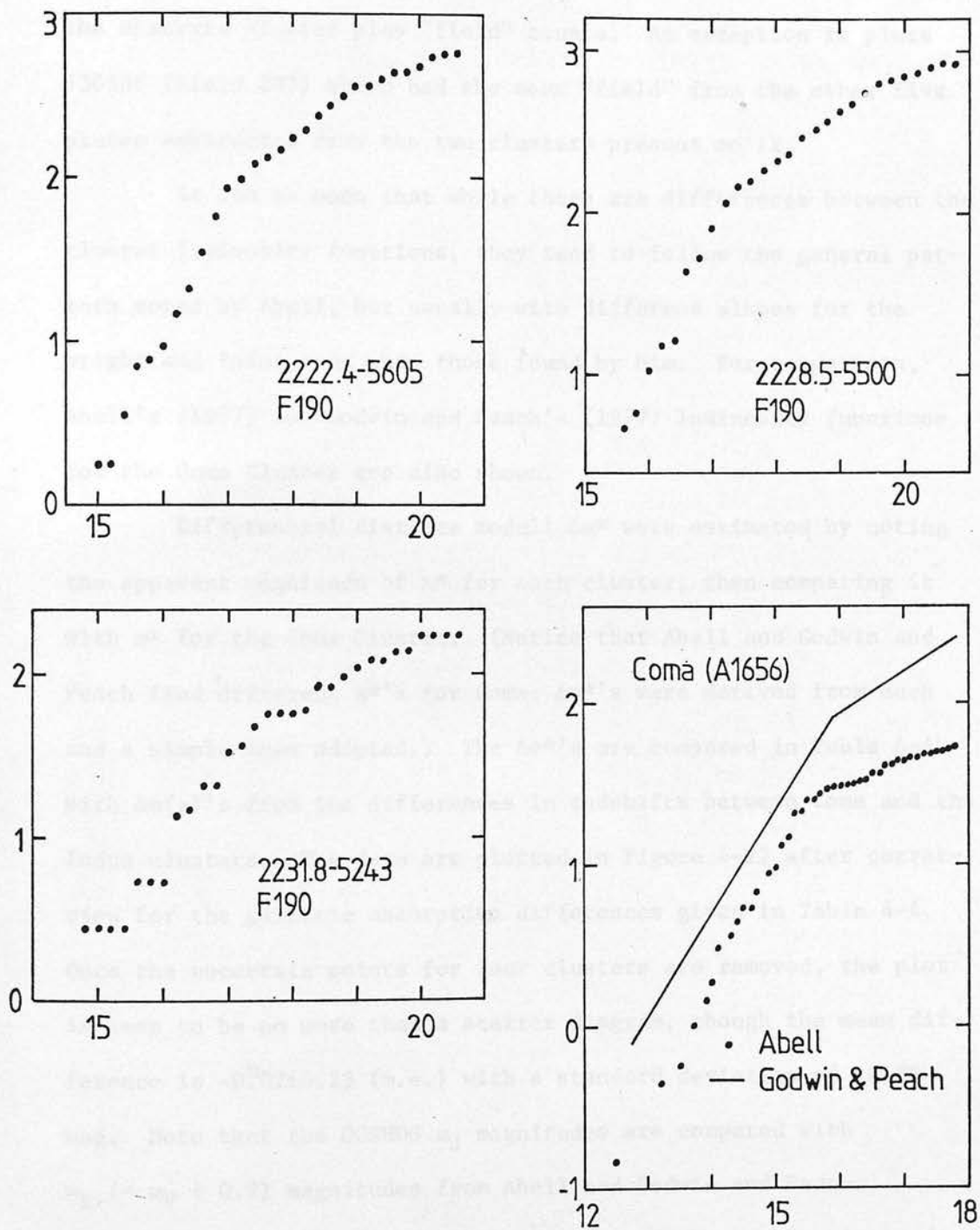


Figure 4-21 (continued).

the observed cluster plus "field" counts. An exception is plate J3658C (field 237) which had the mean "field" from the other five plates subtracted from the two clusters present on it.

It can be seen that while there are differences between the cluster luminosity functions, they tend to follow the general pattern noted by Abell, but usually with different slopes for the bright and faint ends than those found by him. For comparison, Abell's (1977) and Godwin and Peach's (1977) luminosity functions for the Coma Cluster are also shown.

Differential distance moduli Δm^* were estimated by noting the apparent magnitude of m^* for each cluster, then comparing it with m^* for the Coma Cluster. (Notice that Abell and Godwin and Peach find different m^* 's for Coma; Δm^* 's were derived from each and a simple mean adopted.) The Δm^* 's are compared in Table 4-4 with $\Delta m(z)$'s from the differences in redshifts between Coma and the Indus clusters. The data are plotted in Figure 4-22 after correction for the galactic absorption differences given in Table 4-4. Once the uncertain points for four clusters are removed, the plot is seen to be no more than a scatter diagram, though the mean difference is $-0.^m02 \pm 0.23$ (m.e.) with a standard deviation of ± 0.89 mag. Note that the COSMOS m_J magnitudes are compared with m_B ($= m_V + 0.9$) magnitudes from Abell and Godwin and Peach.

Once again, the most likely cause of the problem is inadequate star-galaxy separation combined with calibration uncertainties.

TABLE 4-4

Differential Distance Moduli of Indus Clusters
Referred to the Coma Cluster

Cluster	ΔA_B	$\Delta m(z)$	Δm^*	$\delta \Delta m$
2131.0-5351	0.15	+2.61	+2.5	+0.26
2132.2-5246	0.15	2.21	2.3	+0.06
2132.7-5625	0.15	2.37	2?	+0.5
2143.1-5732	0.15	2.53	2.2	+0.48
2147.0-5533	0.15	1.08	0.8	+0.43
"	"	2.32	"	+1.67
2150.6-5805	0.15	2.58	2.2	+0.53
2152.3-5549	0.15	1.05	2.4	-1.20
2154.9-6040	0.15	2.53	2.4	+0.28
2156.5-5624	0.15	2.56	0.8?	+1.9
"	"	"	2.6?	+0.1
2158.2-6011	0.15	3.17	2.5	+0.82
2201.1-5822	0.15	1.21	2.5	-1.14
2201.2-5019	0.13	0.99	2.4	-1.28
2212.7-5148	0.12	2.34	1.0?	+1.5
"	"	"	3.9?	-1.4
2213.5-5250	0.12	1.80	3.3	-1.38
2218.2-5523	0.12	1.16	1.8	-0.52
2221.0-5644	0.11	0.93	1.8	-0.76
"	"	2.91	"	+1.22
2222.4-5605	0.11	2.66	1.4	+1.37
2228.5-5500	0.12	2.56	1.7	+0.98
2231.8-5243	0.09	+1.89	+2.0	-0.02

Coma Cluster distance taken as 70 Mpc, absorption
as $A_B = 0.20$.

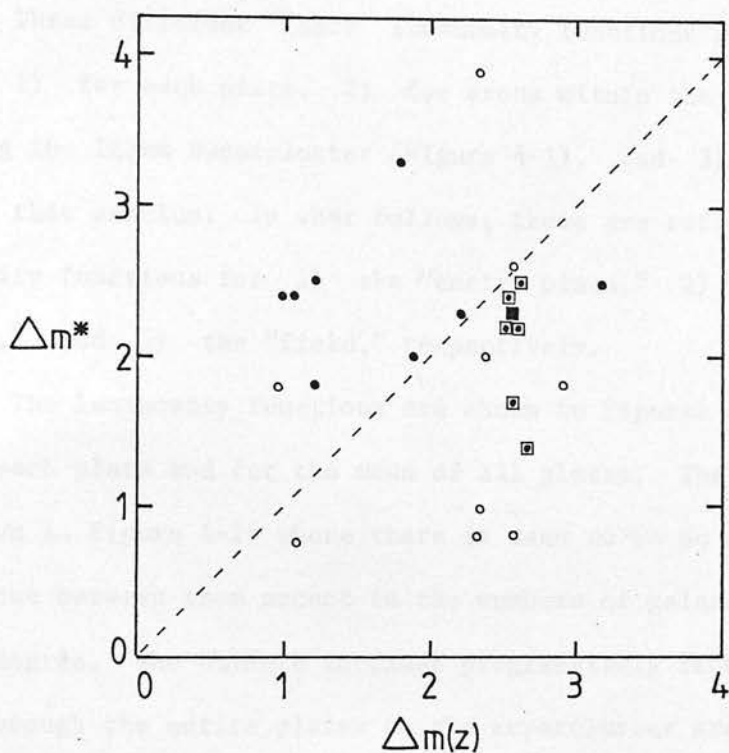


Figure 4-22. Δm^* versus $\Delta m(z)$ for clusters listed in Table 4-4. Uncertain data are shown as open circles. Six Indus Supercluster clusters are enclosed in squares, and the Indus Supercluster data are shown by the solid square. The dashed line is the expected relationship.

C. "Field" Luminosity Functions

Three different "field" luminosity functions were calculated: 1) for each plate, 2) for areas within the annulus defining the Indus Supercluster (Figure 4-1), and 3) for areas outside this annulus. In what follows, these are referred to as luminosity functions for 1) the "entire plate," 2) the "supercluster," and 3) the "field," respectively.

The luminosity functions are shown in Figures 4-23, 24, and 25 for each plate and for the mean of all plates. The means alone are shown in Figure 4-26 where there is seen to be no significant difference between them except in the numbers of galaxies per square degree. The numbers increase progressively from the field areas through the entire plates to the supercluster areas. Abell's finding that the apparent luminosity function is similar in all directions is once again confirmed. The reason for this apparent similarity is that the integration over distance smears out any features that might be present, just as the angular covariance function to any given apparent magnitude limit has most spatial features smeared out.

Since the mean luminosity function for the "entire plate" is probably the most representative here, referring as it does to over 140 square degrees of the sky, it is compared to other luminosity functions in the literature in preference to either the supercluster or "field" luminosity functions. The comparison is shown in Figure 4-27, where the m_J magnitudes have been converted to m_B through equation 4-2b, adopting mean values of B-V from Pence (1976) for each one-magnitude interval. There is still a residual

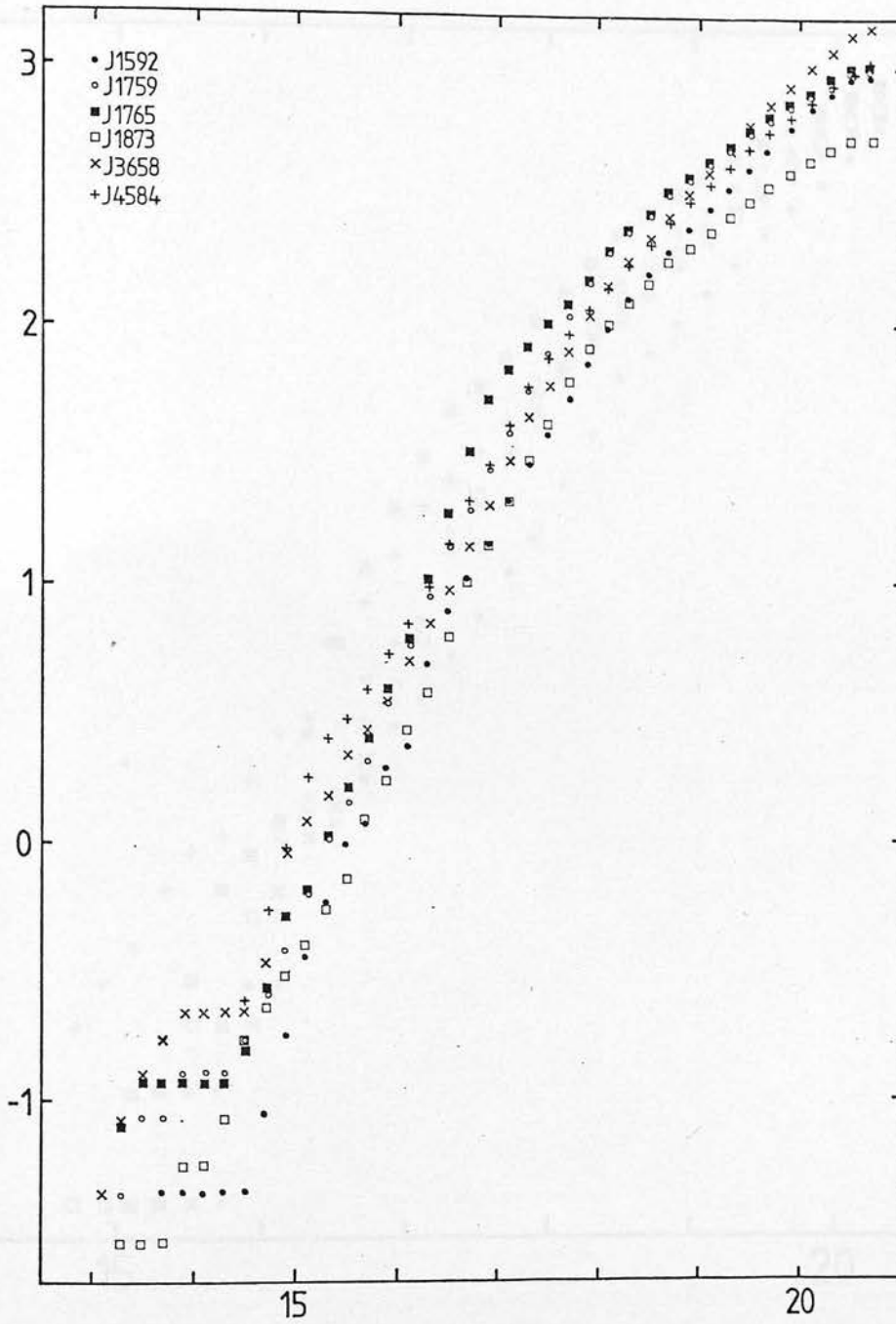


Figure 4-23. Integrated luminosity functions for the "entire plates". Axes as in Figure 4-21.

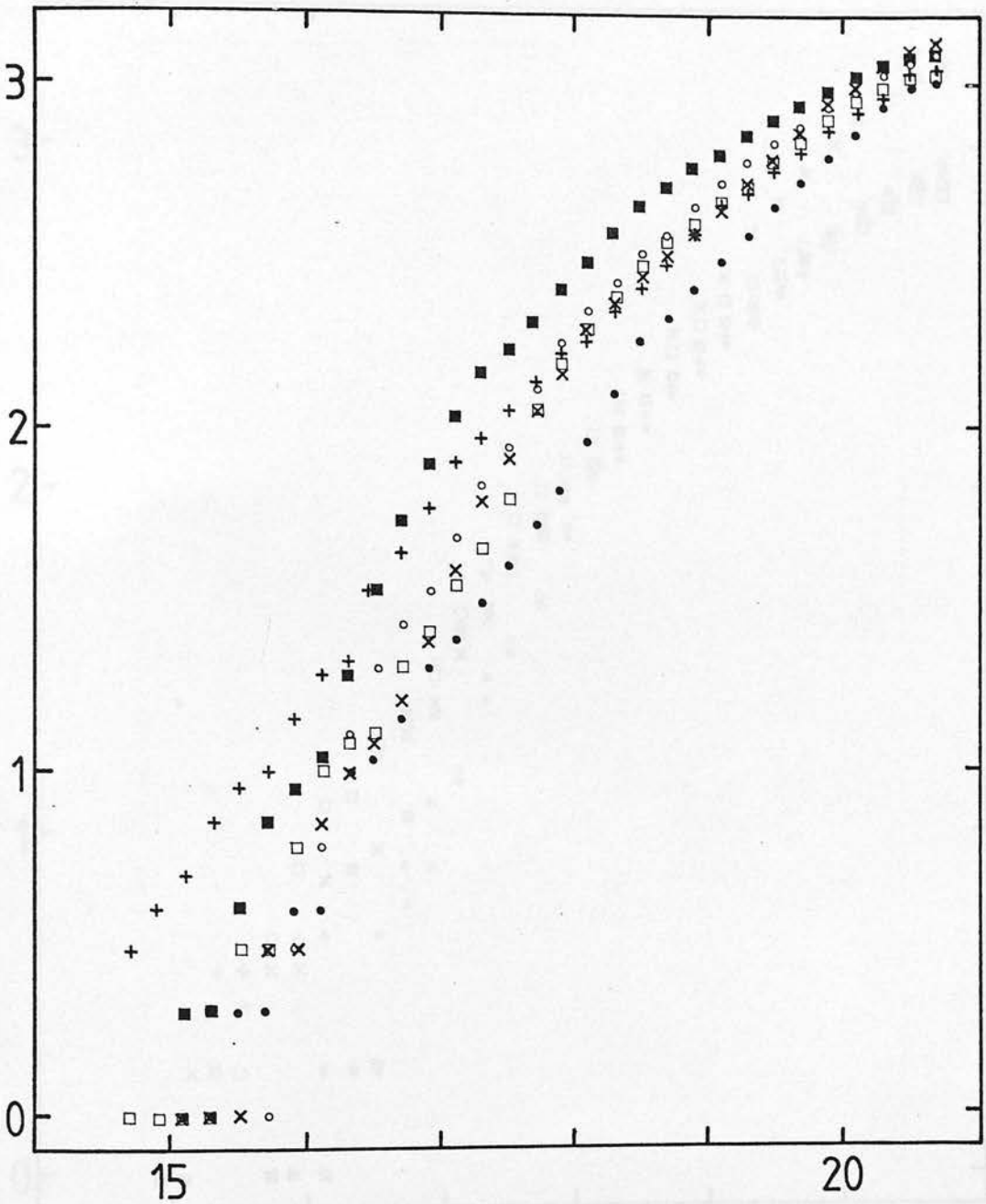


Figure 4-24. Integrated luminosity functions for the supercluster areas. Axes as in Figure 4-21, symbols as in Figure 4-23.

Figure 4-25. Integrated luminosity functions for the "field" areas. Axes as in Figure 4-21, symbols as in Figure 4-23.

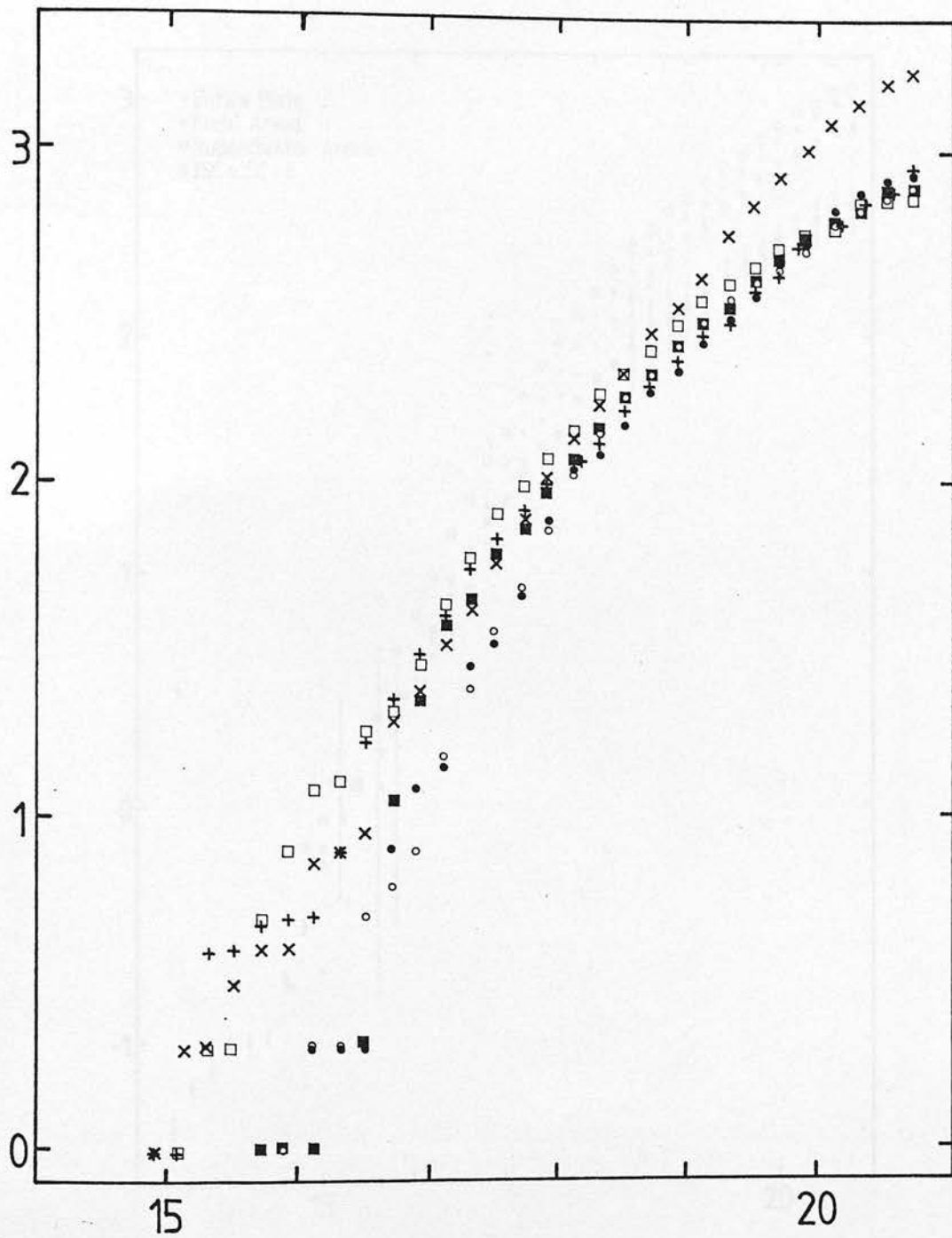


Figure 4-25. Integrated luminosity functions for the "field" areas. Axes as in Figure 4-21, symbols as in Figure 4-23.

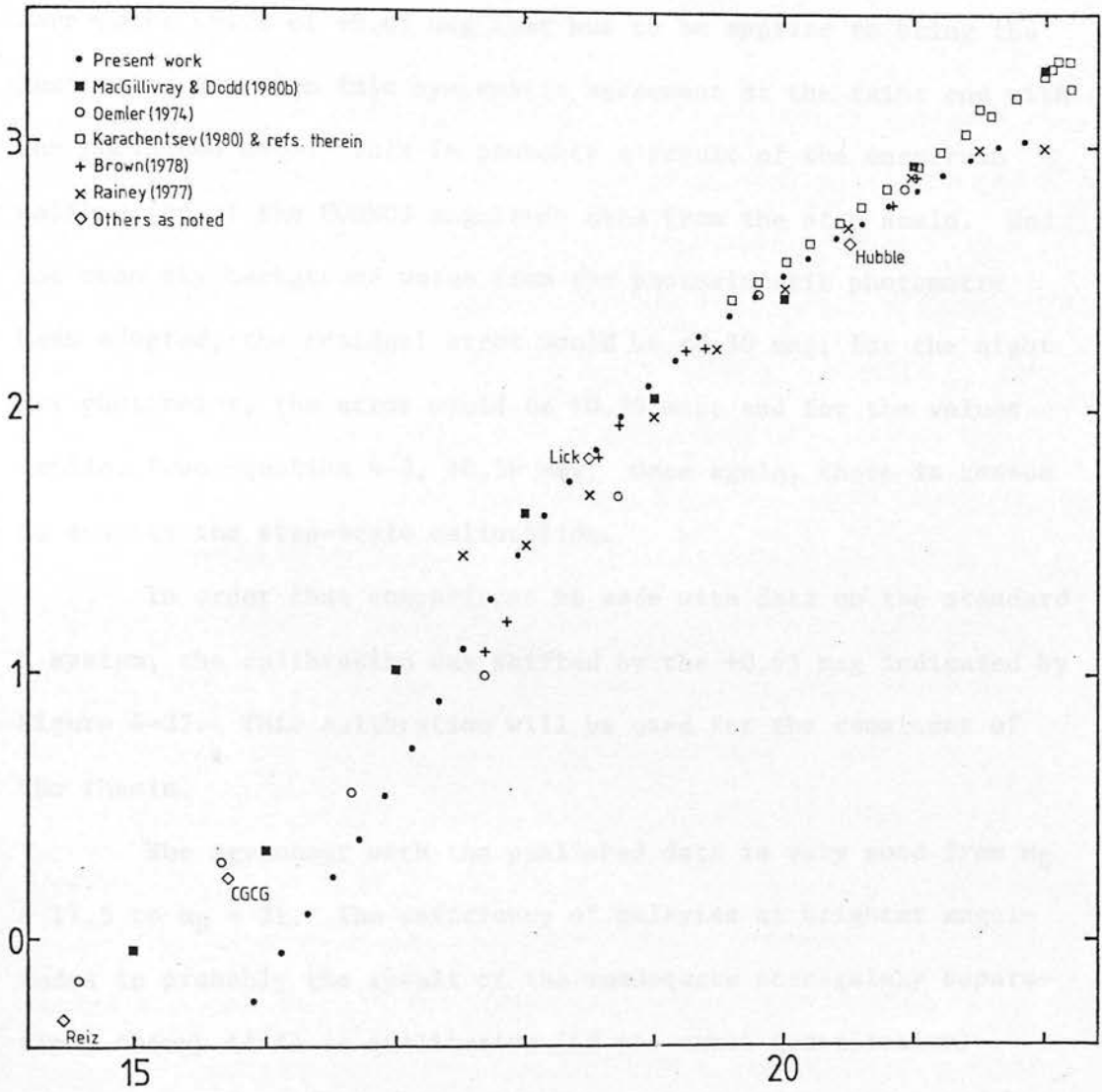


Figure 4-27. Integrated luminosity functions for galaxies from the sources shown. Data from the present work are the mean "entire plate" data from Figure 4-26 and Table 4-6. Axes are m_{pg} and $\log \Sigma N(\leq m)$.

zero-point shift of +0.65 mag that has to be applied to bring the luminosity function into systematic agreement at the faint end with the published data. This is probably a result of the uncertain calibration of the COSMOS magnitude data from the step scale. Had the mean sky background value from the photoelectric photometry been adopted, the residual error would be +0.30 mag; for the night sky photometer, the error would be +0.29 mag; and for the values implied from equation 4-8, +0.39 mag. Once again, there is reason to suspect the step-scale calibration.

In order that comparisons be made with data on the standard B system, the calibration was shifted by the +0.65 mag indicated by Figure 4-27. This calibration will be used for the remainder of the thesis.

The agreement with the published data is very good from $m_B \approx 17.5$ to $m_B \approx 21$. The deficiency of galaxies at brighter magnitudes is probably the result of the inadequate star-galaxy separation, though it is in qualitative (if not exact quantitative) agreement with similar deficiencies seen in the data presented by Brown (1978) and Oemler (1974). These data seem to indicate that the Local Supercluster is located in a volume of space some hundreds of megaparsecs across that is deficient in luminous matter as compared to more distant regions of the universe. The evidence from the present work is not as compelling as that from Brown and Oemler, however, because of the uncertain star-galaxy separation.

D. The Luminosity Function of the Indus Supercluster

In order to look specifically at the luminosity function for the Indus Supercluster, the mean "field" was subtracted from the mean supercluster luminosity function. The result is shown in Figure 4-26 with the other mean luminosity functions. Interestingly, the supercluster luminosity function closely resembles a luminosity function for a rich cluster, though no rich clusters are included in it. If the change in slope at $m_J = 18.0$ is taken as m^* , then the Indus Supercluster is 2.3 magnitudes beyond Coma. This Δm^* is shown in Figure 4-22 where it is seen to agree well with Δm^* 's for four of the six Supercluster clusters represented in the figure (the two discordant points are for clusters on plate J1765, suggesting large systematic errors for that plate, also).

In order to derive other photometric parameters from this luminosity function, it was numerically integrated to give the surface brightness per square degree for the Supercluster. After adjusting the magnitude scale to B magnitudes (as indicated in Section VIII-C above, taking into account the 0.65 mag residual zero-point error found there), the Indus Supercluster's surface brightness was found to be $12.89 \text{ mag deg}^{-2}$, and its mean surface density was found to be $361 \text{ galaxies deg}^{-2}$ to the limiting magnitude of $B = 21.5_5$. A correction for fainter uncounted galaxies is made in the next Chapter.

The same numerical integration was performed for the cluster CL2228.5-5500. This was taken to be typical of the rich clusters in the Supercluster, roughly average in richness. Its

luminosity function was also reduced to numbers per square degree and its surface brightness and density are $10.18 \text{ mag deg}^{-2}$ and $824 \text{ galaxies deg}^{-2}$.

Finally, the total projected area of the Indus Supercluster was taken to be 62.7 deg^2 , the area within the annulus shown in Figures 2-9 and 4-1. The nine rich clusters have their luminosity functions determined within a total area of 4.1 deg^2 , which was subtracted from the area of the Supercluster to give a Supercluster "field" of 58.6 deg^2 . After summing the "field" and "cluster" parameters so defined, and allowing for an average galactic absorption of $A_B = 0.4 \text{ mag}$, the total corrected magnitude of the Indus Supercluster is $B_T^0(\text{ISC}) = 7.9$. With a distance modulus of $\mu_0 = 36.8$, this corresponds to an absolute magnitude of $M_B(\text{ISC}) = -28.9$, or $5.7 \times 10^{13} L_\odot$. Other Supercluster parameters are given in Table 4-5.

The parameters for an "average" galaxy also given in Table 4-5 are calculated simply by dividing the total luminosity of the Supercluster by the total number of galaxies counted to the limiting magnitude $B = 21.5_5$. The numbers are thus sample dependent, but it is interesting to note that the absolute magnitudes agree with previous estimates (by e.g. Brown 1978 and references therein) and that the apparent magnitudes are close to the m^* 's in Table 4-4 for the respective objects. It is thus unlikely that the addition of fainter galaxies missed here will change much the photometric parameters listed in Table 4-5.

The luminosity functions of the mean Supercluster field, the mean "entire plate," and the cluster CL2228.5-5500 are listed in

Table 4-6. The other luminosity functions mentioned in this section are available on request from the writer.

TABLE 4-5

Photometric Parameters for the Indus Supercluster

Parameter	Supercluster "Field"	Rich Clusters	"Field"+ Clusters
Area(deg ²)	58.6	4.1	62.7
$\sum N(\text{deg}^{-2})$	361	824	391
$\sum N$	21130	3410	24540
$\mu_B(\text{deg}^{-2})$	12.89	10.18	12.76
B_T	8.47	10.18	8.27
A_B	0.4	0.4	0.4
B_T^0	8.1	9.8	7.9
μ_0	36.8	36.8	36.8
M_B	-28.7	-27.0	-28.9
$L_0(x10^{-13})$	4.7	1.0	5.7
"Average" Galaxy			
B^0	18.91	18.63	18.87
M_B	-17.89	-18.17	-17.93

TABLE 4-6

B_f	Mean Luminosity Functions			
	Mean Field	Entire Plate	ISC "Field"	Cluster 2228.5-5500
14.10	--	-2.138	--	--
14.30	--	-1.369	--	--
14.50	--	-1.193	--	--
14.70	--	-1.106	--	--
14.90	--	-1.001	--	--
15.10	--	-1.001	--	--
15.30	--	-0.971	--	--
15.51	--	-0.732	-0.770	--
15.71	--	-0.504	-0.174	--
15.91	-0.699	-0.238	-0.174	--
16.11	-0.398	-0.053	+0.114	--
16.31	+0.079	+0.101	0.114	--
16.51	0.079	0.236	0.393	+0.661
16.71	0.342	0.379	0.473	0.769
16.91	0.477	0.542	0.602	1.019
17.11	0.643	0.721	0.748	1.177
17.32	0.732	0.898	0.967	1.213
17.52	0.944	1.092	1.081	1.642
17.73	1.127	1.282	1.211	1.725
17.94	1.301	1.449	1.309	1.896
18.14	1.474	1.595	1.411	2.061
18.34	1.625	1.727	1.526	2.161
18.54	1.747	1.846	1.598	2.197
18.74	1.840	1.967	1.744	2.260
18.95	1.971	2.086	1.815	2.321
19.15	2.079	2.189	1.889	2.373
19.36	2.170	2.280	1.959	2.456
19.57	2.259	2.361	2.044	2.508
19.78	2.332	2.436	2.091	2.571
19.99	2.414	2.508	2.124	2.626
20.19	2.484	2.579	2.179	2.680
20.40	2.551	2.647	2.250	2.738
20.60	2.609	2.714	2.305	2.801
20.81	2.675	2.777	2.351	2.820
21.02	2.731	2.840	2.415	2.836
21.22	2.794	2.899	2.447	2.861
21.43	2.843	2.954	2.498	2.889
21.64	2.890	3.003	2.546	2.916
21.84	2.904	3.019	2.557	2.916

Integral luminosity functions, $\log \sum \langle N \rangle \text{ deg}^{-2}$, summed in ~ 0.2 mag intervals. Mean field is for field areas on all plates except J3658C. Entire plate and ISC "Field" include data from all plates. Cluster is after subtraction of mean field.

CHAPTER 5

The Structure of the Indus Supercluster

I. Introduction

The probable existence of the Indus Supercluster has been demonstrated through galaxy counts, spectroscopy, and photometry leading to luminosity functions. It is still necessary to compare the observed properties of the Supercluster with others that have been previously studied.

First, however, a brief review of the available data seems desirable, along with indications of the data still needed for a more complete study of the Supercluster.

II. Data: Review and Desiderata

A. Galaxy Counts and Redshifts

Counts by eye to a limiting diameter of 12 to 15 arcseconds (roughly corresponding to $B \approx 19$) reveal a large annular structure about $8^\circ \times 10^\circ$ across (Figure 2-9). To some extent, this is the result of projection of galaxies in different discrete redshift ranges, but nine rich clusters with redshifts between $V \approx 22,000$ and $V \approx 24,000$ are confined to this annulus. Evidence from the galaxy counts suggests that the clusters are connected by bridges of galaxies, but no redshifts are available for any galaxies outside of the clusters.

Data obviously needed here are galaxy counts, preferably by machine, to several different magnitude levels. Knowing the sort of galaxy most likely to be counted in such a survey, and its mean

absolute magnitude (Chapter 4, above), it should then be possible to assign a most probable distance to the galaxies seen in the annulus.

This most probable distance could then be confirmed by redshifts of some dozens or hundreds of galaxies both in and out of clusters. (The redshifts are also necessary for a study of the dynamics of the Supercluster, a study presently impossible with a mere fourteen redshifts available in the nine clusters.) The existence of bridges of galaxies to clusters in other velocity ranges might also be revealed by such a redshift survey. Though the Indus Supercluster appears on present evidence to be relatively isolated from its nearest neighbours in space, the writer's present feeling is that there are few if any truly isolated large-scale structures in the universe. The filamentary connections between and involving clusters seem to be the rule rather than the exception in the currently available observations (e.g. Einasto et al 1980a, Davis et al 1981).

B. Photometry

The photometry of thousands of relatively bright galaxies obviously demands measurements made on large-field photographic survey plates (though the application in the future of very large digital array detectors combined with high-speed multi-megabyte computer systems seems possible). These plates will have to be of the highest quality with very low background fluctuations, must have accurate relative and absolute calibration, and must be scanned with a machine having a properly shielded spot to reduce scattered light and increase dynamic range. The plates must also be original

plates — the copies used here are not acceptable material for accurate photometric work, though they might be suitable for distribution studies provided the star-galaxy separation problem could be solved.

C. Non-optical Data

Unfortunately, little is known in the Indus Supercluster area outside of the optical portion of the spectrum. A few of the bright galaxies in the superposed Pavo-Indus Cloud are known radio sources (Haynes et al 1975), but only five fainter galaxies are coincident with radio sources in the initial survey area (Ekers 1970, Savage 1976, Savage et al 1976). Only one of these (PKS2131-537 = A2131-53A) has been observed spectroscopically (Whiteoak 1972 and Appendix A). Though it is a confirmed Supercluster member, it is in no way unusual from other radio sources in its optical or radio characteristics. (This "negative" observation merely offers another small bit of evidence that supercluster galaxies are the typical galaxies in the universe.)

The situation in the X-ray spectrum is even less satisfactory. Of the three X-ray sources in the initial survey area (see Markert et al 1976 and references therein) only one, 2A2155-609, has an error box small enough to allow tentative optical identification. Two rich clusters, CL2154.9-6040 (a confirmed Indus Supercluster member) and CL2158.2-6011 (some 70 Mpc beyond the Supercluster) fall within the error box. Either (or neither) could be the X-ray source — higher resolution data are required.

Other suggested indentifications are much less likely. Markert et al (1976) suggest NGC 7125 or NGC 7126 as possible indentifications for MX2140-60, though neither is a Seyfert galaxy, the most likely kind of individual galaxy to be an X-ray source. Lugger (1978) identifies this source with a "rich" cluster ($R = 2$ on Abell's scale) at 2146.4-5922. However, examination of the area on plates and film copies of Field 145 shows only a poor group of about ten galaxies in Lugger's place.

Finally, 4U2126-60 has too large an error box (24 square degrees) to be identified with anything. However, it does enclose both 2A2155-609 and MX2140-60, so is probably identical with one or the other (or both).

The lack of non-optical information about the Indus Supercluster, while frustrating, is hardly surprising. From a non-optical survey point of view, the ~ 400 square degree initial survey area is simply another randomly chosen one percent of the sky. Hopefully, the present study will direct some attention to this area.

It should be mentioned here that Schuch (1979, 1981) has found the portion of the Ursa Major Supercluster that he surveyed to be completely normal in its radio characteristics when compared with another part of the sky lacking a nearby supercluster. Similarly, while there have been suggestions of diffuse X-ray sources coincident (presumably) associated with superclusters (see e.g. Murray et al 1978, Maccagni et al 1978, Ulmer et al 1978), more detailed work has shown that these sources are either spurious (Culhane 1978) or that the X-ray flux can be adequately explained

as originating entirely in the rich clusters of the superclusters in question (Kellogg 1978, Pravdo et al 1979, Ulmer and Cruddace 1981).

III. Comparison With Other Supercluster Observations

A. Total Luminosity and Mass

As has already been mentioned, it is unfortunate that so few redshifts are available for the Indus Supercluster; this precludes any direct attempt to derive a mass for the system and from that an estimate of its mean density. This remains a task for the next investigation of the Indus Supercluster.

However, the estimate of its total luminosity can be compared with those given recently for the Perseus Supercluster (Einasto et al 1980a) and the Hercules Supercluster (Tarenghi et al 1979b). For the entire Perseus Supercluster ring, Einasto et al find $L = 5.6 \times 10^{13} L_{\odot}$, while Tarenghi et al give $L = 3.8 \times 10^{13} L_{\odot}$ for the part of the Hercules Supercluster that they studied. Reference to the Lick Survey and to the other estimates of the extent of the Hercules Supercluster (Abell 1961, Thuan 1980) suggests that this figure should be at least doubled. The luminosity adopted here for the Hercules Supercluster is $L \sim 8 \times 10^{13} L_{\odot}$ with an uncertainty of at least a factor of two.

Both of these estimates agree with the total luminosity of the Indus Supercluster determined in the previous chapter, $L = 5.7 \times 10^{13} L_{\odot}$. This is likely to be a lower limit as no correction has been made for galaxies fainter than the limiting magnitude of the luminosity function. However, since most of the luminosity of

a system of galaxies is known to come from its brighter members (see e.g. Abell 1977), the estimate is not liable to change much. The circumstantial evidence of the similarity of the integrated luminosity function of the Supercluster to that of rich clusters suggests that less than $\sim 25\%$ of the light has not been included (again, see Abell 1977), making the total luminosity $\sim 7 \times 10^{13} L_{\odot}$.

In any case, the three superclusters have similar total luminosities. If they also have similar mass-to-luminosity ratios ($M/L \sim 150$; Einasto et al 1980a and Tarenghi et al 1979b) then the mass of the Indus Supercluster will be about $m_{ISC} \approx 1 \times 10^{16} m_{\odot}$. This is similar to mass estimates for other superclusters — masses of $\sim 10^{15}$ to $\sim 10^{17}$ have been suggested by de Vaucouleurs (1960), Abell (1974), Schuch (1979), and Dawe et al (1979), as well as by Einasto et al (1980a) and Tarenghi et al (1979b). The mean of these estimates is $8.4(\pm 4.7) \times 10^{15} m_{\odot}$. The Indus Supercluster is thus not unusual when compared to other superclusters, at least regarding its total luminosity and mass.

B. Structural Properties

As has been stressed throughout this thesis, the structure of superclusters has been shown to be annular in projection, with filaments of galaxies joining rich clusters in space, and with neighbouring superclusters sharing adjoining clusters and filaments. Einasto et al (1980a,b) have also suggested that supercluster boundaries are marked in some cases by sheets of galaxies. Though no evidence is yet available in the Indus area for sheets, some supporting evidence comes from redshifts of galaxies in the Virgo Cluster area. The cluster itself is seen in projection

against the "hole" in the middle of the Coma Supercluster. Several galaxies in the "hole" have redshifts somewhat larger than the Coma Cluster itself (Eastmond and Abell 1979, Corwin and Emerson 1981, Appendix A), yet show no strong clustering tendencies. This may be the far "wall" of the Coma Supercluster.

If, then, superclusters are irregular cells, distributed in a roughly sponge-like manner throughout the universe, do they have a characteristic dimension? Data for four superclusters — Perseus, Coma, Hercules, and Indus — plotted in Figure 5-1 (collected in Table 5-1) suggest that there is such a characteristic size. However, Tago (Einasto 1980, private communication) shows that smaller rings of clusters exist in the Coma Supercluster, so this finding of similar sizes for superclusters must be treated with some caution.

In summary, then, the Indus Supercluster is similar to other superclusters, insofar as supercluster properties are currently known. An extensive redshift survey of the Indus Supercluster region is needed to clearly delineate it, however, as well as to study its dynamics and virial properties.

IV. Formation of Superclusters

Though a complete discussion of the formation and evolution of macrostructure in the universe is clearly beyond the scope of this thesis, a short qualitative review of recent work in these areas seems an appropriate conclusion.

Nearly all work on supercluster formation is presently done in the context of big bang cosmological models. Other cosmologies, such as Segal's chronometric universe (Segal 1976, 1980 and

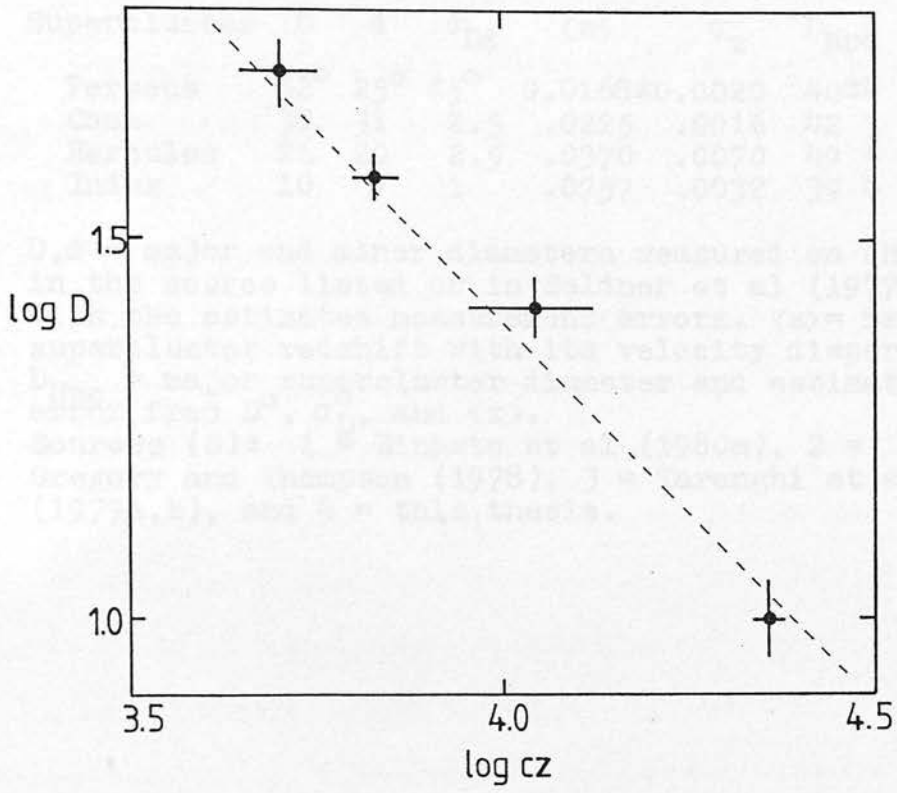


Figure 5-1. Supercluster cell sizes D versus redshift. The dashed line represents a constant linear dimension of 43 Mpc.

Table 5-1 -- Supercluster Cell Sizes

Supercluster	D	d	σ_{Dd}	$\langle z \rangle$	σ_z	D _{Mpc}	S
Perseus	52°	25°	±5°	0.0168±0.0020		40±4	1
Coma	38	31	2.5	.0225	.0016	42 3	2
Hercules	26	20	2.5	.0370	.0070	49 5	3
Indus	10	7	1	.0757	.0032	39 4	4

D,d = major and minor diameters measured on charts in the source listed or in Seldner et al (1977), with the estimated measurement errors. $\langle z \rangle$ = mean supercluster redshift with its velocity dispersion. D_{Mpc} = major supercluster diameter and estimated error from D°, σ_D , and $\langle z \rangle$.

Sources (S): 1 = Einasto et al (1980a), 2 = Gregory and Thompson (1978), 3 = Tarenghi et al (1979a,b), and 4 = this thesis.

references therein), the Hoyle-Narlikar variable-G, steady-state universe (Narlikar 1979 and references therein) and the Pecker tired-light cosmology (Pecker and Vigier 1976, and references therein), have not yet been studied extensively from the points of view of galaxy distribution or the formation of structure among galaxies. Until such studies are made, these cosmological models can only be interesting theoretical constructs, mostly divorced from observational work on large-scale structure. They should be given serious consideration, nevertheless, even if they are eventually shown to be incorrect (Narlikar and Kembhavi (1980) give an extensive review of "non-standard" cosmologies).

Within the more or less "standard" big bang models, work has concentrated on two slightly different approaches: 1) a gravitational instability model where large-scale structure develops after galaxies have formed from an essentially smooth initial distribution of matter and energy and 2) a model invoking large primeval inhomogeneities so that development of macrostructure in the universe precedes galaxy formation (or is at least coeval with it).

The first of these two general models has received much attention from Peebles (1980 and references therein) and others strongly influenced by the apparent homogeneity and isotropy of the cosmic microwave background. If this is taken as an observation of the universe at (or just after) the decoupling era at $z \sim 1300$, it is difficult to see how large-scale adiabatic fluctuations involving both matter and radiation could exist. Fluctuations of the order of size of superclusters ($\sim 10^{16} m_{\odot}$) would be readily detectable in the background radiation — yet these are not seen (e.g. Weiss 1980). There are also theoretical reasons for supposing

that fluctuations of $\sim 10^{16} m_{\odot}$ could either never develop or would be damped out before decoupling (see e.g. Press and Vishniac 1980 as well as Peebles 1980).

Therefore, proponents of the gravitational instability picture have attempted to show that simple gravitational interaction of galaxies since $z \sim 30$ (the galaxies in this picture would form from small isothermal fluctuations in the interval $1300 \gtrsim z \gtrsim 30$) can account for the large scale structure as we see it. Some aspects of this model do match observation — clusters and superclusters form, and the slope of the covariance function (see Chapter 1, Section V-A) is correctly predicted. However, the filamentary sponge-like structure of the distribution of galaxies and clusters cannot be reproduced in this manner (e.g. Davis et al 1981).

This would seem to leave the second alternative as the "correct" one. In this approach, the primeval fluctuations in the universe are generally considered to be adiabatic (see e.g. Doroshkevich et al 1978 and Zel'dovich 1978 and references therein) since isothermal fluctuations in matter alone would be quickly damped out prior to decoupling. This model suggests that the large scale filamentary cell structure that we observe is present before decoupling, perhaps in the form of shock fronts. After decoupling, galaxies and clusters form in these regions of enhanced density. The large-scale structure that we see is thus a reflection of primordial inhomogeneities.

The difficulty here, of course, is that adiabatic fluctuations would leave their mark on the background radiation as small-scale variations that, as mentioned, we do not see. Several ways out of this dilemma have been suggested [e.g. the fluctuations are

actually in the fields associated with Higgs particles (Zel'dovich 1980), or are in gravitationally formed sheets of massive neutrinos (Szalay 1981), or arose after decoupling through perturbations induced by nearly simultaneous supernovae explosions of an initial population of ~ 5 solar mass stars (Saar 1979)], but none of these suggestions or others proposed yet have strong observational evidence in their favour.

It is still apparent, however, that there is structure in the universe. Our inability to adequately account for its formation and evolution can be traced in the end to our lack of observational data. Cosmological theories cannot be tested in a total void — yet even now, many suggested observational tests in cosmology depend on data that we do not yet have (or in some cases, that we can perhaps never obtain).

Lack of data has rendered much of this thesis inconclusive, also. Yet a consistent picture can still be drawn of the structure of the Indus Supercluster. This picture is not in serious conflict with recent views of other superclusters, so perhaps we are finally converging on a satisfactory notion of how luminous matter is distributed in our universe. If this is so, it can only be a matter of time before we also understand how the universe came to be as we see it.

References

- Aaronson, M., Mould, J., Huchra, J., Sullivan, W. T., Schommer, R. A. and Bothun, G. D. 1980. *Ap. J.* 239, 12.
- Abadi, H. I. and Edmunds, M. G. 1977. *A. & A.* 56, 319.
- Abbe, C. 1867. *M.N.R.A.S.* 27, 257.
- Abell, G. O. 1958. *Ap. J. Suppl.* 3, 211 (No. 31).
- Abell, G. O. 1961. *A. J.* 66, 607.
- Abell, G. O. 1962. In *IAU Symp. No. 15*, ed. G. C. McVittie (Macmillan: New York), p. 213.
- Abell, G. O. 1974. In *IAU Symp. No. 63*, ed. M. S. Longair (D. Reidel: Dordrecht), p. 79.
- Abell, G. O. 1975. In *Galaxies and the Universe*, ed. A. Sandage, M. Sandage, J. Kristian (Univ. Chicago Press: Chicago) p. 601.
- Abell, G. O. 1977. *Ap. J.* 213, 327.
- Abell, G. O. 1978. In *IAU Symp. No. 79*, ed. M. S. Longair and J. Einasto (D. Reidel: Dordrecht) p. 253.
- Abell, G. O. and Seligman, C. E. 1965. *A. J.* 70, 317.
- Abell, G. O. and Seligman, C. E. 1967. *A. J.* 72, 288.
- Ables, H. D., Newell, E. B. and O'Neil, E. J. 1974. *P.A.S.P.* 86, 311.
- Agekian, T. A. 1957. *Astron. Zhur.* 34, 371 (Eng. trans.: *Sov. Astron.* 1, 366, 1957).
- Aguero, E. 1971. *P.A.S.P.* 83, 310.
- van Albada, G. B. 1960. *B.A.N.* 15, 165 (no. 500).
- van Albada, G. B. 1962. In *IAU Symp. No. 15*, ed. G. C. McVittie (Macmillan: New York), p. 411.
- Arp, H. C. 1981. *Ap. J. Suppl.* 46, 75.
- Arp, H. C. and Madore, B. F. 1977. *Q.J.R.A.S.* 18, 234.
- Baker, A. E. 1925. *Proc. R. S. Edin.* 45, 166.

- Baker, R. H. 1933. Harv. Ann. 88, No. 3.
- Baker, R. H. 1937. Harv. Ann. 88, No. 6.
- Bautz, L. P. and Abell, G. O. 1973. Ap. J. 184, 709.
- Bell, M. B. 1969. Nature 224, 229.
- van den Bergh, S. 1961. P.A.S.P. 73, 46.
- Bergwall, N. Å. S., Ekman, A. B. G., Lauberts, A., Westerlund, B. E., Borchkhadze, T. M., Breysacher, J., Laustsen, S., Muller, A. B., Schuster, H.-E., Surdej, J. and West, R. M. 1978. A. & A. Suppl. 33, 243.
- Bernheimer, W. E. 1932a. Nature 130, 132.
- Bernheimer, W. E. 1932b. Himmelswelt 42, 223.
- Bogart, R. S. and Wagoner, R. V. 1973. Ap. J. 181, 609.
- Bok, B. J. 1931. Harv. Obs. Circ. No. 371.
- Bok, B. J. 1934. Harv. Obs. Bull. No. 895, 1.
- Bolton, J. G. and Savage, A. 1978. In IAU Symp. No. 79, ed. M. S. Longair and J. Einasto (D. Reidel: Dordrecht) p. 295.
- Borchkhadze, T. M., Breysacher, J., Laustsen, S., Schuster, H.-E. and West, R. M. 1977. A. & A. Suppl. 30, 35.
- Braid, M. K. and MacGillivray, H. T. 1978. M.N.R.A.S. 182, 241.
- Brown, G. S. 1978. Univ. Texas Publ. in Astron. No. 11.
- Brown, G. S. and Tinsley, B. 1974. Ap. J. 194, 555.
- Burbidge, G. R. 1977. In IAU Coll. No. 37, ed. C. Balkowski and B. E. Westerlund (Ed. CNRS: Paris) p. 555.
- Burbidge, G. R. and Burbidge, E. M. 1959. Ap. J. 130, 629.
- Burstein, D. and Heiles, C. 1978a. Ap. Lett. 19, 69.
- Burstein, D. and Heiles, C. 1978b. Ap. J. 225, 40.
- Chandrasekhar, S. and Münch, G. 1952. Ap. J. 115, 103.
- Chincarini, G. 1978. Nature 272, 515.
- Chincarini, G. and Martins, D. H. 1975. Ap. J. 196, 335.
- Chincarini, G. and Rood, H. J. 1976a. Ap. J. 206, 30.
- Chincarini, G. and Rood, H. J. 1976b. P.A.S.P. 88, 388.

- Chincarini, G. and Rood, H. J. 1979. *Ap. J.* 230, 648.
- Chincarini, G., Tarenghi, M. and Bettis, C. 1981. *A. & A.* 96, 106.
- Corwin, H. G. 1967. Thesis, Univ. of Kansas.
- Corwin, H. G. 1971. *P.A.S.P.* 83, 320.
- Corwin, H. G. 1974. *A. J.* 79, 1356.
- Corwin, H. G. 1979. In *Photometry, Kinematics, and Dynamics of
of Galaxies*, ed. D. S. Evans (Astron. Dept. U. T.: Austin)
p. 125.
- Corwin, H. G. 1980. *M.N.R.A.S.* 191, 1. (Appendix B).
- Corwin, H. G. and Emerson, D. 1981. Submitted to *M.N.R.A.S.*
(Appendix A).
- Corwin, H. G., de Vaucouleurs, A. and de Vaucouleurs, G. 1980.
A. J. 85, 1027.
- Corwin, H. G., de Vaucouleurs, A. and de Vaucouleurs, G. 1981.
Submitted to *A. J.*
- Culhane, J. L. 1978. In *IAU Symp. No. 79*, ed. M. S. Longair and
J. Einasto (D. Reidel: Dordrecht) p. 165.
- Davis, M. and Geller, M. J. 1976. *Ap. J.* 208, 13.
- Davis, M., Groth, E. J. and Peebles, P. J. E. 1977. *Ap. J.* 212,
L107.
- Davis, M., Huchra, J., Latham, D. W. and Tonry, J. 1981. Harvard-
Smithsonian Center for Astrophys. Preprint No. 1493.
- Dawe, J. A., Dickens, R. J. and Peterson, B. A. 1977. *M.N.R.A.S.*
178, 675.
- Dawe, J. A., Dickens, R. J., Lucey, J., Mitchell, R. J. and
Peterson, B. A. 1979. *New Zealand J. Sci.* 22, 369.
- Dodd, R. J., MacGillivray, H. T., Smith, G. M. and Ellery, L. A.
1979. In *Image Processing in Astron.*, ed. G. Sedmak, M.
Capaccioli, R. J. Allen (Osserv. Astr.: Trieste) p. 360.
- Doroshkevich, A. G., Saar, E. M. and Shandarin, S. F. 1978. In
IAU Symp. No. 79, ed. M. S. Longair and J. Einasto (D. Reidel:
Dordrecht) p. 423.
- Dressler, A. 1978. *Ap. J.* 223, 765.
- Dreyer, J. L. E. 1890. *Mem. R. A. S.* 49, 1.

- Dreyer, J. L. E. 1895. Mem. R. A. S. 51, 185.
- Dreyer, J. L. E. 1910. Mem. R. A. S. 59, 105.
- Dunlop, J. 1828. Phil. Trans. 118, 113.
- Duus, A. and Newell, B. 1977. Ap. J. Suppl. 35, 209.
- Eastmond, T. S. 1976. Thesis, UCLA.
- Eastmond, T. S. and Abell, G. O. 1978. P.A.S.P. 90, 367.
- Einasto, J., Jõeveer, M. and Saar, E. 1980a. M.N.R.A.S. 193, 353.
- Einasto, J., Jõeveer, M. and Saar, E. 1980b. Nature 283, 47.
- Ekers, R. D. 1970. Aust. J. Phys. 23, 217.
- Ellis, R. S., Fong, R. and Phillipps, S. 1977. M.N.R.A.S. 181, 163.
- Fairall, A. P. 1979. M.N.R.A.S. 188, 349.
- Fairall, A. P. 1981. M.N.R.A.S. 196, 417.
- Fall, S. M. 1979. Rev. Mod. Phys. 51, 21.
- Fall, S. M., Geller, M. J., Jones, B. J. T. and White, S. D. M. 1976. Ap. J. 205, L121.
- Fath, E. A. 1914. A. J. 28, 75.
- Fesenko, B. I. 1979a. Astron. Zh. 56, 928 (Eng. trans.: Sov. Astron. 23, 524, 1980).
- Fesenko, B. I. 1979b. Astrofizika 15, 599 (Eng. trans.: Astrophysics 15, 402, 1980).
- Flin, P. 1974. Mem. Soc. Astron. Ital. 45, 663.
- Ford, H. C., Harms, R. J., Ciardullo, R. and Bartko, F. 1981. UCLA Astron. Astrophys. Preprint No. 114.
- Fullerton, L. W. and Hoover, P. 1972. Ap. J. 172, 9.
- Giovanelli, R., Chincarini, G. and Haynes, M. P. 1981. Ap. J., submitted.
- Glyn Jones, K. 1975. The Search for the Nebulae. (Alpha Academic: Chalfont St. Giles).
- Godwin, J. G. and Peach, J. V. 1977. M.N.R.A.S. 181, 323.

- Golden, L. M. 1974. M.N.R.A.S. 166, 383.
- Green, M. R. 1978. Thesis, Univ. of Oxford.
- Gregory, S. A. and Thompson, L. A. 1978. Ap. J. 222, 784.
- Gregory, S. A., Thompson, L. A. and Tifft, W. G. 1981. Ap. J. 243, 411.
- Gusak, A. I. 1969. Astron. Zhur. 46, 1231 (Eng. trans.: Sov. Astron. 13, 964, 1970).
- Hanes, D. A. 1975. Thesis, Univ. of Toronto.
- Hanes, D. A. 1977. Mem. R. A. S. 84, 45.
- Hardcastle, J. A. 1914. M.N.R.A.S. 74, 699.
- Harms, R. J., Ford, H. C., Ciardullo, R. and Bartko, F. 1981.
In 10th Texas Symp., in press.
- Hauser, M. G. and Peebles, P. J. E. 1973. Ap. J. 185, 757.
- Havlen, R. J. and Quintana, H. 1978. Ap. J. 220, 14.
- Hawkins, M. R. S. 1981. M.N.R.A.S. 194, 1013.
- Haynes, R. F., Huchtmeier, W. K. H., Siegman, B. C. and Wright, A. E. 1975. A Compendium of Radio Measurements of Bright Galaxies (CSIRO: Melbourne).
- Heiles, C. and Cleary, M. N. 1979. Aust. J. Phys. Ap. Suppl. 47, 1.
- Herschel, J. F. W. 1847. Results ... Cape of Good Hope. (Smith, Elder and Co.: London).
- Herschel, J. F. W. 1864. Phil. Trans. 154, 1.
- Herschel, W. 1784. Phil. Trans. 74, 437.
- Herzog, E. 1967. P.A.S.P. 79, 446.
- Hewett, P. C., MacGillivray, H. T. and Dodd, R. J. 1981. M.N.R.A.S. 195, 613.
- Hinks, A. R. 1911. M.N.R.A.S. 71, 588.
- Hoffmann, G. L., Olson, D. W. and Salpeter, E. E. 1980. Ap. J. 242, 861.
- Holmberg, E. 1937. Ann. Lund Obs. No. 6.

- Holmberg, E. 1958. *Medd. Lund Obs., Ser. II*, No. 136.
- Holmberg, E. 1974. *A. & A.* 35, 121.
- Hubble, E. P. 1925. *Ap. J.* 62, 409.
- Hubble, E. P. 1926. *Ap. J.* 63, 263.
- Hubble, E. P. 1934. *Ap. J.* 79, 8.
- Hubble, E. P. 1936a. *The Realm of the Nebulae* (Yale Univ. Press: New Haven).
- Hubble, E. P. 1936b. *Ap. J.* 84, 517.
- Hubble, E. P. and Tolman, R. C. 1935. *Ap. J.* 82, 302.
- Humason, M. L., Mayall, N. U. and Sandage, A. R. 1956. *A. J.* 61, 97.
- von Humboldt, A. 1866. *Cosmos* 4, 28.
- Jöeveer, M. and Einasto, J. 1978. In *IAU Symp. No. 79*, ed. M. S. Longair and J. Einasto (D. Reidel: Dordrecht), p. 241.
- Jöeveer, M., Einasto, J. and Tago, E. 1978. *M.N.R.A.S.* 185, 357.
- Jones, B. J. T. 1976. *M.N.R.A.S.* 174, 429.
- Kalinkov, M. 1967. *Bull. Sec. Astron.* 1, 77.
- Kalinkov, M. 1973. In *Proc. 1st Euro. Reg. Astron. Meet.*, ed. B. Barbanis and J. D. Hadjidemetriou (Springer-Verlag: Berlin) p. 142.
- Kalinkov, M. 1974. *Mem. Soc. Astron. Ital.* 45, 637.
- Kalinkov, M. 1977. In *Highlights of Astronomy*, Vol. 4, Part 1, ed. E. A. Muller (D. Reidel: Dordrecht), p. 279.
- Karachentsev, I. D. 1966. *Astrofizika* 2, 307 (Eng. trans.: *Astrophysics* 2, 159, 1966).
- Karachentsev, I. D. 1970. *Prob. Kosm. fiz.* 5, 201.
- Karachentsev, I. D. 1980. *Pis'ma Astron. Zh.* 6, 3 (Eng. trans.: *Sov. Astron. Lett.* 6, 1, 1980).
- Karachentsev, I. D. and Shcherbanovskii, A. L. 1978. *Astron. Zh.* 55, 449 (Eng. trans.: *Sov. Astron.* 22, 257, 1979).
- Karachentsev, I. D., Tsarevskaya, R. L. and Shcherbanovskii, A. L. 1975. *Astron. Zhur.* 52, 999 (Eng. trans.: *Sov. Astron.* 19, 606, 1976).
- Karoji, H. 1975. *C. R. Acad. Sci. Paris, Sér B*, 280, 421 & 455.

- Karpowicz, M. 1967a. Zs. f. Ap. 66, 301.
- Karpowicz, M. 1967b. Zs. f. Ap. 67, 139.
- Karpowicz, M. 1970a. Acta Astron. 20, 391.
- Karpowicz, M. 1970b. Acta Astron. 20, 395.
- Karpowicz, M. 1971a. Acta Astron. 21, 103.
- Karpowicz, M. 1971b. Acta Astron. 21, 115.
- Karpowicz, M. 1971c. Acta Astron. 21, 391.
- Katz, L. and Mulders, G. F. W. 1942. Ap. J. 95, 565.
- Kellogg, E. M. 1978. Ap. J. 220, L63.
- Kiang, T. 1967, M.N.R.A.S. 135, 1.
- Kiang, T. and Saslaw, W. C. 1969. M.N.R.A.S. 143, 129.
- Kirshner, R. P., Oemler, A. and Schechter, P. L. 1978. A. J. 84, 951.
- Klemola, A. R. 1969. A. J. 74, 804.
- König, A. 1962. In *Astronomical Techniques*, ed. W. A. Hiltner (Univ. of Chicago Press: Chicago), p. 461.
- Konzitas, M. 1977. Thesis, Univ. of Edinburgh.
- Kron, R. G. 1980. Ap. J. Suppl. 43, 305.
- Kron, G. E. and Shane, C. D. 1974. Ap. Sp. Sci. 30, 127.
- Krupp, E. C. 1974. P.A.S.P. 86, 385.
- de Lacaille, N.-L. 1755. Mém. Acad. Roy. des Sci., p. 286.
- Lauberts, A., Holmberg, E., Schuster, H.-E. and West, R. M. 1981a. A. & A. Suppl. 43, 307.
- Lauberts, A., Holmberg, E., Schuster, H.-E. and West, R. M. 1981b. A. & A. Supp., in press.
- Layzer, D. 1956. A. J. 61, 383.
- Layzer, D. 1975. In *Galaxies and the Universe*, ed. A. Sandage, M. Sandage, J. Kristian (Univ. Chicago Press: Chicago) p. 665.
- Limber, D. N. 1953. Ap. J. 117, 134.

- Limber, D. N. 1954. *Ap. J.* 119, 655.
- Limber, D. N. 1957. *Ap. J.* 125, 9.
- Lundmark, K. 1927. *Medd. Uppsala Astron. Obs.* No. 30.
- Lugger, P. M. 1978. *Ap. J.* 221, 745.
- Lutz, R. K. 1979. *The Computer Journal* 23, 262.
- Maccagni, D., Tarenghi, M., Cooke, B. A., Maccacaro, T., Pye, J. P., Ricketts, M. J. and Chincarini, G. 1978. *A. & A.* 62, 127.
- MacGillivray, H. T. and Dodd, R. J. 1979a. *M.N.R.A.S.* 186, 69.
- MacGillivray, H. T. and Dodd, R. J. 1979b. *M.N.R.A.S.* 186, 743.
- MacGillivray, H. T. and Dodd, R. J. 1980a. *M.N.R.A.S.* 193, 1.
- MacGillivray, H. T. and Dodd, R. J. 1980b. *Ap. Sp. Sci.* 72, 315.
- MacGillivray, H. T., Martin, R., Pratt, N. M., Reddish, V. C., Seddon, H., Alexander, L. W. G., Walker, G. S. and Williams, P. R. 1976. *M.N.R.A.S.* 176, 265.
- MacGillivray, H. T., Dodd, R. J. and McNally, B. V. 1980. *Ap. Sp. Sci.* 67, 237.
- MacGillivray, H. T., Dodd, R. J., McNally, B. V. and Corwin, H. G. 1981a. *M.N.R.A.S.*, in press.
- MacGillivray, H. T., Dodd, R. J., McNally, B. V., Lightfoot, J. F., Corwin, H. G., Heathcote, S. R. 1981b. *Ap. Sp. Sci.*, in press.
- Markert, T. H., Canizares, C. R., Clark, G. W., Li, F. K., Northridge, P. L., Sprott, G. F. and Wargo, G. F. 1976. *Ap. J.* 206, 265.
- Materna, J. 1979. *A. & A.* 75, 235.
- Mayall, N. U. 1934. *Lick Obs. Bull.* 16, 177 (No. 458)..
- Mead, R. 1974. *Biometrics* 30, 295.
- Mobray, A. G. 1938. *P.A.S.P.* 50, 275.
- Mottmann, J. and Abell, G. O. 1977. *Ap. J.* 218, 53.
- Mould, J., Aaronson, M. and Huchra, J. 1980. *Ap. J.* 238, 458.
- Murray, S. S., Forman, W., Jones, C. and Giacconi, R. 1978. *Ap. J.* 219, 189.

- Narlikar, J. V. 1979. Lectures on General Relativity and Cosmology (Macmillan: London).
- Narlikar, J. V. and Kembhavi, A. K. 1980. Fund. Cosmic Phys. 6, 1.
- Neyman, J. and Scott, E. L. 1952. Ap. J. 116, 144.
- Neyman, J. and Scott, E. L. 1959. In Handbuch der Physik, Vol. 53, ed. S. Flügge (Springer-Verlag: Berlin) p. 416.
- Neyman, J., Scott, E. L. and Shane, C. D. 1956. In Proc. 3rd Berkeley Symp. Math. Stat. Prob., Vol. III, ed. J. Neyman (Univ. Calif. Press: Berkeley) p. 75.
- Nilson, P. 1973. Uppsala General Catalogue of Galaxies (Uppsala Offset Center, AB: Uppsala).
- Noonan, T. W. 1973. A. J. 78, 26.
- Nottale, L. 1976. Ap. J. 208, L103.
- Oemler, A. 1974. Ap. J. 194, 1.
- Ozernoy, L. M. 1974. In IAU Symp. No. 58, ed. J. R. Shakeshaft (D. Reidel: Dordrecht) p. 85.
- Ozernoy, L. M. and Reinhardt, M. 1976. A. & A. 52, 31.
- Paal, G. 1964. Mitteil. Sternw. der Ungarischen Akad. der Wissensch. No. 54.
- Pecker, J.-C. and Vigier, J.-P. 1976. Astrofizika 12, 315.
- Pedreros, M. 1978. P.A.S.P. 90, 14.
- Peebles, P. J. E. 1980. The Large Scale Structure of the Universe (Princeton Univ. Press: Princeton).
- Pence, W. D. 1976. Ap. J. 203, 39.
- Perrenod, S. C. and Lesser, M. P. 1980. P.A.S.P. 92, 764.
- Peterson, B. A. 1974. In IAU Symp. No. 58, ed. J. R. Shakeshaft (D. Reidel: Dordrecht) p. 75.
- Phillipps, S., Fong, R., Ellis, R. S., Fall, S. M. and MacGillivray, H. T. 1978. M.N.R.A.S. 182, 673.
- Pickering, E. C. 1899. Harv. Obs. Circ. No. 38.
- Pickering, E. C. 1908. Harv. Ann. 60, No. 6.
- Pickup, G. E. 1979. Thesis, Univ. of Edinburgh.

- Pratt, N. M. 1977. *Vistas in Astron.* 21, 1.
- Pravdo, S. H., Boldt, E. A., Marshall, F. E., McKee, J., Mushotzky, R. F., Smith, B. W. and Reichert, G. 1979. *Ap. J.* 234, 1.
- Press, W. H. and Vishniac, E. T. 1980. *Ap. J.* 236, 323.
- Proctor, R. A. 1869. *M.N.R.A.S.* 29, 337.
- Quintana, H. and Havlen, R. J. 1979. *A. & A.* 79, 70.
- Racine, R. 1968. *P.A.S.P.* 80, 326.
- Rainey, G. W. 1977. Thesis, Univ. Calif. Los Angeles.
- Reaves, G. 1968. *P.A.S.P.* 80, 564.
- Reaves, G. 1974. *Astron. Zhur.* 51, 520 (Eng. trans.: *Sov. Astron.* 18, 307, 1974).
- Reaves, G. and Stern, C. 1967. *A.J.* 72, 317.
- Reiz, A. 1941. *Ann. Lund.Obs.* 9, 65.
- Reynolds, J. H. 1921a. *M.N.R.A.S.* 81, 129.
- Reynolds, J. H. 1921b. *M.N.R.A.S.* 81, 598.
- Reynolds, J. H. 1923. *M.N.R.A.S.* 83, 147.
- Reynolds, J. H. 1924. *M.N.R.A.S.* 84, 76.
- Reynolds, J. H. 1934. *M.N.R.A.S.* 94, 196.
- Richter, G. M. 1976. *Astron. Nach.* 297, 145.
- Rood, H. J. 1974. *Ap. J.* 194, 27.
- Rood, H. J. 1976. *Ap. J.* 207, 16.
- Rood, H. J. 1979. *Ap. J.* 233, 431.
- Rood, H. J. 1981. *Gravitational Dynamics of Systems of Galaxies. I.* (Preprint).
- Rood, H. J. and Sastry, G. N. 1971. *P.A.S.P.* 83, 313.
- Rood, H. J., Rothman, V. C. A. and Turnrose, B. E. 1970. *Ap. J.* 162, 411.
- Rose, J. A. 1977. *A. & A. Suppl.* 23, 109.
- Rubin, V. C. 1954. *Proc. Nat. Acad. Sci.* 40, 541.

- Rubin, V. C., Ford, W. K., Thonnard, N., Roberts, M. S. and Graham, J. A. 1976. *A. J.* 81, 687.
- Rudnicki, K., Dworak, T. Z. and Flin, P. 1973. *Acta. Cosmo.* 1, 1.
- Saar, E. 1979. *Estonian Acad. Sci. Preprint No.* A-5.
- Sandage, A. R. 1972. *Ap. J.* 178, 1.
- Sandage, A. R. 1978. *A. J.* 83, 904.
- Sandage, A. R. and Tammann, G. A. 1981. *A Revised Shapley-Ames Catalog of Bright Galaxies* (Carnegie Inst. Publ. No. 635: Washington, D.C.).
- Sandage, A. R. and Visvanathan, N. 1978. *Ap. J.* 223, 707.
- Sanford, R. F. 1917. *Lick Obs. Bull.* 9, 91 (No. 297).
- Savage, A. 1976. *M.N.R.A.S.* 174, 259.
- Savage, A., Bolton, J. G. and Wright, A. E. 1976. *M.N.R.A.S.* 175, 517.
- Schmidt, M. 1978. In *IAU Symp. No. 79*, ed. M. S. Longair and J. Einasto (D. Reidel: Dordrecht) p. 289.
- Schuch, N. J. 1979. *Thesis, Univ. of Cambridge.*
- Schuch, N. J. 1981. *M.N.R.A.S.* 196, 695.
- Scott, E. L., Shane, C. D. and Swanson, M. D. 1954. *Ap. J.* 119, 91.
- Seares, F. H. 1925. *Ap. J.* 62, 168.
- Segal, I. E. 1976. *Mathematical Cosmology and Extragalactic Astronomy* (Academic Press: New York).
- Segal, I. E. 1980. *M.N.R.A.S.* 192, 755.
- Seldner, M., Siebers, B., Groth, E. J. and Peebles, P. J. E. 1977. *A. J.* 82, 249.
- Sérsic, J. L. 1974. *Ap. Sp. Sci.* 28, 365.
- Shane, C. D. 1956. *A. J.* 61, 292.
- Shane, C. D. 1975. In *Galaxies and the Universe*, ed. A. Sandage, M. Sandage, J. Kristian (Univ. Chicago Press: Chicago) p. 647.
- Shane, C. D. and Wirtanen, C. A. 1954. *A. J.* 59, 285.

- Shane, C. D. and Wirtanen, C. A. 1967. Pub. Lick Obs. 22, Part 1.
- Shanks, T. 1979. M.N.R.A.S. 186, 583.
- Shanks, T., Fong, R., Ellis R. S. and MacGillivray, H. T. 1980. M.N.R.A.S. 192, 209.
- Shapley, H. 1929. Proc. Nat. Acad. Sci. 15, 565.
- Shapley, H. 1933. Proc. Nat. Acad. Sci. 19, 591.
- Shapley, H. 1934a. Harv. Obs. Bull. No. 894, p. 5.
- Shapley, H. 1934b. Harv. Obs. Bull. No. 896, p. 3.
- Shapley, H. 1934c. M.N.R.A.S. 94, 791.
- Shapley, H. 1935a. Harv. Ann. 88, No. 5.
- Shapley, H. 1935b. Proc. Nat. Acad. Sci. 21, 587.
- Shapley, H. 1935c. Harv. Obs. Bull. No. 899, p. 17.
- Shapley, H. 1937a. Harv. Obs. Circ. No. 423.
- Shapley, H. 1937b. Harv. Ann. 105, No. 8.
- Shapley, H. 1937c. Proc. Nat. Acad. Sci. 23, 449.
- Shapley, H. 1938a. Proc. Nat. Acad. Sci. 24, 148.
- Shapley, H. 1938b. Proc. Nat. Acad. Sci. 24, 282.
- Shapley, H. 1940. Proc. Nat. Acad. Sci. 26, 166.
- Shapley, H. 1951. Proc. Nat. Acad. Sci. 37, 196.
- Shapley, H. 1957. The Inner Metagalaxy (Yale Univ. Press: New Haven).
- Shapley, H. and Ames, A. 1929. Harv. Obs. Bull. No. 864, 1.
- Shapley, H. and Ames, A. 1930a. Harv. Obs. Bull. No. 873, 1.
- Shapley, H. and Ames, A. 1930b. Harv. Obs. Bull. No. 880, 1.
- Shapley, H. and Ames, A. 1932. Harv. Ann. 88, No. 2.
- Shapley, H. and Jones, R. 1938a. Harv. Ann. 106, No. 1.
- Shapley, H. and Jones, R. 1938b. Harv. Obs. Bull. No. 909, 1.
- Shapley, H. and Jones, R. 1940. Proc. Nat. Acad. Sci. 26, 599.

- Shapley, H. and Paraskevopoulos, J. S. 1940. Harv. Obs. Bull. No. 914, 6.
- Smyth, R. J. 1980. Thesis, Univ. of Edinburgh.
- Snow, T. P. 1970. A. J. 75, 237.
- Sofue, Y., Fujimoto, M. and Kawabata, K. 1968. P.A.S. Japan 20, 388.
- Soneira, R. M. and Peebles, P. J. E. 1977. Ap. J. 211, 1.
- Spitzer, L. 1978. Physical Processes in the Interstellar Medium (Wiley: New York).
- Stobie, R. S., Smith, G. M., Lutz, R. K. and Martin, R. 1979. In Image Processing in Astron., ed. G. Sedmak, M. Capaccioli, R. J. Allen (Osserv. Astr.: Trieste).
- Stratonoff, W. 1900. Publ. Taschkent Obs. No. 2, p. 46.
- Sulentic, J. W. and Tifft, W. G. 1973. The Revised New General Catalogue of Nonstellar Astronomical Objects (Univ. of Arizona Press: Tucson).
- Szalay, A. S. 1981. In 10th Texas Symp., in press.
- Tammann, G. A. and Kraan, R. 1978. In IAU Symp. No. 79, ed. M. S. Longair and J. Einasto (D. Reidel: Dordrecht) p. 71.
- Tarenghi, M., Tifft, W. D., Chincarini, G., Rood, H. J. and Thompson, L. A. 1979a. Ap. J. 234, 724.
- Tarenghi, M., Chincarini, G., Rood, H. J. and Thompson, L. A. 1979b. Ap. J. 235, 793.
- Thuan, T. X. 1980. In Physical Cosmology; ed. R. Balian, J. Audouze, D. Schramm (North Holland Publishing Co.: Amsterdam) p. 277.
- Tifft, W. G. and Gregory, S. A. 1976. Ap. J. 205, 696.
- Tifft, W. G., Hilsman, K. A., and Corrado, L. C. 1975. Ap. J. 199, 16.
- Tombaugh, C. W. 1937. P.A.S.P. 49, 259.
- Tonry, J. and Davis, M. 1981. Ap. J., 246, 680.
- Totsuji, H. and Kihara, T. 1969. P.A.S. Japan 21, 221.
- Tully, R. B. and Fisher, J. R. 1978. In IAU Symp. No. 79, ed. M. S. Longair and J. Einasto (D. Reidel: Dordrecht) p. 31.
- Turner, D. G. 1976. A. J. 81, 1125.

- Turner, E. L. and Gott, J. R. 1976. *Ap. J. Suppl.* 32, 409.
- Turner, E. L. and Sargent, W. L. W. 1974. *Ap. J.* 194, 587.
- Ulmer, M. P. and Cruddace, R. G. 1981. *Ap. J.* 246, L99.
- Ulmer, M. P., Kinzer, R., Cruddace, R. G., Woods, K., Evans, W.,
Byram, E. T., Chubb, T. A. and Friedman, H. 1979. *Ap. J.*
227, L73.
- de Vaucouleurs, G. 1953. *A. J.* 58, 30.
- de Vaucouleurs, G. 1956a. *Mem. Commonwealth (Mt. Stromlo) Obs.*
3, No. 13.
- de Vaucouleurs, G. 1956b. *Vistas in Astron.* 2, 1584.
- de Vaucouleurs, G. 1957. *Ann. Obs. Hougla, Vol. II, Part 1.*
- de Vaucouleurs, G. 1958. *A. J.* 63, 253.
- de Vaucouleurs, G. 1960. *Ap. J.* 131, 585.
- de Vaucouleurs, G. 1961. *Ap. J. Suppl.* 5, 233 (No. 48).
- de Vaucouleurs, G. 1968. *App. Op.* 7, 1513.
- de Vaucouleurs, G. 1970. *Science* 167, 1203.
- de Vaucouleurs, G. 1971. *P.A.S.P.* 83, 113.
- de Vaucouleurs, G. 1975a. In *Galaxies and the Universe*, ed. A.
Sandage, M. Sandage, J. Kristian (Univ. Chicago Press:
Chicago) p. 557.
- de Vaucouleurs, G. 1975b. *Ap. J.* 202, 610.
- de Vaucouleurs, G. 1975c. *Ap. J.* 202, 616.
- de Vaucouleurs, G. 1978. In *IAU Symp. No. 79*, ed. M. S. Longair
and J. Einasto (D. Reidel: Dordrecht) p. 205.
- de Vaucouleurs, G. 1981. *Bull. Astr. Soc. India* 9, 1.
- de Vaucouleurs, G. and Bollinger, G. 1979. *Ap. J.* 233, 433.
- de Vaucouleurs, G. and Corwin, H. G. 1977. *Ap. J. Suppl.* 33, 219.
- de Vaucouleurs, G. and Head, C. 1978. *Ap. J. Suppl.* 36, 439.
- de Vaucouleurs, G. and Pence, W. D. 1979. *Ap. J. Suppl.* 39, 49.
- de Vaucouleurs, G. and de Vaucouleurs, A. 1964. *Reference Cata-
logue of Bright Galaxies* (Univ. of Texas Press: Austin).

- de Vaucouleurs, G. and de Vaucouleurs, A. 1967. *A. J.* 72, 730.
- de Vaucouleurs, G., Corwin, H. G. and Bollinger, G. 1977. *Ap. J. Suppl.* 33, 229.
- de Vaucouleurs, G., de Vaucouleurs, A. and Corwin, H. G. 1972. *A. J.* 77, 1972.
- de Vaucouleurs, G., de Vaucouleurs, A. and Corwin, H. G. 1976. *Second Reference Catalogue of Bright Galaxies* (Univ. Texas Press: Austin).
- Vorontsov-Velyaminov, B. A., Arkipova, V. P. and Krasnogorskaja, A. A. 1962, 1963, 1964, 1968, 1974. *Morphological Catalogue of Galaxies*, 5 volumes. (Moscow State Univ.: Moscow).
- Warwick, C. 1950. *Proc. Nat. Acad. Sci.* 36, 415.
- Waters, S. 1873. *M.N.R.A.S.* 33, 558.
- Waters, S. 1894. *M.N.R.A.S.* 54, 526.
- Webster, A. S. 1976a. *M.N.R.A.S.* 175, 61.
- Webster, A. S. 1976b. *M.N.R.A.S.* 175, 71.
- Weiss, R. 1980. *Ann. Rev. A. & A.* 18, 489.
- Wesson, P. S. 1976. *Ap. Sp. Sci.* 40, 325.
- West, R. M. 1977. *A. & A. Suppl.* 27, 73.
- West, R. M. and Frandsen, S. 1981. *A. & A. Suppl.* 44, 329.
- West, R. M., Borchkhadze, T. M., Breysacher, J., Laustsen, S. and Schuster, H.-E. 1978. *A. & A. Suppl.* 31, 55.
- Whiteoak, J. B. 1972. *Aust. J. Phys.* 25, 233.
- Wirtz, C. 1923. *Medd. Lund Astr. Obs., Ser. 2*, No. 29.
- Yahil, A., Sandage, A. R. and Tammann, G. A. 1980. *Ap. J.* 242, 448.
- Zeiba, A. 1975. *Acta Cosmo.* 3, 75.
- Zeiba, A. and Zeiba, S. 1975. *Acta Cosmo.* 3, 91.
- Zel'dovich, Ya. B. 1978. In *IAU Symp. No. 79*, ed. M. S. Longair and J. Einasto (D. Reidel: Dordrecht) p. 409.
- Zel'dovich, Ya. B. 1980. *M.N.R.A.S.* 192, 663.
- Zonn, W. 1968. *Acta Astron.* 18, 273.

- Zwicky, F. 1938. P.A.S.P. 50, 218.
- Zwicky, F. 1942a. Ap. J. 95, 555.
- Zwicky, F. 1942b. P.A.S.P. 54, 185.
- Zwicky, F. 1951. P.A.S.P. 63, 61.
- Zwicky, F. 1952. P.A.S.P. 64, 247.
- Zwicky, F. 1953. Helv. Phys. Acta 26, 241.
- Zwicky, F. 1957a. Morphological Astronomy (Springer-Verlag: Berlin).
- Zwicky, F. 1957b. P.A.S.P. 69, 518.
- Zwicky, F. and Berger, J. 1964. Ap. J. 141, 34.
- Zwicky, F. and Karpowicz, M. 1965. Ap. J. 142, 625.
- Zwicky, F. and Karpowicz, M. 1966. Ap. J. 146, 43.
- Zwicky, F. and Rudnicki, K. 1963. Ap. J. 137, 707.
- Zwicky, F. and Rudnicki, K. 1966. Zs. f. Ap. 64, 246.
- Zwicky, F., Herzog, E., Kowal, C. T., Karpowicz, M. and Wild, P. 1961, 1963, 1965, 1966, 1968a,b. Catalogue of Galaxies and of Clusters of Galaxies (Calif. Inst. of Tech.: Pasadena).

OPTICAL SPECTRA AND REDSHIFTS FOR 100 DISTANT GALAXIES

WILLIAM G. COOPER, JR. and DAVID BURTON

Appendix A

Department of Astronomy

Blount Hall

University of Michigan

Ann Arbor, Michigan 48106

Printed by D. Burton

Reproduction: Department of Astronomy, University of Texas, Austin, Texas

OPTICAL SPECTRA AND REDSHIFTS FOR EIGHTY GALAXIES

Harold G. Corwin, Jr* and David Emerson

Department of Astronomy

Blackford Hill

University of Edinburgh

Edinburgh EH9 3HJ

Proofs to: D. Emerson

*Present Address: Department of Astronomy, University of Texas, Austin, Texas

ABSTRACT

Spectra of 80 galaxies have been obtained with an image tube spectrograph on the 1.9-metre telescope of the South African Astronomical Observatory at a reciprocal dispersion of 215 \AA mm^{-1} . The spectra have been traced with a microdensitometer to identify features, and have been measured for redshift with a travelling microscope. Complete lists of absorption features and emission lines seen in the spectra have been compiled. The rest wavelengths of the absorption features have been revised and have been used to derive redshifts with external mean errors of the order of $\pm 60 \text{ km sec}^{-1}$. There is, however, marginal evidence of a scale error in our data.

Sandage's finding of systematic differences between HI radio and optical redshifts is confirmed. The differences are not simple zero point or scale errors and zero point corrections are insufficient to bring the optical and radio data into systematic agreement.

The redshifts include values for galaxies in eighteen rich clusters in the Indus Supercluster area, and our data also includes values tending to confirm suggestions of cell structure of the Coma Supercluster.

1. INTRODUCTION

The recent discovery on UK Schmidt IIIaJ southern sky survey plates of an apparent supercluster in the Indus region has prompted a preliminary investigation of galaxies and clusters of galaxies in the area. UBV photoelectric photometry for selected galaxies in Indus has already been reported (Corwin 1980) and a COSMOS machine study of apparent positions, magnitudes and diameters for 120,000 galaxies is nearly complete. This paper presents optical redshifts for about 30 Indus galaxies, most of which lie in rich clusters. Other galaxies outside the Indus area were also observed, and the final sample of 80 spectra is large enough to make possible a detailed comparison of our redshifts with those from other sources.

The selection criteria by which our galaxies were chosen are given in Section 2, Section 3 describes the observations, and Section 4 the measurement of the spectra. The reduction of the spectra for redshifts is described in Section 5, while Section 6 is concerned with the errors in the redshifts. In Section 7 we discuss the general spectral characteristics of the galaxies in our sample. Section 8 remarks on galaxies of special interest, on group and cluster membership, and on galaxies with redshifts discordant with those quoted in other sources. Detailed discussion of the Indus supercluster area is deferred to a later paper where our redshifts will be combined with additional redshifts obtained by Arp, Chincarini and Tarenghi, and Shanks, to allow a more comprehensive study of the structure of the supercluster.

2. SELECTION OF GALAXIES

The galaxies observed were chosen from several lists in more or less the following order or priority:

- (i) Brighter apparent members of rich clusters in the Indus Supercluster area, or brighter objects in the "field" in Indus;
- (ii) Galaxies listed in the Second Reference Catalogue (hereafter RC2; de Vaucouleurs et al, 1976) either
 - (a) unobserved or with single low-weight observations, or
 - (b) with well determined redshifts from several sources, i.e. "standard galaxies";
- (iii) Objects with discordant published redshifts
- (iv) Galaxies in fields for which redshifts can also be obtained from objective prism plates (e.g. Cooke et al 1977); and
- (v) Previously unobserved galaxies in the area of the Virgo Cluster, several of which have photometry by Eastmond (1977) and by Corwin (1980).

Because of problems of sky contamination on our plates, low surface brightness galaxies were generally avoided, as were those with $B_T \gtrsim 16.5$. Our final list is therefore weighted towards early-type galaxies with bright nuclei.

3. OBSERVATIONS

All of the observations were made during a single observing run in June 1978 with the image tube spectrograph (hereafter ITS; see Palmer and Milsom 1972 for a complete description) at the Cassegrain focus of the South African Astronomical Observatory's 1.9 metre Knox-Shaw reflector near Sutherland. We used the number 1 grating which gives a reciprocal dispersion of about 215 \AA mm^{-1} in the first order; the dispersion varies only slowly with

wavelength. The final projected image scale on the plate along the slit is $79.2 \text{ arc sec mm}^{-1}$. We initially set the slit width to 0.4 mm ($= 2.4 \text{ arc sec}$) but soon reduced this to 0.3 mm ($= 1.8 \text{ arc sec}$). Pre-flashed II a-0 plates were used, and each spectrum covered a wavelength range from $\sim 3500 \text{ \AA}$ to $\sim 7500 \text{ \AA}$.

Exposure times ranged from 1 minute to 30 minutes and were preceded and followed by comparison (copper-argon) arc exposures of 10 to 15 seconds. All exposures were untrailed. The slit was usually aligned east-west across the nucleus of the galaxy; exceptions are noted. The slit length was generally set between 40 and 60 arc seconds, though longer slits were used for three exposures; these are also noted. All plates were developed in D-19 for 5 min at 20°C .

4. MEASUREMENT OF THE SPECTRA

All of the spectra were measured by two different methods:

- (a) by D.E. with a Joyce-Loebel scanning microdensitometer, and
- (b) by H.C. with a Hilger and Watts single screw travelling microscope.

The measurements were made independently, and were compared only when all the spectra had been measured by both methods.

The microdensitometer was used to make at least two scans of each spectrum:

- (i) a scan of a strip about 120 microns wide (corresponding to about 10 arc sec) centered on the brightest portion of each spectrum, and
- (ii) a scan corresponding to the full length of the spectrograph slit.

In both cases a slit effectively 30 microns wide (on the plate) was used, and the comparison spectra were scanned and recorded on the same tracing.

In the microscope measures the cross hair was set by eye at the subjectively

estimated centre of the line or feature. Galaxy features were measured in the nucleus when they could be seen there. If the feature was over-exposed in the nucleus but still visible beyond it, the cross-hair was set by interpolation to the estimated nuclear position. Forward and reverse measurements were made for each spectrum during a single sitting. The screw was read to 1 μm . The internal consistency for repeated settings on sharp unblended features was 1-2 μm ; the setting consistency on the more diffuse absorption features was 4-5 μm in the worst cases. All apparent galaxy features, whether absorption or emission, were measured in every spectrum with the exception of No. 1875-1 of NGC 6753, where sky contamination prevented reliable identification of many of the features. Obvious defects were ignored. The night sky emission lines at 5577 \AA , 5892 \AA , 6300 \AA and 6363 \AA were measured whenever they could be seen. The H and K sky absorption features were also occasionally measured.

Curvature manifested itself only as a slight tilt of the spectral lines. As this affected equally comparison and galaxy spectra, it was compensated for in the microscope measures by rotating the cross-hairs by about one degree. This procedure saved a great amount of time with little sacrifice in accuracy, but may have been one source of the small systematic redshift residuals discussed in Section 6 below.

As might be expected, the travelling microscope measurements gave redshifts of much higher internal accuracy (typically, $\sigma_v \sim \pm 40 \text{ km sec}^{-1}$) than did the microdensitometer measures ($\sigma_v \sim \pm 120 \text{ km sec}^{-1}$). A few of the microdensitometer scans were repeated when discrepancies with the travelling microscope values of more than 500 km sec^{-1} were found. The repeat scans always agreed with the microscope values to within the combined errors, suggesting paper slippage during the original scans. However, the microdensitometer scans were found to be far better at detecting features

in over and under-exposed portions of the spectra, except where there was confusion from strong night sky contamination.

Thus, we have decided to adopt redshifts from the travelling microscope measures (Section 5), and to base our discussion of the appearance of spectral features primarily on the Joyce-Loebel scans (Section 7).

5. REDUCTION OF TRAVELLING MICROSCOPE MEASUREMENTS

(a) Comparison Lines and Dispersion Formulae

The comparison lines used to determine the dispersion curves were generally the stronger unblended lines of AI. However, a few blended lines had to be used in some parts of the spectrum. Since the wavelengths of the comparison lines are known to depend on several factors over which observers have little control (contamination of the discharge tube, etc.) residuals from initial dispersion curve solutions were collected and averaged, then applied - where statistically significant - to the laboratory wavelengths tabulated by Zaidel' et al (1961) and Crosswhite and Dieke (1972). The revised wavelengths were then used in final solutions for the dispersion curves for each spectrum. Table 1 lists the comparison lines with their standard and revised wavelengths.

The dispersion coefficients were determined through least squares solutions of a second-order polynomial:

$$\lambda - \langle \lambda \rangle = a + b (x - \langle x \rangle) + c (x - \langle x \rangle)^2$$

where λ is the revised wavelength from Table 1, $\langle \lambda \rangle = 5400 \text{ \AA}$ (except for I 4662 where $\langle \lambda \rangle = 6000 \text{ \AA}$), x is the mean measurement in mm for each line, and $\langle x \rangle$ is the approximate measurement corresponding to 5400 \AA (or 6000 \AA). Higher order polynomials gave no advantage in the least squares fit. Table 3 lists the mean dispersion coefficients determined separately for the

spectra taken with 0.3 and 0.4 mm slit widths. As there is no significant difference between the two sets of coefficients, the spectra are treated identically throughout the remainder of this paper.

The 3948 Å AI comparison blend was absent in many of our spectra. This meant that we had no comparison lines blueward of 4159 Å in more than half of our spectra. To check that the dispersion curves could be safely extrapolated into the ultraviolet, we performed three tests:

- (i) Table 3 shows no significant dependence of the dispersion coefficients on the presence or absence of the 3948 Å blend;
- (ii) Redshift residuals $V - \langle V \rangle$ plotted versus wavelength for individual features in the galaxy spectra showed no systematic trends regardless of the presence or absence of the 3948 Å blend; and
- (iii) Calculated rest wavelengths of galaxy features (Tables 4 and 6) showed no systematic residuals dependent upon the presence or absence of the 3948 Å blend.

We are therefore reasonably confident that extrapolating our dispersion curves into the ultraviolet as necessary has introduced no significant systematic errors in the wavelengths of the measured galaxy features. Only two of the redshifts in our list depend exclusively on lines measured blueward of 4159 Å, and both of these spectra (A 1601-67 B, and a bright star superposed on I4444) had the 3948 Å blend present.

(b) Reduction of redshifts

Once the dispersion curves for each spectrum were known, the apparent wavelength of every measured feature was calculated. Major absorption features were identified from the compilations by/de Vaucouleurs (1967) and by Sandage (1975, 1978) and preliminary redshifts calculated (velocities quoted in this paper are all $V = c \frac{\Delta\lambda}{\lambda_0}$ values). These were then used to find rest wavelengths for all absorption features. Several "new" features

- primarily blends of iron and other metals - were identified in this way. These were used together with the features from the older lists to find second approximation redshifts, which were in turn used to revise the rest wavelengths of all absorption features. The final redshift was determined with these revised wavelengths, but features with rest wavelengths deviating in any particular case by more than two sigma from the mean rest wavelengths were rejected.

The same procedure was tried for the emission lines. However, as the rest wavelengths for these lines were not significantly different from the value in the compilations quoted above, and as no "new" emission lines were found, the initial redshift based on the older wavelength lists was adopted as final.

(c) Absorption Features and Emission Lines seen

A "new" absorption feature had to be present in at least four spectra to be accepted as genuine. All the absorption features used for redshift determination are listed in Table 4; "new" features are marked by an asterisk. Rest wavelengths λ_0 , their mean errors σ_n , the standard deviation σ_1 in a single λ_0 determination, and the numbers of spectra in which the feature was used for redshift determination are listed. A frequency of occurrence parameter $f_0 = 10(n/69)$ was calculated for comparison with Sandage's qualitative estimate of "visibility". For the features in common, the agreement of these two indicators of line strength is good, although f_0 under-estimates "visibility" by about one unit for the less prominent lines. The final column of the table gives tentative identifications of the features based solely on line identifications in the solar spectrum (Moore et al, 1966). These may, of course, be inappropriate to galaxy spectra in several cases.

The mean difference between our adopted wavelengths λ_0 and the values of Sandage and de Vaucouleurs for 17 features is

$$\Delta\lambda_0 = \lambda_0 - \lambda_0 (\text{S,de V}) = +0.06 \pm 0.18 \text{ \AA} \quad \text{with } \sigma_1 = \pm 0.75 \text{ \AA}$$

We have not considered systematic effects due to apparent magnitude, galaxy type etc. (see/de Vaucouleurs 1963, 1967) as our sample is deficient in bright, late-type galaxies.

Eighteen possible absorption features, each seen in fewer than four spectra, are listed in Table 5. This table gives the same information as Table 4, but a Notes column is added. A note such as "4710?" refers to a feature listed by Sandage for which our wavelength agrees only approximately with his. None of the features listed in Table 5 were used for redshift determination, even though they gave the same redshift to within the errors as the accepted features in Table 4. After this table was assembled, we found that lists of features by Williams (1976) and by Dawe et al (1977) confirmed several of these 'new' features. They are marked with a dagger (\dagger).

Table 6 lists the emission lines seen by H.C. in our spectra, and the number of spectra in which each was measured. Comparison of redshifts from emission lines alone with redshifts from absorption features alone for the 24 spectra with both shows $\Delta V = V_{\text{abs}} - V_{\text{ems}} = + 64 \pm 16 \text{ km sec}^{-1}$ and $\sigma_1 = \pm 78 \text{ km sec}^{-1}$. Though the difference is large and significant, we have not corrected either absorption or emission redshifts. The reasons for this are discussed in Section 6d below.

(d) Night Sky Lines

Redshifts for the measured night sky lines were also calculated. Mean values are shown in Table 7. The large negative redshifts for the H and K night sky features are probably caused by asymmetries in the features introduced by the steep continuum gradient blueward of 4000 \AA , combined

with the faintness of the features. The H and K lines were therefore ignored, and a correction to zero night sky redshift was based only on the four emission lines. (No mercury emission lines are visible in the SAAO spectra). The weighted mean of the mean night sky emission redshifts (weights are $W = (10/\sigma_n)^2$) is $-8 \pm 2 \text{ km sec}^{-1}$ with $\sigma_1 = \pm 33 \text{ km sec}^{-1}$ for 211 lines. The adopted correction to zero night sky redshift is therefore $+8 \text{ km sec}^{-1}$; this was applied to all galaxy redshifts.

(e) Adopted Redshifts

The final redshifts are listed in Table 8 which gives in successive columns:

- (1) The galaxy's name;
- (2) The galaxy's 1950 coordinates from RC 2; Dressel and Condon (1976) Reinmuth (1927), Holmberg et al (1980 and references therein), or newly determined by one of us (H.C.) on Palomar Sky Survey (PSS) copy plates, or on UK Schmidt III a-J plates;
- (3) Revised type from RC 2, or estimated by H.C. from PSS or UKS plates;
- (4) SAAO I.T.S. plate number, and spectrum number on that plate;
- (5), (6) and (7). Position angle, width and length of slit;
- (8) Exposure time in minutes;
- (9) Date (in June 1978) of the exposure;
- (10) Redshift reduced to the Sun in km sec^{-1} ;
- (11) Internal mean error in the redshift;
- (12) Redshift corrected for solar motion as in RC 2;
- (13) Subjective estimate of the quality of the spectrum (E = excellent, G = good, F = fair, P = poor);
- (14) Presence (Y), absence (N) or rejection (R) of the 3948 \AA AI blend in the comparison spectrum;
- (15) Subjective emission intensity (10 for spectra showing very strong emission lines, 1 for very weak-lined spectra where the "lines" are probably defects);

- (16) and (17) Number of absorption features (N_{abs}) and emission lines (N_{emis}) used in deriving the redshift;
- (18) Group or cluster (if any) of which the galaxy is probably a member;
- (19) Remarks or references to notes following the table; "UBV" indicates photoelectric aperture photometry given by Corwin (1980);
- (20) Number in the ESO/Uppsala Survey (Holmberg et al 1980 and references therein).

6. INTERNAL AND EXTERNAL ERRORS IN THE REDSHIFTS

(a) Internal Errors

Three estimates of the internal errors in our redshifts are possible, besides the standard deviation in the mean night sky redshift,

$$\sigma_1 = \pm 33 \text{ km sec}^{-1};$$

(i) We have multiple spectra for six galaxies. However, the repeated observations of I4444 and A1740-79 do not refer to the same parts of the galaxies as the first spectra. For the remaining four galaxies, the average deviation of the residuals from the mean redshift is $\pm 33 \text{ km sec}^{-1}$, and the standard deviation in one residual is $\pm 37 \text{ km sec}^{-1}$.

(ii) The mean of the σ_v 's from column (11) of Table 8 is $\langle \sigma_v \rangle = \pm 41 \text{ km sec}^{-1}$.

As expected, emission lines give considerably smaller errors

$$\langle \sigma_{\text{emis}} \rangle = \pm 31 \text{ km sec}^{-1} \text{ than do the absorption features for which}$$

$$\langle \sigma_{\text{abs}} \rangle = \pm 45 \text{ km sec}^{-1}.$$

(iii) Finally, we may convert the mean errors σ_n of the adopted rest wavelengths given in Tables 4 and 6 to redshifts. For the 33 absorption features, this gives $\langle c \frac{\sigma_n}{\lambda_0} \rangle = \pm 36 \text{ km sec}^{-1}$. For 14 emission lines seen in more than one spectrum, $\langle c \frac{\sigma_n}{\lambda_0} \rangle = \pm 21 \text{ km sec}^{-1}$.

The agreement of the four estimates is good, and we adopt as the internal mean error in a redshift measured from a single spectrum $\sigma_1 \sim \pm 40 \text{ km sec}^{-1}$.

(b) True (External) Errors from Optical Redshift Comparisons

It was shown in RC2 and by Sandage (1978) that the true errors in most redshift lists are nearly always larger than the internal errors. Since we have several galaxies in common with RC2, Sandage (1978), and Martin (1976), true external errors in each set may be derived by three-by-three triangular comparisons of the standard deviations of the mean differences between sets. Table 9a gives the relevant data. The comparisons are for all objects in common to the lists except for the RC2 - Sandage comparison which is for a random sample of galaxies in common. To ensure independent samples and unbiased results, we have removed from the RC2 redshifts the data of Sandage (some of which was published in time for inclusion in RC2), and we have removed the $+ 30 \text{ km sec}^{-1}$ correction to the HI system that Sandage applied to his redshifts in 1978.

Table 9b shows the results of the triangular comparisons. The true mean errors are seen to be close to the expected values for RC2 and for Martin, but they are somewhat better than expected for Sandage (cf. his Tables VIII through X). Our redshifts are of comparable quality. Note that we find $f_{\sigma} = \sigma_{\text{Ext}} / \sigma_{\text{int}} \sim \pm 53 / \pm 40 \sim 1.3$ for our data, confirming once again that external errors are larger than internal errors.

We have also calculated zero point offsets for each data set, but delay discussion of these until after a comparison with 21-cm redshifts.

(c) True external errors from 21-cm HI line Redshifts

Redshifts from the 21-cm line of neutral hydrogen are generally very accurate (e.g. RC2, Lewis 1975; Rood 1981, Bottinelli et al 1981a), and so are often assumed to be nearly error-free when making comparisons with much lower weight optical velocities (see e.g. Sandage 1978 and Rood 1981 for such comparisons). We adopt this general approach and assign errors of $\pm 15 \text{ km sec}^{-1}$ to the HI redshifts regardless of their origin; see RC2 and

Lewis (1975) for a justification of this figure.

Eleven of our galaxies have HI redshifts (seven published by Lewis 1975, Whiteoak and Gardner 1977, and Thonnard et al 1978; three unpublished from Parkes observations by Zealey et al., and one from Bottinelli et al., 1981b). The mean residual is $\langle \Delta V \rangle = V_{\text{CE}} - V_{\text{HI}} = -23 \pm 22 \text{ km sec}^{-1}$, with $\sigma_1 = \pm 72 \text{ km sec}^{-1}$. If $\sigma_{\text{HI}} = \pm 15 \text{ km sec}^{-1}$, the mean error in our redshifts is $\pm 70 \text{ km sec}^{-1}$, in fair agreement with the estimate of $\pm 53 \text{ km sec}^{-1}$ from the optical comparisons above. Similar mean residuals and error estimates are set out in Table 10 for the other three optical data sets. Again, the RC2 data set is drawn at random from the catalogue. The large differences between the external errors from HI comparisons and the external errors from the optical triangular comparisons are probably due to the samples being (contrary to expectation) unrepresentative and to scale errors in the various optical data sets.

(d) Zero point and Scale errors

Figure 1 is a plot of the redshift residuals $\Delta V = V_{\text{CE}} - V_{\text{others}}$ vs redshift. The source of the discrepant zero points for our data is apparent: the HI redshifts give mainly negative residuals for galaxies with $V < + 2500 \text{ km sec}^{-1}$ while the optical residuals are systematically positive at $V > + 1000 \text{ km sec}^{-1}$. While the trend in Figure 1 seems clear, it depends almost entirely on the few comparison redshifts at $V > + 4000 \text{ km sec}^{-1}$ for its reality. Therefore we prefer to make no corrections to our redshifts now, although additional comparisons in the future may well confirm the systematically positive residuals at larger redshifts.

If we had corrected our absorption redshifts to the mean system defined by the emission redshifts (see Section 5c above), both HI and optical comparisons would give large negative residuals. Leaving the absorption redshifts uncorrected, as we have, the mean of the optical and HI residuals for the galaxies with $V < + 3500 \text{ km sec}^{-1}$ is not significantly different from zero. Nevertheless, in looking for the cause of the absorption-emission redshift

difference, we have found (see Figure 2) that the residuals from the HI data become larger as emission intensity decreases.

Finally, examination of Table 10 shows that we confirm Sandage's suggestions of a systematic difference between optical redshifts and HI redshifts. Only the RC2 optical redshifts (from which systematic errors have been removed) and Sandage's Palomar "d" series redshifts show no evidence of the systematic difference from HI redshifts in the direction that Sandage suggested (HI redshifts larger). Three of the data sets (our own, Martin's and Sandage's Palomar "a" series) have only marginally significant differences, but all are in the same sense. De Vaucouleurs et al (1979) also find small systematic differences in the same direction between their optical redshifts and recent HI determinations.

Examination of the source of the discrepancy is beyond the scope of this paper. We note, however, that all the optical sources that we have examined seem to show variations in the residuals as a function of redshift (cf. Section 6d above, RC2, and de Vaucouleurs et al 1979). Simple calculations of zero-point differences will not be enough to fully resolve the discrepancies.

In any case the errors in our redshifts are larger than the corrections indicated. Until more precise data from other sources is available for comparison, we prefer to make no corrections to our data.

7. SPECTRAL FEATURES IN THE MICRODENSITOMETER SCANS

The general appearance of galaxy spectra is well known (e.g. Sandage 1975, de Vaucouleurs and de Vaucouleurs 1967) and variations in the stronger features have often been discussed and correlated with other variables such as galaxy type (de Vaucouleurs 1967), metallicity (Faber 1977), and luminosity and/or mass (Faber and Jackson 1976). However, there are few published descriptions of the absorption features in galaxy spectra covering the full wavelength range observed here, and although our sample of 80 galaxies is

weighted towards ellipticals and lenticulars, there are enough spirals to enable a few comments to be made about the variations in spectra observed for different galaxy types.

The comments below must be taken in the context of fairly noisy spectra with no intensity calibration and no sky subtraction. On the other hand, no artificial sky features are present, and the long and short slit scans of each spectrum provide a fairly accurate guide to the relative strengths of sky and galaxy features. It must also be remembered that the 10 arc-sec width of the (short) Joyce-Loebel strip corresponds to linear distances across the face of the galaxy varying from less than 500 parsecs to over 15 Kpc depending on the distance. The well known changes in metallicity with radial distance from a galaxy's nucleus will give rise to much of the galaxy to galaxy variation seen in the tracings, in addition to intrinsic galaxy to galaxy metal abundance variations.

Table 2 lists features frequently seen on the tracings but not appearing in the lists of Sandage (1978) and de Vaucouleurs and de Vaucouleurs (1967). Column (1) gives the name of the feature, asterisked if reported for the first time to our knowledge, columns (2) and (3) give the wavelength of the feature and the mean error in the wavelength, while columns (5) and (6) give the mean error in a single determination of the wavelength and the number of spectra in which the feature was seen within $\pm \sigma$ of the quoted wavelength without possible confusion with night sky or terrestrial absorption features.

A few of these features were noted by H.C. in the travelling microscope measures, and are also listed in Tables 4 and 5, a few were listed by Williams (1976) and some can be seen in the standard spectra used by Kelton (1980). Though these features are strong in the sense of being easily recognised above noise on the microdensitometer tracings, most are broad enough to escape easy detection by eye with a microscope, especially in the well-exposed nuclear regions of a galaxy spectrum. The rather large

uncertainties in the wavelengths of the features are partly instrumental and partly real. Most of the features are blends, and the variation of the fraction of a galaxy being sampled with distance could cause shifts in the apparent wavelength of a feature. The 3579/3612 features could be useful for redshift determinations of distant ellipticals and lenticulars (provided confusion with the similarly separated H and K is avoided) and it may be worth refining the wavelengths of these features using a sample of galaxies at similar redshifts.

(a) Spectra of Elliptical and Lenticular Galaxies

Most of the twenty-seven early type galaxies in our sample with spectral tracings of reasonable signal-to-noise ratio show a basically similar pattern of features in the ultraviolet. The K line and the blends at 3969 ("H") and 3835 ("H η " but with major contributions from MgI and FeI) are all strong, with K typically somewhat deeper than H, and "H η " similar in depth to K but broader. The feature at around 3883 Å, in a region of strong CN absorption in late type stars, is variable in strength and wavelength, and appears to be absent in about half of our E and SO spectra. (In the microscope measurements the 3883 Å feature appears as two components at 3879 Å and 3888 Å.) A feature usually appears at about 3743 Å with a depth somewhat less than "H η ", and is sometimes accompanied by another feature at 3795 Å.

There appears to be an absence of strong absorption features at our dispersion between 3620 Å and 3740 Å. At shorter wavelengths the 3579 Å and 3612 Å features mentioned earlier are seen. The 3579 Å feature is strong and frequently detected, while 3612 Å is weaker and sometimes absent. Though not specifically noted previously in galaxy spectra, these two features can be identified in the spectrophotometry of late type stars by Fay et al (1974). The only galaxies in our sample of 27 that definitely do not show 3579/3612 are A 1238-04, A 2131-62A, and A 2213-52A, although the spectra of these galaxies at longer wavelengths are normal.

The principal features redward of 4000 \AA - the G band around 4304 \AA , the Mg b triplet at around 5174 \AA and the Na D lines at 5892 \AA - show considerable variations in strength from galaxy to galaxy. The G band is particularly strong in A 2212-51A, A 2035-61, and I 4721A, and unusually weak in A 2129-60 and I 4798. The D line appears strongly in A 2035-61 and N 6851, but appears to be completely absent in A 2129-60.

The wavelengths as well as the strengths of the G and b bands vary from galaxy to galaxy, as might be expected for broad features made up of several lines and bands. Histograms of the microscope measured wavelengths show three definite peaks for both of these features. The peaks are designated G_1 , G, and G_2 , and b_1 , b and b_2 in Table 4. (The number ratios $n(G_1)/n(G) = 0.34$, $n(G_2)/n(G) = 0.28$, and $n(b_1)/n(b) = n(b_2)/n(b) = 0.46$ do not, however, change significantly with galaxy type except that $n(b_1)/n(b) = 4.0$ and $n(b_2)/n(b) = 1.5$ for Sc to Im and peculiar galaxies). Such wavelength changes have probably led to lower accuracy in many optically determined redshifts than might have been achieved otherwise.

(b) Spectra of Spirals and Irregulars

Five of the seven galaxies classified SO/a to Sab in our sample have spectra essentially identical to the spectra of the ellipticals and lenticulars. However, the noisy spectrum of A 2111-59 appears to show a very weak K line and a strong b band, while A1601-67A has a discontinuity at 3650 \AA rather than the 3579/3612 pattern typical of early type objects.

The fifteen Sb and Sbc galaxies observed by us include a number of relatively nearby objects for which our spectra refer only to the nucleus. Not surprisingly these have absorption spectra that are very similar to those of the elliptical and lenticular galaxies. In the other Sb and Sbc galaxies, as well as in the Sc to Sm objects, H γ is usually prominent, 3579/3612 no longer dominates shortward of 3700 \AA , and the 3743 \AA feature is often replaced by one at 3769 \AA possibly due to H λ and FeI. The spectra of the two

irregular galaxies (N 5464 and I 4662) are completely dominated by emission lines, with I 4662 showing no absorption at all.

(c) Emission Lines

In general, the number of emission lines present and their strengths, increase along the Hubble spiral sequence. None of our elliptical and lenticular galaxies show any emission, although in some cases under-exposure in the ultraviolet could hide a weak 3727 line, and in the redshift range $z = 0.042$ to 0.055 , weak $H\alpha + NII$ could be masked by OH night sky emission.

The earliest galaxy type in which we see emission lines is Sa (A 1222 + 12, but the type is uncertain). The single HeI line at 4471 \AA measured in the microscope measurements in NGC 7098 (Sa) is probably a defect as it was not recorded on the microdensitometer tracings. The emission spectra of the later type galaxies can for the most part be satisfactorily matched by the spectra of HII regions of various degrees of excitation as given by e.g. Smith (1975). The HeII line at 4686 \AA in the irregular galaxy I 4662 is very surprising, if real. We also note that we occasionally find NII at 6584 \AA to be stronger than $H\alpha$, but only in the nuclei of galaxies. Outside of the nucleus, $H\alpha$ is always stronger than NII, as is usual in HII regions. This reversal of normal line strengths in galaxy nuclei has been previously noted by e.g. Burbidge (1970) and Warner (1973).

8. DISCUSSION

(a) Discordant Redshifts

(i) NGC 4061 and NGC 4065. Turner (1976) has published redshifts for N 4061 and N 4065 that are much lower than those published by Gregory and Thompson (GT, 1978) and by Tifft and Gregory (1979). Our observations confirm the GT redshift for N 4061 to within the measurement errors, but our redshift for N 4065 is over 600 km sec^{-1} larger than GT's. (A similar discrepancy in the redshift for NGC 4104 as observed by GT and by Kirshner et al 1978, also exists, and the sizes and directions of both discrepancies

are of similar magnitude to the redshift errors discussed by Simkin 1977 and Tifft 1978). The internal agreement of the lines measured in our NGC 4065 spectrum is very good (see Table 11) independent of wavelength. However, another observation will be needed to finally resolve the discrepancy.

(ii) NGC 5592. Sandage (1978) gives $V_H = +13, 511 \pm 80 \text{ km sec}^{-1}$ for this galaxy from two Palomar series "d" plates. Our own much lower velocity is based on only a single plate, but, as in the case of N 4065, the internal agreement of the redshift from different lines is very good (Table 11). We also note that our redshift suggests $M_B = -21.4$ (absorption and inclination corrections ignored) using m_h^c from RC2 and assuming (for consistency with Sandage's work) $H_0 = 50 \text{ km sec}^{-1}$. This is in close agreement with the mean value of $M_B = -21.25$ found by Sandage and Tammann (1974) for luminosity class I spirals. Sandage's redshift leads to $M_B = -23.8$, which seems over-luminous. Though Sandage and Tammann have adopted our redshift for the Revised Shapley-Ames Catalogue (RSA; Sandage and Tammann 1981), another spectrum will be necessary to finally resolve the discrepancy.

(iii) IC 4444. Sandage (1978) notes strong absorption lines at zero redshift in this galaxy, with four emission lines giving $V_H = +1979 \pm 14 \text{ km sec}^{-1}$. Our first spectrum for the object (CX 1886-1), centered on a very bright stellar "nucleus" is very similar to Sandage's, though we observe the G-band at the emission redshift and not at $V=0$. Our second spectrum (CX 1886-2) is for a bright knot a few arc-seconds south of the stellar object. Here, all lines - absorption as well as emission - give the same higher redshift. The most reasonable interpretation is that Sandage's spectrum and our first spectrum include a superimposed star.

(iv) A 1610-60 (= PKS 1610-607 = MHS 16-61). Burbidge and Burbidge (1972) give $z = 0.0284$ for this object noting the value to be uncertain, while Whiteoak (1972) gives $z = 0.0176 \pm 0.0001$. Our redshift, and those obtained by Danziger (see Christiansen et al 1977) and by West (1981, in press) confirm

Whiteoak's value. E.M. Burbidge (1981, private communication), has stressed that their redshift is extremely uncertain, being one of three possible fits to their measurements. The RC2 adopted the Burbidge's value and should be corrected.

(v) IC 4721 and IC 4721 A. Sandage's (1978) redshift obviously refers to the small elliptical IC 4721 A 2!2 south of the much larger and lower surface brightness IC 4721. Not only does our redshift for IC 4721 A agree with Sandage's value, but the elliptical is much more easily seen in the eyepiece. On UKS IIIa-J film, IC 4721 A appears to belong to a scattered cloud of galaxies in the background of IC 4721, and there is no sign of interaction between it and IC 4721.

(b) Galaxies of Special Interest

(i) A 1224+13 and A 1233+12. These galaxies are compact dwarf ellipticals in the Virgo Cluster. The integrated photometric properties of A 1233+12 are similar to those for M32 (see Corwin 1980), and it is to be expected that those for A 1224+13 will be much the same. Neither has striking spectral peculiarities at the low dispersion used here, and both should be good candidates as typical members of their class for higher dispersion studies.

(ii) A 2131-62 B and A2212-51 A. These two galaxies were reported to have abnormally small U-B colours by Corwin (1980), but the spectra are apparently normal. Neither shows strong ultraviolet continua or emission lines. The blue U-B colour indices are therefore most probably due to the faintness of the galaxies.

(iii) NGC 7098. The total magnitude ($B_T \approx 12.4$, Corwin 1980) and large size of this neglected southern ringed Sa galaxy easily qualify it for inclusion in the Shapley-Ames Catalogue (1932), though it was not listed there. It has also been detected in neutral hydrogen by Zealey et al (in preparation) and is apparently normal for its type in its integrated HI properties (see Bottinelli et al 1980). Its velocity is such that it could be a member of the Pavo-Indus Cloud (de Vaucouleurs 1956, 1975). However, the large projected

distance to the centre of the Cloud ($\sim 20^\circ \approx 8.5$ Mpc assuming a distance of 24 Mpc for the Cloud; de Vaucouleurs 1975) makes its membership only a possibility.

(c) Groups and Clusters

Included in our sample are galaxies in eighteen rich clusters. Ten of the clusters have only a redshift for one galaxy, and require observation of further galaxies for confirmation of the cluster redshift. We have observed at least two galaxies in four of the clusters, and in four other clusters redshifts of additional galaxies are available from Bergwall et al (1978), Chincarini and Tarenghi (private communication), Fairall (1981), and Green (1978). In all eight clusters, the additional redshifts confirm the initial values.

For our other galaxies, we have made an attempt to identify the groups to which each belongs. The group listings by de Vaucouleurs (1956, 1975) and Corwin (1967) were helpful for the nearer objects, but the continuing lack of data in the southern hemisphere has made it likely that several of our group assignments are incorrect. For the same reason, we have been unable to assign several galaxies to any group.

(d) Superclusters

Galaxies in the Indus Supercluster will be discussed in a subsequent paper. We have also observed a few objects in Virgo that have redshifts in the range covered by the Coma Supercluster (Chincarini and Rood, 1976, 1979; Gregory and Thompson 1978, Tifft and Gregory 1976). The pair of galaxies A 1239-05A, B is on the southern side of the ring of Zwicky clusters defined by Tago (1980, private communication) as the Coma Supercluster. The redshift of the pair is just that of the clusters A 1367 and A1656 (Coma) and of the "bridge" of galaxies between them studied by Gregory and Thompson. N 4061 and N 4065 are the brightest members of a small cluster that is situated in this "bridge".

At a somewhat higher redshift are N 4325, I 775, and A 1222+12. These are in the background of the Virgo cluster, and are located very nearly at the centre of Tago's ring. Several other galaxies in the area observed by e.g. Eastmond and Abell (1978) have similar redshifts. If one accepts the ideas of Joeveer and Einasto (1978), Joeveer et al (1978) and Einasto et al (1980) concerning the cell structure of superclusters, then these galaxies behind the Virgo cluster may be located in, and define, the far "cell wall" of the Coma Supercluster.

ACKNOWLEDGEMENTS

We thank the PATT of the SERC and Dr. Michael Feast for a generous allotment of telescope time; T. Lloyd-Evans, John Menzies, and Roy White for assistance at SAAO, and particularly Richard Dodd for his help with the observations. We would also like to thank Chip Arp, Guido Chincarini, Massimo Tarenghi and Tom Shanks for obtaining additional redshifts in the Indus area for us; Jaan Einasto, Erik Tago and Martin Green for sending data in advance of publication; and especially Kathleen C. Corwin for her invaluable assistance in the reduction of the redshifts.

REFERENCES

- Bergwall, N.Å.S., Ekman, A.B.C., Lauberts, A., Westerlund, B.E., Borchkhadze, T.M., Breysacher, J., Lausten, S., Muller, A.B., Schuster, H.E., Surdej, J., and West, R.M., 1978. Astron. Astrophys. Suppl., 33, 243
- Bottinelli, L., Gouguenheim, L., and Paturel, G., 1980. Astron. Astrophys., 88, 32
- Bottinelli, L., Gouguenheim, L., and Paturel, G., 1981a. Astron. Astrophys. Suppl., in press.
- Bottinelli, L., Gouguenheim, L., and Paturel, G., 1981b. Astron. Astrophys. Suppl., in press
- Burbidge, G., 1970. Ann. Rev. Astron. Astrophys., 8, 369
- Burbidge, E.M. and Burbidge, G.R., 1972. Astrophys. J., 172, 37
- Chincarini, G. and Rood, H.J., 1976. Astrophys. J., 206, 30
- Chincarini, G. and Rood, H.J., 1979. Astrophys. J., 230, 648
- Christiansen, W.N., Frater, R.H., Watkinson, A., O'Sullivan, J.D., Lockhart, I.A., and Goss, W.M., 1977. Mon. Not. R. Astron. Soc. 181, 183
- Cooke, J.A., Emerson, D., Nandy, K., Reddish, V.C., and Smith, M.G., 1977. Mon. Not. R. Astron. Soc., 178, 687
- Corwin, H.G., 1967. Thesis, University of Kansas.
- Corwin, H.G., 1980. Mon. Not. R. Astron. Soc., 191, 1
- Crosswhite, H.M. and Dieke, G.H., 1972. Am. Inst. Phys. Handbook, ed. Gray, D.E. (New York: McGraw-Hill), p.7-1
- Dawe, J.A., Dickens, R.J., and Peterson, B.A., 1977. Mon. Not. R. Astron. Soc., 178, 675
- Dressel, L.L. and Condon, J.J., 1976. Astrophys. J. Suppl., 31, 187
- Eastmond, T.S., 1977. Thesis, Univ. of California, Los Angeles
- Eastmond, T.S. and Abell, G.O., 1978. Publ. Astron. Soc. Pac., 90, 367
- Einasto, J., Joeveer, M., and Saar, E., 1980. Mon. Not. R. Astron. Soc. 193, 353
- Faber, S.M., 1977. The Evolution of Galaxies and Stellar Populations, ed. Tinsley, B.M. and Larson, R.B. (New Haven: Yale Univ. Obs.), p.157
- Faber, S.M. and Jackson, R., 1976. Astrophys. J., 204, 668
- Fairall, A.P., 1981. Mon. Not. R. Astron. Soc., in press
- Fay, T.D., Stein, W.L., and Warren, W.M., 1974. Publ. Astron. Soc. Pac., 86, 772

- Freeman, K.C., Karlsson, B., Lyngå, G., Burrell, J.F., van Woerden, H., Goss, W.M., and Mebold, U., 1977. Astron. Astrophys., 55, 445
- Green, M.R., 1978. Thesis, Univ. of Oxford.
- Gregory, S.A. and Thompson, L.A., 1978. Astrophys. J., 222, 784
- Holmberg, E.B., 1937. Lund Ann. No.6
- Holmberg, E.B., Lauberts, A., Schuster, H.E., and West, R.M., 1980. Astron. Astrophys. Suppl., 39, 173
- Joeveer, M. and Einasto, J., 1978. IAU Symp. No. 79 (Dordrecht: Reidel), p.241
- Joeveer, M., Einasto, J., and Tago, E., 1978. Mon. Not. R. Astron. Soc., 185, 357
- Kelton, P.W., 1980. Astron. J., 85, 89
- Kirshner, R.P., Oemler, A., and Schechter, P.L., 1978. Astron. J., 83, 1549
- Lewis, B.M., 1975. Mem. R. Astron. Soc., 78, 75
- Martin, W.L., 1976. Mon. Not. R. Astron. Soc., 175, 633
- Moore, C.E., Minnaert, M.G.J., and Houtgast, J., 1966. The Solar Spectrum 2935 Å to 8770 Å (Washington, D.C.: U.S. Gov't Printing Office)
- Palmer, D.R. and Milsom, A.S., 1972. "Photoelectronic Image Devices", Advances in Electronics and Electron Physics, Vol.33A, 33B.
- Reinmuth, K., 1927. Veröff. Sternw. Heidelberg, 8, 69
- Rood, H.J., 1981. Preprint
- Sandage, A.R., 1975. Galaxies and the Universe, ed. Sandage, A.R., Sandage, M., and Kristian, J. (Chicago: Univ. of Chicago Press), p.761
- Sandage, A.R., 1978. Astron. J., 83, 904
- Sandage, A.R., and Tammann, G.A., 1974. Astrophys. J., 194, 559
- Sandage, A.R. and Tammann, G.A., 1981. A Revised Shapley-Ames Catalogue of Bright Galaxies (Washington, D.C. : Carnegie Institution)
- Shapley, H. and Ames, A., 1932. Harvard Obs. Ann., 88, No.2
- Simkin, S.M., 1977. Astron. Astrophys., 55, 369
- Smith, H.E., 1975. Astrophys. J., 199, 591
- Thonnard, N., Rubin, V.C., Ford, W.K., and Roberts, M.S., 1978. Astron. J., 83, 1564
- Tifft, W.G., 1978. Astrophys. J., 220, 418
- Tifft, W.G. and Gregory, S.A., 1976. Astrophys. J., 205, 696
- Tifft, W.G. and Gregory, S.A., 1979. Astrophys. J., 231, 23
- Turner, E.L., 1976. Astrophys. J., 208, 20

- de Vaucouleurs, G., 1956. Commonwealth Obs. Mem. No.13
- de Vaucouleurs, G., 1975. Galaxies and the Universe, ed. Sandage, A.R., Sandage, M., and Kristian, J. (Chicago : Univ. of Chicago Press), p.557
- de Vaucouleurs, G. and de Vaucouleurs, A., 1963. Astron. J., 68, 96
- de Vaucouleurs, G. and de Vaucouleurs, A., 1967. Astron. J., 72, 730
- de Vaucouleurs, G., de Vaucouleurs, A., and Corwin, H.G., 1976. Second Reference Catalogue of Bright Galaxies (Austin: Univ. of Texas Press)
- de Vaucouleurs, G., de Vaucouleurs, A., and Nieto, J.L., 1979. Astron. J., 84, 1811
- Warner, J.W., 1973. Astrophys. J., 186, 21
- West, R.M., 1977. Astron. Astrophys. Suppl., 27, 73
- Whiteoak, J.B., 1972. Aust. J. Phys., 25, 233
- Whiteoak, J.B. and Gardner, F.F., 1977. Aust. J. Phys., 30, 187
- Williams, T.B., 1976. Astrophys. J., 209, 716
- Zaidel', A.N., Prokof'ev, V.K., and Raiskii, S.M., 1961. Tables of Spectrum Lines (London : Pergamon Press)

TABLE 1 - ARGON 1 COMPARISON LINES

<u>Line</u>	<u>Std. λ</u>	<u>Adopted λ's</u>		<u>Notes</u>
		<u>0.3 mm</u>	<u>0.4 mm</u>	
3948	3948.9	3948.5	3948.9	Blend with 3947.5
4159	4158.6	4159.1	4159.4	
4345	4345.2	4348.6	4347.5	Blend w. 4348.1 (AII) Contaminated ?
4545	4545.1	4545.2	4545.1	
4764	4764.9	4764.9	4764.9	AII
4879	4879.9	4880.2	4880.6	AII. Contaminated ?
5014	{5014.0}	(5015.4)	(5015.4)	Blend of 5009.4 and 5017.2, both AII
5187	5187.8	(5188.7)	(5188.7)	Used only when λ 5221 not available
5221	5221.3	5218.9	5219.6	Blend with 5216.3
5495	5495.9	5496.3	5495.9	
5606	5606.7	5606.2	5606.2	Contaminated ?
5912	5912.1	5912.0	5912.1	
6032	6032.1	6031.2	6031.0	Contaminated ?
6171	{6171.7}	6171.8	6171.8	Blend of 6170.2 and 6173.1
6416	6416.3	6416.0	6416.3	
6677	6677.3	6677.5	6677.3	
6871	6871.3	6871.7	6871.7	
7147	7147.0	-	-)	Used only for I4662. Std λ 's adopted
7384	7384.0	-	-)	
			-)	
7723	7723.8	-	-)	

TABLE 2

BROAD ABSORPTION FEATURES SEEN ON JOYCE-LOEBEL TRACINGS

<u>Feature</u>	λ_0	σ_n	σ_1	n	<u>Notes</u>
3579*	3579.1	± 1.1	± 4.7	18	Nearly all in E and S0 galaxies
3612*	3612.0	1.3	4.1	10	Mainly in E and S0 galaxies
3680*	3680.8	1.4	4.0	8	
4068	4068.2	1.3	4.7	13	cf 4071 (Table 3)
4153*	4153.8	1.9	6.0	10	
4182*	4182.2	2.0	5.7	8	
4405	4405.6	1.7	5.1	9	cf 4404 (Table 4) Mainly in Sa to Sc galaxies
4460	4460.4	1.5	4.5	9	cf 4457 (Table 4) Nearly all in E and S0 galaxies
4530	4530.3	1.9	4.7	6	cf 4528 (Table 4) Nearly all in E and S0 galaxies
4669*	4669.2	2.1	5.1	6	
5127*	5127.8	1.5	4.5	9	
5148*	5148.4	1.4	3.7	7	
5208*	5208.4	1.2	2.9	6	Nearly all in E and S0 galaxies

TABLE 3 - DISPERSION COEFFICIENTS AND ERRORS

<u>Sample</u>	<u></u>	<u><c></u>	<u><σ></u>
0.3 mm w. λ3948	$214.8 \pm 0.4 \text{ \AA mm}^{-1}$	$-0.624 \pm 0.016 \text{ \AA mm}^{-2}$	$\pm 0.515 \text{ \AA}$
0.3 mm w/o λ3948	$215.0 \pm 0.5 \text{ \AA mm}^{-1}$	$-0.633 \pm 0.019 \text{ \AA mm}^{-2}$	$\pm 0.529 \text{ \AA}$
0.4 mm w. λ3948	$214.3 \pm 0.7 \text{ \AA mm}^{-1}$	$-0.639 \pm 0.027 \text{ \AA mm}^{-2}$	$\pm 0.571 \text{ \AA}$
0.4 mm w/o λ3948	$214.9 \pm 1.1 \text{ \AA mm}^{-1}$	$-0.652 \pm 0.015 \text{ \AA mm}^{-2}$	$\pm 0.508 \text{ \AA}$

TABLE 4 - REST WAVELENGTHS FOR ABSORPTION
FEATURES USED IN CALCULATING REDSHIFTS

<u>Feature</u>	λ_0	σ_n	σ_1	n	f_0	<u>Identity</u>
3742	3742.5	± 0.4	± 1.4	11	1.6	FeI (+ Ti II?)
3769*	3769.0	0.8	2.1	8	1.2	H λ + FeI
3794*	3794.5	0.3	0.7	4	0.6	FeI
H θ	3798.6	0.7	1.7	7	1.0	H θ
3827*	3827.0	0.5	2.0	16	2.3	FeI
H η	3834.66	0.26	1.33	26	3.8	H η (+MgI + FeI)
3879*	3879.1	0.7	2.4	13	1.9	FeI
H ζ	3887.7	0.4	1.1	8	1.2	H ζ
K	3933.44	0.17	1.37	67	9.7	CaII
H	3969.17	0.20	1.68	69	10.0	CaII + He
4071*	4071.1	1.0	2.0	4	0.6	FeI
H δ	4102.8	0.4	2.0	21	3.0	H δ
g	4227.8	0.5	1.3	7	1.0	CaI
4272 [†]	4272.1	0.5	1.0	4	0.6	FeI + CrI
G ₁ [*]	4298.1	0.6	1.7	9	1.3	CH etc.
G	4304.36	0.27	1.49	31	4.5	CH etc.
G ₂ [*]	4310.4	0.5	1.2	6	0.9	CH etc.
H γ	4340.5	0.3	0.6	3	0.4	H γ
4376 [†]	4376.7	0.8	1.7	4	0.6	FeI + CH
4384	4384.1	0.7	2.2	10	1.4	FeI
H β	4864.5	0.5	1.7	11	1.6	H β
b ₁ [*]	5166.6	0.6	2.1	11	1.6	MgI
b	5174.0	0.4	2.1	24	3.5	MgI
b ₂ [*]	5183.2	0.6	2.1	11	1.6	MgI
5268	5268.6	0.6	1.8	11	1.6	FeI + CaI (or MgH)
5591	5591.0	1.2	2.0	3	0.4	CaI + NiI
5709	5709.9	0.4	0.8	4	0.6	FeI + MgI (+NiI ?)
5847*	5847.6	1.1	2.1	4	0.6	FeI (+NiI ?)
5856	5856.3	1.1	3.0	7	1.0	CaI + FeI (or TiO)
D	5892.36	0.26	1.40	28	4.1	NaI
5917*	5917.6	0.6	1.1	4	0.6	FeI ?
5948*	5948.2	0.5	1.0	4	0.6	SiI ?
5955 [†]	5955.3	0.5	1.1	5	0.7	FeI + TiI

TABLE 5 - POSSIBLE ABSORPTION FEATURES MEASURED

<u>Feature</u>	λ_o	σ_n	σ_1	n	\bar{i}_o	<u>Identity</u>	<u>Notes</u>
3752*	3752.4	0.7	1.1	3	0.4	H μ +FeI	
4077 [†]	4077.4	0.4	0.6	3	0.4	FeI+MnI+SrII	
4122*	4122.8	1.0	1.7	3	0.4	FeI (+CoI ?)	
4144 [†]	4144.2	0.5	0.9	3	0.4	FeI + HeI	
4196*	4196.7	0.9	1.5	3	0.4	FeI + CN	
4276*	4276.0	0.9	1.5	3	0.4	FeI + CH (+CrI ?)	
4404 [†]	4404.3	0.6	1.0	3	0.4	FeI	
4457 [†]	4457.3	0.6	1.1	3	0.4	FeI etc.	
4528 [†]	4528.6	-	-	1	0.1	FeI etc.	
4708	4708.0	0.1	0.1	2	0.3	FeI+TiI+CrI	= 4710 ?
4871*	4871.3	0.4	0.7	3	0.4	FeI	
5022	5022.5	0.6	1.0	3	0.4	TiI + FeI	= 5024 ?
5100	5100.5	-	-	1	0.1	FeI (+C ₂ ?)	= 5103 ?
5332	5332.6	1.7	2.3	2	0.3	FeI	= 5331 ?
5403	5403.3	0.6	0.8	2	0.3	FeI + CrI	= 5401 ?
5774*	5774.7	0.7	1.2	3	0.4	FeI	
5783	5783.7	-	-	1	0.1	CrI + FeI + CuI	= 5782?
6021	6021.5	0.8	1.1	2	0.3	FeI	= 6025?

* Features reported for the first time.

[†] Previously reported features independently found by us.

TABLE 6 - EMISSION LINES MEASURED

<u>Line</u>	λ_0	n	<u>Identity</u>
3727	3727.0	23	OII
3868	3868.74	9	Ne III
H ζ	3889.9	1	H ζ (+HeI ?)
He ϵ	3969.56	1	He ϵ (+Ne III ?)
H δ	4101.74	3	H δ
H γ	(4338.6)	5	(He II
	()		(
	(4340.47)		(H γ
4363	4363.2	1	OIII
4471	4471.5	2	HeI
H β	4861.33	13	H β
4958	4958.91	9	OIII
5006	5006.84	11	OIII
5875	5875.63	2	HeI
6548	6548.10	10	NII
H α	6562.81	26	H α
6584	6583.60	25	NII
6678	6678.1	1	HeI
6717	6717.00	12	SII
6731	6731.30	11	SII
7065	7065.2	1	HeI
7135	7135.8	1	AlII

TABLE 7 - NIGHT SKY LINES

<u>Line</u>	<u>K(CaI)H</u>	<u>5577(OI)</u>	<u>5892(NaI)</u>	<u>6300(OI)</u>	<u>6363(OI)</u>	
<V>	-192	-101	±12	-15	+14	-38
σ_n	±31	±54	± 4	± 4	± 4	± 7
σ_1	±120	±210	±31	±30	±42	±31
n	15	15	71	63	59	18

TABLE 8

(1)	(2)	(3)	(4)	(5)	(6)	(7)	(8)	(9)	(10)	(11)	(12)	(13)	(14)	(15)	(16)	(17)	(18)	(19)	(20)
Galaxy	α (1950)	δ	SAAO Plate- Spectrum	Slit P.A.	Slit Width arcsec	Slit Length arcsec	Exposure min.	Date June 1978	V	σ_v	V_0	Quality 39487	Emission Index	n_a	n_e	Group	Remarks	ESO/Upps	
N4061	12 01 28.1 +20 30 38	E3:	CX 1884-3	90°	1.8	59	7	5/6	47215	±34	+7156	F	N	-	9	0	R4065	Note	-
N4065	01 32.9 +20 30 47	E1	1884-4	90°	"	63	5	"	6836	24	6777	PF	N	-	7	0	"	"	-
I775	16 21 +13 11.5	S0:P	1884-1	90°	"	71	10	"	7825	19	7742	F	Y	-	4	0	Coma SC	"	-
N4325	20 34.2 +10 53 56	S0 ⁻	1878-1	0°	"	(107)	20	2/3	7786	35	7696	PF	Y	-	8	0	"	UBV, Note	-
A1222+12	22 00 +12 59.0	Sa?	1884-2	90°	"	71	10	5/6	7695	80	7614	PF	N	-	5	0	"	"	-
A1224+13	24 03 +13 01.0	cE0:	1878-2	0°	"	44	20	2/3	1383	48	1304	PF	Y	-	8	0	Virgo E	Note	-
A1233+12	33 05.9 +12 39 24	cE1:	1884-5	90°	"	63	10	5/6	293	47	208	FG	N	-	3	0	"	UBV, Note	-
A1238-04	38 41 -04 44.2	S0 ⁰	1895-3	90°	"	63	15	8/9	2914	25	2773	FG	N	-	9	0	Virgo II	Note	-
A1239-05A	39 42 -05 31.1	S0p	1895-2	90°	"	63	15	"	6997	62	6854	G	N	-	5	0	Coma SC?	"	-
A1239-05B	39 44 -05 30.2	S0/a P	1895-1	90°	"	63	15	"	6597	62	6454	F	N	-	6	0	Coma SC?	"	-
N4679	12 44 46 -39 18.0	Sbc:	1884-6	90°	"	63	8	5/6	4638	39	4405	F	N	2	7	1	Centaurus	"	372-G82
N5464	14 04 11 -29 46.8	Im:	1885-4	90°	"	59	7	"	2789	25	2629	G	Y	8	1	11	N5494	"	446-G11
A1409-65	09 18 -65 06.3	Sb	1885-1	90°	"	67	2	"	376	28	152	FG	N	4	15	7	N5128?	"	97-G13
N5494	09 29 -30 24.8	Sc	1885-5	90°	"	59	10	"	2775	34	2617	G	Y	2	8	1	N5494	"	446-G25
N5592	21 00 -28 27.7	Sb	1885-6	90°	"	59	5	"	4427	30	4284	F	R	3	10	3	-	"	446-G58
N5612	28 11 -78 10.1	Sb	1885-2	90°	"	55	3	"	2677	59	2451	F	N	-	5	0	N5967?	"	22-C01
I4444	28 27 -43 11.9	Sbc	1886-1	90°	"	59	1	"	2020	31	1841	FG	Y	3	1	3	-	"	272-G14
I4444S	"	"	"	"	"	"	"	"	172	44	-	"	"	-	4	0	-	"	-
I4444	"	"	1886-2	90°	"	59	5	"	2044	15	1865	G	N	6	6	6	-	"	272-G14
N5643	29 28 -43 57.2	Sc	1890-1	90°	"	59	8	6/7	1205	27	1025	F	N	6	9	9	N5643	"	272-G16
I4448	34 22 -78 35.7	Sc P	1885-3	90°	"	63	15	5/6	4625	24	4400	G	Y	5	8	8	-	"	22-C02
N5756	44 48 -14 38.7	Sb?ep	1877-1	45°	2.4	44	20	31 May/ 1 June	2126	19	2049	PF	N	5	3	3	N5728?	"	-
N5757	44 57 -18 52.2	Sb	1876-5	165°	"	44	15	"	2659	30	2566	PF	Y	3	2	3	N5728	"	580-G33
N5791	14 55 56 -19 09.1	E6:	1881-1	90°	1.8	51	5	3/4	3381	28	3297	G	Y	-	10	0	N5796	"	581-C07
"	"	"	1881-2	90°	"	48	5	"	3308	44	3224	FG	Y	-	9	0	"	"	-
N5967	15 42 06 -75 31.0	Sbc	1881-3	90°	"	44	5	"	3037	32	2828	F	Y	3	9	3	N5967?	Note	42-G10
A1601-67A	16 01 26 -67 35.4	Sa	1879-3	90°	"	44	10	2/3	4783	50	4593	FG	N	-	5	0	-	"	68-IG16
A1601-67B	01 34 -67 35.0	S0 ⁰	1879-4	90°	"	48	10	"	4676	16	4486	F	Y	-	2	0	-	"	-
A1610-60	10 43 -60 46.9	E3:	1881-4	90°	"	44	10	3/4	5516	49	5347	FG	Y	-	9	0	Cl 1610-60	"	137-C06
N6221	48 25 -59 08.0	Sc	1886-3	90°	"	59	2	5/6	1383	19	1234	FG	Y	5	3	7	N6300	"	138-C03
N6215A	16 48 30 -58 51.9	Sb	1881-5	90°	"	44	20	3/4	2894	56	2746	PF	Y	2	3	2	-	"	138-C04
N6300	17 12 17 -62 45.9	Sb	1881-6	90°	"	44	10	"	1090	29	938	F	R	2	9	2	N6300	"	101-G25
A1740-79	40 55 -79 00.9	Sb P	1877-2	140°	2.4	48	20	31 May/ 1 June	5384	29	5188	PF	Y	3	0	6	-	"	24-1009
"	"	"	1879-5	90°	1.8	48	30	2/3	5242	33	5046	F	Y	5	0	6	-	"	"
I4662	17 42 12 -64 37.3	Im	1882-1	90°	"	40	5	3/4	299	12	151	G	Y	10	0	18	-	"	102-G14

(1) Galaxy	(2) α	(2) δ	(3) Summary Type	(4) SMO Plate-Spectrum	(5) Slit P.A.	(6) Slit Width arcsec	(7) Slit Length arcsec	(8) Exposure min.	(9) Date June 1978	(10) V	(11) σ_V	(12) V _o	(13) Quality 3948?	(14) Emission n _a	(15) n _e	(16) Group	(17) Remarks	(18) ESO/Upps		
14713	18 24 47	-67 15.4	Sm?p	CX 1882-2	90°	1.8	40	20	3/4	+5548	465	+5401	F	Y	4	3	2	-	Note	103-G23
14714	25 48	-66 41.2	Sed:sp	1886-4	90°	"	71	20	5/6	4593	35	4448	F	Y	2	6	2	-	"	103-G24
14720	29 11	-58 26.6	Sd	1886-5	90°	"	63	15	"	2179	24	2069	F	Y	3	5	6	Pavo-Indus?	"	140-G25
14721	30 03	-58 32.2	Scd p	1886-6	90°	"	63	8	"	2119	30	2009	PF	N	2	10	2	"	"	140-G27
14721A	30 03	-58 34.4	E0	1887-1	90°	"	55	5	"	6121	32	6011	FG	N	-	10	0	-	"	-
N6684	44 03	-65 13.9	SO ⁺	1890-3	90°	"	55	4	6/7	812	30	677	G	N	-	12	0	N6684	"	104-G16
14797	52 25	-54 22.3	SO ⁺	1890-2	90°	"	55	4	"	2606	42	2521	G	Y	-	8	0	Pavo-Indus	"	183-G29
14798	53 44	-62 11.2	SO p	1890-4	90°	"	59	10	"	4546	41	4426	FG	N	-	12	0	N6721	"	141-G15
14806	18 57 15	-57 36.2	Sb sp	1893-1	90°	"	67	15	7/8	4443	36	4345	F	N	-	6	0	"	Note	141-G20
N6744	19 05 02	-63 56.3	Sbc	1893-3	90°	"	67	6	"	700	25	575	E	N	1	11	0	-	"	104-G42
N6753	07 12	-57 08.0	Sb	1875-1	90°	2.4	32	15	30/31 May	3214	55	3120	P	Y	3	4	1	N6753	"	184-G22
"	"	"	"	1883-2	90°	1.8	44	3	4/5	3124	26	3030	F	Y	2	11	4	"	"	"
"	"	"	"	1896-3	90°	"	51	6	8/9	3132	29	3038	P	N	2	9	2	"	"	"
14832	09 53	-56 41.7	Sab sp	1896-4	90°	"	51	20	"	3497	42	3406	P	N	-	5	0	"	"	184-G39
"	"	"	"	1900-6	0°	"	67	15	12/13	3420	39	3329	F	N	2	9	3	"	"	"
N6851	19 59 55	-48 25.5	SO ⁻	1893-2	90°	"	67	6	7/8	3112	36	3072	GE	N	-	8	0	Pavo-Indus	"	233-G21
A2028-63A	20 28 41.9	-63 11 57	E ⁺	1883-3	90°	"	40	20	4/5	22943	34	22832	PF	Y	-	4	0	CI 2029-63 UBV	"	-
A2035-61	35 53.1	-61 30 37	SO ⁺	1879-6	90°	"	44	30	2/3	21377	33	21275	F	Y	-	8	0	CI 2035-61	"	-
A2036-53A	36 33.8	-53 12 38	E0:p	1887-2	90°	"	63	8	5/6	13216	38	13156	G	N	-	5	0	CI 2036-53 UBV	"	186-1671
A2048-52B	48 18.0	-52 56 29	E3	1883-5	100°	"	103	10	4/5	13877	24	13819	F	N	-	5	0	CI 2047-52 Note	"	187-1025
A2048-52A	48 21.7	-52 56 36	SO ⁻	"	"	"	"	"	"	13073	9	13015	F	"	-	3	0	"	Note	"
A2049-52B	49 07.6	-52 13 00	SO ⁻	1896-5	90°	"	51	20	8/9	13794	40	13740	FG	N	-	6	0	CI 2048-52	"	-
A2049-52A	20 49 08.3	-52 21 13	Sbc:	1883-4	90°	"	40	15	4/5	14335	39	14280	P	Y	1	3	0	"	UBV, Note	235-G09
A2111-59	21 11 55.1	-59 47 33	SO/a	1887-3	90°	"	59	20	5/6	17673	63	17581	PF	Y	-	5	0	CI 2113-59	"	-
A2113-59A	13 04.6	-59 43 05	E1:	1880-1	90°	"	40	20	2/3	17502	63	17410	PF	R	-	6	0	"	"	-
A2125-51	25 54.2	-51 06 12	E2	1882-3	90°	"	48	30	3/4	23980	61	23932	F	Y	-	7	0	CI 2126-51	"	-
A2129-60	29 05.3	-60 55 06	SO ⁻	1880-2	90°	"	40	20	2/3	8616	47	8518	F	N	-	5	0	-	UBV, Note	-
A2130-53A	30 38.5	-53 47 40	SO ⁺ p	1901-2	0°	"	63	20	12/13	23555	45	23493	F	N	-	3	0	CI 2131-53	"	-
A2131-62A	31 21.9	-62 18 08	E ⁺ 1	1882-4	90°	"	48	20	3/4	16877	51	16772	F	Y	-	7	0	CI 2130-62	"	-
A2131-62B	31 27.7	-62 10 56	SO/a?	1882-5	90°	"	44	20	"	16774	81	16670	FG	Y	-	4	0	"	UBV	-
A2136-50	36 12.9	-50 55 03	E1	1893-4	90°	"	67	20	7/8	16435	95	16387	F	N	-	3	0	CI 2136-50	"	-
N7098	39 19	-75 20.5	Sa	1883-1	90°	"	40	3	3/4	2399	33	2234	F	N	1	8	1	Pavo-Indus? UBV, Note	"	48-G05
A2142-51	42 08.5	-51 50 17	E ⁺	1896-6	90°	"	51	20	8/9	16119	39	16066	P	N	-	3	0	CI 2142-51	"	-
A2142.57	42 50.4	-57 31 04	E ⁺	1882-6	90°	"	44	30	3/4	22533	52	22451	PF	Y	-	2	0	CI 2143-57 Note	"	-
A2148-57	21 48 27.7	-57 43 14	E3	1880-3	90°	"	44	20	2/3	12074	40	11991	FG	Y	-	6	0	-	UBV, Note	-
A2158-57	"	"	"	1901-1	0°	1.8	63	20	12/13	12021	45	11938	FG	N	-	7	0	-	UBV, Note	-
A2151-57	51 50.3	-57 53 40	SO ⁺	1887-4	90°	"	63	15	5/6	23241	56	23157	FG	Y	-	6	0	CI 2150-58 UBV	"	-
A2158-60D	21 58 21.6	-60 11 12	E ⁺ p	1887-5	90°	"	63	20	"	23917	48	23821	PF	N	-	8	0	CI 2158-60 Note	"	146-1005

(1) Galaxy	(2) α	(3) δ	(4) Summary Type	(5) SAMO Plate- Spectrum	(6) Slit P.A.	(7) Slit Width arcsec	(8) Slit Length arcsec	(9) Exposure min.	(10) Date	(11) V	(12) σ_v	(13) V Quality	(14) F N	(15) Emission n _a	(16) n _e	(17) Group	(18) Remarks	(20) ESO/Upps
N7196	22 02 46	-50 22.0	E3	CX 1877-5	90°	2.4	40	8	31 May/ 1 June	+2884	±45	+2837	F	-	5	0	Pavo-Indus	237-C36
N7200	03 57	-50 14.6	E4:	1877-6	90°	"	44	10	"	2926	121	2879	F	-	3	0	"	237-C37
A2212-51A	12 21.9	-51 45 12	E2:	1887-6	90°	1.8	63	15	5/6	20436	41	20380	G	-	8	0	C1 2212-51 UVV	-
A2213-52A	13 47.8	-52 46 37	S0:	1888-1	90°	"	63	10	"	15973	44	15912	F	-	7	0	C1 2213-52 "	-
N7249	17 15.9	-55 22 36	E2	1890-4	90°	"	44	10	2/3	12005	65	11930	F	-	6	0	C1 2218-55	190-G01
A2230-55A	22 30 18.0	-55 03 08	E1	1888-2	90°	"	63	20	5/6	22619	56	22544	F	-	4	0	C1 2228-55 UVV	-

TABLE 8 - NOTES

- N4061, N4065 - Discordant redshifts (see text). N4061 has a strong continuum with relatively narrow lines. N4065 has a more diffused though still strong continuum with very broad lines. In Coma Supercluster.
- I775 - In Coma Supercluster behind Virgo Cluster.
- N4325 - Comparison spectrum accidentally superposed on outer parts of galaxy spectrum. Strong K, weak H. In Coma Supercluster behind Virgo Cluster.
- A1222+12 = E4-634 (see Eastmond 1977). High surface brightness spiral (?) with strong nuclear continuum and broad, shallow features. Moderately strong $\lambda 3727$ in nucleus only not seen by H.C. but clear on Joyce-Loebel tracing. In Coma Supercluster behind Virgo Cluster.
- A1224+13 = E4-850 (Eastmond 1977). Compact dwarf elliptical in Virgo Cluster. K disturbed by strong night sky.
- A1233+12 = E3-882 (Eastmond 1977). Compact dwarf elliptical in Virgo Cluster. Strong nuclear continuum with strong narrow H & K, weak MgI and $\lambda 4144$. Corwin (1980) has UBV photometry and photometric parameters.
- A1238-04 = No. 19 in Cooke et al (1977). Companion to N4602 (Cooke et al No. 13, 12' south preceding) in Virgo II (V) Cloud. Pretty broad lines.
- A1239-05A = Ho. 440a (Holmberg 1937) = MCG -1-32-38 = No.2 in Cooke et al (1977). Interacting with A1239-05B. In Coma Supercluster behind Virgo II (V) Cloud.
- A1239-05B = Ho 440b = MCG -1-32-39 = No. 1 in Cooke et al (1977). In Coma Supercluster behind Virgo II (V) Cloud.
- N4679 - Weak emission ($H\alpha \approx \lambda 6584$) confined to $\pm 8''$ from nucleus.

- N5464 - Slit on E-W bar. Strong emission lines across central 40" of galaxy show slight rotation. Weak H η (in absorption) and λ 5022.
- A1409-65 = Circinus Galaxy. Diffuse continuum with broad diffuse absorption. Moderate emission within $\pm 12''$ of nucleus. H α = λ 6584 in nucleus, but H α > λ 6584 outside of nucleus. See Freeman et al (1977) for a detailed discussion.
- N5494 - Strong H and K with weak H α slightly tilted across decker.
- N5592 - Redshift disagrees with that by Sandage (1978); see text. Diffuse spectrum, knots either side of bright nucleus, strong H, very weak K. Moderate emission strongly tilted, primarily confined to knots (where H α >> λ 6584), though λ 5006 confined to nucleus (where H α = λ 6584).
- N5612 - Strong, very slightly tilted H, K, G, D. Weaker H δ and H ζ . D band especially strong on Joyce-Loebel tracings.
- I4444 - Peculiar spectrum noted by Sandage (1978) due to superposed star (see text). Longer exposure has pretty strong emission across decker; but λ 3868, H γ , and λ 5006 primarily confined to two knots 6" and 16" west of nucleus.
- N5643 - Pretty strong emission. H δ absorption and emission superposed in and out of nucleus. Strong H γ absorption in nucleus, H γ emission on either side of nucleus. H α \leq λ 6548.
- I4448 - Moderate emission in nucleus. λ 3742 disturbed by strong λ 3727. λ 6717 and λ 6731 disturbed by night sky. Absorption lines faint and diffuse.
- N5756 - Slit aligned on major axis. No evidence for rotation at this dispersion. Emission extends from nucleus to knot 20" south-west on edge of decker. H α > λ 6584.

- N5757 - Slit aligned on bright bar. All features tilted. Emission on east side of galaxy, extending from nucleus (where $H\alpha = \lambda 6584$).
- N5967 - Faint emission ($H\alpha \gg \lambda 6584$) confined to nucleus. H and K tilted.
- A1601-67A, B - Interacting pair, but no emission. B has H and K only, broad and diffuse. H and K narrow in A; $\lambda 3742$, $H\eta$, and G are broad. Observed for A. Longmore.
- A1610-60 = PKS 1610-608. Brightest in cluster. Redshift in RC2 wrong; see text.
- N6221 - Broad emission lines in nucleus narrow to run across decker to knots $\sim 25''$ east and west. $\lambda 6548$ disturbed by very broad $H\alpha$ in nucleus. $H\alpha > \lambda 6584$ and $H\beta > \lambda 5006$.
- N6215A - Faint $H\alpha$ and $\lambda 6584$ only in faint nucleus. Star with strong G band superposed $\sim 10''$ west of nucleus.
- N6300 - Nearly overexposed nucleus with $H\alpha < \lambda 6584$. ($H\alpha$ just seen by H.C. and could not be measured; clear on tracing, however). $\lambda 3727$, $\lambda 4958$, $\lambda 5006$, $H\alpha$, and $\lambda 6584$ confined to nucleus.
- A1740-79 - Spectrum 1877-2 has slit aligned on major axis. Faint emission ($\lambda 3727$, $\lambda 4958$, $\lambda 5006$, $H\alpha \gg \lambda 6584$), slightly twisted, across decker. Spectrum 1879-5 east-west across brightest part of galaxy. Faint emission across decker, tilted. Continuum faint in both spectra; no absorption seen at this dispersion. Observed for A. Longmore.
- I4662 - Nearly overexposed continuum with no absorption and typical HII region emission spectrum. Two knots on slit with the following lines confined to the knots: $H\zeta(+HeI?)$, $He(+NeIII?)$, $\lambda 4363$, $\lambda 4471$, $\lambda 5875$, $\lambda 6548$, $\lambda 6584$, $\lambda 6684$, $\lambda 6717$, $\lambda 6731$, $\lambda 7065$, $\lambda 7135$, and $\lambda 3726$, 29 (2nd order only). Stretching across the decker were $\lambda 3727$ (1st order)

$\lambda 3868$, $H\delta$, $H\gamma$, $H\beta$, $\lambda 4958$, $\lambda 5006$, and $H\alpha$. In nucleus only is a broad emission feature (not seen by H.C.) centred at $\lambda 4686$ that could be HeII.

I4713 - Pretty faint continuum. $H\alpha$ and $\lambda 6584$ tilted across decker.

I4714 - Weak emission confined to nucleus. Star on slit 27" east of nucleus.

I4720 - Diffuse continuum with diffuse absorption lines. Pretty strong $\lambda 3727$, $H\beta$, $\lambda 5006$, and $H\alpha$ within $\pm 15''$ of nucleus (where $H\alpha \gg \lambda 6584$). $\lambda 4958$ and $\lambda 6584$ are very weak. Knot 6" east of nucleus has same emission lines, but broader.

I4721 - Very diffuse continuum with ill-defined absorption lines. $\lambda 3727$, $H\alpha$, and $\lambda 6584$ are very faint across decker. Sandage's (1978) redshift refers to I4721A 2!2 south. See text.

I4721A - High surface brightness elliptical in background of I4721. Sandage's (1978) redshift refers to this object rather than to I4721 2!2 north. See text.

I4806 - Broad lines.

N6744 - Possible $\lambda 3727$ seen by H.C. in nucleus only is probably a defect; not on Joyce-Loebel tracing.

N6753 - Spectrum 1875 -1 overexposed. $\lambda 3727$ seen but not measured. $H\alpha$ pretty weak, tilted. Absorption lines broad and tilted. Spectrum 1883-2 has weak $\lambda 3727$, $\lambda 3868$, $H\alpha$, and $\lambda 6584$. Spectrum 1896-3 slightly trailed, lines diffuse. Emission lines in 1875-1 and 1883-2 cross decker. $H\alpha = \lambda 6584$ in nucleus, but $H\alpha \gg \text{NII}$ in outer regions.

I4832 - Spectrum 1896-4 slightly trailed, nuclear emission only, diffuse absorption lines. Spectrum 1900-6 has faint $\lambda 6548$, $H\alpha$, and $\lambda 6584$. NII lines extend $\pm 12''$ from nucleus, $H\alpha$ confined to nucleus.

N6851 - Broad lines.

A2048-52 A, B - Double elliptical in core of rich cluster. Slit aligned on nuclei of both. Spectra of faint galaxy 22" south-east of A and of faint star 28" north-west of B could not be measured.

A2049-52A - Possible $\lambda 3727$ seen in nucleus by H.C. confirmed on tracing which also shows possible $\lambda 5006$.

A2111-59 - Diffuse lines. Joyce-Loebel tracing noisy with weak K and strong b.

N7098 - Strong continuum with broad absorption features. $\lambda 4471$, measured by H.C., not on tracing and probably a defect.

A2142-57 - No nucleus seen at telescope. Spectrum shows very broad diffuse lines in strong continuum. Brightest in a rich cluster.

A2148-57 - Both spectra show broad lines in strong continuum. In foreground of the two rich clusters near south.

A2158-60D - Brightest of four interacting ellipticals. "B" is a superposed star. West (1977) has a photograph. First in a rich cluster.

TABLE 9a - OPTICAL REDSHIFT COMPARISONS

Sets	CE-RC2	CE-S	CE-M	RC2-S	RC2-M	S-M
$\langle \Delta V \rangle$	+14	+30	+12	+21	-2	-7
σ_n	± 23	± 22	± 32	± 14	± 13	± 14
σ_1	± 80	± 90	± 79	± 70	± 97	± 97
n	12	16	6	25	57	46

TABLE 9b - TRIANGULAR COMPARISONS

Set	CE	RC2	S	M
Sets	σ	σ	σ	σ
CE, RC2, S	± 69	± 40	± 57	-
CE, RC2, M	± 40	± 69	-	± 68
CE, S, M	± 50	-	± 75	± 61
RC2, S, M	-	± 49	± 49	± 83
$\langle \sigma \rangle$	± 53	± 53	± 60	± 71
$\frac{\sigma_n}{\quad}$	± 9	± 9	± 8	± 6
$\langle \Delta V \rangle$	+21	+3	-15	+3

Set Codes:

- CE - Corwin-Emerson (this paper)
- RC2 - Second Reference Catalog (de Vaucouleurs et al 1976)
- S - Sandage (1978)
- M - Martin (1976)

TABLE 10 - HI REDSHIFT COMPARISONS

Set	CE	RC2	M	S(Pa) [§]	S(Pb) [§]	S(Pc) [§]	S(Pd) [§]	S(Sa) [§]	S(Sb) [§]	S(All) [§]
$\langle \Delta V \rangle^*$	-23	+4	-25	-20	-80	-33	+1	-47	-24	-26
σ_n	±22	±13	±14	±15	±21	±13	±11	±14	±11	±6
σ_1	±72	±89	±56	±94	±100	±81	±86	±60	±52	±83
n	11	47	17	42	23	38	65	18	21	233
"True†" σ_1	±70	±88	±54	±93	±99	±80	±85	±58	±50	±82

* $\Delta V = V_{SET} - V_{HI}$

† Assuming $\sigma_{HI} = \pm 15 \text{ Km sec}^{-1}$

§ After 1 cycle of 2σ rejection

TABLE 11 - REDSHIFTS FROM INDIVIDUAL LINES*

FOR NGC 4065 and NGC 5592

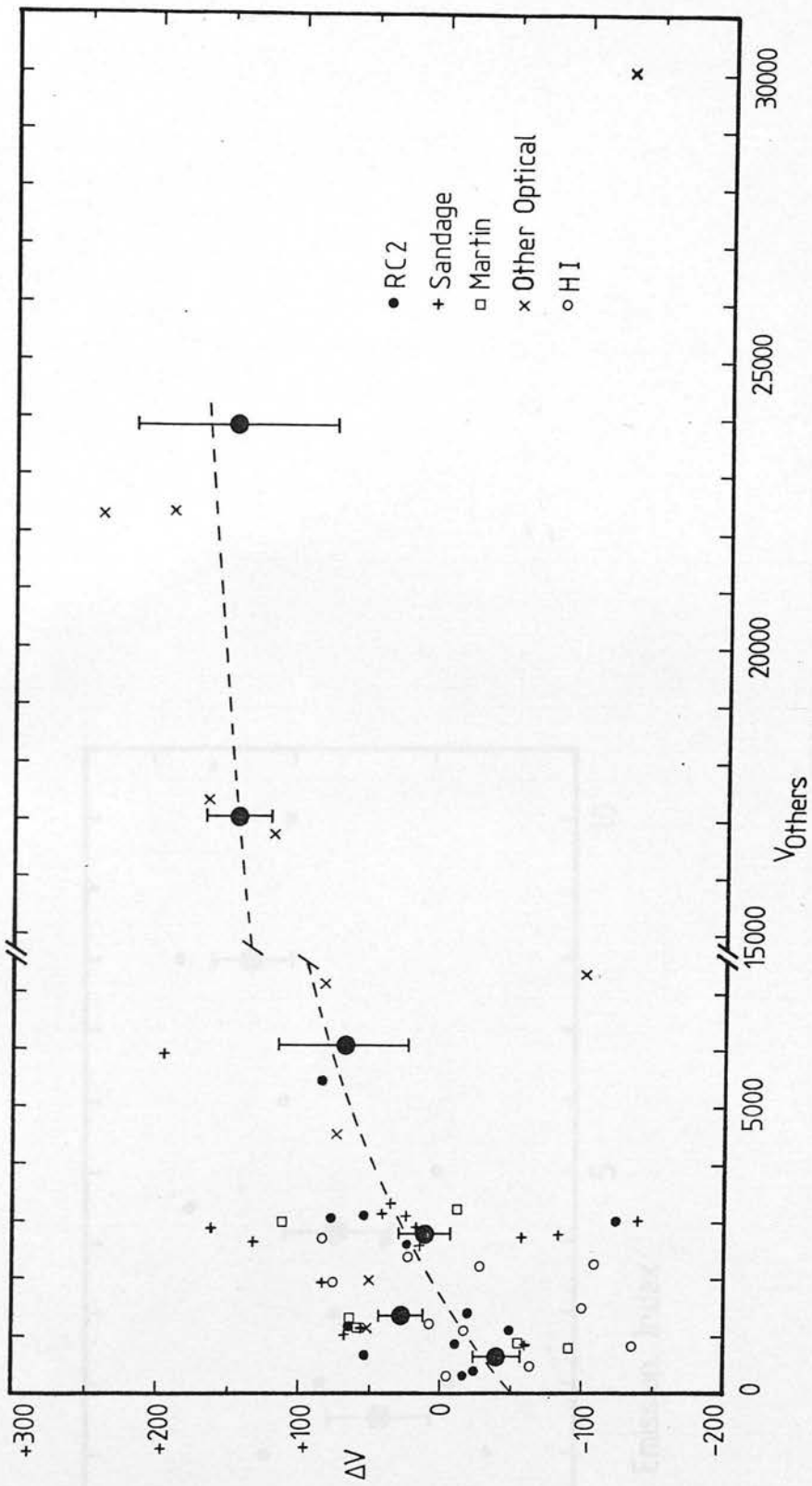
Line	Redshifts	
	N4065	N5592
3742	--	+4542
3769	-	+4486
3827	+6878	-
H η	-	+4405
3879	-	+4227
K	+6795	+4326
H	+6755	+4527
G ₁	+6738	-
G	-	+4620
4376	+6870	-
H β (e)	-	+4383
b ₁	+6725	-
b	-	+4299
b ₂	-	+4419
5268	-	+4347
D	+6840	-
H α (e)	-	+4344
6583(e)	-	+4317

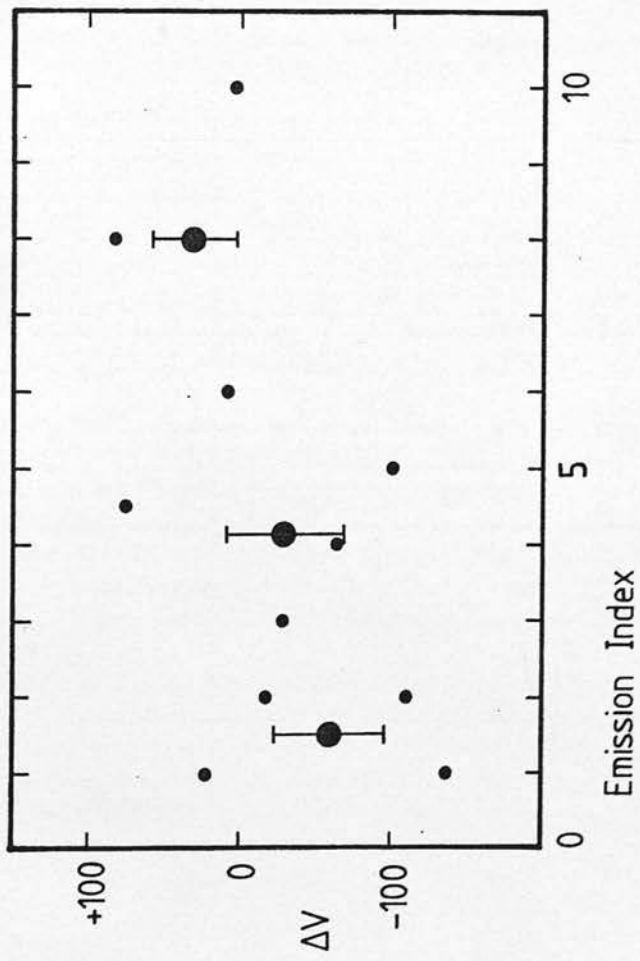
* Absorption unless marked "(e)"

FIGURE CAPTIONS

Figure 1 - Velocity residual $\Delta V = V_{CE} - V_{others}$ vs. V_{others} . The mean points (with error bars) have been calculated assuming equal weight for each point, except for the point at $V = +30046$, $\Delta V = -129$ which was given half weight. The dashed curve is a suggested error function for our data.

Figure 2 - Velocity residual $\Delta V = V_{VE} - V_{HI}$ vs. emission index. The mean points have been calculated assuming equal weight for each point.





UBV photoelectric photometry and photometric parameters for 40 galaxies

Harold G. Corwin, Jr *Department of Astronomy, University of Edinburgh,
Edinburgh EH9 3HJ*

Received 1979 May 31

Summary. Multiaperture photometry with the SAAO 1.0-m reflector for 40 (primarily southern) galaxies is presented. Nineteen of the galaxies are in the area of the Indus Supercluster, and provide calibration for photographic photometry in 16 southern sky survey fields. Observing techniques and reduction procedures receive special attention as many of the galaxies are quite faint and/or of low surface brightness. Photometric parameters are derived through procedures based on those in the *Second Reference Catalogue*, and a few individual objects of special interest are noted.

1 Introduction

The Indus Supercluster covers several southern sky survey fields all of which require photoelectric calibration to establish zero points for photographic photometry. Though previous photoelectric work has been done in the area (see de Vaucouleurs, de Vaucouleurs & Corwin 1976, hereafter referred to as RC2; Graham 1976; Bucknell & Peach 1975; Green & Dixon 1978; Bergwall *et al.* 1978; Wegner 1979; Persson, Frogel & Aaronson 1979) the galaxies observed are generally bright ($B_T < 13$) and do not cover all of the UK Schmidt plates of interest.

Two observing runs with the St Andrews photometer on the 1.0-m Elizabeth reflector at the South African Astronomical Observatory (SAAO) near Sutherland have yielded the necessary *UBV* calibrating data for 19 generally fainter ($B_T > 14$) galaxies. In addition, data for 21 other galaxies were collected, including the Fourcade-Figueroa 'Shred' and eight southern DDO objects (observed at the request of G. de Vaucouleurs; see van den Bergh 1966; Fisher & Tully 1975), as well as galaxies in the Virgo, Hydra (= Abell 1060), Hercules (A2151) and A2670 clusters. These data are being published now because of their potential usefulness to other workers.

Though the data will find their greatest use in the calibration of photographic plates, they can also be used separately to derive photometric parameters of moderate precision (see RC2, pp. 26–38). This is done in Section 5. Sections 2–4 discuss the photometer, observational procedures and reduction in some detail. These generally ignored aspects of galaxy photometry are given considerable space here because of the faintness and low surface

brightness of many of the objects; the quality of the observations could have been easily jeopardized without careful attention to details. Finally, notes on a few objects of special interest are given in Section 6.

2 The photometer

The St Andrews photometer was used in its single-channel pulse-counting mode. The photomultiplier was an EMI 6265A with 1000V EHT applied, and cooled to -10°C . Dark counts were monitored regularly and were no more than 10 per cent of the total counts for even the faintest objects observed ($V \cong 17$). The dark counts were steady at $\sim 25 \text{ s}^{-1}$, except after a malfunction in the electronics late in the second run when they rose to $\sim 120 \text{ s}^{-1}$.

The standard *UBV* filters ($U = 1 \text{ mm}$ Schott UG2; $B = 1 \text{ mm}$ Schott BG12 + 4 mm Schott GG13; $V = 2 \text{ mm}$ Schott OG515) were changed by a stepping motor between integrations according to a preprogrammed sequence. The acquisition eyepiece box had no offsetting facilities so that centring on low surface brightness galaxies had to be accomplished by visual reference to the surrounding star field. However, most of these objects were bright enough to be faintly visible in the Varo image intensifier aperture viewer, so no large centring errors are expected.

Apertures used ranged in angular size from 21 to 85 arcsec. Standard stars were observed through the 30 arcsec aperture; observations with the 21 arcsec aperture are corrected by -0.01 mag for scattering in the telescope and photometer optics. The correction was determined by observations of stars through different apertures on several nights, and proved to be independent of seeing.

Smyth & Stobie (1980) note some uncertainty in the focal plane scale for the 1.0-m reflector used with the St Andrews photometer in its current configuration. This was checked by timing, with a stop watch, polar stars drifting at sidereal rate across the five apertures used here. As explained by Smyth & Stobie, the focal plane scale so derived ($13.8 \text{ arcsec mm}^{-1}$) agreed with a similar determination by them, so has been adopted here also. Smyth & Stobie give the sizes of all apertures presently available on the St Andrews photometer. For convenience, the sizes of the five apertures used in the present work are also listed in Table 1. This gives in successive columns the nominal aperture in arcsec as shown on the aperture wheel of the photometer, the true aperture in arcsec assuming a focal plane scale of $13.8 \text{ arcsec mm}^{-1}$, and the logarithm of the true aperture in tenths of arcmin following RC2.

Table 1. Aperture diameters.

Nominal (arcsec)	True diameter (arcsec)	$\log A$
80	84.6	1.15
56	59.7	1.00
40	42.6	0.85
28	30.2	0.70
20	20.8	0.54

Star drifts by Smyth & Stobie indicated uniform response across the photocathode, and their value of the system 'dead time' — 86 ns — was also adopted for the coincidence correction.

3 Standard stars and reductions

Standard stars were selected from those in the Harvard E and F regions observed by Cousins (1973) and recently revised slightly by him (1978, list circulated at SAAO). These standards gave linear transformations over the colour range of interest ($B-V < 1.4$) with mean errors smaller than ± 0.006 mag in all colours. *Nightly* extinction and transformation coefficients were used in the final reductions as these gave somewhat smaller residuals in the standard stars and the repeated galaxy observations than did mean values of the coefficients. This is contrary to experience at McDonald Observatory where *mean* extinction and transformation values generally give smaller residuals (de Vaucouleurs & de Vaucouleurs 1972, and de Vaucouleurs, de Vaucouleurs & Corwin 1978, hereafter referred to as V^2C). This is probably an indication of the very high quality of the Cousins standards since the observational procedure and reduction was otherwise the same at both observatories.

Under normal conditions (photometric sky throughout the night) 12 standards were observed, four each in the evening, at midnight and in the morning. Abnormally poor weather often limited the number of standards observed, but there were never less than four, and the galaxy observations were never separated by more than 3 hr in time from the standard star observations. When northern galaxies were observed, two Landolt (1973) equatorial standards were added, but these were not included in the final solution for one night's coefficients as they gave significantly larger residuals (in a preliminary solution) than the Cousins standards. In practice then, the number of standards varied from 4 to 14 per night, their colours covered the entire range of galaxy colours encountered, and their maximum air mass ($X \approx 2$) was larger than the maximum air mass for the galaxies.

4 The observations

A single galaxy observation consisted of five 10-s integrations in each colour with the aperture centred by eye on the brightest part of the galaxy (or positioned by reference to field stars as noted above). The five galaxy-plus-sky integrations were interspersed with four integrations on blank sky fields, chosen by eye for the brighter galaxies and containing no stars visible in the Varo tube ($B < 17$). For the fainter galaxies or for those in crowded fields, the sky fields were selected from finding charts and contained no objects brighter than the plate limit of the UK Schmidt telescope ($V \approx 22$). A few galaxies have stars superposed that are bright enough ($V < 16$) to disturb the measurement. With the exception of the star very close to the nucleus of IC 1185, these were measured separately through the 10 arcsec aperture, and their net counts were removed from the galaxy integrations before reduction. Magnitudes and colours for these stars are given in the notes to Table 2 for the galaxies so affected.

Repeated observations at the same aperture on different nights of a dozen galaxies gave overall internal standard deviations of ± 0.02 mag in V and $B-V$, and ± 0.07 mag in $U-B$. Fig. 1 shows, however, that the residuals from the means are dependent upon magnitude. The solid lines in the figure are the adopted internal error functions for the galaxy observations.

Six of the galaxies have observations from other sources. Mean residuals – interpolated between apertures when necessary – for the four galaxies with $12 < V < 14$ are ± 0.02 mag in V , ± 0.025 in $B-V$, and ± 0.06 in $U-B$. These residuals are fortuitously small, so cannot be used to estimate the true external mean errors in the present data. However, the analysis in V^2C suggests that external errors in galaxy photometry are roughly twice as large as internal errors; this is probably true in the present data. There is a marginally significant zero point

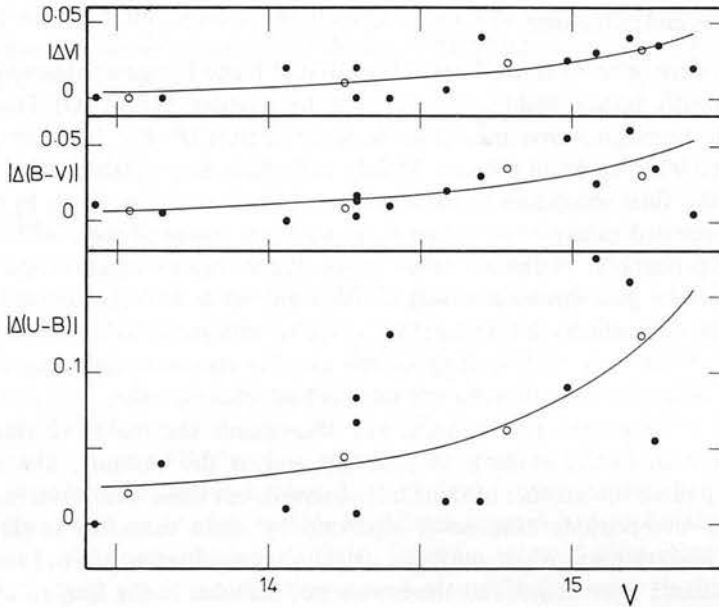


Figure 1. Internal mean error as a function of magnitude. Residuals from mean magnitudes and colours versus V magnitude for repeated galaxy observations are shown as dots. Open circles are mean points and the solid curves are the adopted internal error functions.

difference in $U-B$ of -0.06 ± 0.025 (these data with numerically smaller $U-B$), but there are too few galaxies in common to allow a confident correction to be made.

The data are set out in Table 2 which gives:

Column 1. The galaxy's designation following RC2 except in the cases of A0311-02 = DDO 31 (=N1253A in RC2) and A1331-45 = the Fourcade-Figueroa galaxy (=A1332-45 in RC2).

Column 2. The optical position for 1950.0 from RC2, Reinmuth (1927), Holmberg *et al.* (1978), or - in most cases - measured on UK or Palomar Schmidt plates (the mean errors in the positions are generally ± 1 in the last place given).

Column 3. The revised type, again from RC2 or most often newly estimated from UK or Palomar Schmidt plates.

Table 2. UBV photometry for 40 galaxies.

Galaxy	α	(1950) δ	Type	log A	V	B-V	U-B	Date	Comments
(1)	(2)	(3)	(4)	(5)	(6)	(7)	(8)	(9)	
N0045	00 11 32	-23 27.6	SA(s)dm	1.15	12.70	0.65	0.02	78-09-08	DDO 223
A0031-31	00 31.7	-31 03	SA(s)m	1.15	14.21	0.47	-0.22	78-09-08	DDO 224
I1558	00 33 18	-25 39.1	SAB(s)m	1.15	13.75	0.58	-0.03	78-09-08	DDO 225
I1574	00 40 35	-22 31.4	IBm	1.15	14.37	0.50	-0.03	78-09-08	DDO 226
I0048	00 41 03	-08 27.6	SAB:0 ⁺	1.00	13.33	0.86	0.30	78-09-08	= I1577 = MCG -1-3-1
				0.70	13.63	0.89	0.26	"	See Notes.
A0301-25	03 01 39	-25 28.1	SAB(s)m	1.15	14.74	0.60	-0.07	78-09-08	DDO 227
A0311-02	03 11 52	-02 59.3	SB(s)m	1.15	14.08	0.46	-0.35	78-09-08	DDO 31 = N1253A
N3311	10 34 22	-27 16.1	SA:0 ⁰	1.15	12.16	1.04	0.56	78-06-08	
N4325	12 20 34.2	+10 53 56	SA(s):0 ⁻	1.15	13.53	1.02	0.47	78-06-12	5 day-old moon near.
				0.85	13.86	0.99	0.35	"	
A1222+12	12 22.0	+12 58	Sa?	0.85	15.27	1.09	0.5	78-06-08	= E4-634 (see Eastmond 1977).
				0.70	15.32	0.97	0.4	"	

Table 2 — continued

Galaxy	α (1950)	δ	Type	log A	V	B-V	U-B	Date	Comments
(1)	(2)	(3)	(4)	(5)	(6)	(7)	(8)	(9)	(9)
I3481	12 30 21	+11 41.0	SAB:0 ⁻ pec	1.00	13.62	1.05	0.50	78-06-08	
				0.70	13.97	1.05	0.57	"	
A1233+12	12 33 05.9	+12 39 24	cE1	0.85	14.64	0.90	0.38	78-06-08	= E3-882 (see Eastmond 1977).
				0.70	14.70	0.90	0.53	"	
A1331-45	13 31 39	-45 17.1	SB:m: sp	1.15	13.02	0.70	-0.12	78-06-07	See notes. EU270-G17.
N5264	13 38 47	-29 39.7	IB(s)m	1.15	12.78	0.57	-0.05	78-06-08	DDO 242
N5556	14 17 39	-29 01.1	SAB(rs)d	1.15	12.88	0.69	-0.06	78-06-08	DDO 243. See Notes.
N6034	16 01 17.1	+17 20 01	SO ⁻	1.15	13.73	1.06	0.59	78-06-07	
				0.85	14.03	1.11	0.58	"	
I1185	16 03 29.5	+17 51 03	SA(rs)O/a or a	0.85	14.00	1.05	0.40	78-06-07	See Notes.
N6061	16 04 01.1	+18 22 57	SA:0 ⁻	1.15	13.67	1.11	0.56	78-06-07	
				0.70	14.19	1.08	0.55	"	
A2010-37	20 10 11	-37 20.4	(R')SA(s)O ⁰	1.00	13.21	0.91	0.35	78-09-06	EU399-G25. See Notes.
				0.70	13.45	1.00	0.48	"	
A2028-63A	20 28 41.9	-63 11 57	E ⁺ 3	0.85	15.26	1.39	0.7	78-06-12	
				0.54	15.68	1.29	0.5	"	
A2036-53A	20 36 33.8	-53 12 38	EO: pec	0.85	14.66	1.19	0.30	78-06-07	EU186-IG71A. Brighter and nf of 2.
				0.85	14.74	1.13	0.33	78-09-06	
				0.54	15.00	1.15	0.5	"	
A2049-52A	20 49 08.3	-52 21 13	SB(s):b: pec	0.85	14.27	0.87	0.24	78-06-06	EU235-G09
				0.85	14.31	0.90	0.08	78-06-12	
				0.85	14.29	0.88	0.15	78-09-08	
				0.54	14.90	0.91	0.22	"	
A2059-67	20 59 03	-67 22.7	SA0 ⁻ :	1.15	12.32	0.93	0.44	78-09-06	EU107-G09
				0.85	12.66	0.96	0.43	"	
A2111-59	21 11 55.1	-59 47 33	SA(r)O/a	0.70	15.31	1.04	0.6	78-06-07	
				0.70	15.24	1.11	0.7	78-09-08	
				0.54	15.56	1.07	(0.4)	"	
A2129-60	21 29 05.3	-60 55 06	SA(s)O ⁻	0.85	14.74	0.94	(0.7)	78-06-08	
				0.54	15.00	0.96	(0.3)	"	
A2130-53A	21 30 38.5	-53 47 40	SO ⁺ pec	0.85	14.88	1.21	0.3	78-06-12	Knotty, distorted corona.
				0.54	15.21	1.22	0.4	"	
A2131-62B	21 31 27.7	-62 10 56	SB?O/a?	0.85	15.11	1.01	(0.0)	78-06-08	Normal spectrum; low U-B is
				0.85	15.05	1.06	(0.3)	78-09-08	therefore probably observa-
				0.54	15.35	1.07	(0.1)	"	tional artifact.
A2136-50	21 36 12.9	-50 55 03	E1:	1.00	14.19	1.12	0.49	78-06-06	
				0.70	14.46	1.19	0.52	"	
N7098	21 39 19	-75 20.5	(R)SAB(r)a	1.15	12.04	1.06	0.54	78-09-08	EU48-G05. See Notes.
				0.85	12.53	1.07	0.67	"	
				0.54	13.05	1.10	0.69	"	
A2146-62	21 46 34.9	-62 25 08	SA:0 ⁻	0.85	15.23	1.09	(0.7)	78-06-08	
				0.85	15.15	1.21	(0.4:)	78-09-08	See Notes.
				0.54	15.60	1.18	(0.3)	"	
A2148-57	21 48 27.7	-57 43 14	E3	1.00	14.40	1.05	0.27	78-06-06	
				1.00	14.40	1.07	0.52	78-09-08	
				0.70	14.65	1.13	0.39	"	
A2151-57	21 51 30.3	-57 53 40	SAB(s)O ⁰	0.85	14.96	1.39	0.4	78-06-07	
				0.85	15.01	1.28	0.6	78-09-08	
				0.54	15.42	1.28	0.5	78-09-08	
A2212-51A	22 12 21.9	-51 45 12	E2	1.00	15.42	1.18	(-0.2)	78-09-02	Normal spectrum; low U-B is
				1.00	15.38	1.17	(0.1)	78-09-04	therefore probably observa-
				0.70	15.52	1.17	(0.0)	78-09-02	tional artifact.
A2213-52A	22 13 47.8	-52 46 37	SAB:0 ⁻ :	0.85	14.58	1.14	0.33	78-06-12	
				0.85	14.59	1.10	0.36	78-09-06	
				0.54	15.01	1.14	0.48	"	
A2224-54	22 24 36	-54 59.8	(R')SAB(rs)O/a	1.15	13.78	0.93	0.34	78-09-02	EU190-G12
				0.85	14.04	0.97	0.32	"	
				0.85	14.08	0.97	0.30	78-09-04	
A2225-61A	22 25 29.7	-61 08 16	E ⁺ 3:	1.00	13.43	1.12	0.52	78-06-12	EU146-G28
				1.00	13.43	1.10	0.52	78-09-07	
				0.70	13.91	1.10	0.55	"	

Table 2 – continued

Galaxy	α	(1950)	δ	Type	log A	V	B-V	U-B	Date	Comments
(1)	(2)		(3)	(4)	(5)	(6)	(7)	(8)	(9)	
A2230-55A	22 30 18.0		-55 03 08	E1	0.85	15.83	1.09	(1.3)	78-09-04	
					0.70	16.01	1.13	(0.7)	"	
A2235-67A	22 35 10.2		-67 05 19	SAB0 ⁰	0.85	15.28	0.98	0.3	78-09-06	
					0.54	15.58	0.91	0.4	"	
A2249-60	22 49 59		-60 57.9	SO ⁰ : pec	1.00	13.65	0.96	0.43	78-09-07	EU147-G13. See Notes.
					1.00	13.65	0.97	0.35	78-09-08	
					0.54	14.08	0.98	0.40	78-09-07	
A2351-10B	23 51 07		-10 41.0	SO ⁺ :	0.85	15.52	1.21	(0.2)	78-09-08	
					0.54	15.90	1.10	(0.6)	"	See Notes.

Notes:

148 = 11577. Discovered in 1888 by Barnard (1892) who noted it as variable (see text). IC1 position in error (precession in δ to 1860 applied with wrong sign); IC2 position also wrong (+1 min in α , +3 arcmin in δ). Described in MCG (Vorontsov-Velyaminov & Arkipova 1963) as overexposed in the middle with an outer envelope.

A1331-45. The Fourcade-Figueroa Galaxy, listed as A1332-45 in RC2 where α is incorrect. The aperture was centred on the bright field star ($V = 11.18$, $B-V = 0.66$, $U-B = 0.20$) which was subtracted. See also Graham (1978). EU is the number in the ESO/Upssala Survey (Holmberg *et al.* 1978, and references therein).

N5556 = DDO 243. Superposed star ($V = 14.72$, $B-V = 1.01$, $U-B = 0.91$) subtracted. Not a dwarf galaxy.

I1185. This observation confirms those in V³C and shows those by Pettit (1954) to be incorrect in B , but not V . A superposed star very close to the nucleus could not be removed.

A2010-37. Superposed star ($V = 15.51$., $B-V = 1.39$., $U-B = 0.08$) subtracted from larger aperture. This star, measured only once on 78-06-06, should be remeasured. The v counts were very noisy; the galaxy observation on that date was similarly affected and was discarded.

N7098. A large Sa with well-developed inner and outer rings that is large and bright enough to be a Shapley-Ames galaxy. The RC2 α is incorrect.

A2146-62. In one low u count is not rejected, the $U-B$ (obviously uncertain) for this observation is +0.8.

A2249-60. Superposed star ($V = 15.95$, $B-V = 0.45$, $U-B = -0.03$) subtracted from large aperture.

A2351-10B. Third brightest galaxy in Abell 2670, 8.2 arcmin north preceding the cD. Cluster membership is assumed as there is no published redshift.

Column 4. The aperture, listed in units of log (tenths of arcmin) following RC2. Table 1 lists aperture sizes in arcsec.

Columns 5, 6 and 7. The UBV data with $U-B$ given to the nearest 0.1 mag when $V > 15$, and in parentheses when it seems especially uncertain.

Column 8. The data of the observation (year-month-day).

Column 9. Comments, alternative designations, additional references or references to the notes that follow the table. Most of these galaxies – as well as many others, but not the low surface brightness objects – have been observed spectroscopically with the 1.9-m reflector at SAAO. Their velocities and notes on their spectra will be published separately (Corwin & Emerson, in preparation).

5 Photometric parameters

The present data, combined with previously published photometry for these objects, have been used to derive total magnitudes and colours, as well as isophotal diameters and effective apertures. The procedures used in RC2 have been adopted, but with a few variations:

(1) Annular surface brightness versus aperture (or aperture to the one-quarter power) relations were calculated, and the apertures at $\mu = 25.0$ mag arcsec⁻² were determined by

interpolation or by extrapolation of less than 0.5 mag where necessary. These $\log A_{25}$'s were used instead of $\log D(0)_{25}$ as in RC2.

(2) As there is generally not enough data for these galaxies to justify the use of the three-approximation treatment of RC2, $\log \rho$ ($=\log A_{25} - \log A_e$) was estimated with the relationship

$$\log \rho = 0.35(\pm 0.01) - 0.34(\pm 0.02)(m'_{25} - 14.3), \quad \sigma = \pm 0.11(\text{m.e.}) \quad (1)$$

(compare with RC2, equations 17 and 18) where as usual

$$m'_{25} = B_{25} + 5 \log A_{25} - 5.26. \quad (2)$$

The coefficients and errors of equation (1) were determined by least squares fits to data from RC2, de Vaucouleurs (1977), and de Vaucouleurs & Corwin (1977) for 66 standard galaxies with photometric parameters from detailed surface photometry. Data for NGC 3379 from de Vaucouleurs & Capaccioli (1979) and for the WLM system from Ables & Ables (1977) were added, as were data for 18 DDO objects with photoelectric photometry from V²C or RC2. These latter objects strengthen equation (1) for low surface brightness ($m'_{25} > 14.5$) galaxies.

These modifications make it possible to derive photometric parameters from the aperture photometry alone without *a priori* estimates of (a) diameters and axis ratios and (b) mean effective surface brightnesses which depend on the total magnitude. (Axis ratio corrections to $\log A_{25}$ are in principle necessary. However, since $\log R \lesssim 0.3$ for all galaxies here with sufficient data, the correction is ignored.)

Table 3. Photometric parameters.

Galaxy	T	B_T	$\log A_{25}$	m'_{25}	$\log A_e$	m'_e	$(B-V)_T$	$(U-B)_T$	Δ (Mpc)	M_T^0	$(B-V)_T^0$	$(U-B)_T^0$	$\log A_e$	Group
(1)	(2)	(3)	(4)	(5)	(6)	(7)	(8)	(9)	(10)	(11)	(12)	(13)	(14)	(15)
N0045	8	11.2	1.72	15.1	1.60	14.7	0.60	-0.05	3.5	-16.9	0.52	-0.13	0.61	Pair w. N24.
A0031-31	9	(13.7)	(1.21)	(15.4)	-(1.23)	(15.3)	(0.49)	(-0.21)	10	(-16.7)	(0.42)	(-0.26)	(0.69)	N134 Group
I1558	9	(12.4)	(1.38)	(15.7)	(1.50)	(15.4)	(0.62)	(-0.01)	10	(-18.0)	(0.53)	(-0.07)	(0.96)	N134 Group
I1574	10	(14.3)	(1.12)	(15.2)	(1.07)	(15.1)	(0.54)	(-0.01)	2.5	(-13.3)	(0.41)	(-0.11)	(-0.07)	Sculptor
I0048	-1	13.95	1.04	14.1	(0.55)	(12.2)	0.87	0.26	-	-	-	-	-	Cetus III Cloud?
A0301-25	9	(13.9)	(1.17)	(15.9)	(1.36)	(16.2)	(0.63)	(-0.05)	-	-	-	-	-	Eridanus I Cloud?
A0311-02	9	14.4	1.08	14.8	(0.82)	(14.0)	0.41	-0.33	13	-16.7	0.28	-0.46	0.40	Pair w. N1253.
N3311	-3	12.4	(1.43)	(14.7)	1.18	13.8	1.03	0.56	40	-21.0	0.91	0.49	1.25	A1060 (Hydra)
N4325	-3	14.4	0.99	14.4	(0.6)	(12.9)	1.00	0.4	70	-20.1	0.88	0.4	(0.90)	Coma Supercluster
A1222+12	1?	16.3	(0.2)	(12.2)	-	-	1.0 ₅	(0.5)	70	-18.2	0.9 ₅	(0.5)	-	Coma Supercluster
I3481	-3	14.2	1.03	14.5	0.75	13.4	1.04	0.53	70	-20.3	0.92	0.51	1.06	Coma Supercluster
A1233+12	-6	15.5	0.65	13.0	-	-	0.90	0.4 ₅	12.5	-15.3	0.85	0.4	-	Virgo Cluster
N5264	10	12.7	1.39	14.6	1.11	13.7	0.59	(-0.03)	5.0	-16.3	0.47	(-0.17)	0.28	Centaurus Group
N5556	7	(12.5)	(1.39)	(15.0)	(1.28)	(14.4)	(0.64)	(-0.10)	16	(-18.9)	(0.54)	(-0.17)	(0.95)	-
N6034	-3	14.6	0.97	14.6	(0.7)	(13.6)	1.10	0.54	105	-21.0	0.92	0.51	(1.18)	A2151 (Hercules)
I1185	1	14.9 ₅	0.83	14.0	-	-	1.02	0.39	105	-20.7	0.84	0.31	-	A2151 (Hercules)
N6061	-3	14.6	0.94	14.4	0.65	13.3	1.09	0.51	105	-21.0	0.91	0.49	1.13	A2151 (Hercules)
A2010-37	-2	13.5	(1.17)	(14.4)	0.83	13.1	0.93	0.38	17	-18.2	0.78	0.27	0.52	N6925 Group
A2028-63A	-4	16.4 ₅	0.57	14.5	(0.3 ₅)	(13.7)	1.3 ₅	0.6	230	-21.1	1.0 ₅	0.6	(1.18)	C1 2029-63
A2036-53A	-5	15.6 ₅	0.71	14.3	(0.3 ₅)	(12.9)	1.15	0.31	130	-20.5	0.93	-0.27	(0.95)	C1 2036-53
A2049-52A	3	14.7 ₅	(0.96)	14.5	0.68	13.6	0.80	0.09	140	-21.7	0.56	-0.10	1.29	C1 2048-52
A2059-67	-3	12.8	(1.28)	(14.3)	0.90	12.8	0.93	0.41	-	-	-	-	-	Pavo-Indus Cloud?
A2111-59	0	15.8 ₅	0.75	14.8	0.56	14.1	1.05	(0.6)	170	-21.0	0.78	(0.6)	1.26	C1 2113-59
A2129-60	-3	15.5	0.74	14.2	(0.3)	(12.5)	0.94	(0.5)	85	-19.7	0.77	(0.4 ₅)	(0.70)	-
A2130-53A	-1	15.9	0.70	14.5	(0.4)	(13.4)	1.21	0.3	230	-21.6	0.91	0.3 ₅	(1.23)	C1 2131-53
A2131-62B	0?	16.0	0.67	14.4	(0.3)	(13.0)	1.04	-	170	-20.8	0.78	-	(1.00)	C1 2130-62
A2136-50	-5	15.0 ₅	0.86	14.5	(0.59)	(13.5)	1.15	0.49	160	-21.6	0.92	0.49	(1.26)	C1 2136-50
N7098	1	12.4	(1.43)	(14.5)	1.12	13.5	1.03	0.49	15	-19.1	0.88	0.36	0.76	Pavo-Indus Cloud?
A2146-62A	-3	16.1	0.69	14.7	0.50	14.1	1.15	(0.5)	190	-21.0	0.88	(0.5)	1.24	C1 2147-62
A2148-57	-5	15.2	0.82	14.5	(0.5 ₅)	(13.4)	1.07	(0.36)	120	-20.7	0.88	(0.34)	(1.08)	-

Table 3—continued

Galaxy	T	B_T	$\log A_{25}$	m'_{25}	$\log A_e$	m'_e	$(B-V)_T$	$(U-B)_T$	Δ (Mpc)	M_T^0	$(B-V)_T^0$	$(U-B)_T^0$	$\log A_e$ (kpc)	Group
(1)	(2)	(3)	(4)	(5)	(6)	(7)	(8)	(9)	(10)	(11)	(12)	(13)	(14)	(15)
A2151-57	-2	16.1 ₅	0.67	14.6	(0.4)	(13.6)	1.30	0.5	230	-21.4	0.99	0.5	(1.23)	C1 2150-58
A2212-51A	-5	16.5	(0.52)	(14.1)	-	-	1.17	-	200	-20.6	0.91	-	-	C1 2212-51
A2213-52A	-3	15.3	0.84	14.7	0.60	13.8	1.12	0.3 ₅	160	-21.3	0.89	0.34	1.27	C1 2213-52
A2224-54	0	14.6	0.96	14.4	(0.6)	(13.1)	0.94	0.30	-	-	-	-	-	C1 2224-54
A2225-61A	-4	14.0	(1.09)	(14.6)	0.85	13.7	1.10	0.49	-	-	-	-	-	C1 2226-61
A2230-55A	-5	16.6	(0.58)	(15.0)	-	-	1.10	(0.7)	220	-20.7	0.82	(0.7 ₅)	-	C1 2228-55
A2235-67A	-2	16.2	0.60	14.2	-	-	0.94	0.37	-	-	-	-	-	Group 2234-67
A2249-60	-2	14.4	0.95	14.1	0.47	12.2	0.96	0.37	-	-	-	-	-	-
A2351-10B	-1	16.7	0.53	14.4	-	-	1.1 ₅	(0.6)	220	-20.7	0.87	(0.6 ₅)	-	A2670

Table 3 gives photometric parameters for all but one of the galaxies observed. (A1331-45 is too large and too highly inclined to allow determination of even preliminary parameters.) The columns in the table are:

Column 1. The designation as in Table 2.

Column 2. The numerical type index (see RC2, Table 2a).

Column 3. The total blue magnitude.

Column 4. $\log A_{25}$ determined as described above, except for the five DDO galaxies with data at only one aperture. For these

$$\log A_{25} = \log D(0)_{25} - 0.12(\pm 0.03) \quad (3)$$

where $\log D(0)_{25}$ is from RC2. This relationship was found using data for 19 DDO galaxies also used in deriving equation (1) above. Though differences between $\log A_{25}$ and $\log D(0)_{25}$ might be expected to depend on surface brightness, magnitude, diameter and inclination, no such correlations were found in this sample.

Column 5. The mean surface brightness within A_{25} .

Column 6. $\log A_e$, the effective aperture containing half the light of the galaxy.

Column 7. The mean surface brightness within A_e .

Columns 8 and 9. Total $B-V$ and $U-B$ colours derived using the RC2 procedure.

Column 10. The galaxy's estimated distance in megaparsecs taken from (a) de Vaucouleurs (1979b) for NGC 45, (b) application of the precepts of de Vaucouleurs (1979a) for galaxies in the Hercules Cluster (Corwin, in preparation), (c) application of de Vaucouleurs' (1958) rotating-expanding Local Supercluster model with $R_{1\epsilon_1} = 1100 \text{ km s}^{-1}$, $R_1\omega_1 = 250 \text{ km s}^{-1}$ and $R_1 = 12.5 \text{ Mpc}$ for galaxies with $V < 4000 \text{ km s}^{-1}$, (d) a free-space Hubble parameter $H_0 = 100 \text{ km s}^{-1} \text{ Mpc}^{-1}$ (de Vaucouleurs & Bollinger 1979) for galaxies with $V > 4000 \text{ km s}^{-1}$, (e) the mean velocity of the Coma Supercluster ($V = 6900 \text{ km s}^{-1}$; see Gregory & Thompson 1978) with H_0 as above.

Column 11. The absolute total blue magnitude, corrected for inclination, galactic absorption and redshift following RC2.

Columns 12 and 13. The intrinsic colours similarly corrected following RC2.

Column 14. The log of the intrinsic effective diameter containing half the galaxy's light, in kiloparsecs.

Column 15. Group or cluster membership if known.

Distances and intrinsic parameters are not given where the redshift is unknown. Uncertain values are enclosed in parentheses. The parameters for the five DDO galaxies with observations at one aperture only are especially uncertain; they were derived using the standard magnitude-aperture curves in RC2, and should be reviewed completely when more data become available.

The similarity of intrinsic parameters for many of the galaxies with $T < 0$ is not surprising as most of these objects are among the first few brightest in rich clusters. The early-type galaxies in groups or in the 'field' (e.g. A2010-37, 2129-60, 2148-57) are generally fainter and smaller than the bright cluster galaxies.

6 Discussion: galaxies of special interest

6.1 DDO GALAXIES

These low surface brightness, late-type objects are generally rich in neutral hydrogen (see e.g. Balkowski *et al.* 1974; Fisher & Tully 1975; Thuan & Seitzer 1979). Thus, H I parameters for these galaxies are easier to determine at present than are optical parameters. Since the few observations presented here go only a short way toward redressing the imbalance, they will be combined with the much larger body of optical data on DDO galaxies now being collected at McDonald Observatory by de Vaucouleurs. Full discussion of the optical photometric parameters of the DDO objects will be published by de Vaucouleurs at a later date.

6.2 IC 48

This galaxy was described as variable by Barnard (1892) in his note on its discovery. The present observations and one other made by T. G. Hawarden with the same equipment ($\log A = 1.00$, $V = 13.29$, $B - V = 0.87$, $U - B = 0.27$ on 1978 December 27) show that Barnard's supposition of variability is probably incorrect. The galaxy's normal colours for its type make it unlikely that it has a Seyfert nucleus, though a spectrum will be necessary for confirmation. Barnard's observations are also consistent with his having seen a supernova near the centre of the galaxy. This would again require confirming observations, perhaps on early patrol camera plates.

6.3 A 1233+12

First noted by Reinmuth (1927) as 'considerably faint, very small, round and brighter in the middle', this galaxy was also listed by Eastmond (1977) as E3-822. Eastmond gives magnitudes for the galaxy from two methods: the Abell-Mihalas (1966) extrafocal technique, and iris-diaphragm measurements. Comparison of data for this and other of Eastmond's objects for which photoelectric observations are available (including A 1222 + 12 = E4-634) show that the iris-diaphragm measurements are affected by errors dependent upon surface brightness, magnitude and galaxy type. The extrafocal magnitudes have errors depending on magnitude and type, the latter effect also noted by Smyth & Stobie (1980). Details of this magnitude comparison will be published separately by Abell & Corwin.

A spectrum of A 1233 + 12 shows it to have the same velocity as NGC 4552 which is 11 arcmin north (NGC 4551 with a slightly larger velocity is 7 arcmin south). A 1233 + 12 is thus a dwarf member of the Virgo Cluster, morphologically and photometrically very similar to M32 (for which $M_T^0 = -15.3$, $(B - V)_T^0 = 0.85$, $(U - B)_T^0 = 0.38$ and $\log A_e(\text{kpc}) = -0.68$). However, it is relatively isolated from its nearest neighbours, so may have a different luminosity distribution in its outer regions (M32, of course, is disturbed photometrically and dynamically by M31). On the basis of the present data alone, however, A 1233 + 12 is a good example of a compact dwarf elliptical. (The galaxy is not included in Zwicky's lists of compact galaxies (Zwicky 1971; Zwicky, Sargent & Kowal 1975) though he is known to have searched the Virgo Cluster area.)

6.4 GALAXIES IN THE INDUS SUPERCLUSTER AREA

The 19 galaxies in this part of the sky for which data are given here will help to calibrate southern sky survey fields 106–109, 144–147, 187–190 and 235–238. As far as possible, the galaxies were chosen to be in the unvignetted portions of the UK Schmidt plates covering these fields. They were also selected so that calibrating objects – including those with previously published data – would be available over at least a 2 mag range in each field. For most fields, the range is 3–4 mag. A COSMOS study of the Indus Supercluster is currently being carried out at the Royal Observatory, Edinburgh; results will be published when available.

Acknowledgments

I am grateful to the Director of SAAO, Dr M. W. Feast and to PATT for generous allotments of telescope time; and to SRC for travel and subsistence grants. The staff at SAAO was very helpful – special thanks are due Roy White, Pete Read, Rona Banfield, Tom Lloyd-Evans and John Menzies. Robert Smyth, Bob Stobie, Martin Green, Keith Dixon, Tim Hawarden and Andy Longmore very kindly supplied data in advance of publication. Several of my colleagues at ROE had helpful comments on an earlier version of this paper. Finally, I am especially grateful for G. de Vaucouleurs' continued encouragement and inspiration.

References

- Abell, G. O. & Mihalas, D. M., 1966. *Astr. J.*, **71**, 635.
 Ables, H. D. & Ables, P. G., 1977. *Astrophys. J. Suppl.*, **34**, 245.
 Balkowski, C., Bottinelli, L., Chamaraux, P., Gouguenheim, L. & Heidmann, J., 1974. *Astr. Astrophys.*, **34**, 43.
 Barnard, E. E., 1892. *Astr. Nachr.*, **130**, 7 (see also Barnard, E. E., 1895, *Mon. Not. R. astr. Soc.*, **55**, 451).
 Bergwall, N. A. S., Ekman, A. B. G., Lauberts, A., Westerlund, B. E., Borchkhadze, T. M., Breysacher, J., Laustsen, S., Muller, A. B., Schuster, H.-E., Surdej, J. & West, R. M., 1978. *Astr. Astrophys. Suppl.*, **33**, 243.
 Bucknell, M. J. & Peach, J. V., 1976. *Observatory*, **96**, 61.
 Cousins, A. J. W., 1973. *Mem. R. astr. Soc.*, **77**, 223.
 de Vaucouleurs, G., 1958. *Astr. J.*, **63**, 253.
 de Vaucouleurs, G., 1977. *Astrophys. J. Suppl.*, **33**, 211.
 de Vaucouleurs, G., 1979a. *Astrophys. J.*, **227**, 380.
 de Vaucouleurs, G., 1979b. *Astrophys. J.*, **227**, 729.
 de Vaucouleurs, G. & Bollinger, G., 1979. *Astrophys. J.*, **233**, 433.
 de Vaucouleurs, G. & Capaccioli, M., 1979. *Astrophys. J. Suppl.*, **40**, 699.
 de Vaucouleurs, G. & Corwin, H. G., 1977. *Astrophys. J. Suppl.*, **33**, 219.
 de Vaucouleurs, G. & de Vaucouleurs, A., 1972. *Mem. R. astr. Soc.*, **77**, 1.
 de Vaucouleurs, G., de Vaucouleurs, A. & Corwin, H. G., 1976. *Second Reference Catalogue of Bright Galaxies* (RC2), University of Texas Press, Austin.
 de Vaucouleurs, G., de Vaucouleurs, A. & Corwin, H. G., 1978. *Astr. J.*, **83**, 1331. (V²C).
 Eastmond, T. S., 1977. *PhD thesis* (unpublished), University of California at Los Angeles.
 Fisher, J. R. & Tully, R. B., 1975. *Astr. Astrophys.*, **44**, 151.
 Graham, J. A., 1976. *Astr. J.*, **81**, 681.
 Graham, J. A., 1978. *Publs astr. Soc. Pacif.*, **90**, 237.
 Green, M. R. & Dixon, K. L., 1978. *Observatory*, **98**, 166.
 Gregory, S. A. & Thompson, L. A., 1978. *Astrophys. J.*, **222**, 784.
 Holmberg, E. B., Lauberts, A., Schuster, H.-E. & West, R. M., 1978. *Astr. Astrophys. Suppl.*, **34**, 285.
 Landolt, A. U., 1973. *Astr. J.*, **78**, 959.

- Persson, S. E., Frogel, J. A. & Aaronson, M., 1979. *Astrophys. J. Suppl.*, 39, 61.
- Pettit, E., 1954. *Astrophys. J.*, 120, 413.
- Reinmuth, K., 1927. *Veröff. Sternw. Heidelberg*, 8, 69.
- Smyth, R. J. & Stobie, R. S., 1980. *Mon. Not. R. astr. Soc.*, 190, 631.
- Thuan, T. X. & Seitzer, P. O., 1979. *Astrophys. J.*, 231, 327.
- van den Bergh, S., 1966. *Astr. J.*, 71, 922.
- Vorontsov-Velyaminov, B. A. & Arkipova, V. P., 1963. *Morphological Galaxy Catalogue (MCG)*, Vol. 3, Moscow State University, Moscow.
- Wegner, G., 1979. *Astrophys. Space Sci.*, 60, 15.
- Zwicky, F., 1971. *Catalogue of Selected Compact Galaxies and of Post-Eruptive Galaxies*, Berne, Switzerland.
- Zwicky, F., Sargent, W. L. W. & Kowal, C. T., 1975. *Astr. J.*, 80, 545.